Underpinning replication of protein-bound DNA by the accessory replicative helicase Rep

Jan-Gert Brüning

Doctor of Philosophy

University of York

Biology

September 2014

Abstract

Accurate DNA replication must occur prior to every cell division. However, replication forks often stall at sites of DNA damage and protein-DNA complexes. If not removed, these blocks can threaten the viability of both daughter cells by preventing the completion of genome duplication or by targeting of blocked forks by recombination enzymes that can result in gross chromosomal rearrangements and genome instability. The importance of minimising fork blockage has resulted in cells evolving repair systems to remove lesions from DNA whilst accessory replicative helicases can underpin replication fork movement through hard-to-replicate sites including protein-DNA complexes.

This thesis investigates the *Escherichia coli* accessory replicative helicase Rep. It is shown that efficient recruitment of Rep to the replisome via an interaction with the replicative helicase DnaB is dependent on the extreme Rep C-terminus. This work also indicates that the DnaB C-terminus is necessary for this interaction.

Secondly, this work determines the function of the 2B subdomain, a conserved feature of Superfamily 1A (SF1A) helicases. Characterisation of a Rep mutant lacking this domain (RepΔ2B) showed greatly reduced levels of protein displacement from DNA, indicating a central role of the 2B subdomain in the removal of nucleoprotein blocks. Complementation of this mutation by a 2B subdomain of the homologous helicase UvrD supports the idea that the accessory replicative helicase function of Rep is dependent on a 2B subdomain. These data also demonstrate that the function of 2B subdomains is conserved among other SF1A helicases.

Previous work had also shown that the 2B subdomain of SF1A helicases is flexible. Mutations in the hinge that connect the 2B subdomain to the rest of the helicase resulted in activation of DNA helicase activity and increased levels of nucleoprotein removal from single-stranded (ss) and double-stranded (ds) DNA.

These data shed new light on how translocation along DNA is coupled to protein displacement during helicase catalysis, a conserved function of many helicases. A model is proposed where ATP hydrolysis is closely linked to conformational changes of the 2B subdomain of Rep, facilitating protein displacement by Rep.

Table of Contents

List of Tables

List of Figures

Acknowledgements

First and foremost, I want to thank my PhD supervisor Prof Peter McGlynn for all the support and advice during the last four year, starting from an exciting Bachelor project that encouraged me to apply for this PhD project. I also want to thank Dr Jonathan Pettitt, who supervised my work on *C. elegans* back at the University of Aberdeen.

I am also extremely grateful to Dr Kamila Myka for her comments on my first draft of my thesis and most importantly for all her patience and support, especially in the last few stressful months of my PhD.

Furthermore, I want to thank Dr John Atkinson and Dr Milind Gupta for their general help and advice during the initial stages of my PhD. Additionally, I want to thank all current members of our lab, Dr Michelle Hawkins, Dr Jamieson Howard, especially for his assistance with protein purifications and Dr Aisha Syeda, particularly for help P1 transduction.

In general, I want express my gratitude also to all members of the Prof Maggie Smith and Prof Mike Brockhurst research groups for the great atmosphere in the lab and various lab outings.

Additionally, thanks to all my friends from home, from Aberdeen and from York for giving me much appreciated breaks from work and help me maintain a basal level of sanity.

Finally, I want to thank my family, my parents Engelbert and Maria, my sisters Nadine and Verena, my brother-in-laws Thomas and Tobias and my nieces and nephews, Freya, Joschka and Jenne. They have always supported and helped me and this PhD would not have been possible without them!!!

Declaration

I hereby declare that this thesis has been composed by the undersigned, Jan-Gert Brüning, for the degree of Ph.D. at the University of York. This work has not been presented in any previous application for a degree. All the work was performed by the undersigned unless otherwise stated in text. All sources of information have been specifically acknowledged in the text.

Jan-Gert Brüning

September 2014

Chapter 1

INTRODUCTION

Chapter 1 – Introduction

1.1 Helicases

The DNA molecule forms a double helix of two antiparallel phosphate-sugar chains that are connected via complementary base pairs (Watson & Crick, 1953). It is the sequence of these bases that contains all the information necessary to build an organism. In order to access the information encoded in DNA, it is necessary to gain access to these bases. This function is provided by enzymes called helicases. Helicases are a subclass of translocases that couple directional movement along DNA and/or RNA substrates to the disruption of hydrogen bonds between nucleic acid duplexes (Lohman *et al.*, 2008; Singleton *et al.*, 2007). Helicases are an essential class of enzymes that participate in virtually every aspect of nucleic acid metabolism (Brennan *et al.*, 1990; Chaudhury & Smith, 1984; Chuang *et al.*, 1997; Company *et al.*, 1991; Lahue *et al.*, 1989; LeBowitz & McMacken, 1986; Liu & Marians, 1999; Mendonca *et al.*, 1993). The importance of helicases is reflected by the fact that as much a 1-2% of all genes in eukaryotes encode helicases (Eki *et al.*, 2007; Shiratori *et al.*, 1999).

The minimal structural unit of helicases and translocases resembles the ATP binding site of the *Escherichia coli* DNA strand exchange protein RecA. Helicases and translocases bind and hydrolyse nucleoside triphosphates (NTPs) between two opposing RecA-like folds. The energy derived from NTP hydrolysis is converted into conformational changes within the RecA-like core domains and translated into directional movement on nucleic acid (Subramanya *et al.*, 1996; Ye *et al.*, 2004).

Helicases in which two RecA-like folds oppose each other in the tertiary structure of the protein can unwind DNA as monomers. However, in the absence of additional factors or protein/protein interactions, some monomeric helicases require additional helicase molecules to translocate behind the leading helicase molecule for efficient nucleic acid unwinding *in vitro* (Figure 1.1A) (Cheng *et al.*, 2001; Maluf *et al.*, 2003; Yang *et al.*, 2008). These additional molecules do not actively participate in the unwinding of a nucleic acid duplex but rather prevent the leading helicase molecule from backslipping, thereby increasing the processivity of the

leading helicase molecule (the so-called cooperative inchworm model) (Byrd & Raney, 2005; Byrd & Raney, 2006). A few exceptions of monomeric helicases exist that can unwind DNA via translocation along the nucleic acid duplex (Singleton *et al.*, 2001).

Other helicases form quaternary structures, usually hexameric rings, and bind NTP between opposing RecA-like folds of two neighbouring subunits. These hexameric helicases encircle a single strand of nucleic acid and separate the nucleic acid duplex by steric exclusion of the complementary strand (Figure 1.1B) (Enemark & Joshua-Tor, 2006; Kaplan, 2000).
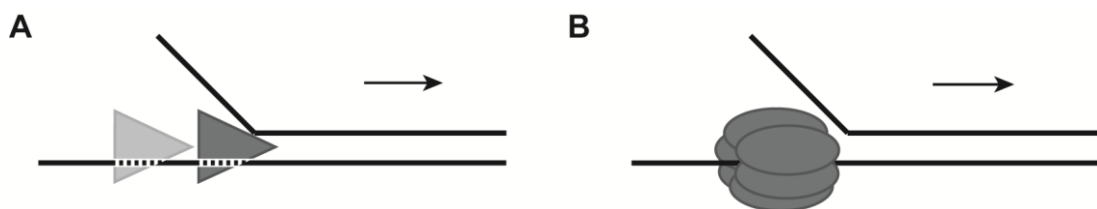
Figure 1.1 Unwinding of nucleic acids by helicases
(A) Unwinding by monomeric helicases (dark grey). Helicases interact with a single strand of nucleic acid (indicated by the dashed line) and couple directional translocation with destabilisation of the duplex. Additional trailing helicase molecules (light grey) can increase the efficiency of nucleic acid unwinding (cooperative inchworm model (Byrd & Raney, 2006)) (B) Hexameric helicases encircle and translocate along a single strand of nucleic acid resulting in unwinding of the duplex by steric exclusion of the complementary strand. The black arrows indicate direction of translocation of the helicases.

1.1.1 Active and passive helicases

Nucleic acid unwinding can occur in an active or a passive fashion. Active helicases directly interact with the duplex junction and result in the destabilisation of the base pairs. Translocation along single-stranded nucleic acid and unwinding of a nucleic acid duplex occur at approximately the same rate in a fully active helicase and these rates are not affected by the stability of the duplex substrate (GC content). Active helicases are often monomeric helicases, such as *E. coli* UvrD (Superfamily 1A, see below), T4 bacteriophage Dda (SF1B) or *E. coli* RecG (SF2) (Byrd *et al.*, 2012; Manosas *et al.*, 2013; Manosas *et al.*, 2010; Sun *et al.*, 2008).

Unwinding by passive helicases depends on thermal fraying of the base pairs at the duplex junction with translocation of the helicase trapping the resultant single-stranded nucleic acid. Passive helicases are defined functionally by a four-fold or larger reduction in the velocity of nucleic acid duplex unwinding compared to translocation along single-stranded nucleic acid (Manosas *et al.*, 2010). Hexameric replicative helicases, such as *E. coli* DnaB are often passive by this definition (Manosas *et al.*, 2010). Coupling of DnaB to the replisome however increases the rate of DNA unwinding (Kim *et al.*, 1996; Stano *et al.*, 2005), illustrating that protein-protein interactions that stabilise helicases at the duplex junction can result in DNA unwinding in an active mode (see section 1.2.4).

1.1.2   Protein displacement by helicases

Another factor regarding nucleic acid translocation and unwinding are protein-DNA complexes. Protein complexes that are able to bind single-stranded or double-stranded nucleic acids are abundant in cells (Ali Azam *et al.*, 1999; Wang *et al.*, 2011). Hence, helicases are bound to encounter such nucleoprotein complexes during translocation along and unwinding of nucleic acids. While some protein-DNA complexes have evolved specifically to block the progression of helicases (section 1.2.3), the majority of nucleoprotein complexes present accidental barriers to helicase movement along DNA (Brewer & Fangman, 1988; Gautam *et al.*, 2001; Khatri *et al.*, 1989). Thus, in addition to the disruption of hydrogen bonding between the nucleic acid base pairs, helicases are also required to break non-covalent bonds between proteins and DNA. The inability to do so can result in helicase dissociation from nucleic acid and incomplete duplex unwinding.

The mean energy required to unwind a single base pair of DNA is 6.7 kJ mol^{-1}, whereas the free energy from ATP hydrolysis is about 42 kJ mol^{-1} (von Hippel & Delagoutte, 2001). Thus, a single ATP hydrolysis event provides enough energy to unwind about six base pairs. However, helicases generally show lower step sizes (defined as the number of base pairs translocated per NTP hydrolysis event). The step sizes of some helicases have been reported as 1 or 2 base pairs (Galletto *et al.*,

2004a; Kornberg *et al.*, 1978; Lee & Yang, 2006). Even taking into account higher step size estimates of 4-5 base pairs, not all the free energy from ATP hydrolysis would be required for DNA unwinding (Ali & Lohman, 1997; Yang *et al.*, 2008). Indeed, many helicases are able to remove protein blocks from single-stranded nucleic acids and also unwind protein-bound nucleic acid duplexes, suggesting that some energy of NTP hydrolysis might be utilised for protein displacement. However, the efficiency in protein displacement varies from helicase to helicase (Byrd & Raney, 2006; Jankowsky *et al.*, 2001; Morris *et al.*, 2002; Morris & Raney, 1999; Yancey-Wrona *et al.*, 1992).

The exact mechanisms by which helicases displace protein-DNA blocks are still unclear. ATPase activity of Dda is increased upon encounter of model nucleoprotein block on ssDNA. This is not the case when this helicase translocates away from this block (Raney & Benkovic, 1995), suggesting that the displacement of protein-DNA complexes by helicases requires an increased energy input and is likely a multi-step process (Teulon *et al.*, 2011).

1.1.3 Classification of helicases

Helicases and translocases have been classified into Superfamilies based on conserved amino acid motifs (Gorbalenya & Koonin, 1993). The presence of a Walker A and a Walker B motif that mediate NTP binding and hydrolysis and a conserved arginine finger, which is required for energy coupling, are ubiquitous among all of these enzymes (Crampton *et al.*, 2004; Scheffzek *et al.*, 1997; Singleton *et al.*, 2007; Walker *et al.*, 1982). Other motifs are diagnostic of certain superfamilies of helicases and translocases.

Helicases are further differentiated according to their polarity. Type A helicases translocate with 3' to 5' polarity along nucleic acids, while type B helicases translocate with 5' to 3' polarity. Additionally, translocation can occur along single-stranded (type α) or double-stranded (type β) nucleic acids or in some cases both (Figure 1.2) (Singleton *et al.*, 2007).
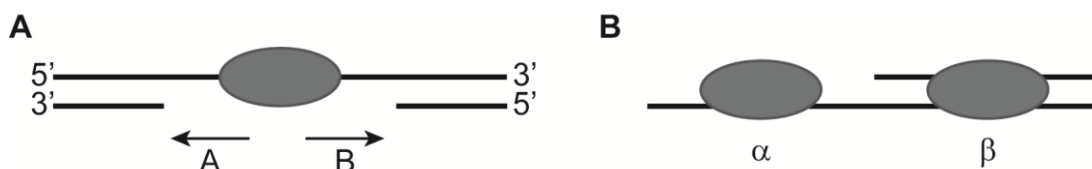
Figure 1.2 Different types of helicases
(A) Type A helicases translocate and unwind nucleic acids with 3' to 5' polarity, while type B helicases display 5' to 3' polarity. (B) Translocation along single-stranded nucleic acids is performed by type α helicases and translocases, while β enzymes can translocate along double-stranded nucleic acids.

1.1.4   Monomeric helicases

1.1.4.1   Superfamily 1 helicases

Superfamily 1 helicases were originally classified based on seven conserved helicase motifs (Gorbalenya & Koonin, 1993). Two more motifs have been added as a characteristic for SF1 helicases in a more recent classification (Singleton *et al.*, 2007). All SF1 helicases that have been identified to date translocate along single stranded nucleic acids (type α) (Gilhooly *et al.*, 2013; Singleton *et al.*, 2007).

Superfamily 1 helicases share a conserved domain structure with two main domains, 1 and 2, that are subdivided into A and B (Figure 1.3A). Subdomains 1A and 2A form the motor core of the helicase which is required for NTP and ssDNA binding. The subdomains 1B and 2B are insertions in the 1A and 2A subdomains, respectively, and are generally considered to have an accessory role for helicase function. They have been proposed to assist DNA unwinding (Lee & Yang, 2006; Saikrishnan *et al.*, 2008) or have autoinhibitory functions with respect to helicase activity (Brendza *et al.*, 2005). These domains show large variations in size among different SF1 helicases. Some 1B and 2B subdomains are longer than 100 amino acids, while other helicases have a very small 1B or no 2B subdomain (Dillingham, 2011; Saikrishnan *et al.*, 2008).

A

domain		1A			1B		1A	2A		2B			2A		
motif	Q	I	Ia	Ib			II	III	IVa	IV			V	VI	
DNA	-	-	+	+			-	+	+	-			+	-	
ATP	+	+	-	-			+	+	-	+			-	+	

B

IVa   V   III Ia II Ib

AMP-PNP

VI   IV   I   Q

C

i) 2A 1A

ii)

iii)
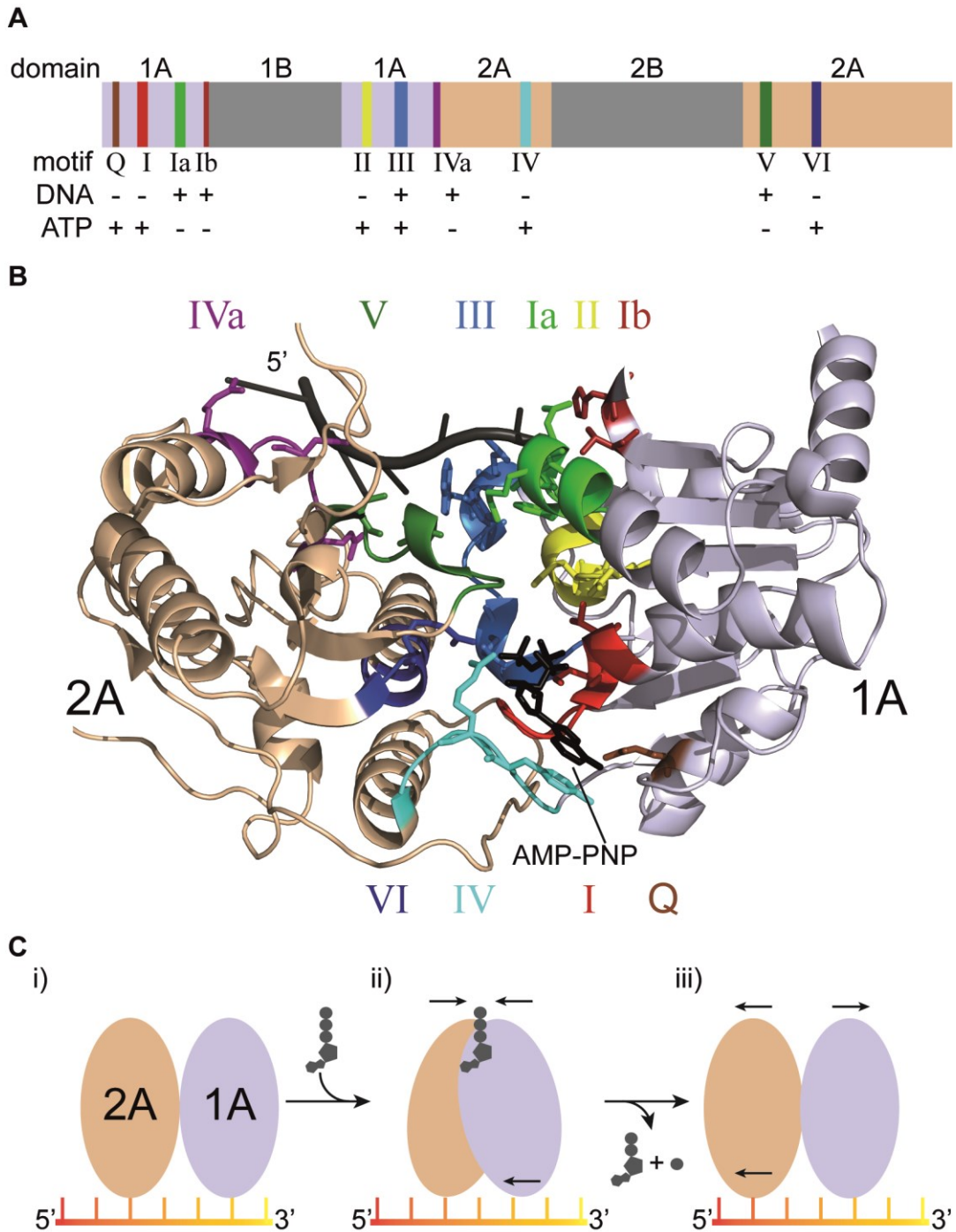
Figure 1.3 The Superfamily 1 helicase motor core

(A) Position of conserved helicase motifs of a representative SF1 helicase, PcrA. These positions may vary between different helicases. (B) Crystal structure of the PcrA motor core (subdomains 1A in light blue and 2A in wheat; subdomains 1B and 2B are not shown) bound to ssDNA and the ATP analogue AMP-PNP (PDB: 3PJR, (Velankar *et al.*, 1999)) in cartoon representation. Residues of helicase motifs that contact the ssDNA or the nucleoside are in stick representation. Details about the function of the motifs are given in the text. The crystal structure lacked a magnesium cation, which is required for ATP hydrolysis. (C) Inchworm model of translocation by a SF1A helicase: (i) the helicase motor core bound to ssDNA in the absence of a nucleoside. (ii) The motor core closes on ATP binding, loosening the contacts of the 1A subdomain to ssDNA. This reduces the distance of the two subdomains on the ssDNA. (iii) ATP hydrolysis and release of ADP and P_i results in a forward motion of the 2A subdomain. The motor core returns into its original conformation, having translocated a single base pair.

1.1.4.1.1 Superfamily 1A helicases

Superfamily 1A helicases translocate with 3' to 5' polarity along ssDNA. All conserved helicase motifs in SF1A helicases line the cleft between the 1A and 2A subdomains (Figure 1.3B) (Subramanya *et al.*, 1996). These conserved motifs are involved in NTP binding as well as single-stranded nucleic acid interactions.

The Walker A and B motifs (motifs I and II, respectively) are located in the 1A subdomain at the interface between the 1A and 2A subdomains. In concert with the Walker A motif, motif IV positions ATP between the two core regions, while the Q-motif provides specificity for ATP binding over other nucleosides (Hall & Matson, 1997; Tanner *et al.*, 2003; Walker *et al.*, 1982). The conserved arginine finger is part of motif VI in the 2A subdomain and is located opposite to the invariant lysine of the Walker A motif (Velankar *et al.*, 1999). Binding of ATP by SF1A helicases induces conformational changes in the motor core that result in motifs VI and III moving closer together (Velankar *et al.*, 1999).

ATP hydrolysis is promoted by a divalent cation at the active site, which is coordinated by conserved threonine and aspartate residues in motif I and II, respectively (Velankar *et al.*, 1999). The release of ADP and organic phosphate opens the cleft between the motor core and returns to the initial conformation. These ATP hydrolysis-induced conformational changes alter the interaction of the N-terminal (1A subdomain) and C-terminal (2A subdomain) motor cores with single-stranded nucleic acid via motifs Ia, Ib, III, IVa and V, such that a single subdomain is always tightly bound to the ssDNA, allowing the other subdomain to move forward in the 3' to 5' direction in an inch-worm like fashion. Subsequent cycles of ATP hydrolysis result in the directional movement of the helicase along the nucleic acid lattice in single base pair steps (Figure 1.3C) (Caruthers & McKay, 2002; Korolev *et al.*, 1997; Korolev *et al.*, 1998; Velankar *et al.*, 1999).

The best studied SF1A helicases are the *E. coli* helicases Rep and UvrD and the *Bacillus stearothermophilus* helicase PcrA. All three helicases are closely related, sharing about 40% amino acid identity (Gilchrist & Denhardt, 1987; Iordanescu, 1993). Crystallisation of these helicases in complex with different DNA substrates,

revealed the typical domain architecture of SF1 helicases of four subdomains (Figure 1.4) (Korolev *et al.*, 1997; Lee & Yang, 2006; Velankar *et al.*, 1999).
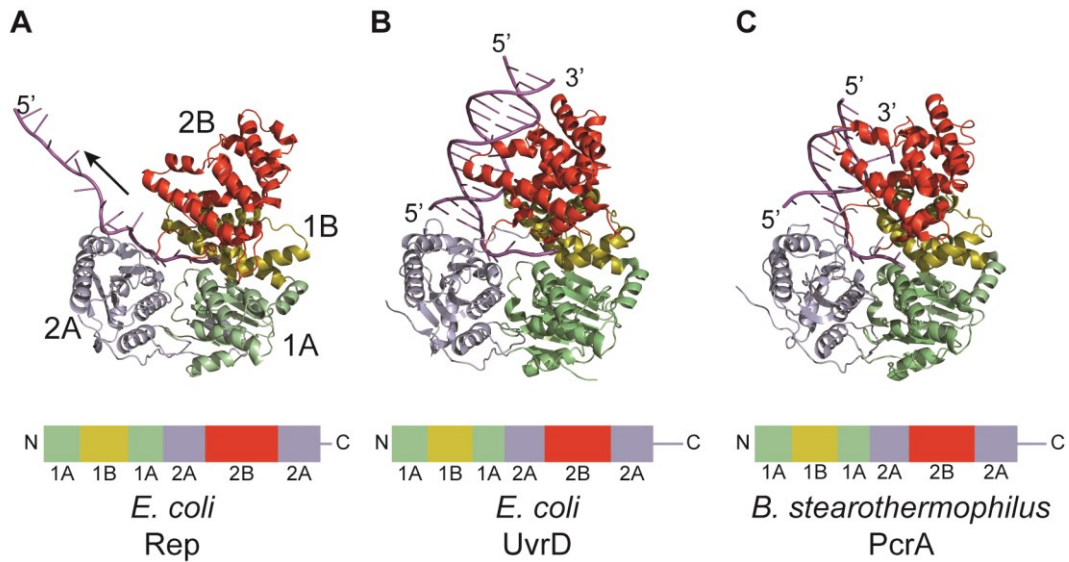
Figure 1.4 Conserved domain structure of Superfamily 1A helicases
Crystal structures of (A) *E. coli* Rep (PDB: 1UAA, (Korolev *et al.*, 1997)), (B) *E. coli* UvrD (PDB: 2IS2, (Lee & Yang, 2006)) and (C) *B. stearothermophilus* PcrA (PDB: 3PJR, (Velankar *et al.*, 1999)) in cartoon representation. The conserved domain structure is illustrated by colour coding with the 1A subdomain in green, 1B in yellow, 2A in blue, 2B in red and DNA in magenta. The arrow in (A) indicates translocation polarity of all the helicases (3'-5').

A single homologue of these helicases is present in almost all prokaryotes (Gilhooly et al., 2013). Biochemical and genetic characterisation of PcrA and UvrD showed that these two helicases have almost identical functions. They both function as antirecombinases, removing RecA filaments from ssDNA to suppress illegitimate recombination (section 1.3.6) (Anand *et al.*, 2007; Veaute *et al.*, 2005). Both helicases function in nucleotide excision repair (section 1.3.1) (Atkinson *et al.*, 2009; Manelyte *et al.*, 2009; Petit *et al.*, 1998) and are also involved in the replication of certain plasmids (Bruand & Ehrlich, 2000; Soultanas *et al.*, 1999). In contrast, Rep is functionally diverse from these helicases, having roles in replication restart (section 1.3.2) (Heller & Marians, 2005b) and the replication of several phages (Calendar *et al.*, 1970; Denhardt *et al.*, 1967). It was shown recently that all three helicases promote replication fork movement through nucleoprotein complexes *in vitro*, which suggests crucial roles in the maintenance of genome stability for these helicases (section 1.5) (Guy *et al.*, 2009).

Efficient DNA unwinding by Rep, UvrD and PcrA required multimerisation either in the form of self-dimerization or via interactions with other accessory proteins *in vitro* (Cheng *et al.*, 2001; Guy *et al.*, 2009; Maluf *et al.*, 2003; Soultanas *et al.*, 1999; Soultanas *et al.*, 1998; Yancey & Matson, 1991; Yang *et al.*, 2008).

SF1A helicases are generally less abundant in eukaryotes. The best studied example is *Saccharomyces cerevisiae* Srs2, which is a homologue of UvrD and displays antirecombinase activity by removing Rad51 filaments from ssDNA (Krejci *et al.*, 2003; Veaute *et al.*, 2003). Similar activities have been shown for Fbh1, the homologue of Srs2 in *Schizosaccharomyces pombe* and human cells (Fugger *et al.*, 2009; Lorenz *et al.*, 2009).

1.1.4.1.2   Superfamily 1B helicases

The best studied Superfamily 1B helicase is Dda from bacteriophage T4. The crystal structure of Dda revealed the typical Superfamily 1 domain structure. (Figure 1.5A) (He *et al.*, 2012). Dda is an optimally active helicase, unwinding DNA with almost the same velocity as it translocates along ssDNA (Byrd *et al.*, 2012). Additionally, Dda is able to remove protein blocks from both ss- and dsDNA (Byrd & Raney, 2004; Byrd & Raney, 2005; Byrd & Raney, 2006; Morris & Raney, 1999; Yancey-Wrona & Matson, 1992). During DNA unwinding by Dda, the 2B subdomain interacts with the 1B subdomain, forming an arch through which one strand of ssDNA is passed. Mutations affecting this interaction reduce the efficiency of DNA unwinding (He *et al.*, 2012). Similarly, a deletion of the 1B subdomain of the SF1B helicase RecD2 from *Deinococcus radiodurans* (Figure 1.5B) abolishes DNA helicase activity (Saikrishnan *et al.*, 2008). The relatively small 1B subdomain of Superfamily 1B helicases therefore acts as a pin against which the dsDNA junction is pressed resulting in duplex destabilisation and consequently DNA unwinding.

SF1B helicases not only show the same domain architecture as SF1A helicases but they also bind ssDNA in the same orientation with respect to their motor core, i.e. the 3' end of the ssDNA faces towards the 1A subdomain and the 5' end is closer to the 2A subdomain (Figure 1.5). However, SF1B helicases translocate with the

opposite polarity (5'-3') than that of SF1A helicases. Comparisons of the crystal structures of SF1A PcrA and SF1B RecD2 revealed that Superfamily-specific interactions of helicase motifs Ia and III with ssDNA restrict the translocation polarity of SF1A and SF1B helicases to the 3'-5' and 5'-3' direction, respectively (Saikrishnan *et al.*, 2009).
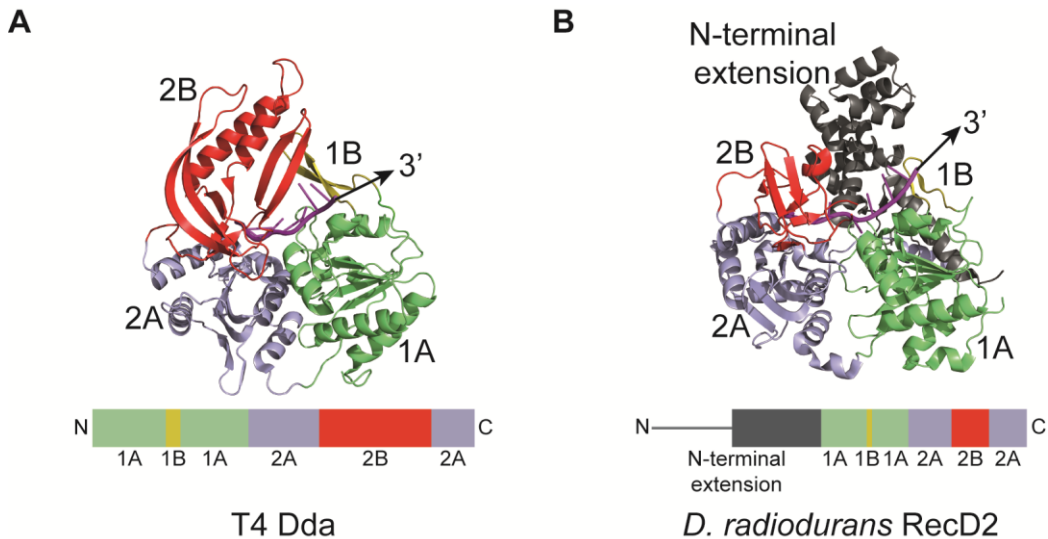
Figure 1.5 Structure of Superfamily 1B helicases
Crystal structures of (A) T4 Dda (PDB: 3UPU, (He *et al.*, 2012)) and (B) *D. radiodurans* RecD2 (PDB: 3GP8, (Saikrishnan *et al.*, 2009)) in cartoon representation. The conserved domain structure is illustrated by colour coding with the 1A subdomain in green, 1B in yellow, 2A in blue, 2B in red and ssDNA in magenta. The N-terminal domain of RecD2 is shown in grey. The initial 150 amino acids of RecD2 are missing in the crystal structure and are indicated by a grey line below. The arrows indicate translocation polarity of the helicases along ssDNA.

*Dr*RecD2 is a homolog of *E. coli* SF1B helicase RecD. While *Ec*RecD forms part of the RecBCD helicase/nuclease complex, which is involved in homologous recombination (section 1.3.5), *Dr*RecD2 functions in the absence of a larger molecular complex (Amundsen *et al.*, 2000; Walsh *et al.*, 2014). *D. radiodurans* does not encode any RecB or RecC homologs but instead *Dr*RecD2 encodes an N-terminal extension that in missing from the *E. coli* RecD protein (Rocha *et al.*, 2005).

RecD helicases are closely related to the eukaryotic Pif1 family of helicases (Fairman-Williams *et al.*, 2010; Zhang *et al.*, 2006). Most eukaryotes encode a single Pif1 helicase, while *S. cerevisiae* encodes two Pif1 members, Pif1 and Rrm3 (Bessler *et al.*, 2001). Pif1 helicases have been implicated in telomere maintenance and Okazaki fragment processing and have roles in genome maintenance in the nucleus

and the mitochondria (Budd *et al.*, 2006; Futami *et al.*, 2007; George *et al.*, 2009; Lahaye *et al.*, 1991; Schulz & Zakian, 1994; Zhou *et al.*, 2002). *Sc*Rrm3 and the single Pif1 homolog Pfh1 from *S. pombe* also function as accessory replicative helicases by assisting replication fork progression through protein-DNA complexes (section 1.5) (Ivessa *et al.*, 2002; Sabouri *et al.*, 2012).

Another phylogenetic group of SF1B helicases, classified as Upf1-like helicases, are involved in various RNA processing pathways and are mostly found in eukaryotes (Clerici *et al.*, 2009; Fairman-Williams *et al.*, 2010; Ideue *et al.*, 2007). Some of these helicases have been shown to translocate both on DNA and RNA (Guenther *et al.*, 2009; Tackett *et al.*, 2001; Taylor *et al.*, 2010).

1.1.4.2   Superfamily 2 helicases

Superfamily 2 helicases are also monomeric helicases and share several of the conserved helicase motifs with SF1 helicases. SF2 helicases however lack the SF1 motif IV (SF2 motif 4 corresponds to SF1 motif IVa) and do not display conservation within helicase motif III (Figure 1.6A) (Korolev *et al.*, 1998). All helicase domains localise into the cleft between the opposing N- and C-terminal motor core domains (Figure 1.6B), allowing NTP binding and hydrolysis by monomers.

SF2 helicases form the largest class of helicases. The majority of SF2 helicases belong to the groups of DEAH/RHA and DEAD-box RNA helicases including both type A and B enzymes that participate in all cellular processes involving RNA, starting from transcription to RNA decay (Cordin *et al.*, 2006; Fairman-Williams *et al.*, 2010). Some other notable examples of DNA-dependent SF2 helicases are PriA (SF2Aα, involved in replication restart; section 1.3.2) and RecG (SF2Aβ, branch migration; section 1.3.3) (McGlynn & Lloyd, 1999; Sandler, 2000). Some SF2 class enzymes, such as the transcription-coupled repair (TCR) factor Mfd only display translocase rather than helicase activity (SF2Aβ), by which Mfd can push stalled RNA polymerases from DNA (section 1.4.2) (Park *et al.*, 2002).
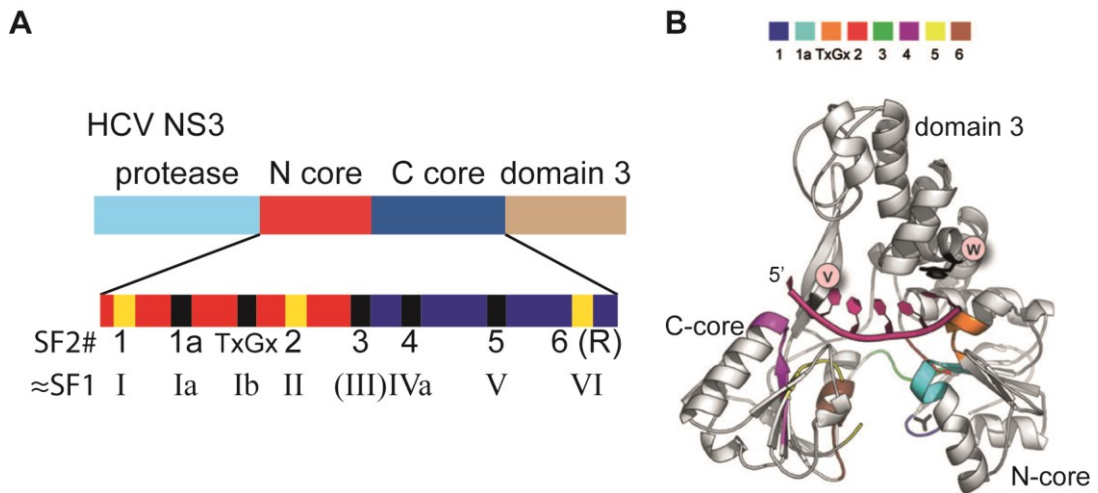
Figure 1.6 Conserved helicase domains of Superfamily 2 helicases
(A) Domain structure of a representative SF2 helicase, NS3. The positions of conserved SF2 helicase motifs in the N and C core are indicated and the corresponding SF1 helicase motifs are given. Motifs 3/III lack conservation of residues. (B) Crystal structure of NS3h in complex with a deoxyuridine substrate (PDB: 1A1V, (Kim *et al.*, 1998)). Note: the protease domain is lacking. Adapted from Singleton *et al.* (2007).

1.1.5 Hexameric helicases

Helicases of the remaining Superfamilies 3 to 6 are all active as hexamers that form toroidal quaternary structures. They bind a single strand of nucleic acid in their central channel and unwind the nucleic acid duplex by steric exclusion of the complementary strand (Enemark & Joshua-Tor, 2006; Kaplan, 2000). These helicases require hexamerisation to be active, because the motor cores do not oppose each other within a single monomer. Instead, hexameric helicases bind NTPs at the interface between two neighbouring helicase subunits of the hexameric ring. However, the mechanistic details how NTP hydrolysis between the six subunits is coordinated to result in nucleic acid translocation and duplex unwinding are still unknown and could also vary from helicase to helicase (Lyubimov *et al.*, 2011).

All hexameric helicases contain the Walker A and B motifs as well as a conserved arginine finger. Other helicase motifs are diagnostic for each different Superfamily (Figure 1.7).

Superfamily 4 helicases comprise replicative helicases from bacteriophages (e.g. T7 gene protein 4, T4 gp41) and prokaryotes, such as *E. coli* DnaB (see section 1.2) (Ilyina *et al.*, 1992). SF4 helicases from bacteriophages have additional N-terminal

primase domains (Figure 1.7B), while in prokaryotes the primase and helicase are separate entities. All SF4 helicases are type B helicases, translocating with 5' to 3' polarity (Singleton *et al.*, 2007). DnaB can also act as β type translocase and participate in branch migration *in vitro*, as it can accommodate two DNA strands in its central channel. However, evidence of DnaB translocating over duplex DNA has not been found *in vivo* (Kaplan, 2000; Kaplan & O'Donnell, 2002).
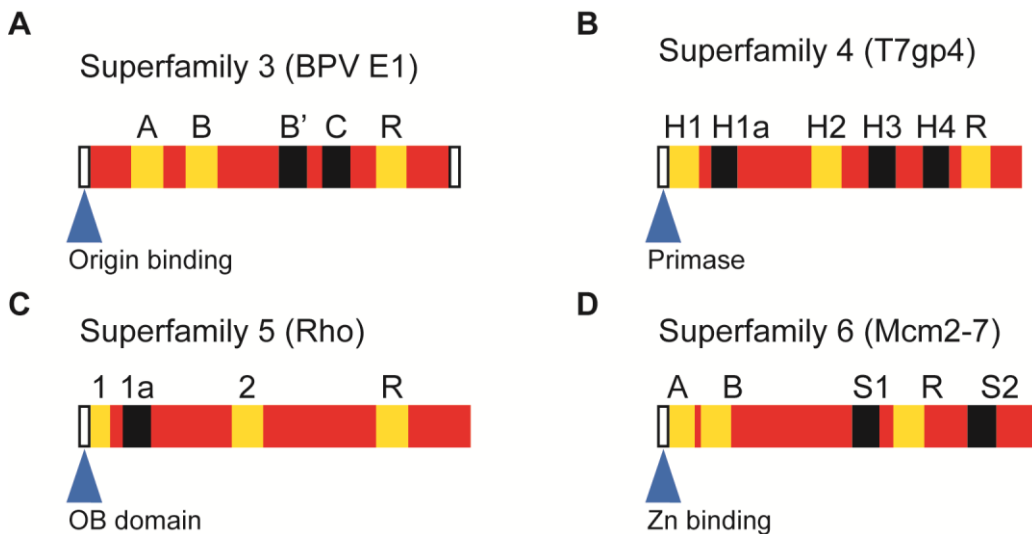
Figure 1.7 Conserved motifs of hexameric helicases
Conserved helicase motifs of (A) Superfamily 3, (B) Superfamily 4, (C) Superfamily 5 and (D) Superfamily 6 helicases with representative members in parentheses. The blue triangles indicate the location of accessory domains of the exemplary helicase. These vary between helicases of the same Superfamily. SF5 OB domain stands for oligosaccharide/oligonucleotide binding. Taken from Singleton *et al.* (2007).

Based on the DnaB crystal structure, ssDNA translocation and DNA unwinding was proposed to occur in a hand-over-hand mechanism via sequential NTP hydrolysis (Figure 1.8C) (Itsathitphaisarn *et al.*, 2012). The DnaB hexamer makes contacts with about 10 base pairs of ssDNA and forms a spiral staircase around the DNA (Figure 1.8C.i). NTP hydrolysis of the DnaB molecule furthest away from the fork junction disrupts the interface with the neighbouring DnaB monomer (Figure 1.8C.ii). The free subunit moves downwards towards the fork junction, resulting in the unwinding of two base pairs of DNA. In this position it can bind NTP with the newly adjacent DnaB molecule (Figure 1.8C.iii). Recurring NTP hydrolysis of the top subunit and NTP binding between subunits at the bottom of the staircase would result in unwinding of 2 base pairs per NTP hydrolysis event (Figure 1.8C.iv), similar

to the experimentally determined step size of 1.4 base pairs per ATP (Galletto *et al.*, 2004a).
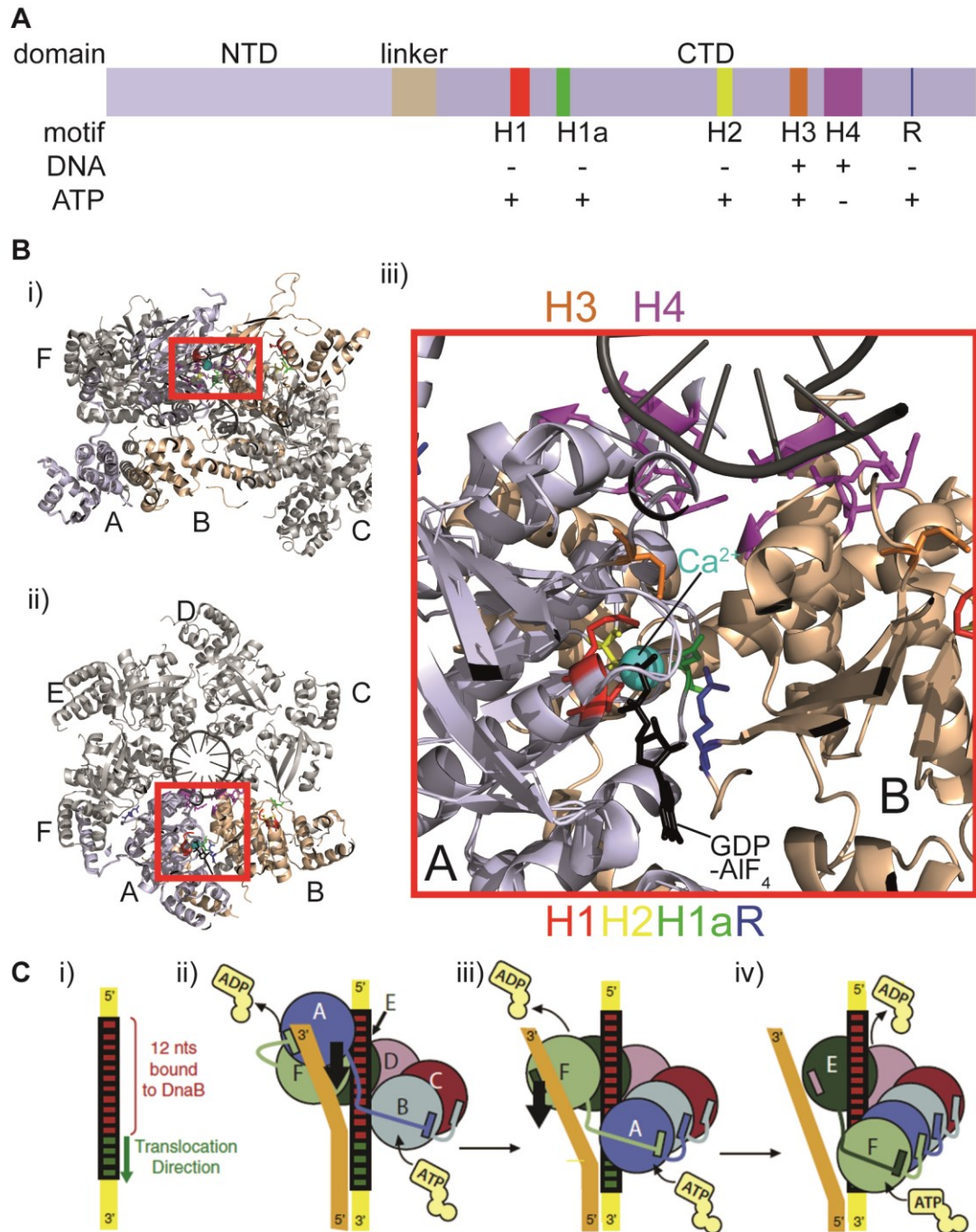
Figure 1.8 Helicase mechanism the hexameric Superfamily 4 helicase DnaB
(A) Positions of conserved helicase motifs of a hexameric SF4 helicase, DnaB from *B. stearothermophilus*. The positions may vary between different helicases. (B) (i) Side and (ii) top view of the of *Bst*DnaB hexamer encircling ssDNA molecule (PDB: 4ESV, (Itsathitphaisarn *et al.*, 2012)). Monomers are labelled A to F. (iii) Detailed view of the nucleoside (GDP-AlF4₄; black) and ssDNA (grey) contacts between DnaB monomers A (light blue) and B (wheat) in cartoon representation. Residues of helicase motifs that contact the ssDNA or the nucleoside are in stick representation. (C) Model of the hand-over-hand mechanism of DnaB hexamer translocation along ssDNA. Details in the text. Taken from Itsathitphaisarn *et al.* (2012).

1.2 DNA Replication

DNA replication is challenging given the vast amount of DNA that is present in a cell. Errors made during this process, although rare, cannot be completely prevented. Mistakes during DNA replication can be advantageous and are linked to evolution. On the other hand, a change, a partial loss or a duplication of the genetic material can be disastrous for the progeny, leading to reduced fitness or even lethality. DNA replication is therefore tightly controlled and several mechanisms have evolved to ensure a high fidelity of genome copying.

1.2.1 The initiation of DNA replication

Timely replication prior to cell division is ensured by controlling the initiation of DNA replication. In *E. coli*, the replication machinery is assembled at a single origin of replication, *oriC*, allowing bidirectional replication of the circular chromosome (Prescott & Kuempel, 1972). In order for DNA polymerases to gain access to the ssDNA strands, the duplex DNA must be separated.

Binding of the *oriC* region by the ATP-bound initiator protein DnaA and subsequent ATP hydrolysis leads to melting of the DNA duplex in the AT-rich DNA unwinding element (DUE), creating a ssDNA bubble (Figure 1.9A) (Bramhill & Kornberg, 1988; Hwang & Kornberg, 1992; Kowalski & Eddy, 1989). DnaA can then recruit and deposit two heterododecameric DnaB-DnaC complexes onto each strand of the melted DNA bubble (Figure 1.9B) (Kobori & Kornberg, 1982; Seitz *et al.*, 2000; Wickner & Hurwitz, 1975). This DnaA-DnaB-DnaC complex is called the pre-initiation complex.

DnaB is the main replicative helicase in *E. coli* and forms a hexameric ring encircling a single strand of DNA (Kaplan, 2000; LeBowitz & McMacken, 1986). DnaC is an accessory protein that binds to the DnaB C-terminus in 1:1 stoichiometry and is responsible for DnaB loading onto the ssDNA by acting as a "ring-breaker" (Arias-Palomo *et al.*, 2013; Galletto *et al.*, 2003). In complex with DnaC, DnaB adopts a conformation where the central channel on the N-terminal end of the helicase is

almost completely closed and DnaB is therefore unable to translocate along ssDNA (Barcena *et al.*, 2001).
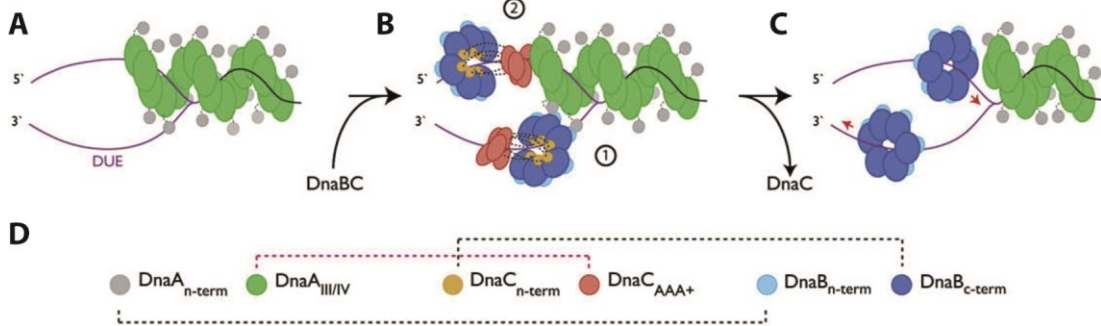
Figure 1.9 Formation of the pre-initiation complex
(A) ATP hydrolysis by DnaA.ATP multimers (green) assembled at *oriC* results in opening of the DNA at DUE. (B) DnaB-DnaC complexes (blue and red) are recruited to the ssDNA via (1) DnaA-DnaB interactions or via (2) DnaA-DnaC interactions. (C) DnaC dissociates from DnaB, allowing DnaB to translocate towards the dsDNA junction with 5' to 3' polarity. (D) Protein-protein interactions of the pre-initiation complex at *oriC*. Taken from Mott *et al.* (2008)

The principle of replication initiation is conserved in eukaryotes, with the origin recognition complex (ORC; similar to DnaA) binding to autonomous replication sequences (ARS; equivalent to *oriC*), which are scattered along the linear eukaryotic chromosomes (Bell & Stillman, 1992). Cdc6p and Cdt1p load the heterohexameric replicative helicase Mcm2-7 onto the ssDNA, forming the pre-replication complex (pre-RC) (Perkins & Diffley, 1998; Randell *et al.*, 2006).

1.2.2 The components of the replisome

In order to commence DNA unwinding and replication, DnaB translocation needs to be activated. ATP hydrolysis by DnaC, which is stimulated by DnaB and ssDNA leads to dissociation of DnaC from the helicase (Biswas *et al.*, 2004; Gupta *et al.*, 2010; Wahle *et al.*, 1989). This enables DnaB to translocate with 5' to 3' polarity along ssDNA towards the dsDNA junction of the initiation bubble (LeBowitz & McMacken, 1986). The primase DnaG is recruited to DnaB via an interaction between the DnaB N-terminus and the DnaG C-terminus. This positions DnaG away from the fork junction directly behind DnaB and allows DnaG to synthesise short RNA primers of

10 to 12 nucleotides (Bailey *et al.*, 2007; Chang & Marians, 2000; Yoda & Okazaki, 1991; Zechner *et al.*, 1992). These RNA primers recruit a DNA polymerase III holoenzyme on each ssDNA strand, from which DNA synthesis is initiated using the parental DNA strands as a template (Hiasa & Marians, 1994).
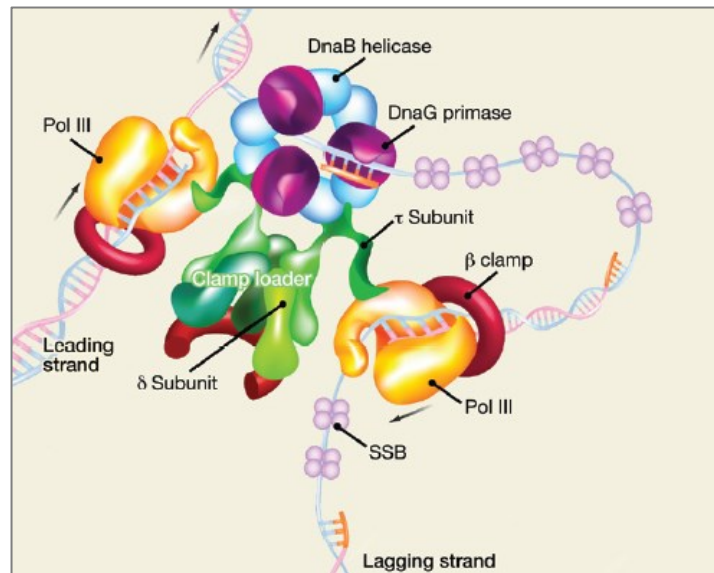
Figure 1.10 The components of the *E. coli* replisome
In the *E. coli* replisome, a hexamer of DnaB separates the DNA into a leading and a lagging strand template. On the leading strand template, DNA polymerase III copies the DNA continuously and its interaction with the DNA is ensured by the ß clamp. On the lagging strand template, the DnaG primase, which interacts with DnaB, synthesises short RNA primers every 1-2 kb. The DNA pol III extends the DNA from one RNA primer to the next and displaces single-strand binding protein (SSB), which prevent the formation of secondary structures in the ssDNA. This whole complex is orchestrated by interactions with the clamp loader. Taken from Yao & O'Donnell (2010). Note that a third Pol III complex has been shown to be associated with the clamp loader, which does is not bound to DNA and not depicted in this figure (Reyes-Lamothe *et al.*, 2010).

The DNA polymerase III holoenzyme is composed of ten different proteins and can be subdivided into three functional units: DNA polymerase III cores, the β clamp loading complex and the β clamp (Onrust *et al.*, 1995).

A polymerase core consisting of the subunits α, ε and θ is present on each arm of the replication fork. The α subunit is the DNA polymerase that synthesises DNA from a 3' OH group of the RNA primer with 5' to 3' polarity (Gefter *et al.*, 1971; Welch & McHenry, 1982). ε is the proofreading subunit that possesses 5' to 3' exonuclease activity to correct possible misincorporations of nucleotides. ε

proofreading activity is further stimulated by the θ subunit (Scheuermann & Echols, 1984; Studwell-Vaughan & O'Donnell, 1993).

Both DNA polymerases are coupled via the clamp loader complex, consisting of seven subunits ($\tau_3\delta\delta'\chi\psi$). The τ subunits each make contacts with DNA pol III and DnaB via their C-termini (Dallmann *et al.*, 2000). Thus, the DNA polymerase III holoenzyme can couple three DNA pol III core molecules (Reyes-Lamothe *et al.*, 2010). The clamp loader complex also interacts with the β clamp, which is a homodimer of the *dnaN* gene product. An interaction with the δ subunit opens the β clamp dimer and allows its loading onto DNA-RNA primer duplexes (Stewart *et al.*, 2001). The β clamp interacts with the DNA pol III core via an interaction with the α subunit and tethers the polymerase to the DNA (Kong *et al.*, 1992; O'Donnell *et al.*, 1992; Stukenberg *et al.*, 1991). Subunits χ and ψ stabilise the β clamp loader complex and interact with single-strand binding protein (SSB), which binds to ssDNA and prevents the formation of secondary DNA structures (Glover & McHenry, 1998; Olson *et al.*, 1995).

The principle of replication in eukaryotes is homologous to prokaryotes. The most notable difference in the context of this work is that the replicative helicase Mcm2-7, a heterohexamer, translocates along the leading strand template with 3' to 5' polarity (Fu *et al.*, 2011; Lee & Hurwitz, 2000; Moyer *et al.*, 2006), the opposite polarity to prokaryotic replicative helicases, such as *E. coli* DnaB.

1.2.3 Replication elongation and termination

Once the DNA polymerase III holoenzyme has been assembled, DNA synthesis commences from RNA primers, which are extended by the DNA pol III cores with 5' to 3' polarity (Hiasa & Marians, 1994). Due to the antiparallel nature of the DNA molecule, DNA is replicated in a semiconservative manner (Meselson & Stahl, 1958). Only one strand – the leading strand – can be synthesised continuously. The lagging strand template is re-primed every 1-2 kb, due to a cyclic interaction between DnaB and DnaG (Wu *et al.*, 1992). DNA synthesis then occurs from one primer to the next in short, so called Okazaki fragments (Okazaki *et al.*, 1968).

During DNA unwinding by DnaB, negative supercoiling of the *E. coli* chromosome is lost, while positive supercoiling of the DNA is induced ahead of the replication fork (Postow *et al.*, 2001). This poses torsional stress that can slow down and eventually halt replication fork progression. Hence, the accumulation of positive supercoiling needs to be actively counteracted. This is mediated by the type II topoisomerase DNA gyrase. In complex with ATP, DNA gyrase is able to relieve positive supercoiling by creating a transient dsDNA break. DNA gyrase then passes another intact DNA strand through the break before the DNA is resealed, thereby generating negative supercoiling in the chromosome (Brown & Cozzarelli, 1979; Gellert *et al.*, 1976; Gore *et al.*, 2006).

After bidirectional translocation of the replication forks away from *oriC*, DNA replication terminates at a site opposite to *oriC*. Replication fork movement past this region is prevented by binding of the termination utilisation substance (Tus) protein to *Ter* sites positioned on each chromosome arm, resulting in the formation of polar replication barriers (Figure 1.11) (Khatri *et al.*, 1989; Mulcair *et al.*, 2006). DNA replication therefore ceases opposite to *oriC*, where the replication forks ultimately converge (Louarn *et al.*, 1977).
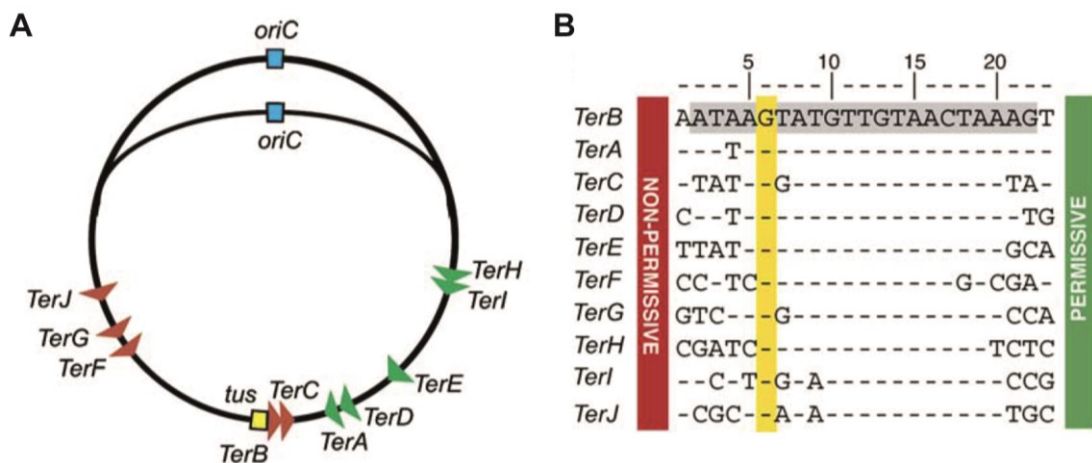
Figure 1.11 The *Ter* sites of the *E. coli* chromosome
(A) Replication forks translocate bidirectionally away from *oriC*. The left and right replication fork encounters the red and green *Ter* sites in the permissive orientation, respectively. Replication forks meet opposite to *oriC*. Translocation of replication forks past this region is prevented due to encounters with Tus-*Ter* complexes in the non-permissive orientation. (B) Consensus sequence of the ten *Ter* sites from *E. coli*. The conserved G-C (6), which is essential for blocking replication forks arriving from the non-permissive side, is shown in yellow. Taken from Mulcair *et al.* (2006).

1.2.4 High processivity and synthesis rates of the *E. coli* replisome

In order to replicate the whole *E. coli* chromosome with only two active replication forks within 40-50 minutes, each replisome needs to copy DNA at a rate of 1000 bp s^{-1} (Chandler *et al.*, 1975).

The DNA pol III core enzyme (αεθ) is able to synthesise DNA on a primed ssDNA template on its own. However, translocation speed and processivity are very low with approximately 15-20 nucleotides copied per binding event and a velocity of only 10 nt s^{-1} (Fay *et al.*, 1981; Maki *et al.*, 1985). Stabilisation of the polymerase on the DNA via the β clamp increases complementary polymerisation of DNA to a rate of 350-500 bp s^{-1} (Tanner *et al.*, 2008). Within the context of the replisome this rate is doubled, resulting in DNA synthesis rates of about 1000 bp s^{-1} (McHenry, 1988).

Similarly, DnaB displays very low DNA helicase activity of only 50 bp s^{-1} (passive helicase), while within the context of the replisome DnaB is able to unwind DNA at approximately 1000 bp s^{-1} (active helicase) (Galletto *et al.*, 2004a; LeBowitz & McMacken, 1986). The interaction of DnaB with DnaG is mutually stimulatory for the activity of both proteins. Nucleotide polymerisation by DnaG is enhanced 300-fold, while DNA helicase activity of DnaB is increased six-fold by the presence of primase and SSB (LeBowitz & McMacken, 1986; Tougu *et al.*, 1994). Additionally, the processivity of DNA replication is increased by the formation of the replisome, allowing for the synthesis of tens of thousands base pairs without dissociating (Naktinis *et al.*, 1995; Stano *et al.*, 2005; Stukenberg *et al.*, 1991). Formation of the replisome complex is therefore essential for fast rates of DNA replication and for rapid cell growth.

1.3 Replication fork processing and repair mechanisms

1.3.1 Excision repair

Excision repair pathways act at all times during cell growth to repair DNA damage (Lindahl, 1993; Lindahl, 1996). Excision repair is subdivided into base excision repair (BER) and nucleotide excision repair (NER).

BER repair pathway corrects single nucleotide changes, such as abasic sites, nicks a single strand of DNA and excises only a short stretch of DNA, which is subsequently filled by DNA polymerase I and sealed by DNA ligase (Doetsch & Cunningham, 1990).

NER repairs bulky lesions such as inter-strand crosslinks, protein-DNA crosslinks or pyrimidine dimers (Sancar & Sancar, 1988; Weiss & Grossman, 1987). Briefly, DNA damage recognition occurs via the UvrA-UvrB complex (Truglio *et al.*, 2004). During TCR, Mfd increases the recruitment of these dimers to sites of DNA damage (Selby & Sancar, 1993). UvrC can bind to the UvrA-UvrB dimer and nick the phosphate backbone of the damaged DNA strand close to the lesion (Verhoeven *et al.*, 2000). UvrD unwinds the nicked DNA creating a ssDNA gap that is filled by DNA polymerase I and sealed by DNA ligase (Orren *et al.*, 1992).

1.3.2   Replication fork reloading away from the origin

As mentioned above, loading of DnaB onto DNA is a highly regulated process. Replication initiation via DnaA-mediated loading of DnaB occurs only at *oriC*, while the presence of SSB on ssDNA inhibits DnaC-DnaB loading elsewhere on the chromosome (Xu & Marians, 2000). However, replication forks often stall at DNA lesions or nucleoprotein complexes, which can eventually lead to the dissociation of the replisome from the DNA. Reloading of the replisome onto the DNA is therefore essential to finish the DNA replication. In *E. coli* two pathways exist that facilitate reloading of the replisome onto structure-specific DNA substrates (Figure 1.12) (Heller & Marians, 2007; McGlynn *et al.*, 1997; Nurse *et al.*, 1999).

The first pathway involves the SF2 helicase PriA, which binds to DNA forks with a 3' OH of the leading strand close to the fork branch point (Lee & Marians, 1987; McGlynn *et al.*, 1997; Mizukoshi *et al.*, 2003). Hence, PriA can also recognise and restart replication from D-loop structures (a process called recombination-dependent replication) (McGlynn *et al.*, 1997; Mizukoshi *et al.*, 2003). Leading strand gaps that are more than five nucleotides away from the branch point greatly reduce the affinity of PriA for the substrate and consequently PriA-directed

replication fork reloading (Mizukoshi *et al.*, 2003). If necessary, PriA can unwind the lagging strand DNA to provide a ssDNA stretch that is sufficient in length for DnaB loading. PriA binding to a DNA substrate recruits DnaT. Another protein called PriB acts as an accessory factor by stabilising the PriA-DnaT interaction (Liu *et al.*, 1996; Ng & Marians, 1996). A DnaB-DnaC complex can subsequently bind the PriA-PriB-DnaT complex and initiate the assembly of a functional replisome (section 1.2.2) (Heller & Marians, 2005a; Liu & Marians, 1999; Liu *et al.*, 1996; Lopper *et al.*, 2007).
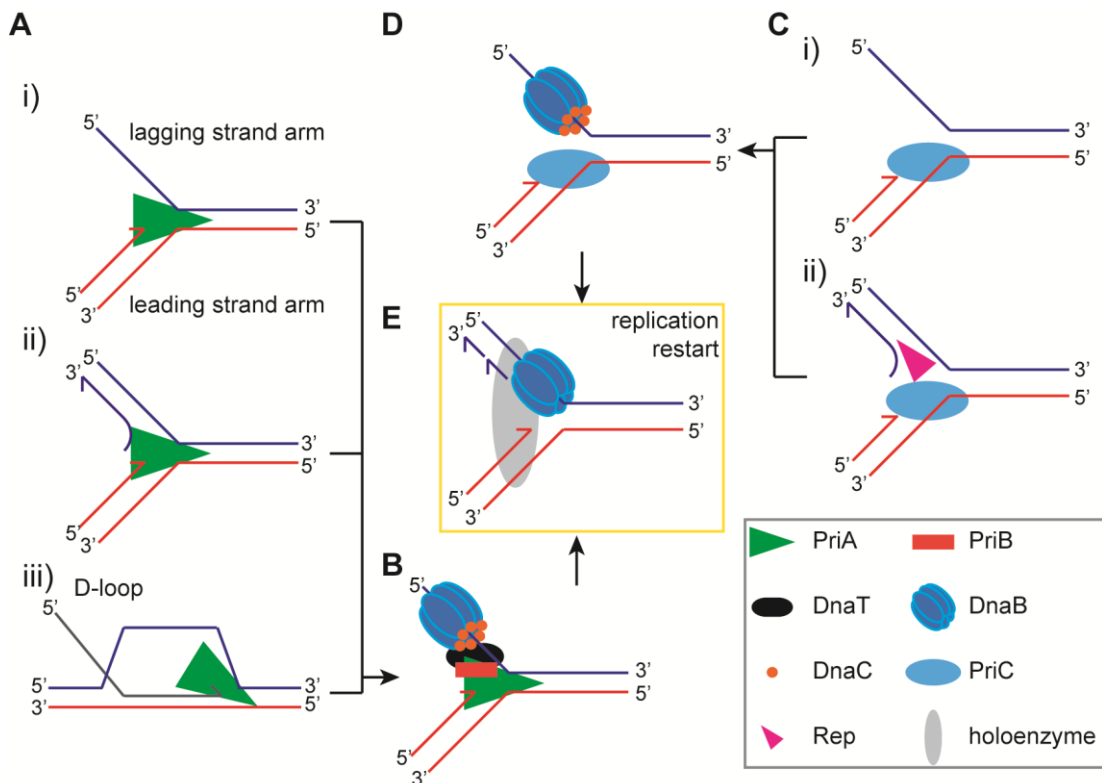
Figure 1.12 Replication fork reloading
(A) DNA structures that are recognised by PriA have a 3' OH group close to the branch point and can include D-loops. (B) PriA binding recruits PriB and DnaT, which facilitate DnaB-DnaC loading onto the lagging strand. (C) PriC binding to DNA structures requires a leading strand gap. Lagging strand DNA can be unwound by additional type A helicases, such as Rep or PriA. (D) PriC can mediate DnaB-DnaC loading without additional factors. (E) After DnaC dissociates, DnaB unwinding can start. DnaG can form a primer and initiate the formation of the DNA pol III holoenzyme, resulting in the formation of a functional replisome.

Alternatively, fork reloading can occur via PriC at fork structures with leading strand gaps of at least five base pairs (Heller & Marians, 2005a). PriC interacts with SSB and alters the SSB-ssDNA interaction, exposing ssDNA to deposit a DnaB-DnaC complex on the lagging strand directly (Wessel *et al.*, 2013). If a lagging strand gap is absent,

additional DNA unwinding by the 3'-5' helicases Rep or PriA is required to provide sufficient ssDNA for DnaB binding (Heller & Marians, 2007; Sandler, 2000; Sandler *et al.*, 2001).

Single mutants of either *priC* or *priA* are viable, although *priA* mutants show severe growth defects (Kogoma *et al.*, 1996; Lee & Kornberg, 1991; Nurse *et al.*, 1991; Sandler *et al.*, 1999). This reflects the larger scope of DNA substrates that are targeted by PriA and the role of PriA in recombination-dependent replication (section 1.3.5). *priA priC* as well as *priA rep* double mutants, which are inactivated for both replication fork reloading pathways, are synthetically lethal (Sandler & Marians, 2000), indicating that even in wild-type cells replisome reloading is a frequent and essential process .

1.3.3 Replication fork reversal

If the initial replication block that led to replication fork collapse is not removed, simple reloading of a replication fork via the PriA or PriC restart pathways will not necessarily result in successful replication. It is possible that additional attempts increase the likelihood of overcoming a certain replication block but this is not always the case (Payne *et al.*, 2006).

Collapsed replication forks can undergo replication fork reversal, a process that creates a four-way DNA molecule, called "chicken-foot structure" in which the two nascent DNA strands anneal (Figure 1.13) (Fujiwara & Tatsumi, 1976; Higgins *et al.*, 1976; Hotchkiss, 1974).
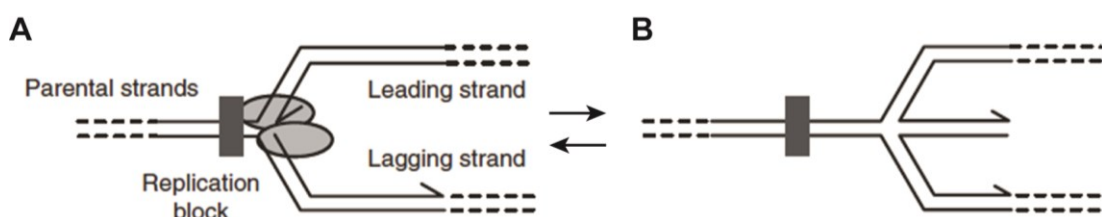
Figure 1.13 The principle of replication fork reversal
(A) Replication fork progression is blocked leading to the collapse of the replisome. (B) Reversal of the replication fork results in annealing of the nascent DNA strands creating four-way DNA structure. Taken from Atkinson and McGlynn (2009).

In case replication fork reversal generates a nascent ssDNA portion, a process called template switching can occur, where the undamaged nascent ssDNA strand is used as a DNA template to replicate the shorter nascent strand. Alternatively, replication fork reversal could promote the recruitment of repair enzymes by increasing the distance between the original replication block and the DNA fork. Exonucleolytic cleavage of the nascent duplex strand or branch migration of the chicken foot structure can generate a replication fork structure onto which a replisome can be loaded after bypass or removal of the block (Baharoglu *et al.*, 2008; Flores *et al.*, 2001; McGlynn & Lloyd, 2001; Michel *et al.*, 2004; Seigneur *et al.*, 1998).

1.3.4   Repair of ssDNA lesions by single-stranded gap repair

DNA replication can leave single-stranded DNA gaps (section 1.4.1), which need to be repaired and filled in, as otherwise a dsDNA break would be generated in the subsequent round of DNA replication (Kogoma *et al.*, 1996).

Repair of ssDNA gaps via RecA-mediated strand exchange can create base pairing with an intact homologous DNA strand that can be used as a template to remove the DNA lesion. RecA is the main strand exchange protein in *E. coli*. RecA is an ATPase that stably binds to ssDNA in a complex with ATP and forms filaments by multimerisation of RecA on the ssDNA in the 5' to 3' direction (Cox & Lehman, 1981; Cox *et al.*, 1983; West *et al.*, 1980). In the presence of SSB, RecA requires the mediator complex RecFOR for RecA loading on ssDNA (Cox & Lehman, 1982; Morimatsu & Kowalczykowski, 2003). The RecA filament can then invade and anneal to the complementary parental strand while displacing the non-complementary nascent strand, giving rise to another type of four-way DNA structure, called Holliday junction (Holliday, 1964). With the DNA lesion in the context of duplex DNA, excision repair pathways can now repair the lesion. Subsequent DNA replication of the remaining ssDNA gap restores integrity of the DNA duplex. The four-way DNA structure can then be resolved by branch migration or by cleavage of the Holliday junction (Iwasaki *et al.*, 1992; Iwasaki *et al.*, 1991; Parsons *et al.*, 1992). Cleavage of the Holliday junction can result in non-crossover or crossover products.

Ligation of the nicked DNA restores two intact DNA molecules and prevents problems in subsequent rounds of replication.
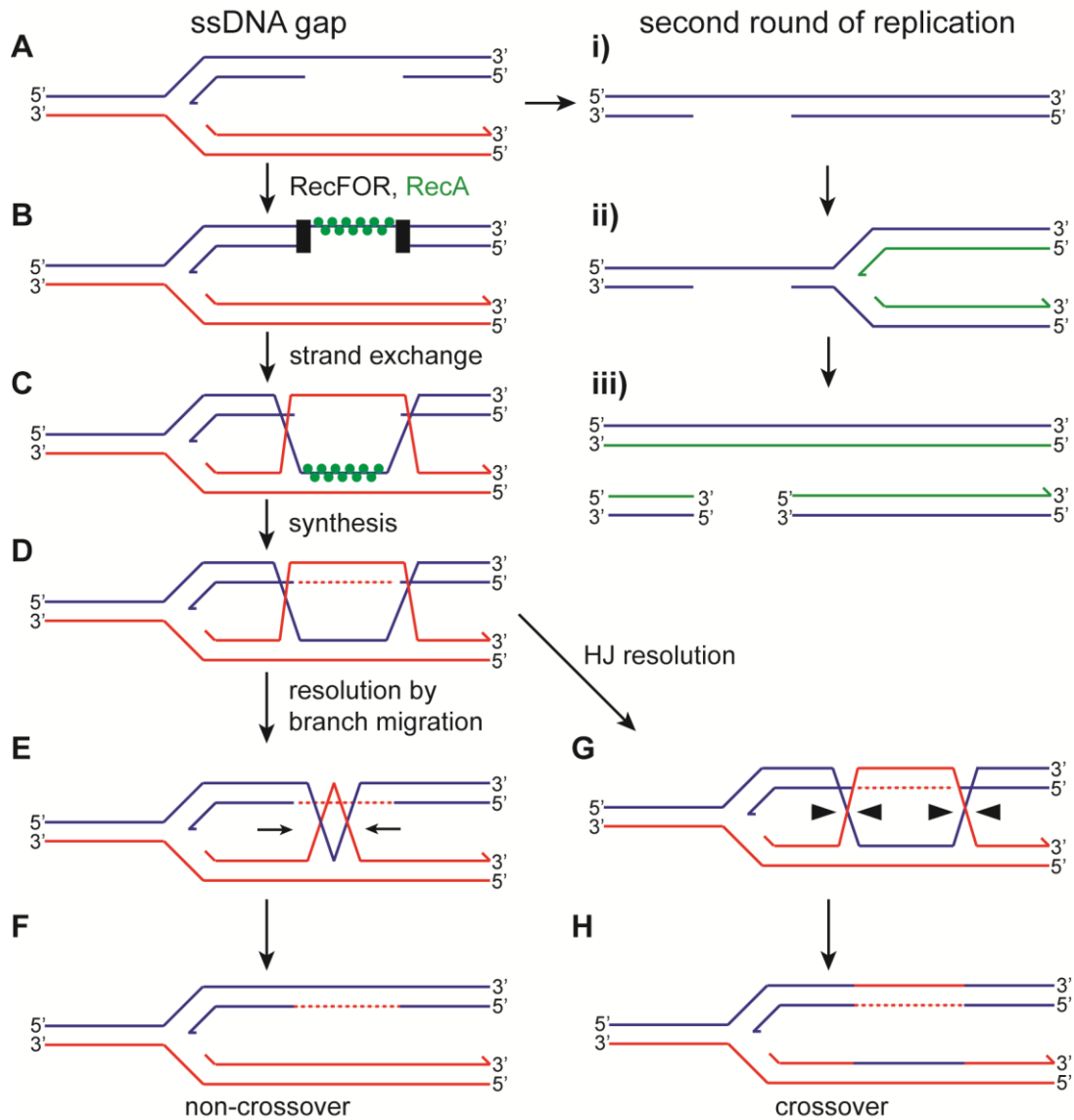
Figure 1.14 Single-strand gap repair
(A-D) A single stranded gap is repaired by RecFOR-mediated RecA loading onto ssDNA. Strand exchange provides complementary strand to fill the DNA gap. (E-F) Branch migration leads to non-crossover products, (G-H) while Holliday junction resolution via cleavage creates crossover products. (i-iii) A second round of replication on a gapped DNA template creates a dsDNA break, which requires further processing by recombination enzymes.

1.3.5 Double-strand break repair

Double-stranded DNA breaks can result from various sources. These include DNA damaging agents, irradiation or replication of gapped DNA (Figure 1.14i-iii) (Kogoma

et al., 1996). Additionally, double-strand breaks can be created during the repair of arrested replication forks (Michel *et al.*, 1997; Seigneur *et al.*, 1998). The inability to process such a DNA lesion is a lethal event.
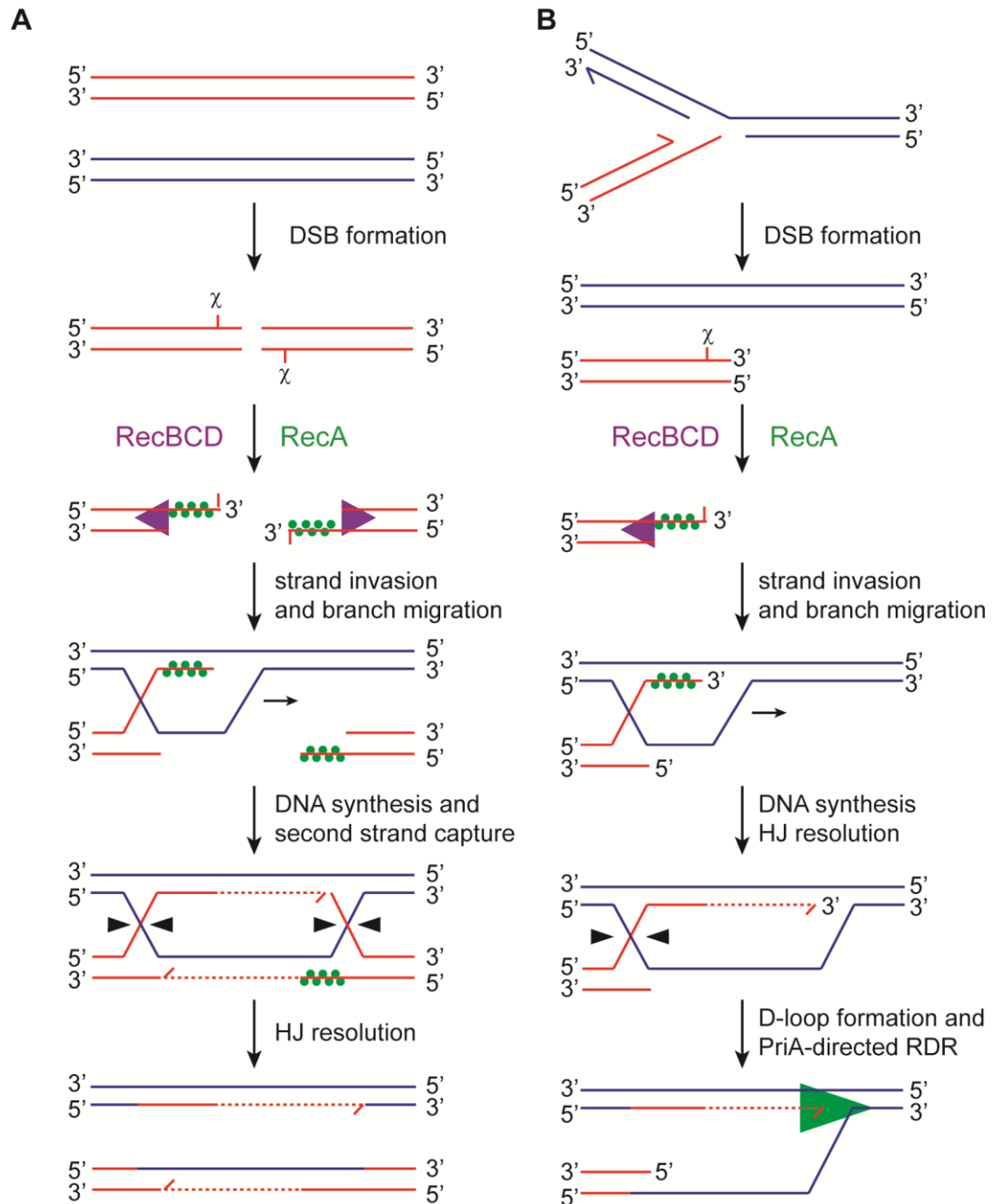
Figure 1.15 Double-strand break processing by RecBCD
(A) Recombination-dependent DSB repair. Two dsDNA ends processed by RecBCD and RecA loading onto the 3' ssDNA strand after the encounter of a χ sequence. The ssDNA-RecA filament performs homology search and strand invasion. The donor DNA serves as a template for DNA synthesis. After resolution of the structure two intact DNA strands have been produced. (B) Recombination-dependent replication. A single dsDNA end is processed by RecBCD. Strand invasion forms a D-loop structure that serves as a substrate for PriA-directed replication fork reloading. Adapted from Dillingham and Kowalczykowski (2008).

In *E. coli* the heterotrimeric helicase/nuclease complex RecBCD can bind and process dsDNA ends (Taylor & Smith, 1985). RecBCD has a bipolar motor activity with the SF1 helicases RecB and RecD translocating along the complementary DNA strands with 3'–5' and 5'–3' polarity, respectively (Boehmer & Emmerson, 1992; Dillingham *et al.*, 2003). During dsDNA unwinding the C-terminal nuclease domain of RecB cleaves both ssDNA strands. The RecC protein is an inactive nuclease that binds behind RecB and scans the incoming ssDNA for a specific nucleotide recognition sequence called crossover hotspot instigator (χ, 5'-GCTGGTGG-3') (Amundsen *et al.*, 2007). Upon recognition of this sequence, RecB nuclease activity is attenuated on the 3' ssDNA tail, while the 5' ssDNA tail is further degraded (Bianco & Kowalczykowski, 1997). A second conformational change in the complex by RecD results in RecA loading onto the 3' ssDNA tail (Amundsen *et al.*, 2000; Taylor *et al.*, 2014). Continuous DNA unwinding and RecA loading creates a long ssDNA-RecA filament which can perform homology search (Churchill *et al.*, 1999). Strand invasion and branch migration leads to the formation of a Holliday junction, where the complementary DNA sequences can be used as templates to fill in the ssDNA gaps. Resolution of the Holliday junction restores two intact duplex strands (Figure 1.15A) or a D-loop structure for recombination-dependent replication via replisome reloading by PriA (Figure 1.15B).

1.3.6   The interplay between recombination and genome stability

The repair of replication forks by recombination is an error-prone process that has been linked to genome instability. Recombination-dependent replication can be initiated at non-homologous sites downstream of the original lesion, allowing the cell to finish replication in the presence of an otherwise insuperable block. This process however leads to deletions between the block and the site of re-initiation that can affect cell viability if vital genetic information is lost (Ahn *et al.*, 2005; Lambert *et al.*, 2005; Payne *et al.*, 2006). Similarly, recombination at inverted repeats can result in the excision of DNA circles (Mizuno *et al.*, 2012).

Just as the initiation of replication is a highly regulated process, several control mechanisms therefore also underlie recombination and consequently recombination-dependent restart pathways.

Antirecombinases, such as *E. coli* UvrD, are enzymes that remove strand-exchange proteins from ssDNA thereby preventing the formation of D-loops (Krejci *et al.*, 2003; Simandlova *et al.*, 2013; Veaute *et al.*, 2005; Veaute *et al.*, 2003).

Additionally, R-loops have been implicated in genome instability as these structures are prone to cause double strand breaks (Helmrich *et al.*, 2013; Wahba *et al.*, 2011). The formation of R-loops is prevented by digestion of RNA by RNase HI or by the disruption of RNA-DNA hybrids via *E. coli* Rho, *S. cerevisiae* Sen1 or human Senataxin (Alzu *et al.*, 2012; Mischo *et al.*, 2011; Wahba *et al.*, 2011; Washburn & Gottesman, 2011).

Thus, recombination acts as a double-edged sword. On the one hand, recombination ensures cell survival via its role in processing of otherwise lethal DNA damage and replicative blocks. On the other hand, unrestricted recombination in itself can result in lethal genome rearrangements.

1.4 Blocks to replication fork progression

During DNA replication the replisome encounters various obstacles, such as DNA lesions or nucleoprotein complexes (French, 1992; Lindahl, 1993). In order to accurately complete genome duplication various mechanisms exist to overcome these blocks.

1.4.1 Single-stranded DNA lesions

Due to the nature of semicontinuous DNA replication, DNA lesions on the lagging strand are not considered to impede replication fork progression as long as DNA unwinding by the replicative helicase is not obstructed (McInerney & O'Donnell,

2004; Nelson & Benkovic, 2010). Replication can simply proceed from the next primer leaving a short ssDNA gap, which can be filled in by ssDNA gap repair (section 1.3.4). In contrast, a leading strand lesion uncouples leading strand synthesis from DNA unwinding and lagging strand synthesis (Pages & Fuchs, 2003). Re-priming can occur downstream of a DNA lesion in the leading strand and DNA replication can therefore continue via the original replisome (Figure 1.16A) (Yeeles & Marians, 2011). Alternatively, leading strand lesions can lead to the dissociation of the replisome, requiring replication fork processing and replication fork reloading (Figure 1.16B) (section 1.3.2) (Heller & Marians, 2006). In both scenarios, bypass of the lesion allows DNA replication to finish without major delays but leaves a ssDNA gap that needs to be repaired to prevent DNA damage in subsequent rounds of replication (section 1.3.4).
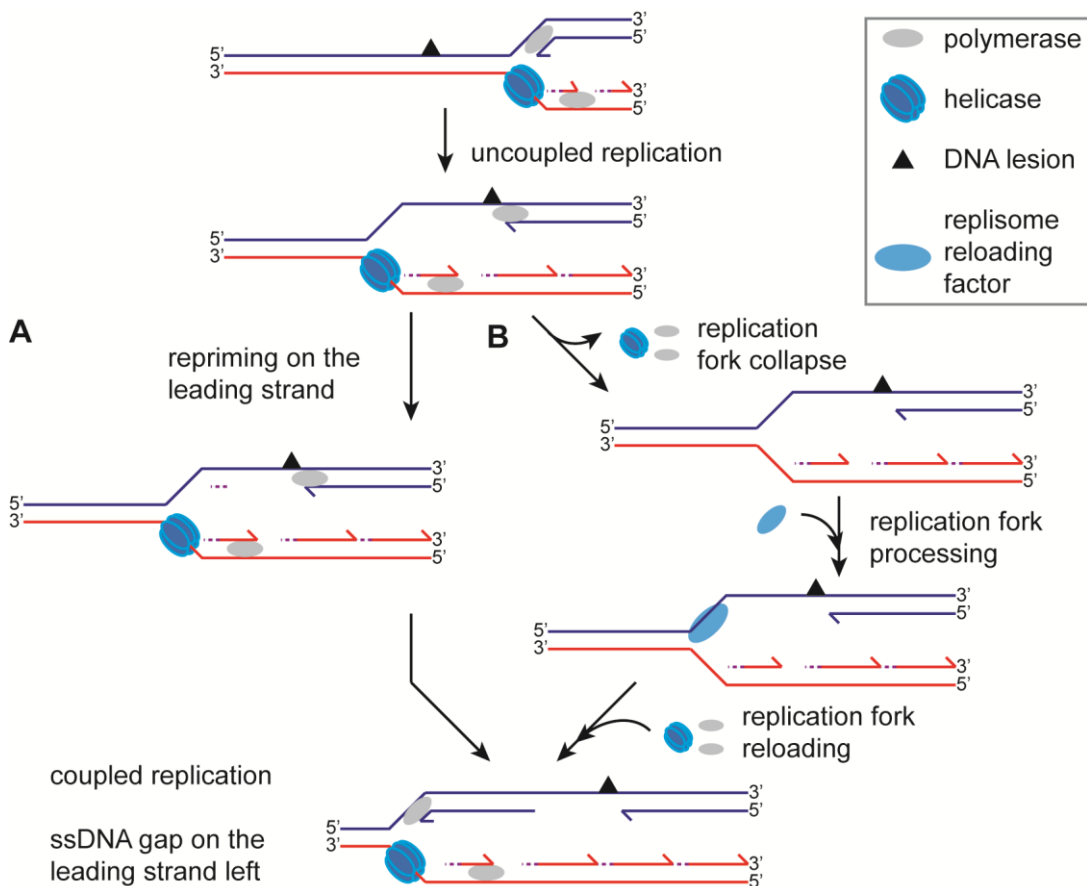
Figure 1.16 Bypass of a leading strand lesion
DNA replication of the leading strand is blocked by a DNA lesion, leading to uncoupling of DNA replication. (A) Re-priming by DnaG (indicated as a purple dotted line) can occur on the leading strand downstream of the lesion, allowing the replisome to resume replication. (B) The replisome dissociates from the fork requiring replisome reloading to continue replication. The outcome in both scenarios is a ssDNA gap on the leading strand. Adapted from Yeeles *et al.* (2013).

1.4.2 Replication/transcription conflicts

The DNA is coated in protein complexes *in vivo* (Ali Azam *et al.*, 1999; Wang *et al.*, 2011). Thus, DNA replication frequently encounters dsDNA blocks, such as nucleoprotein complexes, which are the main sources of replication fork pausing in *E. coli* (Gupta *et al.*, 2013). Extended replication fork pausing can lead to loss of function of the replisome *in vitro* (Marians *et al.*, 1998; McGlynn & Guy, 2008). Since replication fork collapse can result in recombinogenic substrates that can have deleterious effects on cell viability *in vivo* (section 1.3.6), it is essential to minimise the frequency of dsDNA blocks.

Transcription complexes in particular are a potent threat to genome stability *in vivo* (Merrikh *et al.*, 2011; Prado & Aguilera, 2005). Conflicts between transcription and replication are unavoidable, simply given the approximately ten-fold faster translocation rate of the replisome compared to RNA polymerases and result in the reduction of replication speed (Figure 1.17A) (Brewer, 1988; Liu & Alberts, 1995). Furthermore, encounters between both complexes in a head-on fashion lead to the accumulation of positive supercoiling between the replisome and the RNA polymerase, which can stall replication fork movement (Figure 1.17B) (Elias-Arnanz & Salas, 1999; French, 1992; Liu & Alberts, 1995). Consequently, head-on conflicts are thought to be more detrimental for cells (Boubakri *et al.*, 2010; Prado & Aguilera, 2005). Highly transcribed genes, such as the rDNA loci, are therefore usually transcribed co-directionally with respect to replication fork movement (Paul *et al.*, 2013; Rocha, 2004; Srivatsan *et al.*, 2010).
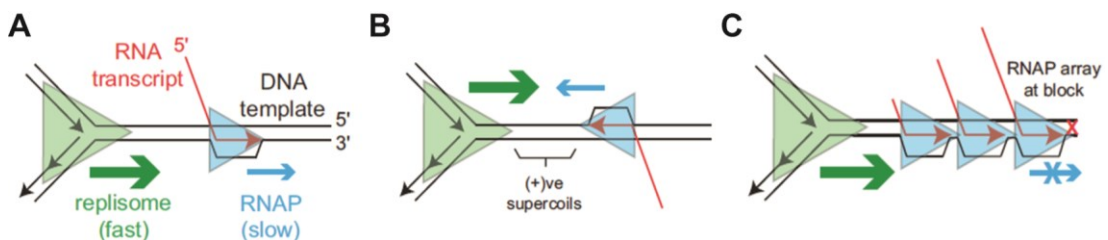
Figure 1.17 Replication/transcription conflicts
(A) Co-directional encounters between the replication fork and transcription complexes slow down replication forks because of their different speeds. (B) Head-on collisions between the replisome and RNA polymerases lead to the accumulation positive supercoiling between the complexes. (C) A single stalled RNA polymerase can lead to the accumulation of additional RNA polymerases. Taken from McGlynn *et al.* (2012).

RNA polymerases can stall at DNA lesions or they can backtrack on the DNA template *in vivo* (Selby *et al.*, 1997; Tornaletti, 2005; Tornaletti *et al.*, 2006). In backtracked RNA polymerases, the 3' OH of the mRNA transcript is not present at the active site anymore and the RNA polymerase is in a highly stable but inactive state (Komissarova & Kashlev, 1997). Although the replisome is able to displace a single RNA polymerase block (Pomerantz & O'Donnell, 2010), stalling of an RNA polymerase in a highly transcribed gene is thought to cause an accumulation of trailing RNA polymerases that form a complete block to replisome progression (Figure 1.17C) (Trautinger *et al.*, 2005).

Wild-type cells actively reduce the number of stalled RNA polymerase complexes on DNA. The anti-backtracking factors GreA and GreB can cleave the extruding 3' end of the mRNA of a backtracked RNA polymerase, thereby restoring a 3' OH group at the active site and allowing the continuation of transcription (Orlova *et al.*, 1995). The SF5 translocase Rho actively terminates transcription and can also remove stalled RNA polymerase from the DNA (Dutta *et al.*, 2011; Washburn & Gottesman, 2011). The SF2 translocase Mfd, which interacts with RNA polymerase, can "push" stalled RNA polymerases off the DNA (Park *et al.*, 2002). Mfd additionally functions in TCR by coupling the displacement of RNA polymerases to the recruitment of the enzymes of the NER pathway via an interaction with UvrA (section 1.3.1). This enhances the repair of a DNA lesion and prevents further stalling of other RNA polymerases at the same site of DNA damage (Selby & Sancar, 1993).

1.5 Accessory replicative helicases and the displacement of nucleoprotein blocks

Accessory replicative helicases safeguard genome stability by reducing the levels of replication fork breakdown caused by nucleoprotein complexes, allowing the original replisome to continue genome duplication. DNA unwinding by the replicative helicase DnaB is inhibited by a repressor-operator complex, whereas this block does not obstruct DNA unwinding by the SF1A helicase Rep (Yancey-Wrona & Matson, 1992). This observation initially suggested that DNA replication could be

assisted by additional helicases. Since then it has been shown that the helicase Rep can directly promote replication fork movement through a nucleoprotein complex that otherwise completely blocks DnaB-driven fork progression *in vitro* (Guy *et al.*, 2009).

Cells that lack Rep are viable but show a reduction in the speed of replication fork progression, which is suggestive of increased replication fork stalling *in vivo* (Lane & Denhardt, 1975). Indeed, overexpression of a helicase that targets and inactivates only stalled but not actively translocating replication forks is lethal in a *rep* mutant but not in wild-type cells (Gupta *et al.*, 2013). Similarly, Rep is essential in cells that contain an inversion of a highly transcribed operon, which increases the levels of head-on collisions between the replication fork and transcription complexes (Boubakri *et al.*, 2010).

E. coli cells possess a second homologous helicase, UvrD that can act as an accessory replicative helicase *in vitro* (Guy *et al.*, 2009). Single mutants of *rep* or *uvrD* are viable, whereas the double mutant is synthetically lethal under fast growth conditions (Guy *et al.*, 2009; Taucher-Scholz *et al.*, 1983). The lethality can be relieved by either a reduction of the growth rate or by additional mutations that destabilise the interaction of RNA polymerase with DNA, suggesting that accessory replicative helicases are required to underpin replication fork movement through nucleoprotein blocks, especially RNA polymerases *in vivo* (Guy *et al.*, 2009).

In the absence of *rep*, cells depend on the helicase activity of RecBCD, as indicated by a synthetic lethality between *rep* and *recB* or *recC*. However, a *rep recD* mutant, lacking only RecBCD exonuclease activity can still function in homologous recombination and is therefore viable (Uzest *et al.*, 1995). The *rep recB* and *rep recC* lethality is suppressed by additional mutations in *ruvABC*, as these mutations prevent the generation of dsDNA breaks from the resolution of regressed forks and Holliday junctions (Seigneur *et al.*, 1998). It was therefore concluded that Rep is required to reduce the amounts of replication fork breakdown.

A similar function has been observed for the *S. cerevisiae* helicase Rrm3. In the absence of Rrm3, replication fork movement is retarded (Azvolinsky *et al.*, 2006; Ivessa *et al.*, 2002). Stalling of the replisome occurs at various non-histone protein

complexes, such as rDNA, tRNA genes, replication fork barriers, telomeres and inactive or late-firing replication origins (Azvolinsky *et al.*, 2006; Azvolinsky *et al.*, 2009; Ivessa *et al.*, 2003). Thus, Rrm3 is required to assist replication fork movement through nucleoprotein complexes.

Pfh1, a homologue of Rrm3, has been identified to function as an accessory replicative helicase in *S. pombe*. Pfh1 is required to reduce fork stalling at highly transcribed RNAPII genes, especially when transcription occurs in a head-on direction with respect to replication (Sabouri *et al.*, 2012). Pfh1 depletion results in increased levels of genome instability and the survival of these cells is dependent on mechanisms that stabilise stalled replication forks (Pinter *et al.*, 2008; Steinacher *et al.*, 2012).

1.5.1 Polarity

Rep, UvrD, Rrm3 and Pfh1 are all Superfamily 1 helicases that bind and translocate along ssDNA. However, the prokaryotic accessory replicative helicases are SF1A helicases, translocating with 3' to 5' polarity, while the eukaryotic counterparts Rrm3 and Pfh1 translocate with 5' to 3' polarity (Ivessa *et al.*, 2002; Matson, 1986; Tanaka *et al.*, 2002; Yarranton & Gefter, 1979). The opposite polarities of accessory replicative helicases in pro- and eukaryotes are also reflected in opposing polarities of the respective main replicative helicases. The prokaryotic replicative helicase DnaB translocates along the lagging strand template with 5' to 3' polarity (LeBowitz & McMacken, 1986). On the other hand, eukaryotic Mcm2-7 translocates along the leading strand template with 3' to 5' polarity (Fu *et al.*, 2011; Lee & Hurwitz, 2000; Moyer *et al.*, 2006). This suggests that translocation on the ssDNA arm that is not bound by the replicative helicase at the replication fork might be a conserved feature of accessory replicative helicases (Figure 1.18) (Guy *et al.*, 2009).

The SF1A helicase PcrA from Gram-positive bacteria can complement the lethality of *Δrep ΔuvrD* strains *in vivo* and promote fork movement of a reconstituted *E. coli* replisome along protein-bound DNA *in vitro*, in accordance with the 3'-5' polarity of PcrA. On the other hand, the helicases T4 Dda and *D. radiodurans* RecD2 that

translocate with the same polarity as the replicative helicase DnaB (5'–3') do not restore growth in a *Δrep ΔuvrD* mutant and cannot promote fork movement along protein-bound DNA *in vitro* (Guy *et al.*, 2009), despite the fact that Dda is able to remove various protein blocks, including transcribing RNA polymerases, from DNA *in vitro* (Bedinger *et al.*, 1983; Byrd & Raney, 2006; Yancey-Wrona & Matson, 1992). These data all support the hypothesis that primary and accessory replicative helicases translocate along different template strands at the fork.
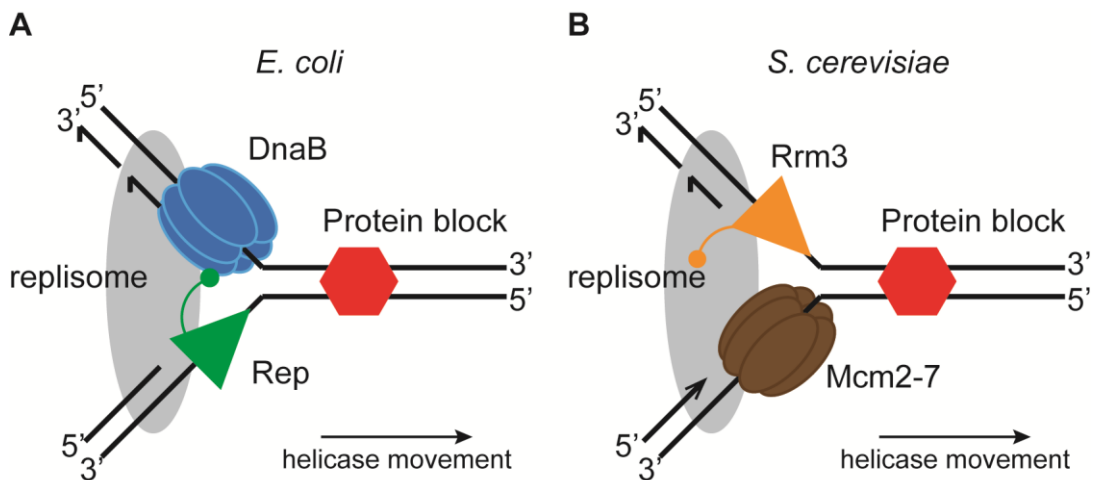
Figure 1.18 Complementary translocation polarities by replicative and accessory replicative helicases at the replication fork
(A) In *E. coli* and other prokaryotes the replicative helicase DnaB (blue) translocates with 5'-3' polarity along the lagging strand template. A SF1A helicase, acting as accessory replicative helicase (Rep in *E. coli*; green), translocates with 3'-5' polarity along the leading strand template. Thus, both helicases translocate towards the fork junction with Rep assisting in the displacement of protein blocks (red). (B) Replicative (Mcm2-7; brown) and accessory replicative helicase (SF1B helicase Rrm3 in *S. cerevisiae*; orange) occupy the opposite strands than their prokaryotic counterparts. Replisome movement is driven towards the protein block by both helicases.

1.5.2 Accessory subdomains

All helicase motifs of Superfamily 1 helicases are found in the motor core domains 1A and 2A. On the other hand, the exact function of the accessory subdomains is still unknown. In particular, the role of the 2B subdomain in SF1A helicases is unclear. In the crystal structures of UvrD and PcrA, the 2B subdomain makes contact with dsDNA, which led to the conclusion that the 2B subdomain plays a role in DNA unwinding (Lee & Yang, 2006; Velankar *et al.*, 1999). However, a Rep mutant that lacks the 2B subdomain is not only a functional helicase but even displays

higher rates of DNA unwinding than the wild-type helicase, suggesting that the 2B subdomain is dispensable for DNA unwinding (Cheng *et al.*, 2002).

The effect of DNA-bound proteins on unwinding by SF1A helicases shows different degrees of efficiency. DNA unwinding by HelD, which lacks a 2B subdomain, is largely inhibited, whereas Rep and UvrD are more or less unaffected by the same protein-DNA block (Dillingham, 2011; Yancey-Wrona & Matson, 1992). Thus, the 2B subdomain in SF1A helicases could play a role in nucleoprotein displacement by these helicases.

1.5.3 Localisation

Rep and Rrm3 interact directly with the replisome. Rep binds to DnaB via the Rep C-terminus, while Rrm3 binds to the catalytic subunit Pol2p of the leading strand polymerase and/or to the sliding clamp PCNA (Azvolinsky *et al.*, 2006; Guy *et al.*, 2009; Schmidt *et al.*, 2002). However, it is unclear when these accessory replicative helicases are recruited to the replisome. The interaction of DnaC with DnaB that is required for replication initiation is inhibitory for Rep binding to DnaB. The relatively high affinity for Rep to DnaB could however enable a continuous association of Rep with the replication fork to occur away from sites of replication (re)initiation (Guy *et al.*, 2009). However, DNA unwinding by Rep is much slower compared to the replisome (Cheng *et al.*, 2001; Yao *et al.*, 2009). Rep could therefore simply translocate along ssDNA formed by the replisome at the fork, since Rep translocation along ssDNA occurs at a speed similar to that of the progressing replication fork (Brendza *et al.*, 2005; Yao *et al.*, 2009). However, DNA unwinding by Rep can be stimulated by protein-protein interactions (Yancey & Matson, 1991). It was shown that Rep and DnaB display cooperativity in DNA unwinding (Atkinson *et al.*, 2011a; Guy *et al.*, 2009). Thus, the interaction of Rep with DnaB could stimulate Rep helicase activity to actively participate in replication fork movement.

Similarly, Rrm3 is excluded from the pre-RC complex but Rrm3 generally associates with translocating replication forks during S-phase and is further enriched at sites of persistent replisome stalling (Azvolinsky *et al.*, 2006), suggesting that reduced

replication fork movement facilitates Rrm3 recruitment to the replisome. However, increased levels of Rrm3 at stalled replication forks could simply be a reflection of an accumulation of replication forks at such sites in general.

UvrD can complement for the absence of Rep and act as an accessory replicative helicase by the virtue of the high intracellular concentration of UvrD (Guy *et al.*, 2009). Rather than interacting with components of the replisome, UvrD interacts with RNA polymerase and might therefore act more distributively across the chromosome (Epshtein *et al.*, 2014; Gwynn *et al.*, 2013; Noirot-Gros *et al.*, 2002). Since Rep is only present in γ-proteobacteria, accessory replicative helicase function could be supplied by UvrD homologues in bacteria that only contain a single UvrD-like helicase. As PcrA in *Bacillus* also interacts with RNA polymerases (Gwynn *et al.*, 2013), the localisation of helicases to sites of frequent replisome stalling rather than the replisome itself might be a common feature of accessory replicative helicases. Association directly with the replisome however seems to provide a more efficient mechanism of replication fork progression, which is reflected by the higher efficiency of plasmid-encoded Rep compared to UvrD to restore growth to *Δrep ΔuvrD* mutants (Guy *et al.*, 2009). This is likely due to the fact that replication blocks that are not associated with transcription can also be efficiently targeted by Rep but not UvrD.

Thus, accessory replicative helicases are Superfamily 1 helicases that translocate with a polarity opposite that of their respective replicative helicases and underpin replication fork movement through hard-to-replicate sites.

1.6 Aims and objectives

The overall aim of this work was to investigate how Rep functions as an accessory replicative helicase to underpin replication fork movement along protein-bound DNA.

The objectives are:

1) to further characterise the interaction between Rep and DnaB to identify potential residues in DnaB that are critical for this interaction.
2) to characterise the role of the 2B subdomain for Rep function.
3) to investigate the importance of conformational flexibility between the subdomains of Rep with respect to accessory helicase function.

Chapter 2

MATERIALS AND METHODS

Chapter 2 – Materials and Methods

2.1 Materials and Suppliers

All chemicals, unless stated otherwise, were purchased from Sigma-Aldrich, VWR-BDH, Fisher Scientific or Melford. Media ingredients and materials used for nucleic acid manipulations can be found in Appendix A.1.

2.2 Growth Media

2.2.1 Lysogeny broth (LB) and agar

Lysogeny broth (LB) (Bertani, 1951) for rich growth conditions was prepared in deionised water (dH_2O) containing 5 g l^{-1} NaCl, 5 g l^{-1} yeast extract and 10 g l^{-1} tryptone. The pH was adjusted to 7.0 with 5 M NaOH. For LB agar, 18 g l^{-1} agar was added to LB. LB and LB agar were autoclaved and cooled before the addition of any supplements.

LB containing only 0.5 g l^{-1} NaCl ("LB$^{0.5}$") was used for P1 transductions (section 2.5.10.2) and in plasmid loss assays (section 2.7.2).

2.2.2 Minimal Medium (MM)

56 salts was prepared in dH_2O with the following ingredients before autoclaving.

Table 2.1 Composition of 56 salts

Chemical	Amount per litre
KH_2PO_4	5.28 g
$Na_2HPO_4 \times 12 \ H_2O$	8.68 g
$(NH_4)_2SO_4$	2 g
10% $Ca(NO_3)_2$	2 ml
1% $MgSO_4$	1 ml
1% $FeSO_4$	50 µl

For liquid minimal medium (MM), 56 salts was diluted in an equal volume of autoclaved dH_2O and supplemented with glucose (0.32% w/v) and thiamine (vitamin B1; 0.1% w/v) as well as additional antibiotic or supplement when necessary.

Minimal agar (MA) was prepared by mixing 56 salts with and equal volume of autoclaved agar (30 g l^{-1} in dH_2O).

2.2.3 F medium

Overexpression of His-tagged Rep variants was performed in autoclaved F medium containing 14 g l^{-1} yeast extract, 8 g l^{-1} tryptone, 12 g l^{-1} KH_2PO_4 and 1.2 g l^{-1} K_2HPO_4 (Kim & McHenry, 1996).

2.2.4 Antibiotics and Supplements

All antibiotics used, including their stock and final concentrations can be found in Table 2.2. Antibiotics were prepared in dH_2O and filter-sterilised using a 0.22 µm pore filter. All antibiotic stock solutions were stored at -20°C.

Table 2.2 Antibiotics used in this study

Antibiotic	Stock concentration (mg ml^{-1})	Final concentration (µg ml^{-1})
Ampicillin (Ap)	100	50 or 100
Carbenicillin (Cb)	100	50
Kanamycin (Kn)	80	30

All media supplements used, including their stock and final concentrations can be found in Table 2.3. Supplements dissolved in water were filtered through a 0.22 µm pore sterile filter.

Table 2.3 Media supplements used in this study

Supplement	Stock concentration	Solvent	Final concentration	Storage
Arabinose	20% (w/v)	dH_2O	0.2% (w/v)	RT°C
Calcium Chloride (CaCl$_2$)	0.5 M	dH_2O	5 mM	RT°C
Glucose	20% (w/v)	dH_2O	0.2% (w/v)	RT°C
Isopropyl β-D-1-thiogalactopyranoside (IPTG)	1 M	dH_2O	1 mM	-20°C
Sodium citrate	1 M	dH_2O	2.5 mM	RT°C
5-bromo-4-chloro-3-indolyl-β-D-galactopyranoside (X-Gal)	20 mg ml^{-1}	DMSO	120 µg ml^{-1}	-20°C

2.2.5 Growth Conditions

E. coli strains were stored at -80°C in LB with 30% glycerol (v/v) as a cryoprotectant and streaked out onto LB agar containing the appropriate antibiotics. Liquid growth was achieved in 10 ml LB with the appropriate antibiotics at 37°C and shaking at 220 rpm for 16 h, unless stated otherwise. Temperature sensitive strains were grown at their permissive temperature, 30°C.

2.3   Bacterial strains used in this study

Table 2.4 List of all *E. coli* strains used in this work

Strain name	Genotype	Source
a) General strains		
AB1157	*thr-1, ara-14, leuB6, Δ(gpt-proA)62, lacY1, tsx-33, supE44, galK2, rac⁻, hisG4(Oc), rfbD1, mgl-51, rpsL31, kdgK51, xyl-5, mtl-1, argE3 (Oc), thi-1, qsr⁻*	(Bachmann, 1996)
BL21 AI	*F⁻ ompT gal dcm lon hsdS$_B$(r$_B$⁻ m$_B$⁻) araB::T7RNAP-tetA*	Invitrogen
DH5α	*F⁻ endA1 glnV44 thi-1 recA1 relA1 gyrA96 deoR nupG Φ80dlacZΔM15 Δ(lacZYA-argF)U169, hsdR17(r$_K$⁻ m$_K$⁺), λ−*	(Hanahan, 1983)
HB222	BL21 AI Δ*rep::cat*	H. Bell, unpublished
MG1655	*F⁻ rph-1*	(Guyer *et al.*, 1981)
STL1324	AB1157 *lacZ::bla⁺ tetAdup787 dnaB107ᵗˢ malE::*Tn*10kan*	(Saveson & Lovett, 1997)
TB28	MG1655 Δ*lacIZYA::<>*	(Bernhardt & de Boer, 2004)
b) TB28 derivatives		
AM2158	MG1655 Δ*lacIZYA::<> rpoB G1260D*	(Trautinger & Lloyd, 2002)
HB278	MG1655 Δ*lacIZYA::<>* Δ*rep::cat rpoB G1260D*	(Gupta *et al.*, 2013)
JGB045	MG1655 Δ*lacIZYA::<> dnaB107ᵗˢ malE::*Tn*10kan*	TB28 x P1.STL1324 to Knʳ
JGB070	MG1655 Δ*lacIZYA::<> dnaB107ᵗˢ malE::*Tn*10kan /* pAM403 *(lac⁺ rep⁺)*	JGB045 x pAM403 to Apʳ
JGB103	MG1655 Δ*lacIZYA::<>* Δ*rep::cat dnaB107ᵗˢ malE::*Tn*10kan /* pAM403 *(lac⁺ rep⁺)*	JGB070 x P1.N6577 to Knʳ
N5925	MG1655 Δ*lacIZYA::<> rpoB*35*	(Guy *et al.*, 2009)
N6524	MG1655 Δ*lacIZYA::<>* pAM403 *(lac⁺ rep⁺)*	(Guy *et al.*, 2009)

Table 2.4 continued

Strain name	Genotype	Source
N6540	MG1655 Δ*lacIZYA::<>* Δ*rep::cat* / pAM403 *(lac⁺ rep⁺)*	(Guy *et al.*, 2009)
N6556	MG1655 Δ*lacIZYA::<>* Δ*rep::cat* Δ*uvrD::dhfr* / pAM403 *(lac⁺ rep⁺)*	(Guy *et al.*, 2009)
N6568	MG1655 Δ*lacIZYA::<>* Δ*uvrD::dhfr* / pAM403 *(lac⁺ rep⁺)*	(Guy *et al.*, 2009)
N6577	MG1655 Δ*lacIZYA::<>* Δ*rep::cat*	(Guy *et al.*, 2009)
N6632	MG1655 Δ*lacIZYA::<>* Δ*uvrD::dhfr*	(Guy *et al.*, 2009)
N7919	MG1655 Δ*lacIZYA::<>* *recB268::*Tn*10* Δ*rep::cat* / pAM403 *(lac ⁺ rep⁺)*	(Atkinson *et al.*, 2011b)
N7604	MG1655 Δ*lacIZYA::<>* Δ*rep::cat rpoB*35*	(Gupta *et al.*, 2013)

2.4 List of plasmids used in this study

A detailed list of all plasmids used and created for this study can be found in the appendix section A.4.

2.5 General molecular and genetic techniques

2.5.1 Plasmid DNA isolation

Plasmid DNA was isolated from 5 ml LB stationary phase cultures. The cultures were centrifuged at 6000 × g for 10 min. The cell pellet was processed according to the manufacturer's instructions (QIAGEN QIAprep Spin Miniprep Kit) and plasmid DNA was eluted in 50 µl 10 mM Tris-HCl pH 8.5.

2.5.2 Agarose gel electrophoresis

DNA was analysed on 0.8 – 2% agarose (w/v) gels prepared in 1× Tris-borate-EDTA (TBE) buffer (Table A.6) with 0.1 µg ml^{-1} ethidium bromide. DNA samples were mixed with 6× gel loading buffer (GLB; Table A.2) and run at 100 V for 1 h. The DNA was visualised using a UV transilluminator system (BioRad).

2.5.3 Restriction digestion

To obtain DNA fragments to be used for DNA cloning, 3-8 µg plasmid DNA or PCR products were digested with 20 units (U) restriction enzymes in final reaction volumes of 25-100 µl resulting in the excision of the desired fragments. Reactions took place in the recommended buffer systems (NEB) and at the recommended temperature overnight.

For plasmid DNA screens, 100-300 ng plasmid DNA was digested by 2 U of restriction enzyme as either a single or double digest in the recommended buffer

system (NEB). Reactions took place in a final volume of 10 µl at the recommended temperature for 1.5 h. For digestion with two or more restriction enzymes, single digests were set up as controls.

2.5.3.1 Conversion of DNA 5' overhangs to blunt ends

For ligation of otherwise incompatible DNA overhangs, DNA fragments from restriction digestion were blunt ended. 0.2 mM dNTPs (final concentration) and 0.05 U µl^{-1} DNA polymerase I Klenow Fragment (NEB) were added to restriction digests after overnight incubation (section 2.5.3) for 15 min at room temperature. Afterwards, Klenow was heat inactivated at 75°C for 20 min.

2.5.3.2 Removal of phosphate groups from 5' DNA ends

Samples from the restriction digestion that were used as vectors for ligations were dephosphorylated by the addition of 0.1 U µl^{-1} of calf intestine alkaline phosphatase (CIP; NEB) for 1 h at 37°C.

2.5.3.3 DNA clean-up for two step DNA digestion

To remove any enzymes or other impurities for sequential DNA digestion, the DNA samples were processed according to the manufacturer's instructions (Qiagen PCR purification kit). DNA was eluted in 30 µl 10 mM Tris-HCl pH 8.5.

2.5.4 Purification of linear DNA fragments

Products from restriction digests were separated on agarose-TBE gels at 100 V for 1 h. The DNA was visualised under UV-light and fragments of interest were excised from the gel. The excised fragments were treated following the manufacturer's instructions (Qiagen QIAquick Gel Extraction Kit) and eluted in 30 µl 10 mM Tris-HCl pH 8.5.

2.5.5   Polymerase Chain Reaction (PCR)

PCR reactions were performed in a PTC-100 Thermal cycler (MJ Research, now BioRad) or in a T-professional Basic Gradient Thermocycler (Biometra). Plasmid DNA (0.2 – 2 ng μl^{-1}) or genomic DNA were used as PCR templates. For genomic DNA, either a single colony of *E. coli* or 5 µl from a stationary LB culture were resuspended in 100 µl dH$_2$O and boiled at 95°C for 5 min. From this 100 µl reaction, 1 µl was used as template DNA.

2.5.5.1   PCR primers

All primers were purchased from Integrated DNA Technologies (www.idtdna.com). Primers were resuspended in 10 mM Tris pH 8 and 1 mM EDTA and stored at -80°C as 100 µM stocks.

For a table of all PCR primers used, refer to the appendix section A.3 Table A.13.

PCR products intended for restriction digestion were amplified with PCR primers additionally carrying 5' extensions including six random nucleotides to allow for efficient DNA cleavage close to the 5' DNA end upstream of the palindromic DNA recognition sequence for the respective restriction enzyme.

2.5.5.2   Non-proofreading polymerase

Taq DNA polymerase (NEB) was used for diagnostic PCR reactions of plasmids and chromosomal DNA. PCR reactions were set up as follows:

Table 2.5 PCR reactions with *Taq* polymerase

DNA template	$0.1 - 1$ ng μl^{-1} for plasmid DNA or 1 µl for colony PCRs
Taq DNA polymerase (NEB)	0.0125 U μl^{-1}
10x standard *Taq* buffer (NEB)	1x
dNTPs (Roche)	0.125 mM
forward and reverse primer	0.1 µM
dH$_2$O	to 50 µl

Table 2.6 PCR cycles for PCR reactions with *Taq* polymerase

Initial denaturation	95°C	4 min	
Denaturation	95°C	15 s	
Annealing	55-65°C*	30 s	30-35 cycles
Extension	68°C	1 min per kb	
Final extension	68°C	5 min	

* The annealing temperature was calculated by the formula:

$$T_m (°C) = 2x\ nt_{primer\ length} + 2x\ nt_{(G\ and\ C)} - 5°C$$

2.5.5.3 Proofreading polymerase

PCR products that were intended for DNA ligations were amplified with the proofreading polymerase Phusion (NEB). Typical PCR reaction conditions were as follows:

Table 2.7 PCR reactions with Phusion polymerase

DNA template	$0.1 - 1$ ng μl^{-1} for plasmid DNA or 1 µl for colony PCRs
Phusion (NEB)	0.02 U μl^{-1}
5x HF buffer (NEB)	1x
dNTPs (Roche)	0.2 mM
forward and reverse primer	0.5 µM
dH$_2$O	to 50 µl

Table 2.8 PCR cycles for PCR reactions with Phusion polymerase

Initial denaturation	98°C	30 s	
Denaturation	98°C	10 s	
Annealing	55-65°C*	30 s	30-35 cycles
Extension	72°C	0.5 min per kb	
Final extension	70°C	10 min	

* The annealing temperature was determined using the NEB Tm Calculator (https://www.neb.com/tools-and-resources/interactive-tools/tm-calculator).

2.5.6 Site directed mutagenesis (SDM)

Point mutations of the *rep* gene were introduced via site directed mutagenesis of pPM657 (pET22b*bio-rep*). Forward and reverse primers were designed as complementary sequences and contained the desired base changes flanked by 10-12 base pairs of the wild-type sequence of the gene (for the complete list of primers, refer to Table A.15 in the appendix section A.3). PCR reactions were performed as described in 2.5.5.3 for 18-22 cycles with the addition of 5% dimethyl sulfoxide (DMSO). Annealing occurred at 60°C.

The template plasmid was digested by the addition of 0.3 U µl^{-1} DpnI (NEB) to the PCR reaction at 37°C for 16 h, before PCR purification and elution in 30 µl 10 mM Tris-HCl pH 8.0 (section 2.5.3.3).

2.5.7 DNA ligation

Ligations were performed in a final volume of 10 µl containing 1× NEB ligation buffer (50 mM Tris-HCl pH 7.5, 10 mM magnesium chloride, 10 mM dithiothreitol (DTT) and 1 mM ATP). Approximately 10-50 ng of vector DNA and a fourfold molar excess of the insert DNA were used. The reaction took place at room temperature for 2-4 h after the addition of 400 U of T4 DNA ligase (NEB).

2.5.8   DNA sequencing

DNA sequencing of purified plasmids or PCR products was performed by GATC Biotech (www.gatc-biotech.com) using BigDye Terminator v3.1 chemistry on the Sanger ABI 3730xl automated capillary DNA sequencer.

A full list of the sequencing primers used in this study can be found in the appendix A.3 Table A.14.

2.5.9   Calcium Chloride (CaCl₂) transformation

E. coli strains with the desired genotype were grown to an absorbance at 650 nm (A_{650}) of ~0.4 in 10 ml LB in the presence of the appropriate antibiotic(s). The culture was cooled on ice and centrifuged (6000 × g, 10 min, 4°C). The pellet was resuspended in 1 ml 0.1 M CaCl₂ and kept on ice for at least 20 min. 100 µl of CaCl₂-competent cells were then added to 100 ng plasmid DNA or to 10 µl ligation reactions in a microcentrifuge tube and incubated for a further 30 min on ice. Afterwards the cells were heat-shocked at 42°C for 45 s and placed back on ice for 2 min. To recover the cells, 900 µl of LB was added for 1 h at 37°C. The cells were centrifuged at 12000 × g for 1 min and the pellet was plated onto LB agar plates with the selective antibiotic. The plates were incubated at 37°C for 16 h.

2.5.10 P1 transductions

2.5.10.1 P1 lysate preparation

To generate lysates from *E. coli* strains, 300 µl of a fresh overnight culture of a donor strain was mixed with 10^7 plaque forming units (pfu) P1 phage from an *E. coli* MG1655 strain (P1.MG1655) and 10 µl of 0.5 M CaCl₂. The reactions were incubated at 37°C for 15 min (or 30°C for 30 min for temperature sensitive strains) to allow adsorption of the phage to the donor strain. Afterwards, 10 ml LB and additional 100 µl of 0.5 M CaCl₂ were added. The cultures were incubated at 37°C (or 30°C) and 220 rpm until cell debris, indicating cell lysis, was visible.

At this point, 300 µl of chloroform (CHCl₃) was added for 10 min to lyse any remaining cells. The P1 phage particles were separated from cellular debris by centrifugation (6000 × g, 10 min, 4°C) and the supernatant containing P1 phage particles was transferred to a fresh 15 ml conical tube. The lysates were mixed with 1 ml CHCl₃ and stored at 4°C.

To check P1 titres, 2.5 ml 0.6% LB agar were mixed with 100 µl TB28 culture (A_{650} >0.8) and poured onto LB agar plates supplemented with 5 mM $CaCl_2$ and 0.13% glucose (soft top agar plates). Serial dilutions of the P1 lysates were spotted on the soft top agar plates and after 16 h incubation at 37°C, the titre (pfu ml^{-1}) was calculated from the number of plaques on the agar plates.

2.5.10.2 P1 transductions

For P1 transductions, 500 µl of a fresh overnight culture of the *E. coli* acceptor strain was mixed with 50 µl of the P1 lysate (>10^8 pfu/ml) from a strain with the mutation of interest and 5 µl of 0.5 M $CaCl_2$ to allow adsorption of the phage to the cells. A control lacking P1 was also set up. The reactions were incubated for 15 min at 37°C (or 30 min at 30°C) before centrifugation (6000 × g, 5 min) to remove the supernatant containing free P1 phage particles. The pellet was resuspended in 1 ml LB broth containing 20 mM sodium citrate, to bind the calcium ions and prevent further phage adsorption. After 1 h at 37°C (or 30°C) and subsequent centrifugation (6000 × g, 5 min), the cell pellets were plated on LB$^{0.5}$ agar with 2.5 mM sodium citrate and antibiotic(s) to select for the desired transductants. After 24 h incubation at 37°C (or 36 h at 30°C), colonies were restreaked to single colonies on fresh LB$^{0.5}$ agar with antibiotic(s) and 2.5 mM sodium citrate and to remove any remaining P1 phage particles and incubated at 37°C (or 30°C) for 16 h. Single colonies from these plates were then grown in 10 mL LB broth for 16 h, pelleted by centrifugation (6000 × g, 10 min), confirmed by PCR (section 2.5.5.2) and frozen away as glycerol stocks at -80°C.

2.6   Protein Purification

Rep, bio-Rep, bio-RepΔ2B, UvrD, DnaB, DNA polymerase III αεθ complex, τ clamp loader complex, DnaC, SSB, β sliding clamp, HU, DnaG, DnaA, EcoRI E111G and LacI were purified as described in (Abarzua *et al.*, 1984; Atkinson *et al.*, 2009; Guy *et al.*, 2009; Hiasa & Marians, 1994; Hodgman, 1988; King *et al.*, 1989; Marians, 1987; Marians, 1995; Parada & Marians, 1991) by former members of our laboratory. RecD2 was a gift from Dale Wigley (CRUK). Streptavidin was purchased from Sigma.

Purification of His-Rep G543A/S545A, His-Rep G373T/G374T and His-RepΔ2B^{uvrD2B} from pET14b plasmids followed the optimised overexpression and purification protocol for pET14b*rep* that was established for His-Rep by Dr Jamieson Howard in our lab.

2.6.1 Overexpression

BL21 AI *Δrep::cat* (HB222) strains were CaCl$_2$ transformed with different pET14b versions encoding the gene of interest and grown on LB agar supplemented with 50 mg ml^{-1} carbenicillin at 37°C for 16 h. On the next day, 10 ml F medium with 50 mg ml^{-1} carbenicillin was inoculated with a single colony from the transformations and incubated at 37°C for 16 h. The cultures were centrifuged and the pellet was resuspended in 1 ml F medium, which was used to inoculate 1 l F medium. The culture was incubated at 37°C and 220 rpm until an A$_{650}$ ~0.5 was reached. Expression of the T7 RNA polymerase was induced by the addition of arabinose (0.2% final concentration) and incubation continued at 20°C and 220 rpm for 3 h.

Afterwards, the culture was centrifuged (4000 rpm, 20 min, 4°C, Sorvall SLC-6000 rotor). The pellet was resuspended in 10 ml 50 mM Tris pH 7.5 and 10% (w/v) sucrose, then added dropwise to liquid nitrogen and stored at -80°C until cell lysis.

2.6.2   Cell lysis

The cell pellets were thawed on ice and resuspended in 50 mM Tris-Cl pH 8.4, 20 mM EDTA pH 8.0, 150 mM KCl and 0.2 mg ml^{-1} lysozyme. After 10 min incubation on ice, Brij-58 was added to 0.1% (v/v; final concentration) with further 20 min incubation on ice. The supernatant was recovered after centrifugation (38000 rpm, 1 h, 4°C, type 70.1 ti rotor) and DNA was precipitated by dropwise addition of polymin P to 0.075% (v/v; final concentration) with stirring at 4°C for 10 min. After centrifugation (16000 rpm, 20 min, 4°C, Sorvall SS-34 rotor), solid ammonium sulphate was added to the supernatant to 50% saturation with stirring at 4°C for 10 min. After centrifugation (16000 rpm, 20 min, 4°C, Sorvall SS-34 rotor), the pellet was stored on ice at 4°C overnight.

2.6.3   Purification by nickel affinity chromatography

His-tagged Rep proteins were purified by affinity chromatography on a 5 ml His-trap FF column (GE Healthcare) charged with 0.2 M aqueous NiSO$_4$ solution. The protein pellet was diluted in 20 mM Tris-HCl pH 7.9 and 5 mM imidazole until the conductivity matched that of 20 mM Tris-HCl pH 7.9, 5 mM imidazole and 500 mM NaCl (binding buffer). After injection of the protein sample, the His-trap FF column was washed in binding buffer (3 column volumes, CV) at 2.5 ml min^{-1}, prior to a linear imidazole gradient (20 CVs; 5 mM to 1 M). Fractions with an absorbance peak at 280 nm were analysed on an 8% sodium dodecyl sulphate polyacryl gel electrophoresis (SDS-PAGE) gel (Table A.10; 220 V, 50 min) for the presence of Rep and pooled.

2.6.4   Purification by heparin affinity chromatography

Proteins were further purified by affinity chromatography on a 3 ml heparin-agarose C 10/10 column (GE Healthcare). The conductivity of the peak fraction from the His-trap FF column purification was adjusted to the conductivity of heparin

buffer (50 mM Tris pH 7.5, 1 mM EDTA and 50 mM NaCl) by dilution in 50 mM Tris pH 7.5 and 1 mM EDTA. After injection of the protein sample, the column was washed in heparin buffer (3 CVs) at 2.5 ml min^{-1}, prior to a linear NaCl gradient (20 CVs; 50 mM to 1 M). Fractions with high UV absorbance peaks (280 nm) were analysed on an 8% SDS-PAGE gel (220 V, 50 min) for the presence of Rep. Fractions corresponding to 60%-100% or 30-60% of the UV peak were pooled as peak and side fractions, respectively.

2.6.5 Gel filtration

Gel filtration was performed on a HiLoad 26/60 Superdex 200 preparative grade column (GE Healthcare). The column was equilibrated in 50 mM Tris pH 8.4, 200 mM NaCl, 1 mM EDTA and 5 mM DTT. The peak fraction from the previous purification step was loaded on the column and eluted in 2 CVs at a flow rate of 1 ml min^{-1}. Samples were collected as 3 ml fractions, analysed on an 8% SDS-PAGE gel (220 V, 50 min) for the presence of Rep and pooled as peak and side fractions.

2.6.6 Dialysis

Proteins were dialysed in 4 l of 50 mM Tris pH 7.5, 1 mM EDTA, 1 mM DTT, 100 mM NaCl and 50% glycerol (v/v) with mixing at 4°C overnight. The concentration of the proteins was estimated using a Nanodrop 2000C (ThermoScientific). Proteins were aliquoted and stored at -80°C.

2.7   Genetic Techniques

2.7.1 Viability Assays (Spot Tests)

E. coli strains carrying the pAM403 (pRC7 *rep$^+$ lac$^+$*) (Mahdi *et al.*, 2006) construct were transformed with different pBAD constructs and grown on LB agar with

120 µg ml^{-1} X-gal, 1 mM IPTG, 30 µg ml^{-1} kanamycin and 100 µg ml^{-1} ampicillin and selected for blue transformants. Blue colonies were streaked to single colonies on minimal agar plates with kanamycin, X-gal and IPTG but without ampicillin to allow for the loss of pAM403, indicated by the appearance of white colonies. Single white pAM403-less colonies were restreaked onto a second minimal agar plate to confirm the absence of pAM403. Single white colonies from these plates were then grown in liquid minimal medium with kanamycin overnight (selecting for pBAD derivatives), serially diluted and spotted on rich medium and minimal agar with kanamycin and without or with 0.2% (w/v) arabinose. Plates were photographed after 16 h (LB agar) or 72 h (minimal agar) incubation at 37°C.

2.7.2 Blue/white screening assays

2.7.2.1 Plasmid loss assays

To test the viability of certain mutants in absence of a complementing plasmid, plasmid loss assays were performed. TB28 and derivatives carrying the plasmid pAM403 (pRC7 rep^+ lac^+) were streaked out on LB$^{0.5}$ agar with 100 µg ml^{-1} ampicillin and grown for 16 h. Single colonies were inoculated in 10 ml LB$^{0.5}$ broth and grown for 16 h before plating of 100 µl of 10^{-5} – 10^{-6} dilutions on LB$^{0.5}$ or minimal agar supplemented with 120 µg ml^{-1} X-Gal and 1 mM IPTG. The plates were incubated at 25°C and 30°C either for 48 h on LB$^{0.5}$ or for 6 days for growth on minimal agar. The plates were photographed after incubation and loss of pAM403, indicated as the appearance of white colonies, was assayed by blue/white screening.

2.7.2.2 Plasmid complementation assays

Different pBAD plasmids (pPM638 derivatives) were tested for the ability to complement the synthetic lethality of the *rep recB* double mutant. For this, HB268 (*Δrep recB268* / pAM403) was transformed with different pBAD constructs and plated on LB$^{0.5}$ agar with 30 µg ml^{-1} kanamycin, 100 µg ml^{-1} ampicillin, 120 µg ml^{-1} X-Gal and 1 mM IPTG. After 16 h incubation at 37°C, single blue colonies were

grown in 10 ml LB$^{0.5}$ broth containing 30 µg ml^{-1} kanamycin for 16 h at 37°C, before 100 µl of 10^{-4} and 10^{-5} dilutions were plated on LB$^{0.5}$ with 30 µg ml^{-1} kanamycin, 120 µg ml^{-1} X-Gal and 1 mM IPTG in the absence or the presence of 0.2% arabinose. Ampicillin was omitted to allow for the loss of the pAM403 plasmid, which resulted in white colonies if the *rep* genes expressed from the pBAD plasmids were able to complement the synthetic lethality. Plates were photographed after 48 h incubation at 37°C and complementation was assayed by blue/white screening.

2.8 Biochemical Assays

2.8.1 *In vitro* replication assays

In vitro replication assays were performed in 40 mM HEPES pH 8.0, 10 mM DTT, 10 mM magnesium acetate, 2 mM ATP, 0.2 mM of G/C/UTP each, 0.04 mM of dNTPs and 0.1 mg ml^{-1} bovine serum albumin (BSA) as described in Guy *et al.* (2009).

Replication enzymes (50 nM DNA polymerase III αεθ complex, 25 nM τ clamp loader complex, 160 nM DnaB and DnaC monomers, 1 µM SSB, 80 nM β, 30 nM HU, 200 nM DnaG) were premixed on ice. Final reaction volumes were 15 µl.

2.8.1.1 EcoRI E111G Replication Block Assays

Plasmid pPM594 (containing the *E. coli oriC* and an array of 8 EcoRI sites; 2 nM) was incubated with 250 nM EcoRI E111G dimers on ice prior to the addition of replication enzymes. Replication was induced after the addition of 300 nM DnaA and shifting of the reaction to 37°C for three min, followed by the addition of 47 U of SmaI to release positive supercoiling in the absence of a topoisomerase and 0.4 MBq [α^{32}P]-dCTP (222 TBq mmol^{-1}) for 1.5 min. The denoted helicases (100 nM) were added for 2 min before the reactions were stopped by the addition of 5 µl of 10 M ammonium acetate, ethanol precipitated and evaluated by denaturing agarose gel electrophoresis (Hiasa & Marians, 1994), phosphorimaging and autoradiography. Replication efficiency was determined by the amount of the

4.7 kb full length replication product relative to control reactions (- E111G, no helicase and + E111G, no helicase).

2.8.1.2   Replication Fork Stability Assays

The *oriC* and *lacO$_{22}$* containing plasmid pPM561 (2 nM) was incubated with 400 nM LacI on ice in replication buffer prior to the addition of replication enzymes. Replication was induced after the addition of DnaA and shifting of the reaction to 37°C for 3 min. Afterwards, 47 U of SmaI to release positive supercoiling in the absence of a topoisomerase and 0.4 MBq [α^{32}P]-dCTP (222 TBq mmol^{-1}) were added for 1.5 min. The denoted helicases (100 nM) were added for 1.5 min before the addition of 1 mM IPTG to dissociate LacI from the *lac* operator sequences. The reactions were continued for 2 min and then stopped by the addition of 5 µl of 10 M ammonium acetate, ethanol precipitation and evaluated by denaturing agarose gel electrophoresis (Hiasa & Marians, 1994), phosphorimaging and autoradiography. Replication efficiency was determined by the amount of the full length replication product (6.5 kb) relative to control reactions (- LacI, no helicase and + LacI, no helicase).

2.8.2   Oligonucleotide preparation for *in vitro* assays

2.8.2.1   Oligonucleotide purification

All oligonucleotides used in the following assays were urea PAGE-purified. For this, 1 µg bp^{-1} of the oligonucleotide was mixed with sequencing loading dye (Table A.4; 1× final concentration) and heated to 95°C for 5 min prior to loading on a denaturing urea polyacrylamide gel (Table A.3) and electrophoresis on a SequiGen apparatus (BioRad). The samples were run at 55 W for 1-3 h depending on their sequence length. The oligonucleotides were visualised by UV shadowing. Full length sequences were excised from the gel and eluted in 50 mM Tris-HCl pH 8.0 and 1 mM EDTA (1× TE) at 4°C overnight.

2.8.2.2   5' radiolabelling of DNA oligonucleotides

To 5' radiolabel single oligonucleotides, 25 μl reactions were set up containing 500-1000 ng oligonucleotide, 10 U of T4 Polynucleotide Kinase (PNK; NEB) and $1\times$ PNK buffer (70 mM Tris-HCl pH 7.6, 10 mM $MgCl_2$ and 5 mM DTT). The reaction was incubated at 37°C for 1 h in the presence of 0.4 MBq [γ^{32}P]-ATP (222 TBq $mmol^{-1}$) before heat inactivation of PNK at 65°C for 15 min. Unincorporated [γ^{32}P]-ATP was removed by passing the reaction through a Micro Bio-Spin™ P-6 Gel Columns (BioRad) following the manufacturer's instructions, eluting the radiolabelled oligonucleotide in 10 mM Tris pH 7.4.

2.8.2.3   Generation of radiolabelled DNA fork substrates

To generate forked DNA substrates, 200-400 nM radiolabelled oligonucleotide was mixed with a threefold molar excess of the complementary oligonucleotide in $1\times$ SSC buffer (Table A.5). The reactions were incubated at 95°C for 5 min in a Dri-Block (Techne) and left in the aluminium block to slowly cool down to room temperature. Afterwards, the fork substrate was separated from ssDNA by non-denaturing polyacrylamide gel electrophoresis (Table A.8) at 180 V for 90 min. The radiolabelled DNA was visualised by autoradiography, excised from the gel and eluted in $1\times$ TE at 4°C overnight.

The concentration of the dsDNA fork was calculated from the amount of incorporated radioactivity of the single radiolabelled oligonucleotide determined on a TriCarb 2900TR Liquid Scintillation Counter (Packard, now PerkinElmer).

2.8.3 Helicase assays

Helicase assays were performed as described previously (Guy *et al.*, 2009). Helicase assays were set up in 50 mM HEPES pH 8.0, 10 mM DTT, 10 mM magnesium acetate, 2 mM ATP, and 0.2 mg ml^{-1} BSA ("unwinding buffer") with 1 nM forked DNA structures. All DNA unwinding reactions were carried out at 37°C. Final reaction volumes were 10 μl.

The unwinding buffer with the forked DNA substrate (60 base pairs dsDNA, 38 bases ssDNA arms; CC139 annealed to CC140; Table A.16) was assembled on ice and shifted to 37°C for 2 min before the addition of any protein. Increasing concentrations of different helicases (0-100 nM) were added for 10 min, before the reactions were terminated by the addition of 2.5 µl of 100 mM Tris-HCl pH 7.5, 200 mM EDTA, 10 mg ml^{-1} proteinase K and 0.5% SDS ("stop buffer"). The products were separated on 10% polyacrylamide/TBE gels (Table A.8) at 180 V for 90 min and analysed by phosphorimaging and autoradiography. Unwinding efficiency was given as relative amounts of ssDNA compared to total DNA and corrected for the respective no helicase control.

To test the cooperativity between Rep mutants and DnaB, DnaB (100 nM hexamers) was added to the reactions 2 min prior to the addition of different Rep variants (0-10 nM). Reactions continued for 10 min before stopping by the addition of 2.5 µl stop buffer. The reactions were processed and analysed as in described above. Cooperativity of DNA helicases was calculated by the fraction of DNA unwinding by Rep in presence of DnaB divided by the levels of DNA unwinding by Rep and DnaB on their own. Cooperativity in case of co-incubation of two helicases was indicated by values greater than 1.

2.8.4 Nucleoprotein displacement assays

2.8.4.1 Streptavidin displacement from ssDNA

Streptavidin displacement assays from ssDNA were adapted from Byrd and Raney (2004). Reactions containing 1 nM of biotinylated dT$_{60}$-mers (PM326-328; Table A.16) and 50 mM HEPES pH 8.0, 10 mM DTT and 0.2 mg ml^{-1} BSA were assembled on ice. The reactions were shifted to 37°C for 2 min, 1 µM streptavidin was added and further incubated for 5 min to allow the streptavidin to bind to the biotin. Different helicases (0-50 nM) along with 100 µM free biotin (to prevent any streptavidin that has been removed by the helicases to rebind the biotinylated DNA) were added with 2 min further incubation. Helicase translocation was initiated by the addition of 10 mM magnesium acetate and 2 mM ATP to the final

reaction volume of 10 µl. The reactions were stopped after 10 min by the addition of 2.5 µl 0.5 M EDTA pH 8.0 and separated on a 10% polyacrylamide/TBE gel at 180 V for 90 min. The gels were dried and analysed by phosphorimaging and autoradiography. Streptavidin displacement was calculated by the fraction of ssDNA generated in the presence of the helicases and normalised to a ssDNA control (set to 100%) and a ssDNA + streptavidin bandshift (set to 0%).

To test the cooperativity in streptavidin displacement between Rep and DnaB from ssDNA, ssDNA was bound to streptavidin as above on ice for 5 min. Afterwards, 100 µM biotin was added without or with DnaB (2, 10 or 50 nM hexamers) on ice for a further 5 min. Next, different Rep variants (2 or 10 nM final concentration) were added on ice for 2 min. Initiation of helicase translocation and processing of the reactions was performed as above. The cooperativity in streptavidin displacement was calculated as in section 2.8.3.

2.8.4.2   Unwinding of streptavidin-bound duplex DNA

Unwinding of streptavidin-bound DNA forks was tested in unwinding buffer (see section 2.8.3) in a final reaction volume of 10 µl. The biotinylated DNA fork (CC139B53 annealed to CC140B47; Table A.16) was incubated with 1 µM streptavidin for 5 min to allow the streptavidin to bind to the biotin-modified bases close to the ss/dsDNA junction.

Different helicases (0-100 nM) were added together with free biotin (100 µM) for 10 min at 37°C, before termination of the reaction by the addition of 2.5 µl stop buffer and separation on a 10% polyacrylamide/TBE gel at 180 V for 120 min. The gels were dried and analysed as before (section 2.8.3). Total streptavidin displacement was given as relative amounts of ssDNA and dsDNA compared to total DNA and corrected for the respective no helicase control.

Cooperativity between Rep variants and DnaB was assayed in the same way as above, except that 100 nM DnaB hexamers and 100 µM free biotin were added together and incubated at 37°C for 2 min after the addition of streptavidin. Rep (0-10 nM) was added with a further 10 min incubation at 37°C before termination and

processing of the reactions as above. Cooperativity in DNA unwinding was calculated as in described in section 2.8.3.

2.8.4.3   LacI displacement assays

Reactions were assembled in unwinding buffer with 1 nM $lacO_1$ DNA fork (oJA025 annealed to oJA026; Table A.16) in the absence or presence of 1 mM IPTG and incubated at 37°C for 10 min. LacI (20 nM tetramers) was added for 5 min at 37°C, to allow binding of $LacI_4$ to the *lac* operator. Different helicases (0-100 nM) were added for 10 min at 37°C, before the reactions were terminated by the addition of 2.5 μl stop buffer and processed as described in 2.8.3. DNA unwinding was determined as in 2.8.3. Blockage of DNA unwinding was calculated by the amount of DNA unwinding in presence of LacI (with and without IPTG) divided by the amount of DNA unwinding in absence of LacI and IPTG for each different helicase concentration.

To test the cooperativity of Rep and DnaB for unwinding of LacI-bound DNA, 100 nM DnaB hexamers were added 2 min prior to the addition of Rep (0-10 nM). Reactions continued for 10 min before processing as above. Cooperativity was determined as in 2.8.3.

2.8.5   Electrophoretic Mobility Shift Assays (EMSA)

DnaB-Rep bandshifts were performed as described previously (Guy *et al.*, 2009). The reaction were set up with 1 nM DNA fork (CC139 annealed to CC140) in 50 mM HEPES pH 8.0, 10 mM magnesium acetate, 10 mM DTT, 10 μM ADP and 50 μg ml^{-1} BSA. These concentrations of magnesium and ADP have been shown to stabilise DnaB hexamerisation (Bujalowski *et al.*, 1994; Ng & Marians, 1996). 100 nM DnaB hexamers were added and incubated at 37°C for 2 min before the addition of the Rep variants (0-25 nM) to the final reaction volume of 10 μl. Incubation was continued for 10 min, prior to the addition of 2 μl 30% glycerol and loading on a 4% polyacrylamide gel with 89 mM Tris base, 89 mM boric acid and 10 μM ADP.

Electrophoresis was performed at 160 V for 90 min with 89 mM Tris base, 89 mM boric acid and 10 μM ADP as running buffer. The gels were dried and analysed by phosphorimaging and autoradiography.

2.8.6 Surface Plasmon Resonance (SPR)

Surface Plasmon Resonance was performed at 25°C on a Series S Sensor Chip SA (GE Healthcare) in a BiaCore T200 (GE Healthcare).

The streptavidin coated sensor chips were primed in 10 mM HEPES pH 7.4, 150 mM NaCl, 3 mM EDTA and 0.05% surfactant P20 (HBS-EP+ buffer, GE Healthcare) and activated with three 1 min washes with a solution of 1 M NaCl and 50 mM NaOH at 30 μl min^{-1} intermitted with 1 min HBS-EP+ buffer until a stable baseline signal was reached.

2.8.6.1 DNA interaction with immobilised proteins

Biotinylated proteins were diluted to a final concentration of 10 μg ml^{-1} by passing them through Micro Bio-Spin 6 columns (Bio-Rad) that had been equilibrated in HBS-EP+ buffer. Different biotinylated proteins were immobilised to flow channels 2, 3 or 4 at a flow rate of 10 μl min^{-1} to approximately equimolar concentrations of about 30 RU per kDa of the immobilised protein (i.e. about 2300 RU for the 77 kDa protein bio-Rep). Stable immobilisation was ensured by three washes in 1 M NaCl at 30 μl min^{-1} intermitted with 1 min HBS-EP+ buffer until a stable baseline signal was reached. Flow channel 1 served as a control and did not contain any immobilised protein.

To test the interaction between DNA and the biotinylated proteins, different DNA substrates were diluted in HBS-EP+ buffer to the denoted concentrations and passed over the chip at a flow rate of 10 μl min^{-1} for 5 min before injections of 1 M NaCl for 1 min at 30 μl min^{-1}.

2.8.6.2 Interaction of helicases with immobilised DNA

DNA substrates with a 5' biotin tag (100 nM; Table A.16) were diluted in HBS-EP+ and immobilised in single flow channels of the chip at a flow rate of 10 µl min^{-1} to 50-200 RU depending on the length of the oligonucleotide. Stable binding of the DNA to the chip surface was ensured by three washes in 1 M NaCl at 30 µl min^{-1} intermitted with 1 min HBS-EP+ buffer until a stable baseline signal was reached. Flow channel 1 served as a control and no DNA was immobilised.

Different His-tagged Rep mutants (3 nM – 1 µM) were diluted in HBS-EP+ buffer and passed over the chip at a flow rate of 10 µl min^{-1} for 15 min at which the response in RUs plateaued. This was followed by HBS-EP+ buffer with the same flow rate for 5 min to allow for dissociation of the helicases from the DNA. Remaining protein was removed by two injections of 1 M NaCl and 50 mM NaOH followed by HBS-EP+ for 60 s at a flow rate of 30 µl min^{-1}.

2.8.7 Size Exclusion Chromatography-Multiangle Laser Light Spectroscopy (SEC-MALLS)

To determine the oligomeric state of the Rep-DnaB interaction, SEC-MALLS was performed. For this, a SPD20A UV/Vis detector and a Shimadzu HPLC system, linked to a Wyatt Dawn HELEOS-II 18-angle light-scattering detector and Wyatt Optilab rEX refractive index monitor were used. A Superdex 200 10/300 size exclusion column (GE Healthcare) column was equilibrated in 50 mM HEPES pH 8, 10 mM MgAc, 10 mM DTT, 2 mM ATP and 150 mM potassium glutamate and attached to the HPLC. 120 µl of 1.0 mg ml^{-1} of either Rep or DnaB or 0.9 mg ml^{-1} of Rep and DnaB were injected onto the column via a SIL-20A Autosampler. Data was analysed with the Astra software using dn/dc values of 0.186 for proteins.

Chapter 3

INVESTIGATION OF THE INTERACTION BETWEEN REP AND DNAB

Chapter 3 – Investigation of the interaction between Rep and DnaB

3.1 Introduction

Protein-DNA complexes are the main source of genome instability in *E. coli* (Gupta *et al.*, 2013). The replicative helicase DnaB, which drives replication fork movement in *E. coli*, is at the leading edge of the replication fork and is therefore also the first to encounter any nucleoprotein block. However, DnaB on its own is not able to unwind DNA bound by a single repressor-operator complex *in vitro* (Yancey-Wrona & Matson, 1992). During DNA replication, the replisome is also likely to encounter multiple protein-DNA complexes that can fully block replication fork progression. For example, a single stalled RNA polymerase is thought to cause traffic jams formed by trailing transcription complexes *in vivo*, especially in highly transcribed genes (Trautinger *et al.*, 2005). If such conflicts between replication and transcription are not resolved, replication either fails or results in gross chromosomal rearrangements (Colavito *et al.*, 2010; Lambert *et al.*, 2010; Payne *et al.*, 2006).

In *E. coli*, the Superfamily 1A helicases Rep and UvrD act as accessory replicative helicases that promote replisome movement through such protein-DNA complexes (Guy *et al.*, 2009). Cells lacking one of these helicases are viable but the deletion of both helicases is lethal when cells are grown in rich medium, suggesting a redundant function between these helicases (Taucher-Scholz *et al.*, 1983). However, these *Δrep ΔuvrD* mutants are viable under slow growth conditions on minimal medium, a phenotype that correlates with reduced levels of transcription and hence fewer nucleoprotein barriers to replication (Guy *et al.*, 2009).

Rep directly interacts with the replisome via DnaB and this interaction depends on the last 33 amino acids of the Rep C-terminus. Efficient recruitment of Rep to the replisome facilitates complementation of the *Δrep ΔuvrD* lethality on rich medium. In the absence of the Rep C-terminus high levels of plasmid-expressed RepΔC33 are required to restore growth (Guy *et al.*, 2009). UvrD does not interact with the replisome and functions as an accessory replicative helicase by virtue of its high

intracellular concentration (Atkinson *et al.*, 2011b; George *et al.*, 1994; Guy *et al.*, 2009).

Questions remain concerning how Rep interacts with DnaB and how this interaction affects the positioning of Rep at the replication fork to efficiently underpin replication fork movement past nucleoprotein blocks. In this chapter, the interaction between Rep and DnaB will therefore be further investigated and characterised.

3.2   Results

3.2.1   The C-terminal four residues of Rep are critical for proper function *in vivo*

The last 33 amino acids of the Rep C-terminus contain residues that are essential for the interaction with the replicative helicase DnaB (Guy *et al.*, 2009). This interface was subsequently narrowed down to the final 15 amino acids of Rep (C. Guy, unpublished data).

To determine the exact residues necessary for the interaction of the Rep C-terminus with DnaB, C-terminal truncations of Rep were tested for complementation of the *Δrep ΔuvrD* lethality on rich medium (Guy *et al.*, 2009; Taucher-Scholz *et al.*, 1983). Different C-terminal deletions of Rep were cloned under the control of an arabinose inducible promoter, P_{BAD}.

These pBAD plasmids were transformed into *ΔlacIZYA rep⁺ uvrD⁺* (N6524) and *ΔlacIZYA Δrep ΔuvrD* (N6556) strains that also carried the *lac⁺* pRC7*rep* plasmid to complement the lethality of the double helicase mutant on rich medium. pRC7 derivatives can be lost at a high frequency in the absence of selection by omitting ampicillin if the plasmid is not required for the viability of the strain (Bernhardt & de Boer, 2004). The viability of *Δrep ΔuvrD* cells on minimal medium therefore allowed for loss of pRC7*rep*, which could be monitored by blue/white screening on plates containing X-gal, IPTG and kanamycin (to select for the pBAD derivatives). White colonies containing only the pBAD derivatives were then grown in liquid minimal medium, serially diluted and spotted onto LB without and with arabinose, resulting in low and high levels of expression from the P_{BAD} promoter, respectively (Figure 3.1A).

In a wild-type background, none of the helicases had an effect on viability even at high levels of expression, indicating that none of the constructs was toxic (Figure 3.1B). In a *Δrep ΔuvrD* strain, cells lacking an accessory replicative helicase were inviable on rich medium (see pBAD in Figure 3.1C.i and C.ii), in line with previous reports (Guy *et al.*, 2009; Taucher-Scholz *et al.*, 1983). Only full length Rep and
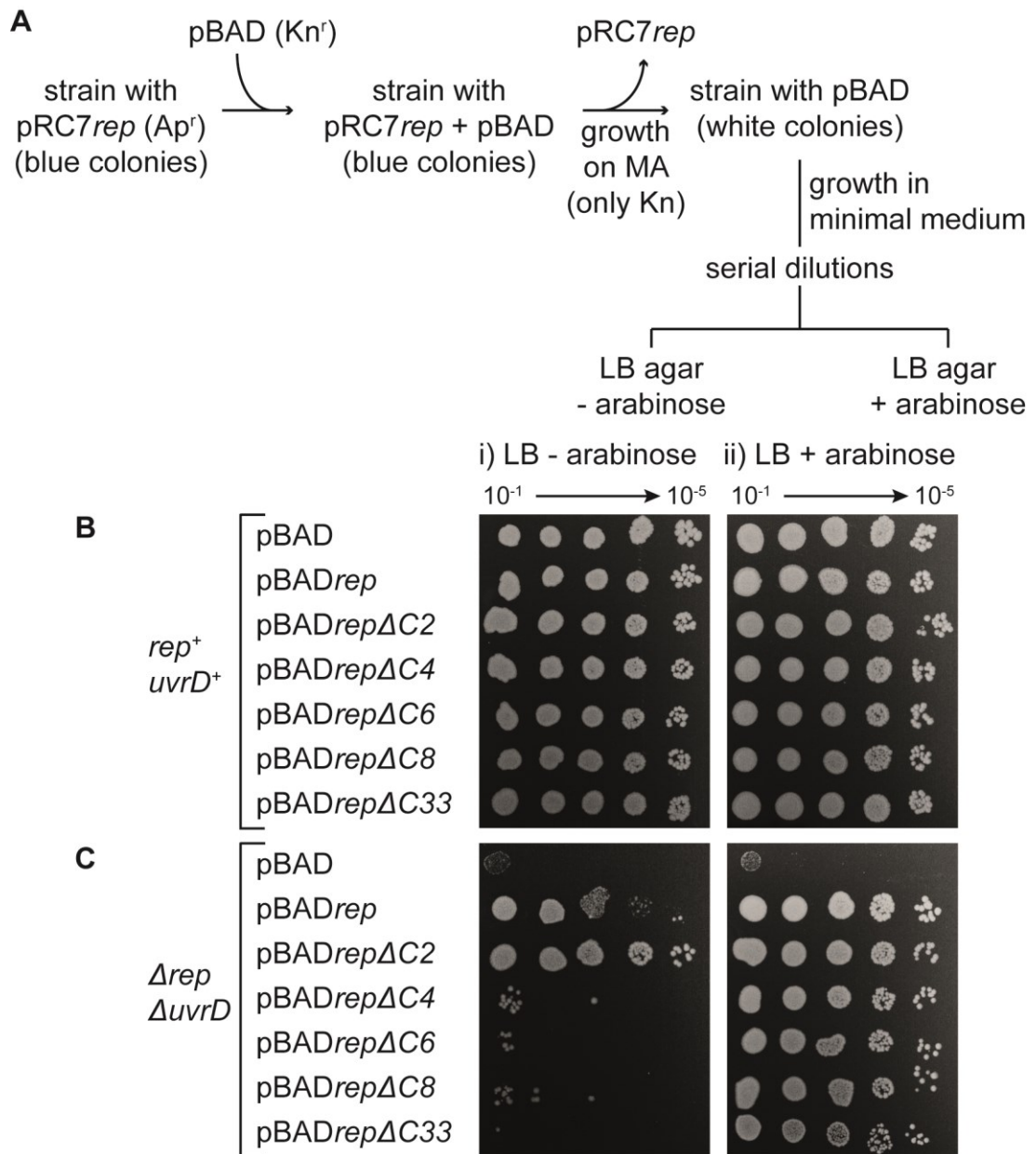
Figure 3.1 The last four amino acids of the Rep C-terminus are crucial for Rep function *in vivo*.
(A) Experimental protocol for the introduction of arabinose inducible pBAD derivatives and loss of pRC7*rep*. Kanamycin was present at all stages to select for pBAD derivatives, whereas ampicillin was omitted to lose pRC7*rep* during growth on minimal medium. Colony formation of (B) *rep*[+] *uvrD*[+] (N6524) and (C) *Δrep ΔuvrD* (N6556) strains with different pBAD derivatives after loss of pRC7*rep* (the experiment was performed as two independent replicates; n=2). Cells were grown in minimal medium, prior to plating of serial dilutions on LB agar with kanamycin ± arabinose.

RepΔC2 complemented the viability defect of *Δrep ΔuvrD* cells on rich medium already at low levels of expression. The deletion of the last two amino acids resulted in a slight improvement of the complementation at low levels of expression compared to the full length protein (Figure 3.1C.i). In contrast, deletions of four or more amino acids from the Rep C-terminus required high levels of expression to

restore growth (Figure 3.1C.ii). Previous work has demonstrated that complementation of the *Δrep ΔuvrD* growth defect in the absence of arabinose correlates with the ability of Rep to interact with DnaB as demonstrated by the requirement for high intracellular concentrations of RepΔC33 to complement the *Δrep ΔuvrD* lethality (Guy et al., 2009). The data in Figure 3.1 suggests that the last four amino acids of the Rep C-terminus are crucial for the Rep-DnaB interaction.

DNA translocation by Rep and all other helicases is dependent on NTP hydrolysis, usually ATP. NTP binding is mediated via the conserved Walker A and B motifs (Walker *et al.*, 1982). The invariant lysine (residue 28 in Rep), which is part of the conserved helicase motif I (Walker A motif), interacts with the phosphate tail of ATP (Korolev *et al.*, 1997; Lee & Yang, 2006; Ramakrishnan *et al.*, 2002; Story *et al.*, 1992; Velankar *et al.*, 1999). Mutations of this residue in ATP hydrolysing proteins abolish ATPase activity (Rehrauer & Kowalczykowski, 1993; Zavitz & Marians, 1992). RepK28A is an inactive DNA helicase and fails to promote replisome movement past protein blocks *in vitro* (Atkinson *et al.*, 2011a). However, it should still retain the interaction with DnaB as it contains the full Rep C-terminus. To test the impact of an ATPase-deficient helicase on cell growth *in vivo*, RepK28A was overexpressed in wild-type cells and single mutants of *rep* and *uvrD*.
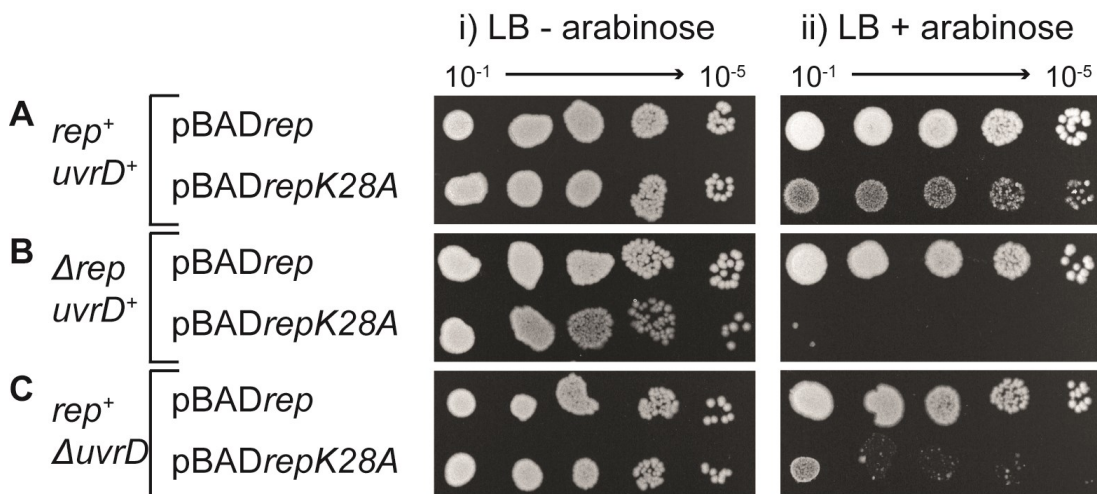
Figure 3.2 The overexpression of the ATPase deficient Rep mutant RepK28A is toxic.
Colony formation of (A) *rep⁺ uvrD⁺* (N6524), (B) *Δrep uvrD⁺* (N6540) and (C) *rep⁺ ΔuvrD* (N6568) strains with different pBAD*rep* derivatives after growth in LB and plating of serial dilutions on LB agar with kanamycin ± arabinose (n=2).

Overexpression of RepK28A in the *rep⁺ uvrD⁺* wild-type background was toxic as it resulted in a smaller colony size compared to overexpression of wild-type Rep (Figure 3.2A). The *ΔuvrD* strain with pBAD*repK28A* showed a reduction in the number of colony forming units in addition to a reduction in colony size (Figure 3.2C), while in cells lacking Rep, overexpression of RepK28A was lethal (Figure 3.2B). The reduced toxicity by RepK28A in the presence of chromosomal Rep (*ΔuvrD*, Figure 3.2C) as compared to UvrD (*Δrep*, Figure 3.2B), suggests that wild-type Rep counteracts the toxicity resulting from RepK28A overexpression more efficiently than UvrD.

Efficient complementation of the *Δrep ΔuvrD* rich medium lethality by low levels of Rep proteins was dependent on the last four amino acids of the Rep C-terminus (Figure 3.1C.i). It was tested if deletions of the last four amino acids of RepK28A were able to reduce the toxicity of overexpression of this helicase-deficient Rep mutant. For this, the *repK28A* mutation was combined with the same C-terminal deletions that had been generated in wild-type Rep and cloned under the control of the arabinose-inducible promoter P_{BAD}.

Only the expression of RepK28AΔC2 phenocopied RepK28A, since it resulted in smaller colony sizes compared to overexpression of Rep in a wild-type strain (Figure 3.3A), lethality in a *Δrep* strain (Figure 3.3B) and reduced growth in a *ΔuvrD* strain (Figure 3.3C). Deletions of four or more amino acids from the RepK28A C-terminus restored viability to the *Δrep* strain upon overexpression of the helicase mutant. However, these mutants still retained some toxicity in the *rep* mutant, as colony size was reduced compared to wild-type Rep (Figure 3.3B). This toxicity was still slightly visible in the *ΔuvrD* mutant, but absent in the wild-type background (Figure 3.3C).

These data demonstrate the toxicity of RepK28A was dependent on the last four amino acids of the Rep C-terminus. Thus, complementation of *Δrep ΔuvrD* lethality by truncated wild-type Rep (Figure 3.1) and the toxicity of truncated ATPase mutants of Rep showed an inverse pattern. Deletion of the final two amino acids (G672 and K673) did not have a significant effect in both assays, inferring that

amino acids K670 and R671 (fourth and third from the C-terminus) are essential for the Rep-DnaB interaction.
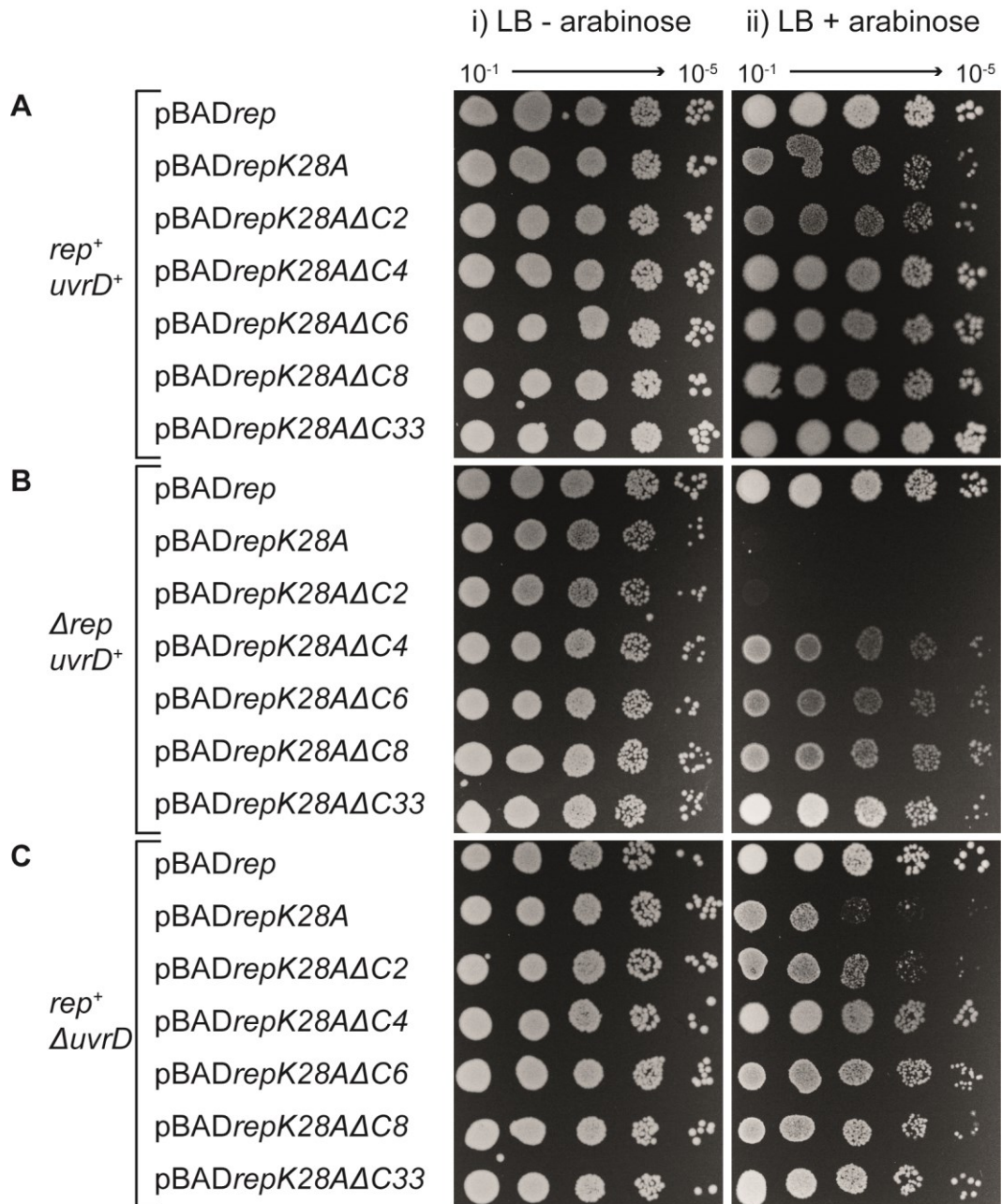
Figure 3.3 RepK28A toxicity depends on the final four amino acids of the Rep C-terminus
Colony formation of (A) *rep*[+] *uvrD*[+] (TB28), (B) *Δrep uvrD*[+] (N6577) and (C) *rep*[+] *ΔuvrD* (N6632) strains with different pBAD*rep* derivatives after growth in LB and plating of serial dilutions on LB agar with kanamycin ± arabinose (n=3).

SPR experiments were going to be performed on a streptavidin coated chip to test the interaction between DnaB and the C-terminal four residues of Rep directly using surface-immobilised biotinylated Rep peptides. However, DnaB interacted non-

specifically with the SPR chips (data not shown) and could not be removed using different buffer conditions. Due to time constraints these experiments were abandoned.

A Weblogo (Crooks *et al.*, 2004) of the Rep C-terminus from 44 Rep genes was created to identify the conservation of residues among different Rep genes (Figure 3.4) (Chen *et al.*, 2011; Papadopoulos & Agarwala, 2007). This comparison indicates that the final four amino acids among most Rep genes are enriched in positively charged residues. The importance the C-terminal four residues in Rep for Rep function *in vivo*, as indicated above, and the conserved basic nature of these residues in other Rep homologues suggests that these residues may be involved in ionic interactions with acidic residues in DnaB.

Figure 3.4 Sequence conservation of the Rep C-terminus
A Weblogo motif showing the sequence conservation of the last 34 amino acids of the Rep C-terminus. The Weblogo (Crooks *et al.*, 2004) was created from a multiple sequence alignment implemented in COBALT (Papadopoulos & Agarwala, 2007) from 44 Rep sequences retrieved from representative protein sets (Chen *et al.*, 2011). Reference numbering refers to residues of *E. coli* Rep.

3.2.2   A Rep and DnaB interaction is not observed by SEC-MALLS

DnaB forms a hexameric ring that encircles ssDNA of the lagging strand template at the replication fork (Kaplan, 2000) and unwinds DNA with 5'-3' polarity (LeBowitz & McMacken, 1986). Rep is likely to bind to the leading strand template, translocating in the 3'-5' direction (Figure 1.18A) (Atkinson *et al.*, 2011a; Yarranton & Gefter, 1979). It is not known whether all six binding sites within the DnaB hexamer are usually occupied by Rep or whether steric hindrance limits the Rep interaction at the replication fork, either in the presence of the hexamer alone or in the context of the replisome.

Size exclusion chromatography multi-angle laser light scattering (SEC-MALLS) was performed to identify the stoichiometry of the Rep-DnaB complex *in vitro* (Figure 3.5). Rep and DnaB on their own as well as Rep and DnaB together in an equimolar ratio were passed through the size exclusion column. Measurements of the UV signal, the refractive index and light scattering were taken to indicate the elution of the protein from the column, the concentration and the size of the analyte, respectively. The molecular weight of the proteins was estimated from the fraction of light scattering divided by the refractive index.
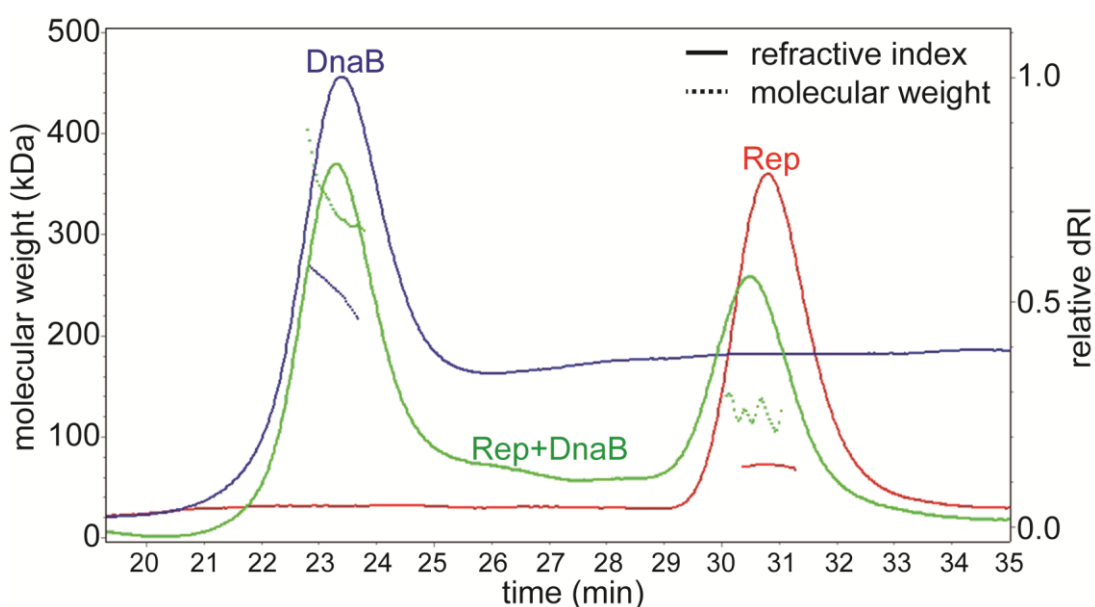
Figure 3.5 Rep and DnaB do not interact to form a detectable complex by SEC-MALLS
SEC-MALLS traces of the molecular weight and differential refractive index (dRI) over time of elution of 1 mg ml^{-1} of Rep (red lines) or DnaB (blue) alone or 0.9 mg ml^{-1} of Rep and DnaB together (green) from a Superdex 200 HR 10/30 column. The continuous line represents the refractive index. The shorter dashed lines underneath the dRI peaks are molecular weight estimates calculated from the refractive index and light scattering.

The molecular weight of Rep on its own was estimated at 71 kDa, close to the literature value of 77 kDa. No DnaB monomers were detected (52 kDa). However, the molecular weight of DnaB was only estimated at 245 kDa, lower than the theoretical mass of 314 kDa for a hexamer, likely due to problems with the refractive index of the DnaB sample that did not return the baseline. In the Rep+DnaB sample, only peaks corresponding to a Rep monomer (co-elution with the Rep only peak) and a DnaB hexamer (330 kDa) but no Rep-DnaB complex was detected. Although the Rep-DnaB interaction was observed by SPR, it is possible

that DNA is required to form a stable complex in solution. A DNA-Rep-DnaB complex can form, as indicated by bandshift analyses (Guy *et al.*, 2009). However, due to time constraints, this could not be followed up.

3.2.3   The DnaB C-terminus is a candidate for the interaction with Rep

The residues in DnaB that interact with Rep are unknown. However, the conservation of basic residues in the C-terminus among most Rep genes (Figure 3.4) suggests that acidic residues in DnaB may form an important part of the Rep-DnaB interface. Rep is found only in γ-proteobacteria, while other bacteria only encode a single UvrD, rather than Rep, homolog (Gwynn *et al.*, 2013). It was therefore investigated whether DnaB displays highly conserved acidic residues that are specific to γ-proteobacteria. Hence, sequence alignments of DnaB homologs were generated for γ-proteobacteria only (Figure 3.6) and for proteobacteria except γ-proteobacteria (Figure 3.7), to compare the conservation of DnaB sequences in general and to detect conserved acidic residues within γ-proteobacteria that would be candidates for the Rep-DnaB interaction.

DnaB among γ-proteobacteria is highly conserved, showing only some variation at the N-terminus (Figure 3.6A). The C-terminus also displays high sequence conservation and contains several conserved acidic amino acids, three at the very end of the *E. coli* DnaB C-terminus (D469, D470 and E471) as well as an aspartate eleven amino acids away from the end of the sequence (D461) (marked with *; Figure 3.6B). An additional aspartate is found in the DnaB C-terminus of several γ-proteobacteria (residue 534, Figure 3.6A), but this is not present in *E. coli* DnaB (Figure 3.6B).

DnaB genes from other proteobacteria revealed little sequence similarity (Figure 3.7). Although acidic residues were present in the C-terminus, they were much less conserved than in γ-proteobacteria (Figure 3.7). These differential patterns of sequence conservation support the hypothesis that acidic residues within DnaB from γ-proteobacteria form part of the interaction interface with Rep. These data also suggest that it is the C-terminus of DnaB that interacts with Rep.
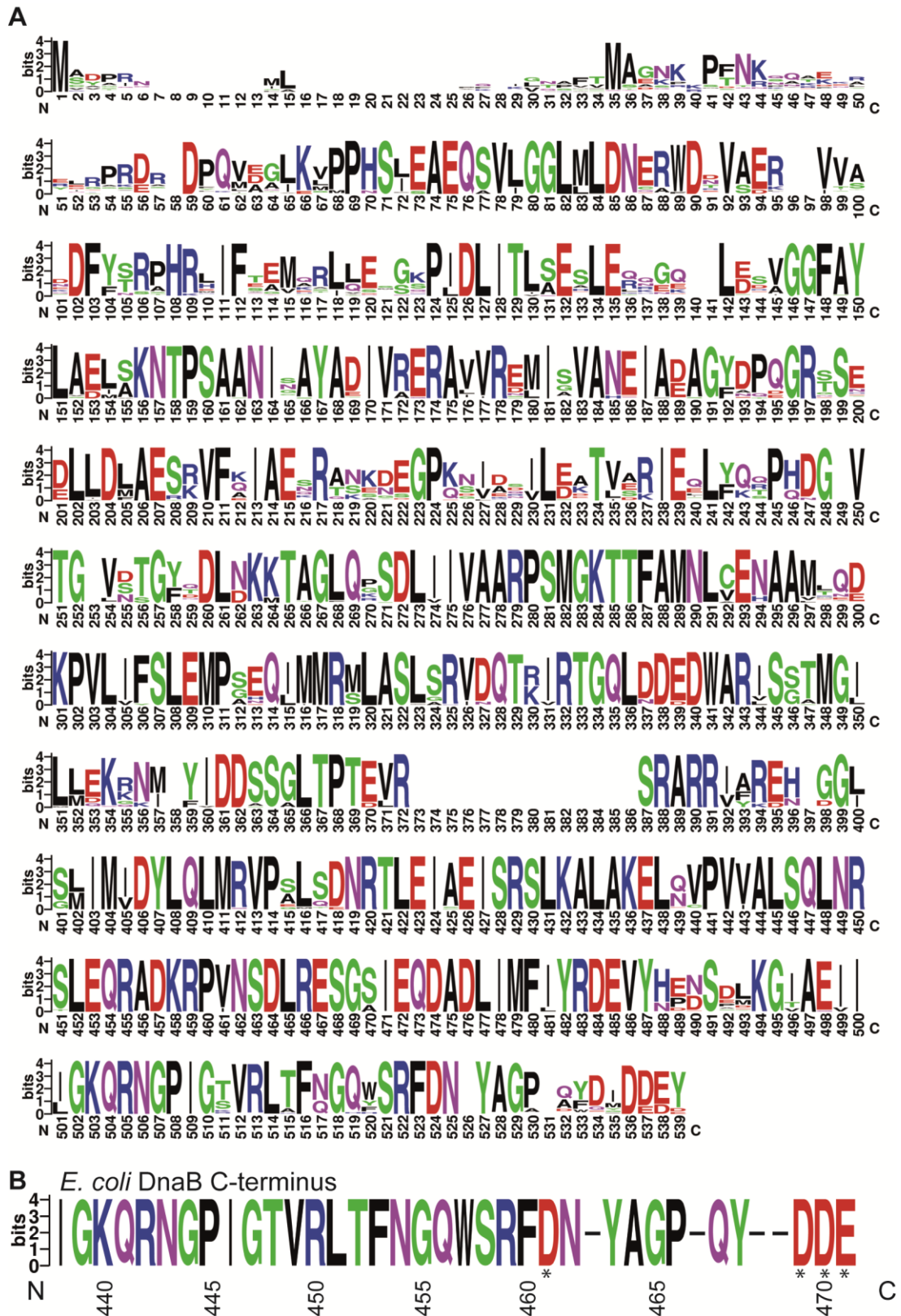
Figure 3.6 DnaB from γ-proteobacteria have conserved acidic residues in the C-terminus
(A) A Weblogo motif showing the sequence conservation of the DnaB genes from γ-proteobacteria. The Weblogo (Crooks *et al.*, 2004) was created from a multiple sequence alignment implemented in COBALT (Papadopoulos & Agarwala, 2007) from 471 DnaB sequences form γ-proteobacteria (Dereeper *et al.*, 2008). Note that the residue numbers do not represent the actual amino acid positions in individual DnaB genes (B) *E. coli* DnaB C-terminus from DnaB alignments. Numbering refers to *E. coli* DnaB residues. Asterisks indicating acidic residues of *E. coli* DnaB that could form a potential interaction interface with the *E. coli* Rep C-terminus.
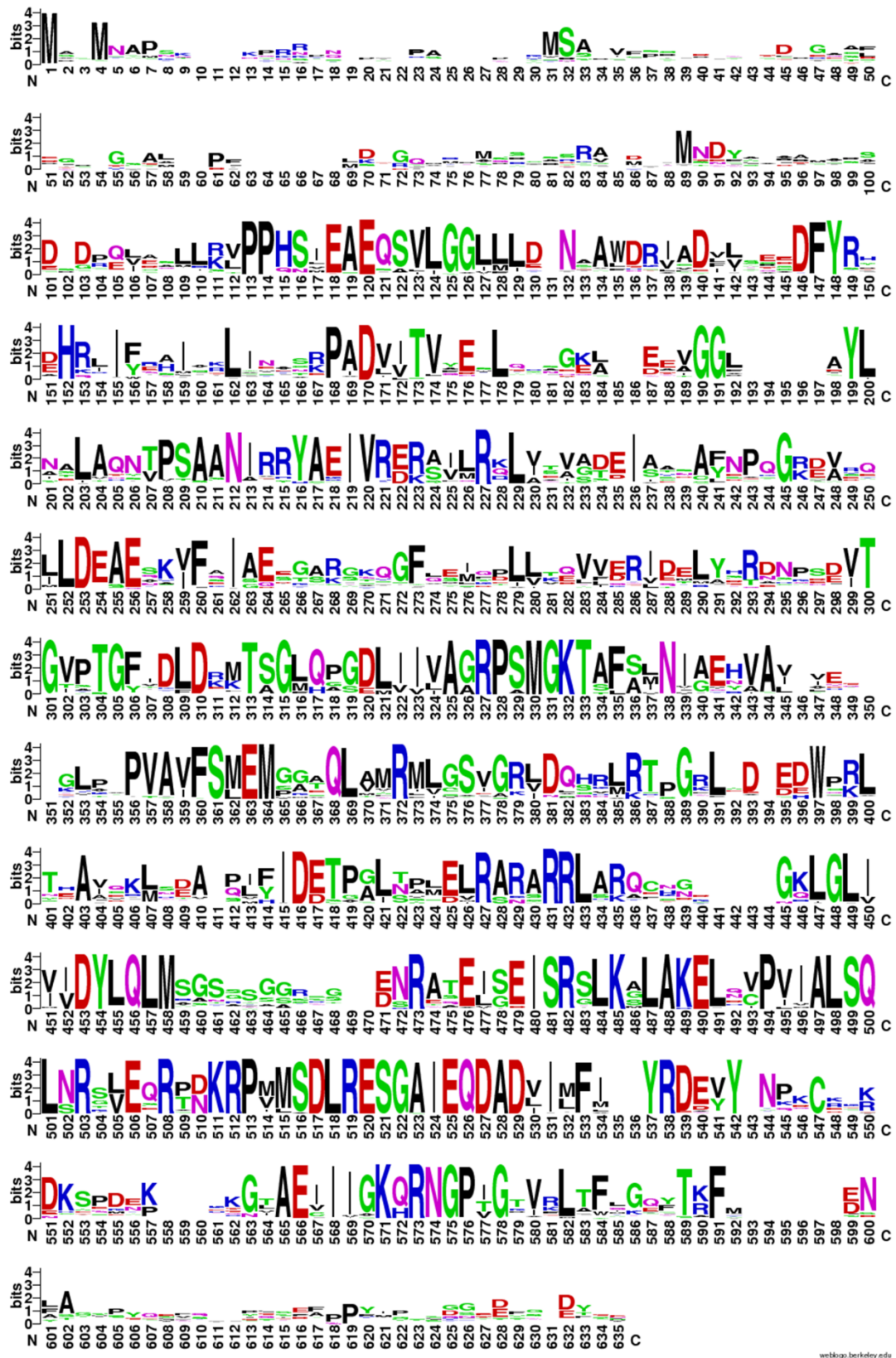
Figure 3.7 High sequence variation among DnaB genes outside of γ-proteobacteria
A Weblogo motif showing the sequence conservation of DnaB genes from different proteobacteria excluding γ-proteobacteria. The Weblogo (Crooks *et al.*, 2004) was created from a multiple sequence alignment implemented in COBALT (Papadopoulos & Agarwala, 2007) from 489 DnaB sequences with an e-value of 1e^{-100} (Dereeper *et al.*, 2008).

3.2.4 The *dnaB107^{ts}* allele

DnaB is an essential gene and cannot be deleted (Carl, 1970; Wechsler & Gross, 1971). Since cloning of a pRC7*dnaB* construct to complement a chromosomal deletion of *dnaB* failed (data not shown), genetic analysis to address the DnaB-Rep interaction was performed in a strain encoding a temperature sensitive *dnaB* allele, *dnaB107^{ts}* (Lark & Wechsler, 1975). The mutation of this *dnaB* allele was unknown and therefore sequenced. The *dnaB107^{ts}* allele contained a single base change (g617a) resulting in an amino acid substitution from glycine 206 to glutamate (Figure 3.8B). This residue is conserved among proteobacteria (corresponds to G301 in the sequence alignments in Figure 3.7; G252 Figure 3.6A. Note these numbers do not represent the actual amino acid positions in individual DnaB proteins). A sequence alignment of DnaB from *E. coli* and *B. stearothermophilus* (appendix Figure A.1) revealed that residue 206 in *E. coli* DnaB is located in the RecA-like C-terminal domain just after a linker domain (Figure 3.8A.ii), which is involved in DnaB hexamer formation (Bailey *et al.*, 2007; Itsathitphaisarn *et al.*, 2012).
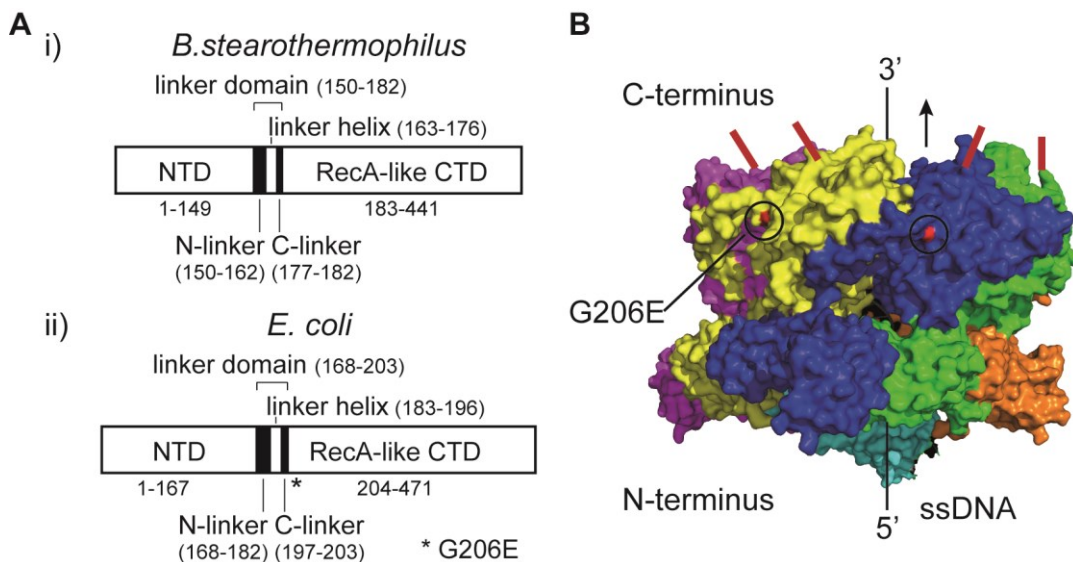
Figure 3.8 The mutation of the *dnaB107^{ts}* allele is located close to the linker region
(A) Domain organisation of the (i) *B. stearothermophilus* (adapted from (Itsathitphaisarn *et al.*, 2012)) and (ii) the *E. coli* DnaB monomer. The position of the domains of *Eco*DnaB is homologous to *Bst*DnaB based on a sequence alignment (Figure A.1). The asterisk indicates the G206E mutation in the *dnaB107^{ts}* allele. (B) Side view of *B. stearothermophilus* DnaB hexamer (PDB: 4ESV; (Itsathitphaisarn *et al.*, 2012)). DnaB monomers are differently coloured and encircle a strand of ssDNA in the central channel. The final 13 residues (ERRFDEAQIPPGA) of the DnaB C-terminus are unresolved and are indicated by a red line. The residue homologous to the *E. coli* G206E mutation is labelled red and encircled.

3.2.5   Complementation of *dnaB107*[ts] depends on the DnaB C-terminus

To identify a potential interaction interface of the DnaB C-terminus with Rep, different C-terminal truncations of DnaB (Figure 3.9A) were cloned under the control of an arabinose inducible promoter and tested for complementation of the temperature sensitivity of the *dnaB107*[ts] allele.

Overexpression of DnaB and the C-terminal truncations did not reduce colony formation in a wild-type background (*dnaB*[+]) at any temperature tested (Figure 3.9B), suggesting that the DnaB constructs are not toxic in a wild-type background.

DnaB107[ts] strains containing the empty vector were viable at 30°C, displaying growth up to the highest dilution tested (pBAD, Figure 3.9C.i). However, no growth was observed at 37°C or 42°C in the absence of a complementing *dnaB* gene (pBAD, Figure 3.9C.ii and iii), confirming the temperature sensitivity of this *dnaB*[ts] allele (Lark & Wechsler, 1975).

Expression of wild-type *dnaB* did not affect the growth of the strain at the permissive temperature, suggesting that DnaB overexpression is not toxic in a *dnaB107*[ts] background (pBAD*dnaB*, Figure 3.9C.i). Additionally, expression of wild-type *dnaB* restored growth of the strain at the non-permissive temperatures (pBAD*dnaB*, Figure 3.9C.ii and iii). However, high levels of expression (+arabinose) were required to fully complement viability to levels compared to the non-permissive temperature, while in the absence of arabinose growth was two orders of magnitude lower.

Overexpression of DnaB with deletions of up to nine amino acids from the C-terminus phenocopied wild-type DnaB. These mutants slightly improved colony size at the permissive temperature (Figure 3.9C.i), suggesting that these DnaB mutants are also not toxic in a *dnaB107*[ts] background. Growth at the non-permissive temperatures was restored at low levels of expression to similar levels than wild-type DnaB and also required the presence of arabinose for full complementation (Figure 3.9C.ii and iii). DnaB mutants with longer truncations (DnaBΔC12-33) did not affect the growth of the *dnaB107*[ts] strain in the absence of
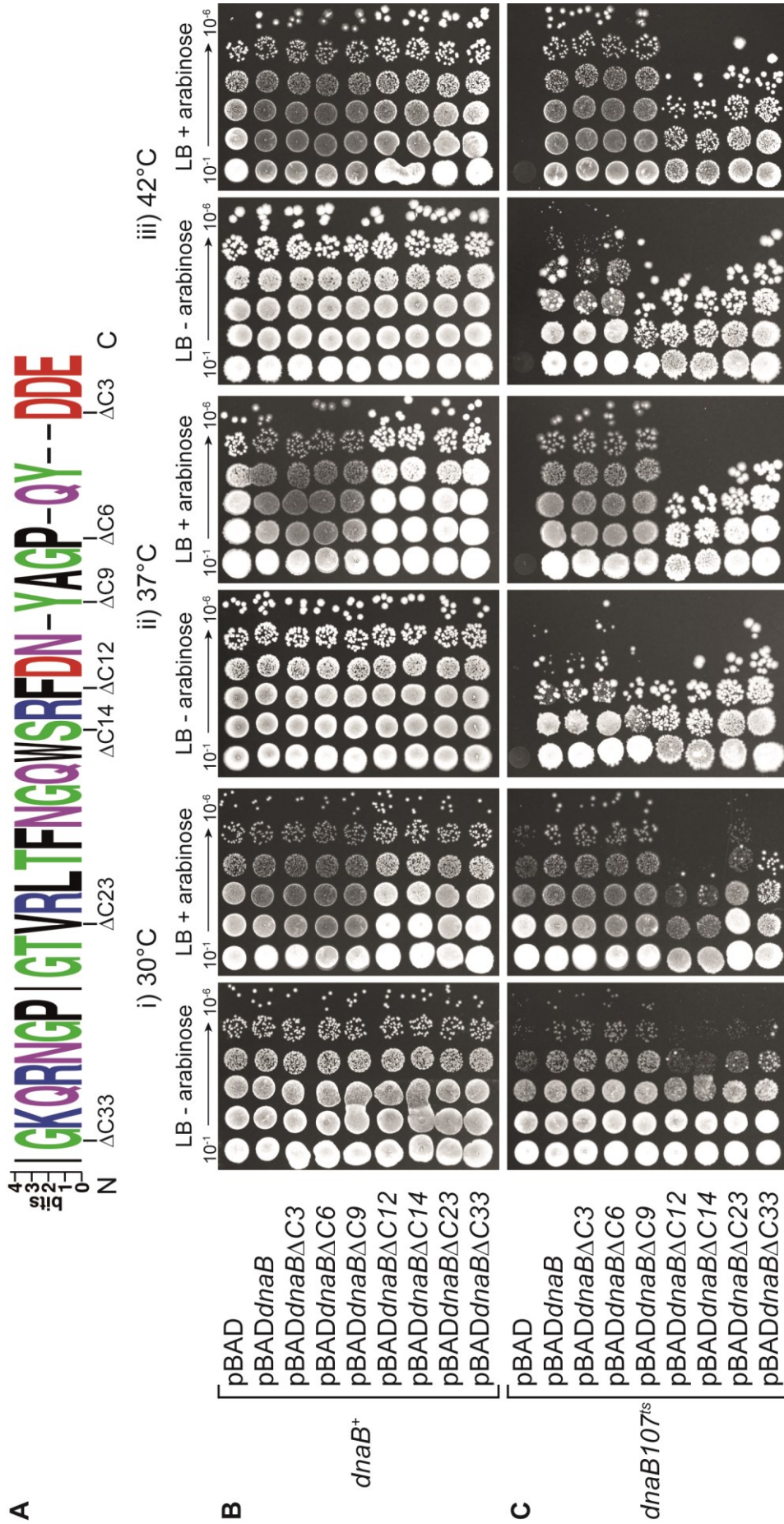
Figure 3.9 Efficient complementation of *dnaB107^ts* is dependent on the last 12 amino acids of the DnaB C-terminus
(A) *E. coli* DnaB C-terminal amino acids with indicated truncations of the respective C-terminal deletions. Colony formation of (B) *dnaB^+* (TB28) and (C) *dnaB107^ts* (JGB045) strains with different pBAD derivatives at (i) 30°C, (ii) 37°C and (iii) 42°C after growth at 30°C in LB and plating of serial dilutions on LB agar with ampicillin ± arabinose (n=2).

arabinose. Overexpression of these constructs however caused a slight reduction in viability (Figure 3.9C.i). At the non-permissive temperatures, these mutants restored growth similar to wild-type *dnaB* in the absence of arabinose but did not further improve the viability at increased levels of expression (+arabinose) (Figure 3.9C.ii and iii).

Thus, efficient complementation of the temperature sensitivity of *dnaB107^ts* was dependent on the last twelve amino acids of the DnaB C-terminus. Truncated proteins harbouring deletions of more than twelve amino acids lacked all four acidic residues of the *E. coli* DnaB C-terminus (Figure 3.9A), which were proposed to be required for the interaction between Rep and DnaB (see above).

To test whether the complementation of the temperature sensitivity by the DnaB mutants was an effect resulting from the interaction between Rep and DnaB, *dnaB107^ts rep* or *dnaB107^ts uvrD* double mutants were going to be generated. It was hypothesised that in a *Δrep dnaB107^ts* mutant, where the Rep-DnaB interaction is absent in the first place, complementation of the temperature sensitivity by the DnaB mutants should be independent of the C-terminal deletion of DnaB. However, in a *ΔuvrD dnaB107^ts* strain efficient complementation of the temperature sensitivity would depend on the Rep-DnaB interaction. DnaB C-terminal mutants that failed to recruit Rep to the replisome were expected to show a reduction in growth compared to DnaB C-terminal mutations that retained the Rep-DnaB interaction.

Transductions of the *dnaB107^ts* allele into *Δrep* or *ΔuvrD* mutants or vice versa failed (data not shown), suggesting a synthetic lethality between the *dnaB107^ts* allele and these helicase mutants. Transductions of the *dnaB107^ts* allele were therefore attempted in *Δrep* and *ΔuvrD* strains bearing complementing pRC7*rep* or pRC7*uvrD* plasmids, respectively (Guy *et al.*, 2009; Mahdi *et al.*, 2006). However, only a *dnaB107^ts Δrep* strain (JGB103) was obtained, but no *dnaB107^ts ΔuvrD* strain could be generated. Additional attempts and alternative transduction strategies had to be abandoned due to time constraints.
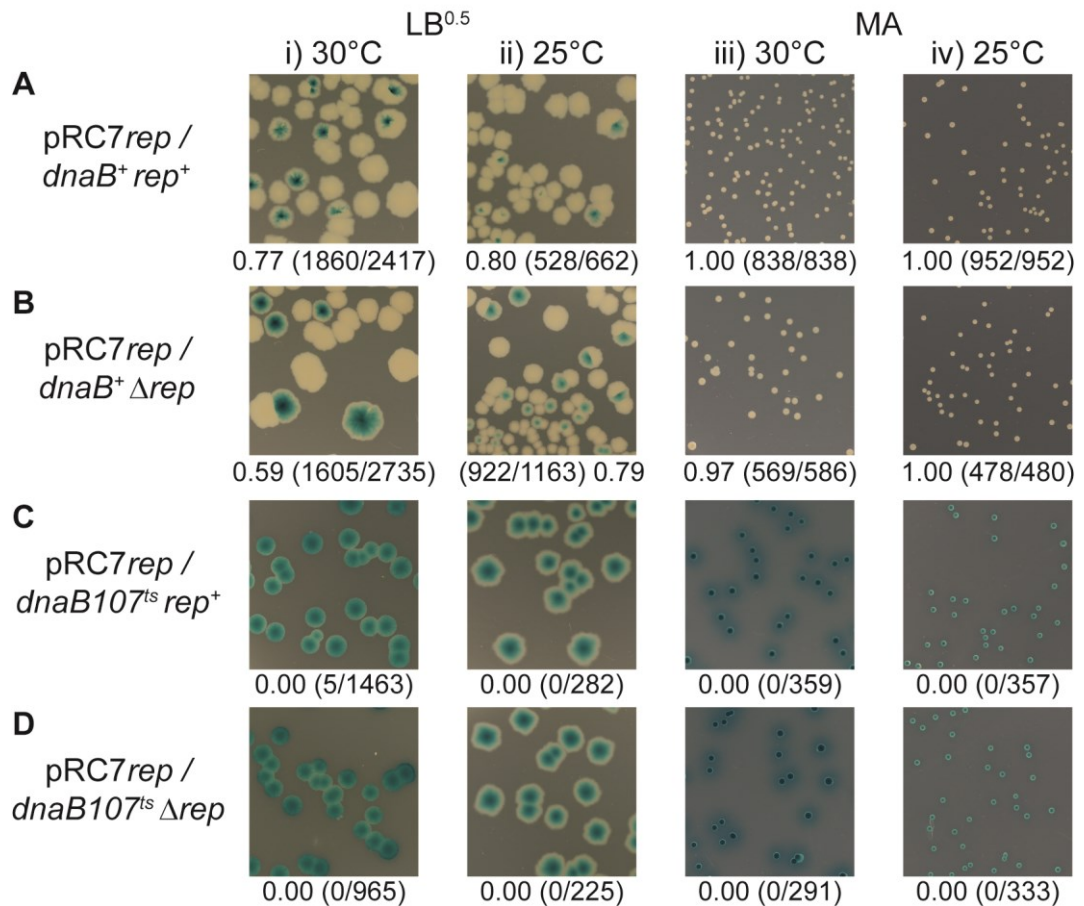
Figure 3.10 Strains bearing the *dnaB107^{ts}* allele do not lose pRC7*rep*
Blue/white screening for loss or retention of pRC7*rep* in (A) *rep^+ dnaB^+* (TB28), (B) *Δrep dnaB^+* (N6540), (C) *rep^+ dnaB107^{ts}* (JGB070) and (D) *Δrep dnaB107^{ts}* (JGB103) strains on LB$^{0.5}$ plates grown at (i) 30°C and (ii) 25°C or minimal agar plates grown at (iii) 30°C or (iv) 25°C in presence of IPTG and X-Gal. Fractions of white colonies are given from three independent experiments, with numbers of white and total numbers of colonies in brackets.

To test for complementation of the *dnaB107* temperature sensitivity by different pBAD*dnaB* derivatives, the pRC7*rep* plasmid had to be lost from the *Δrep dnaB107^{ts}* strain. This was monitored by blue/white screening of the *Δrep dnaB107^{ts}* strain and the respective single mutant and wild-type controls on plates containing X-gal and IPTG. The strains were grown at 30°C and also 25°C on LB$^{0.5}$ and minimal agar to maintain the temperature sensitive *dnaB* allele and also decrease the growth rates to reduce the need for Rep activity by decreasing the amounts of replication/transcription conflicts.

In a *rep^+ dnaB^+* (wild-type) or *Δrep dnaB^+* strain loss of pRC7*rep*, indicated by the appearance of white colonies, occurred under all conditions tested (Figure 3.10A and B). On the other hand, the pRC7*rep* plasmid could not be lost from the *Δrep*

dnaB107[ts] or even the *rep*[+] *dnaB107*[ts] strain (Figure 3.10C and D). This was not affected by growth at a lower temperature (Figure 3.10 ii and iv) or growth on minimal medium (Figure 3.10 iii and iv). Since single mutations of *dnaB107*[ts] are viable at 30°C, this suggests that increased levels of Rep due to the presence of pRC7*rep* are advantageous for cell survival in the presence of the *dnaB107*[ts] allele. Alternatively, it is possible that pRC7*rep* has integrated into the chromosome, given that the *dnaB107*[ts] allele displays increased levels of recombination even at its permissive temperature of 30°C (Saveson & Lovett, 1997).

3.2.6   Overexpression of *dnaB* is toxic in the absence of Rep

Due to the synthetic lethality between *dnaB107*[ts] and *rep* or *uvrD* mutants, the overexpression of the C-terminal truncations of DnaB had to be tested in *dnaB*[+] Δ*rep* and *dnaB*[+] Δ*uvrD* strains.

Approximately 500 DnaB hexamers are present in a wild-type cell (TB28) (Atkinson, 2007). Due to time constraints, the levels of pBAD-expressed DnaB could not be tested. However, Rep and UvrD overexpression from the same plasmid background results in approximately 4000-8000 and 1000-3000 molecules per cell in the presence of arabinose, respectively (J. Atkinson, unpublished data). At similar levels of expression of the pBAD*dnaB* constructs, DnaB hexamers would largely be composed of the DnaB mutants. If these truncated DnaB mutants would not interact with Rep anymore, colony formation could be reduced in the absence of UvrD, similar to a Δ*uvrD rep*Δ*C33* strain (Atkinson *et al.*, 2011b), as accessory replicative helicase function of Rep would not be efficiently targeted to replication forks anymore. In contrast, growth in a Δ*rep* background would not be affected by the overexpression of DnaB mutants compared to the control, since the Rep-DnaB interaction would be absent in all cases and accessory replicative helicase function would be provided by UvrD, due to its high intracellular concentration.

Since efficient complementation of the temperature sensitivity of *dnaB107*[ts] showed a significant difference between DnaBΔC9 and DnaBΔC12, only DnaBΔC9,

DnaBΔC12 were tested in the *dnaB*⁺ backgrounds using full length DnaB and DnaBΔC33 as controls.

In a wild-type background, the overexpression of DnaB mutants did not have a significant effect on cell growth (Figure 3.11A), as seen before (Figure 3.9A.ii). In a *Δrep* mutant, cells grew as good as the wild-type strain in the presence of the empty vector control (Figure 3.11B). Low levels of expression of the DnaB truncations did not affect the viability of the strain (Figure 3.11B.i). However, overexpression of any DnaB construct in the absence of Rep was lethal. Overexpression of full length DnaB and DnaBΔC9 completely prevented cell growth, whereas DnaBΔC12 and DnaBΔC33 retained colony formation at a low level (Figure 3.11B.ii). In contrast, DnaB overexpression did not have any effect on a *ΔuvrD* strain apart from a slight reduction in colony size upon growth in the presence of arabinose (Figure 3.11C).
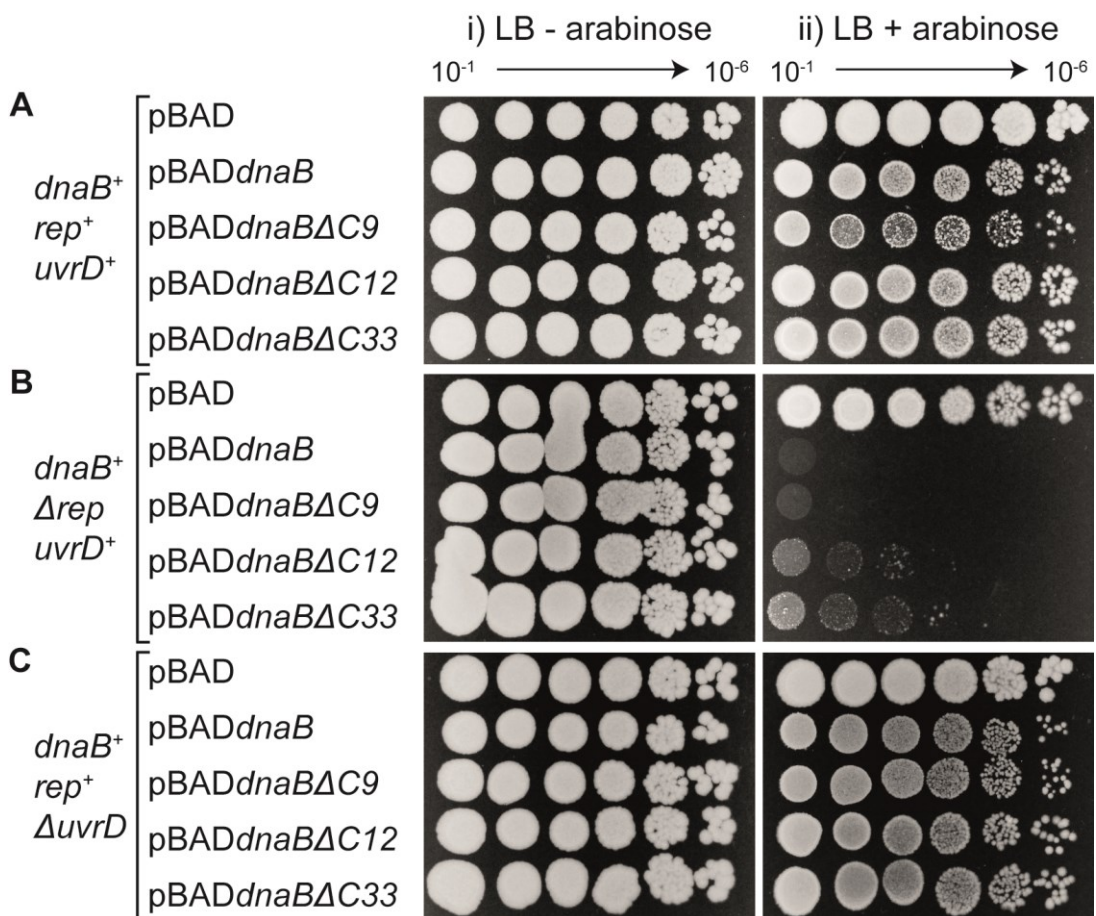
Figure 3.11 Overexpression of DnaB is toxic in the absence of Rep
Colony formation of (A) *rep*⁺ *uvrD*⁺ (TB28), (B) *Δrep uvrD*⁺ (N6577) and (C) *rep*⁺ *ΔuvrD* (N6632) strains with different pBAD derivatives after growth in LB and plating of serial dilutions on LB agar with kanamycin ± arabinose (n=3).

These results are out of line with the hypothesis postulated above and the toxicity resulting from DnaB overexpression in a *Δrep* strain is likely not related to the presence or absence of the Rep-DnaB interaction but due to time constraints, further investigation of this phenotype and the reason for the toxicity could not be performed.

3.3   Discussion

In this chapter, the interaction between the replicative helicase DnaB and the accessory replicative helicase Rep from *E. coli* was investigated. This interaction is crucial for efficient promotion of replication fork movement through nucleoprotein blocks *in vitro* and correlates with complementation of viability by low levels of Rep *in vivo* (Figure 3.1) (Guy *et al.*, 2009). In crystal structures of Rep, the final 33 amino acids of the C-terminus are not resolved and it was initially shown that these residues are involved in the interaction with DnaB (Guy *et al.*, 2009; Korolev *et al.*, 1997). The data presented here indicate that the interaction between Rep and DnaB requires the last four amino acids of the Rep C-terminus, K670 R671 G672 and K673 (Figure 3.1 and Figure 3.4). In line with this, sequence alignments of Rep proteins from different bacteria showed that positive charges are a conserved feature of the Rep C-terminus. Due to time constraints and experimental difficulties it could not be tested whether the DnaB-Rep interaction was dependent on a specific residue (e.g. R671, based on a high level of conservation of a positively charged amino acid; Figure 3.4) or on positively charged residues in the Rep C-terminus in general. However, in the light of these results it is likely that the interaction between Rep and DnaB is mediated via ionic interactions between the positively charged Rep C-terminus and negatively charged residues on DnaB.

In line with this hypothesis, sequence analysis of DnaB genes from proteobacteria indicated high levels of conservation of acidic residues only in γ-proteobacteria, the only class of bacteria where *rep* genes have been found (Gwynn *et al.*, 2013) (Figure 3.6 and Figure 3.7). Moreover, the Rep-DnaB interaction has been shown to be species specific, with Rep showing only a very low affinity interaction with DnaB of the Gram-positive bacterium *B. stearothermophilus* (Guy *et al.*, 2009), which lacks acidic residues in the C-terminus.

DNA replication in a *dnaB107^{ts}* strain is almost immediately shut-down upon the change to the non-permissive temperature (Sclafani & Wechsler, 1981), which made this allele ideal to test the effect of the DnaB C-terminal mutants. However, the G206E mutation in *dnaB107^{ts}* is located close to the flexible linker domain, which is involved in the formation of DnaB hexamers (Bailey *et al.*, 2007; Barcena *et*

al., 2001) (Figure 3.8). It was proposed that hexamerisation is less stable resulting in more frequent replication fork breakdown, explaining why even at the permissive temperature, *dnaB107^{ts}* strains display increased levels of recombination (Lovett, 2006; Saveson & Lovett, 1997; Saveson & Lovett, 1999). Consequently, the possible synthetic lethality of *dnaB107^{ts}* and *rep* or *uvrD* (section 3.2.5) could be caused by the absence of antirecombinase activity of UvrD and a lack of accessory replicative helicase activity to prevent replication fork breakdown by Rep (and UvrD) (Guy *et al.*, 2009; Veaute *et al.*, 2005). More detailed investigations of the effect of DnaB mutant overexpression with respect to Rep interaction were therefore not possible in the *dnaB107^{ts}* background. Generation of *dnaB^{ts} rep* or *uvrD* double mutants could be attempted in a different temperature sensitive *dnaB* strain that does not show such severe growth defects (Sclafani & Wechsler, 1981; Wechsler & Gross, 1971).

Genetic analysis of C-terminal DnaB deletion mutants in the temperature sensitive *dnaB107^{ts}* mutant however indicated a crucial role for the final twelve amino acids of the DnaB C-terminus (Figure 3.9). The C-terminal side of the DnaB hexamer faces towards the 3' end of ssDNA (Galletto *et al.*, 2003; Itsathitphaisarn *et al.*, 2012). In the context of the replication fork the C-terminal side of DnaB is therefore closest to the ss/dsDNA junction (Jezewska *et al.*, 1998b). An interaction of Rep with the DnaB C-terminus would therefore place Rep close to the fork junction (as shown in Figure 1.18A), where Rep would be in an ideal position to remove nucleoprotein complexes ahead of the replication fork. *E. coli* DnaB has not been crystallised yet. However, in the crystal structures of the *B. stearothermophilus* DnaB hexamer, the last 13 amino acids of the DnaB C-terminus are not resolved (Figure 3.8B; PDB: 4ESV (Itsathitphaisarn *et al.*, 2012) and PDB: 2R6D (Bailey *et al.*, 2007)), suggesting that they are flexible and potentially available to form protein-protein interactions. In support of this hypothesis, it was shown that binding of the helicase loader protein DnaC to DnaB prevents the formation of the Rep-DnaB interaction (Guy *et al.*, 2009). DnaC interacts with the C-terminal face of DnaB and the DnaB-DnaC complex might therefore block or even occupy a shared interaction interface of Rep on DnaB (Barcena *et al.*, 2001). Indeed, yeast-2-hybrid screens in our lab showed that

DnaBΔC3 had a reduced affinity for DnaC and Rep compared to the full length DnaB protein (M. Gupta, unpublished data).

Since the *dnaB107^{ts}* temperature sensitivity was complemented by DnaBΔC3 as efficiently as by full-length DnaB, the complementation was likely not related to the recruitment of Rep to DnaB. Therefore, more direct approaches, such as SPR or pull downs are necessary to verify whether the Rep-DnaB interaction is dependent on the last three DnaB amino acids. It is possible that the DnaB truncations can increase the stability of DnaB heterohexamers with DnaB107, thereby complementing the hexamerisation defects and consequently the temperature sensitivity of *dnaB107^{ts}* (Saveson & Lovett, 1997).

The reason for different phenotypes between DnaBΔC9 and DnaBΔC12 still remains unclear. DnaB mutants that lack the C-terminal region only form DnaB dimers but not hexamers (Biswas & Biswas, 1999). Hexamerisation could therefore also be compromised in DnaBΔC12-33. This could be tested *in vitro*, e.g. by SEC-MALLS (Figure 3.5). Nonetheless, in the presence of chromosomal full-length DnaB107 proteins hexamer formation might occur, as DnaBΔC12 to DnaBΔC33 complemented the temperature sensitivity of *dnaB107^{ts}* (Figure 3.9B.ii and iii).

DnaB overexpression in a *dnaB^{+} Δrep* background was lethal (Figure 3.11B). It had been reported before that DnaB overexpression induces recombination due to increased DNA breaks (Yamashita *et al.*, 1999). Rep is likely required to prevent replication fork stalling and collapse in these strains. Further investigation of this phenotype is required to shed light on the effects of DnaB overexpression on other repair pathways.

In summary, the data presented here suggest an interaction between Rep and DnaB that is mediated via ionic interactions of their C-termini positioning Rep in an ideal location at the replication fork junction for nucleoprotein displacement.

Chapter 4

ANALYSIS OF THE FUNCTION OF THE 2B SUBDOMAIN OF REP

Chapter 4 – Analysis of the function of the 2B subdomain of Rep

4.1 Introduction

Superfamily 1A helicases like Rep, UvrD or PcrA are the most extensively studied DNA helicases. They share a common structure with two main domains (1 and 2) that are further subdivided into two subdomains (A and B; Figure 4.1A) (Bird *et al.*, 1998). All seven conserved helicase motifs necessary for the translocation along ssDNA are found in subdomains 1A and 2A (Figure 1.3) (Gorbalenya & Koonin, 1993; Korolev *et al.*, 1997; Lee & Yang, 2006). Crystal structures of UvrD and PcrA revealed that the 2B subdomain makes contacts with the DNA duplex (Figure 1.4) and it was proposed that the 2B subdomain acts as a wrench to assist DNA unwinding (Lee & Yang, 2006; Velankar *et al.*, 1999). In contrast to this idea, the 2B subdomain of Rep is dispensable for helicase function, with RepΔ2B, a mutant lacking the 2B subdomain (Figure 4.1B), displaying increased levels of DNA unwinding (Cheng *et al.*, 2002).
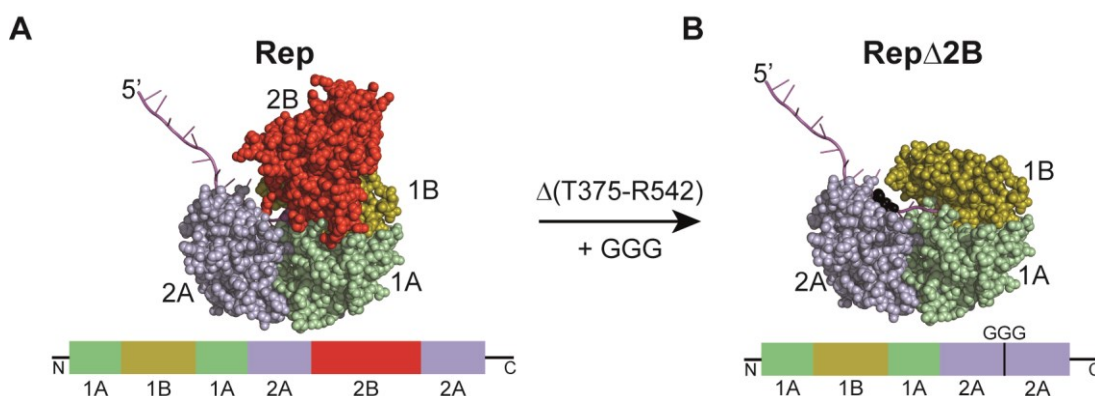
Figure 4.1 The RepΔ2B mutation
(A) Crystal structure of wild-type Rep (PBD: 1UAA; (Korolev *et al.*, 1997)). (B) Hypothetical structure of RepΔ2B, where the 2B subdomain has been replaced with three glycines (in black). Colour legend: 1A – green, 1B – yellow, 2A – blue, 2B – red, DNA – magenta.

Wild-type Rep and other SF1 helicases are thought to require multiple monomers for DNA unwinding in the absence of other factors, e.g. SSB (Byrd & Raney, 2005; Cheng *et al.*, 2001; Maluf *et al.*, 2003; Yang *et al.*, 2008). However, in the absence of

the 2B subdomain, monomers of RepΔ2B were activated for DNA unwinding, albeit displaying only a low processivity. The processivity of ssDNA translocation by RepΔ2B (800 nt) was similar to that of wild-type Rep (700 nt), but RepΔ2B displayed an approximately twofold increase in ssDNA translocation speed (Brendza *et al.*, 2005). It was therefore proposed that the 2B subdomain has an autoinhibitory function with respect to Rep helicase activity and ssDNA translocation (Brendza *et al.*, 2005).

RepΔ2B is a functional helicase *in vivo*, as it supports replication of φX174 at a similar efficiency to wild-type Rep (Cheng *et al.*, 2002). Nonetheless, only a few SF1 helicases exist that naturally lack the 2B subdomain (e.g. *E. coli* HelD; Figure A.2) (Dillingham, 2011) and the exact function of the 2B subdomain remains elusive. However, the inability of HelD, but not Rep, to efficiently unwind a DNA duplex that was bound by a single *lac* repressor-operator complex (Yancey-Wrona & Matson, 1992), first suggested a function of the 2B subdomain in nucleoprotein displacement.

In this chapter, the function of the 2B subdomain of SF1A helicases is investigated via the characterisation of RepΔ2B and RepΔ2B^{uvrD2B}, a Rep mutant that contains the 2B subdomain of the related (38% amino acid identity) and structurally similar SF1A helicase UvrD (Figure 4.2) (Gilchrist & Denhardt, 1987).
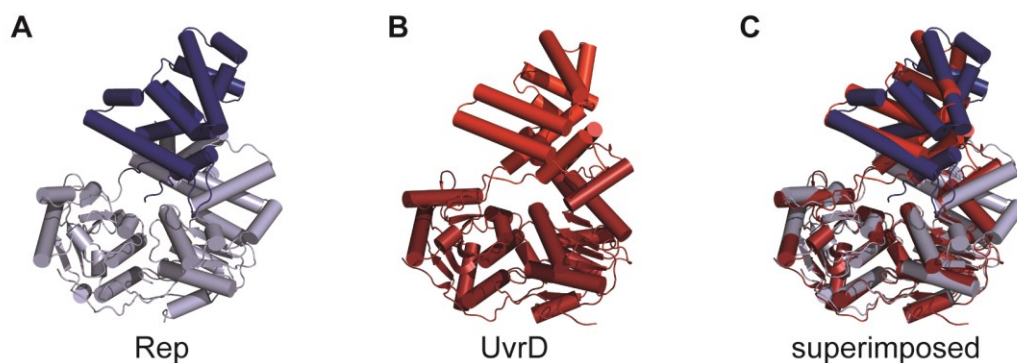
Figure 4.2 Rep and UvrD are highly similar in structure
(A) Crystal structure of Rep (PDB: 1UAA; (Korolev *et al.*, 1997)) and (B) UvrD (PDB: 2IS1; (Lee & Yang, 2006)) in cartoon representation (C) Superimposition of Rep and UvrD structures illustrating the structural similarity between both helicases.

4.2   Results

4.2.1   The hyperactive helicase RepΔ2B

It was shown previously, that the 2B subdomain of Rep is dispensable for Rep function as RepΔ2B (untagged and His-tagged) displayed increased levels of DNA unwinding on short duplex substrates (Cheng *et al.*, 2002).

DNA unwinding by biotinylated Rep and biotinylated RepΔ2B was tested on a DNA fork with 60 base pairs duplex DNA and two ssDNA arms of 38 bases. DNA unwinding of bio-RepΔ2B resulted in increased helicase activity compared to bio-Rep (Figure 4.3). Thus, RepΔ2B was a hyperactive helicase also on the DNA substrate used in this assay.
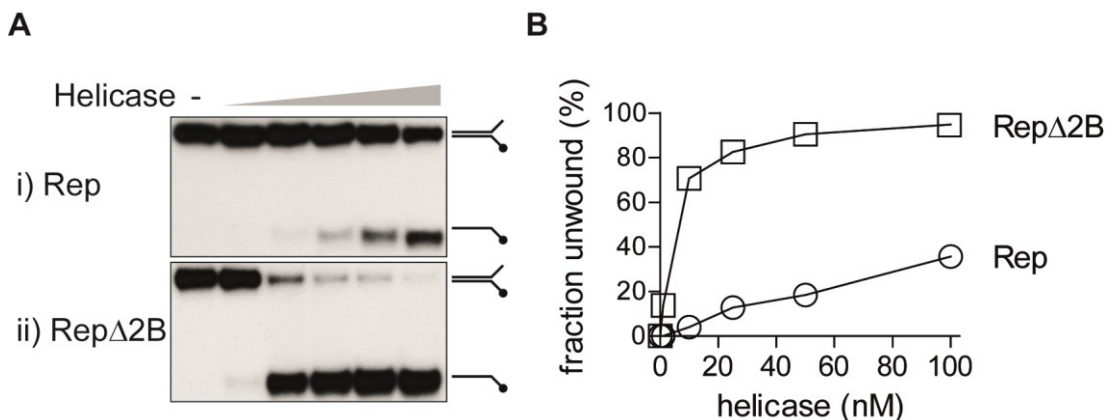
Figure 4.3 RepΔ2B is a hyperactive helicase
(A) DNA unwinding by (i) Rep and (ii) RepΔ2B (1, 10, 25, 50 and 100 nM) on DNA fork structures with 60 bp dsDNA (CC139+CC140). (B) Fractions of unwound DNA for different helicase concentrations. Error bars represent standard error of the mean (n=5).

In addition to (or because of) the physical interaction between Rep and DnaB (see Chapter 3), Rep and DnaB also display functional cooperativity as displayed by enhanced levels of DNA unwinding when both helicases are present at a DNA fork (Guy *et al.*, 2009). Such cooperativity was not observed with a helicase-deficient Rep mutant, Rep K28A (Atkinson *et al.*, 2011a), which indicates that the helicase activity of Rep is essential for the cooperativity.

The level of DNA unwinding by Rep and DnaB was stimulated about 2-2.5 fold compared to the sum of DNA unwinding by Rep and DnaB on their own (Figure 4.4A.i and C), similar to what was reported before (Guy *et al.*, 2009). RepΔ2B did not display cooperativity with DnaB (Figure 4.4C), although it was shown that the 2B subdomain is dispensable for the Rep-DnaB interaction (Guy *et al.*, 2009). However, the levels of DNA unwinding by RepΔ2B alone were already higher than the levels of DNA unwinding by Rep and DnaB together (Figure 4.4B), suggesting that either no further stimulation of the RepΔ2B helicase activity could occur or that the 2B subdomain of Rep is essential for the Rep-DnaB cooperativity.
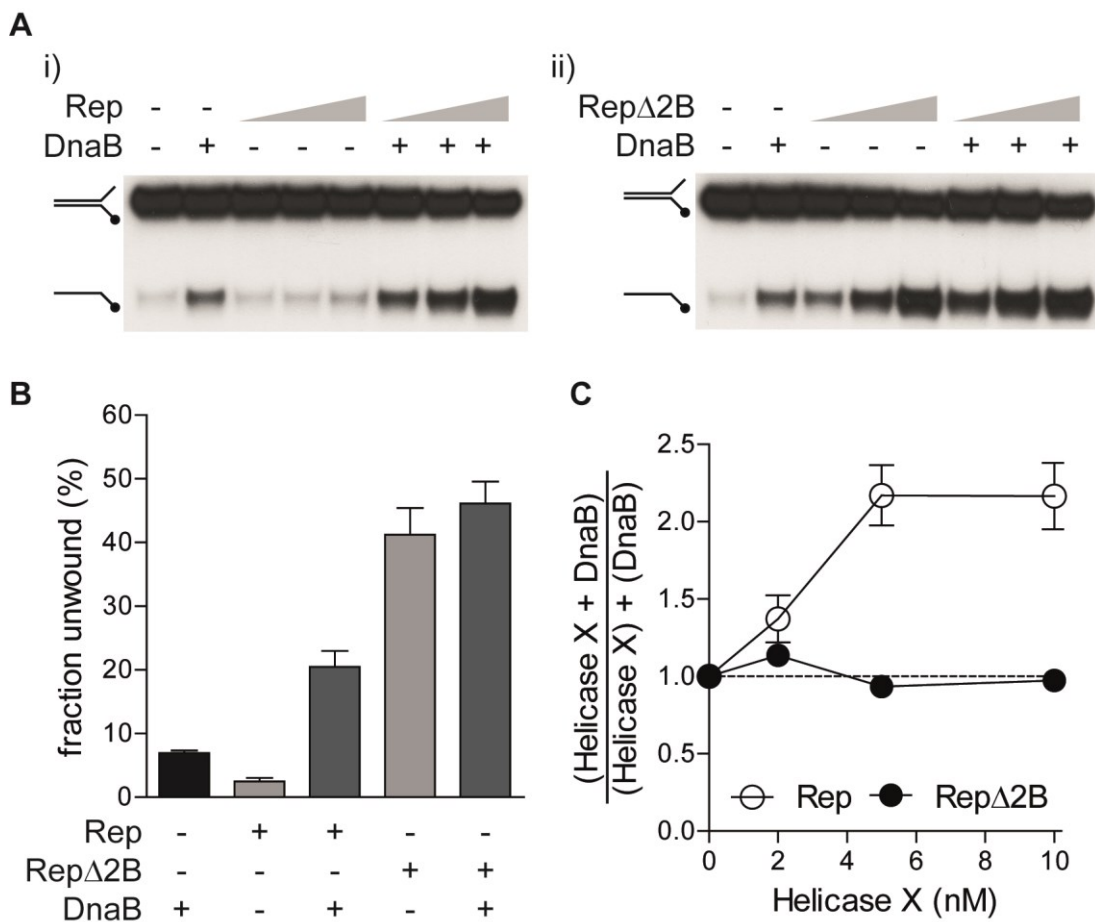
Figure 4.4 RepΔ2B does not cooperate with DnaB in DNA unwinding
(A) Cooperativity of DNA unwinding by (i) Rep and (ii) RepΔ2B (2, 5 and 10 nM) without and with DnaB (100 nM hexamers) on DNA fork structures with 60bp duplex DNA (CC139+CC140). (B) Fractions of unwound DNA by 10 nM Rep(Δ2B) without and with DnaB. (C) Cooperativity in DNA unwinding shown as fractions of unwound DNA by Rep(Δ2B) with DnaB compared to the sum of the individual levels of DNA unwinding by the two individual helicases. Error bars represent standard error of the mean (n=5).

4.2.2   RepΔ2B does not complement wild-type Rep function *in vivo*

4.2.2.1   RepΔ2B does not complement the *Δrep ΔuvrD* lethality on rich medium

It was reported that RepΔ2B is a functional helicase *in vivo*, since RepΔ2B is able to promote replication of phage ϕX174, which is dependent on unwinding of the double stranded replicative form of the phage by Rep *in vivo* (Cheng *et al.*, 2002). However, this assay failed to address the role of Rep in the context of the *E. coli* replisome. It was suggested that the lethality of *Δrep ΔuvrD* double mutants on rich medium could be caused by the lack of accessory replicative helicase activity to cope with replication-transcription conflicts (Guy *et al.*, 2009). Therefore, different plasmid-encoded Rep constructs were expressed from an arabinose inducible promoter (P_{BAD}) and assayed for their ability to complement the *Δrep ΔuvrD* rich medium lethality *in vivo*.

In a wild-type background (*rep$^+$ uvrD$^+$*), only RepΔ2B significantly affected the growth of the strain (Figure 4.5A.ii). The expression of RepΔ2B was toxic, as indicated by smaller colony sizes at high levels of expression (+arabinose; Figure 4.5A.ii). This toxicity was dependent on the interaction of RepΔ2B with DnaB, since RepΔ2BΔC33, which lacks the Rep C-terminus that is required for the interaction between Rep and DnaB, restored normal colony size (Figure 4.5A.ii).
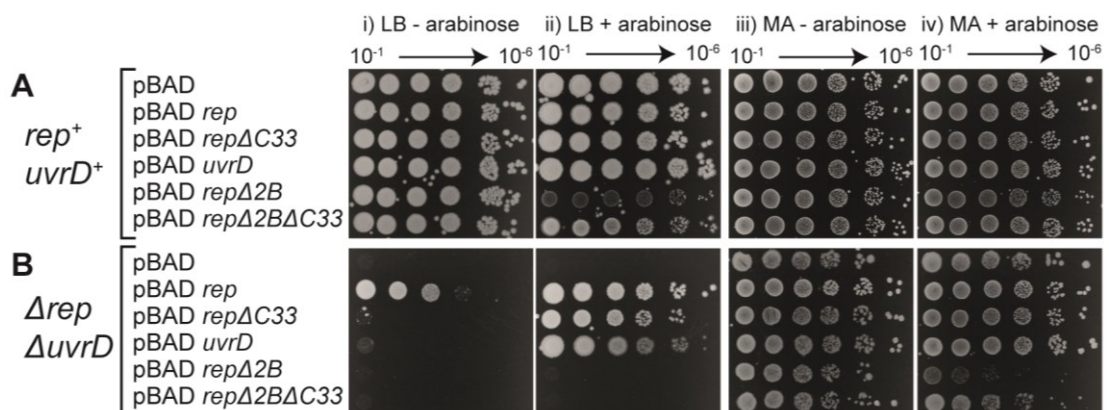
Figure 4.5 RepΔ2B cannot complement growth of a *Δrep ΔuvrD* strain on rich medium *in vivo*
(A) *rep$^+$ uvrD$^+$* (N6524) and (B) *Δrep ΔuvrD* (N6556) cells lacking the pRC7*rep* plasmid but carrying the denoted helicases were grown in liquid minimal medium, serially diluted and spotted on LB or MM agar containing kanamycin ± arabinose (n=2).

In a *Δrep ΔuvrD* background in the absence of a plasmid-encoded helicase (the empty pBAD), growth occurred only on minimal agar, but not rich medium (Figure 4.5B.ii and iv). This is because under slower growth conditions the levels of replication/transcription conflicts are reduced and cells therefore do not require an accessory replicative helicase (Guy *et al.*, 2009). Wild-type Rep was the only helicase tested that was able to restore growth in the absence of arabinose (Figure 4.5D.i). On the other hand, RepΔC33 which does not interact with DnaB needed increased levels of expression to compensate for the reduced efficiency of recruitment to the replisome (Guy *et al.*, 2009). Similarly, UvrD, which interacts with RNA polymerases rather than components of the replisome (Gwynn *et al.*, 2013), was therefore only able to complement the synthetic lethality of the *Δrep ΔuvrD* mutant by the virtue of high cellular concentrations (Figure 4.5D.ii). RepΔ2B, despite being functional in the replication of φX174 DNA (Cheng *et al.*, 2002), was not able to complement the rich medium lethality either at low or high levels of expression (Figure 4.5D.i and ii). Additionally, RepΔ2B was toxic when overexpressed in cells grown on minimal agar, as shown by the decrease in growth by three orders of magnitude (Figure 4.5B.iv). In the absence of the interaction with DnaB, RepΔ2BΔC33 was still unable to support growth on rich medium (Figure 4.23D.i and ii), but the toxicity seen for RepΔ2B on minimal agar was reduced (Figure 4.5D.iv). These results suggest that RepΔ2B is toxic when it interacts with DnaB and consequently with the replisome and that the 2B subdomain of Rep is essential for Rep function *in vivo*.

4.2.2.2 RepΔ2B cannot complement the *rep recB* lethality *in vivo*

The deletion of Rep is synthetically lethal in combination with the deletion of the helicase/exonuclease complex RecBCD, which is involved in DNA end-resection at double strand breaks and subsequent RecA loading onto ssDNA (Dillingham & Kowalczykowski, 2008; Uzest *et al.*, 1995). In the absence of Rep, replication forks are more prone to DNA breaks, where RecBCD is necessary for recombination-mediated repair (Michel *et al.*, 1997). Strains lacking *rep* and *recB* can be maintained by supplying *rep in trans* via the low copy number plasmid pRC7*rep*

(strain HB268), which is lost at a high frequency in the absence of selection if the plasmid is not required for the viability of the strain (Bernhardt & de Boer, 2004). Complementation of the *rep recB* synthetic lethality by different pBAD constructs was assayed by blue/white screening on plates containing X-Gal and IPTG without and with arabinose (low and high levels of expression of *rep* form the P_{BAD} promoter, respectively).
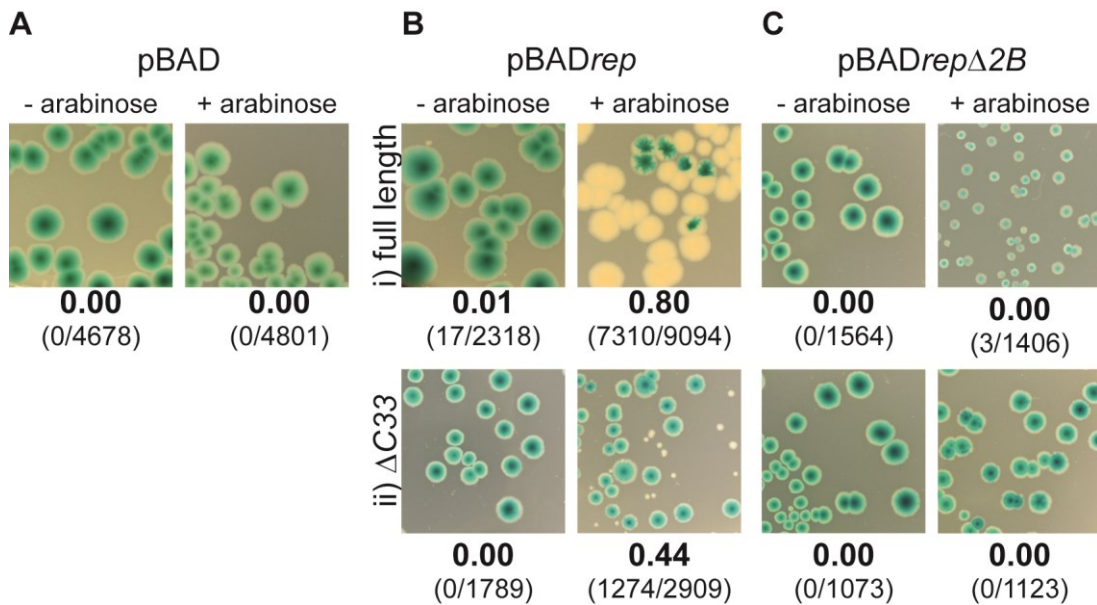
Figure 4.6 RepΔ2B cannot complement the *rep recB* lethality *in vivo*
Blue/white screening for loss or retention of pRC7*rep* in *rep recB* (N7919) strains with different pBAD derivatives encoding (i) full length versions or (ii) C-terminal truncations of *rep* mutants on LB$^{0.5}$ agar with kanamycin ± arabinose in presence of IPTG and X-Gal. Fractions of white colonies are given, with numbers of white and total numbers of colonies in brackets from at least four independent replicates.

The plasmid pRC7*rep* could not be lost in the absence of a pBAD-expressed helicase, as indicated by the lack of white colonies with the empty vector control (pBAD; Figure 4.6A). In the presence of pBAD*rep*, a very small fraction of white colonies appeared (-arabinose). At high levels of expression of wild-type *rep* (pBAD*rep* +arabinose) pRC7*rep* was lost at a high frequency (80% white colonies; Figure 4.6B.i). Fewer and also smaller white colonies appeared when the Rep C-terminus was absent (44%; Figure 4.6B.ii), which correlated with the reduced efficiency of complementation of the *Δrep ΔuvrD* rich medium lethality (Figure 4.5D.i). RepΔ2B did not complement Rep function and at high levels of expression even resulted in

smaller colony sizes (Figure 4.6C.i), reflecting the toxicity of RepΔ2B that was observed previously (Figure 4.5B.iv). Overexpression of RepΔ2BΔC33 did not result in complementation; however colonies were bigger than after overexpression of RepΔ2B (Figure 4.6C.i and ii), again linking the toxicity of RepΔ2B to the interaction with DnaB.

4.2.2.3 Overexpression of Superfamily 1 helicases lacking a 2B subdomain is toxic

Most SF1A helicases possess a 2B subdomain, but there are a few exceptions, like HelD from *E. coli* (appendix Figure A.2) (Dillingham, 2011). Since the overexpression of RepΔ2B was toxic, it was tested whether this was a general feature for SF1A helicases lacking a 2B subdomain, or whether this was an artefact resulting from the overexpression of an artificial helicase, such as RepΔ2B.

Overexpression of HelD was toxic in a wild-type and in a *Δrep ΔuvrD* strain. HelD overexpression was more toxic than RepΔ2B both on LB and minimal agar (Figure 4.7A ii and iv), suggesting that the toxicity upon helicase overexpression is linked to the absence of the 2B subdomain in SF1A helicases.
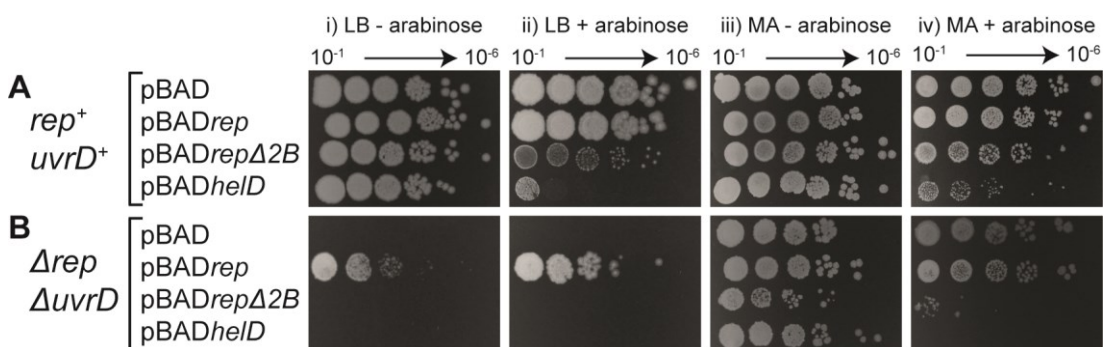
Figure 4.7 Overexpression of Superfamily 1A helicases lacking a 2B subdomain is toxic
Colony formation of (A) *rep⁺ uvrD⁺* (TB28) and (B) *Δrep ΔuvrD* (N6556) strains with different pBAD derivatives after loss of pRC7*rep*. Cells were grown in minimal medium, prior to plating of serial dilutions on LB or minimal agar with kanamycin ± arabinose (n=2).

4.2.2.4   The toxicity of RepΔ2B is not caused by an increased helicase activity

The deletion of the 2B subdomain increased levels of DNA unwinding for Rep (Figure 4.3) (Cheng *et al.*, 2002). It was therefore tested whether this increased helicase activity of RepΔ2B was the reason for its toxicity *in vivo*, by combining RepΔ2B with RepK28A, a mutation that prevents ATP hydrolysis and abolishes DNA helicase activity of Rep (Atkinson *et al.*, 2011a).
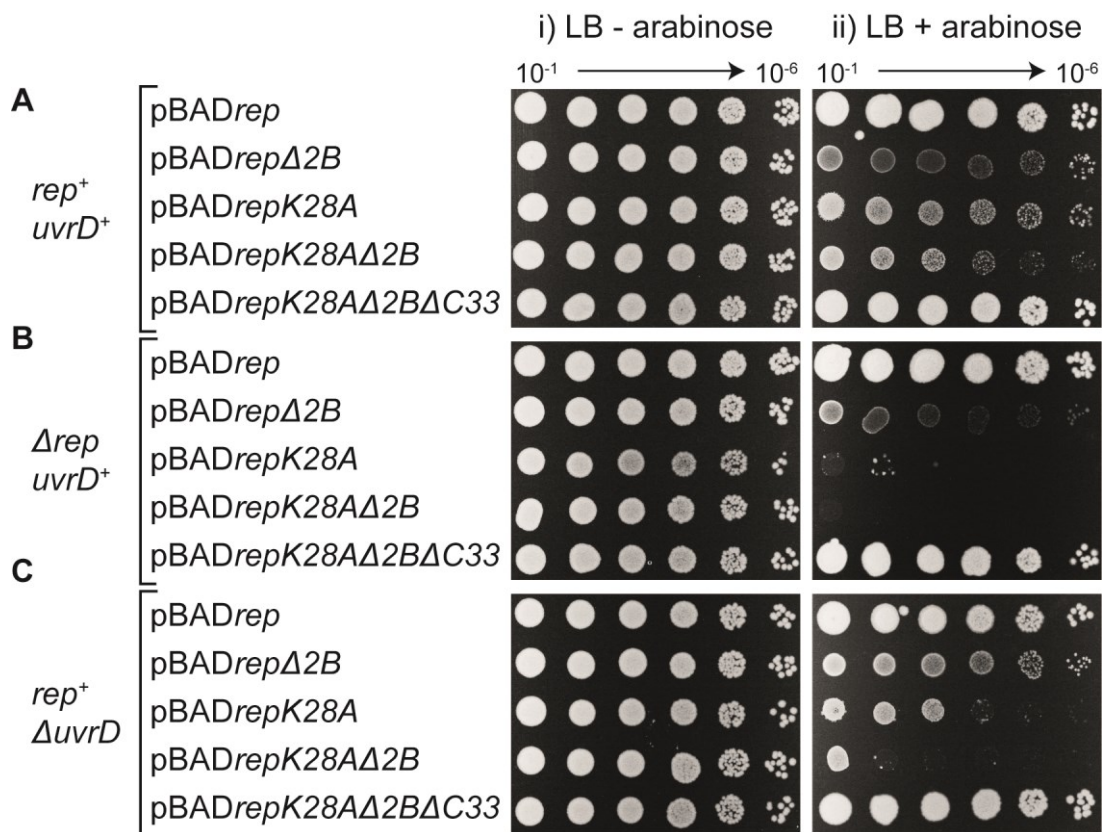
Figure 4.8 The toxicity of Rep is not caused by the increased helicase activity of RepΔ2B
Colony formation of (A) *rep*[+] *uvrD*[+] (TB28), (B) *Δrep uvrD*[+] (N6577) and (C) *rep*[+] *ΔuvrD* (N6632) strains with different pBAD*rep* derivatives after growth in LB and plating of serial dilutions on LB agar with kanamycin ± arabinose (n=2).

Overexpression of RepΔ2B resulted in slightly smaller colonies than RepK28A in a wild-type background (Figure 4.8A). On the other hand, overexpression of RepK28A caused a greater reduction in colony size in the single mutant backgrounds than RepΔ2B, with RepK28A overexpression being nearly lethal in the *Δrep* background (Figure 4.8B and C). A helicase-deficient RepΔ2B mutation (RepK28AΔ2B) showed

an additive effect in toxicity, which was most prominent in a *ΔuvrD* background (Figure 4.8C). These data indicate that the increased helicase activity of RepΔ2B (Figure 4.3) is at least not the only reason for the toxicity of RepΔ2B *in vivo*. The disruption of the interaction of this mutant with DnaB (RepK28AΔ2BΔC33) restored viability (Figure 4.8B and C), suggesting that the chromosomal helicases compete with the Rep mutants for access to the replication fork.

4.2.3 RepΔ2B does not form a stable complex with a DnaB-bound DNA fork

Several SF1A helicases have been crystallised in complex with various DNA substrates. These complexes revealed that the ssDNA is bound between subdomains 1A and 2A (Figure 1.4) (Korolev *et al.*, 1997; Lee & Yang, 2006; Velankar *et al.*, 1999). In crystal structures of PcrA and UvrD, the 2B subdomains make contacts with dsDNA (Figure 1.4) (Lee & Yang, 2006; Velankar *et al.*, 1999). To test whether the 2B subdomain of Rep affects DNA binding, EMSAs were performed that tested the ability of Rep and RepΔ2B to form stable complexes without and with DnaB on a forked DNA substrate (Figure 4.9).
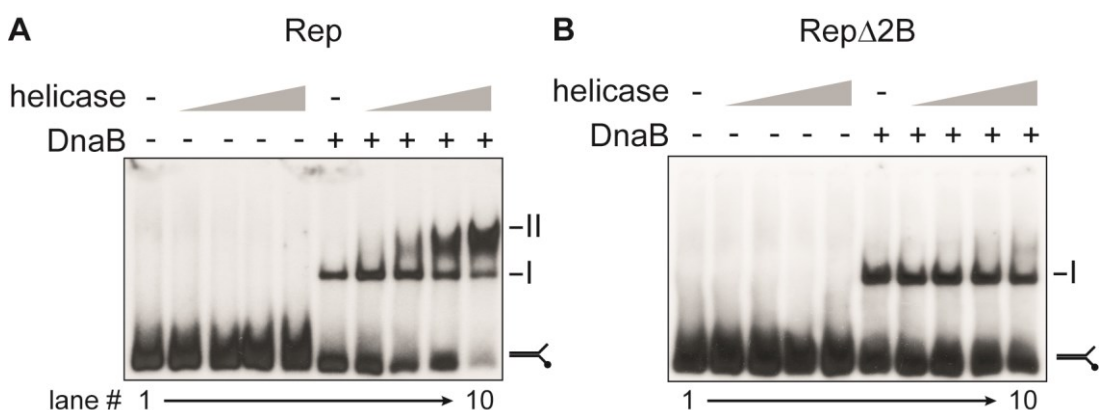
Figure 4.9 RepΔ2B does not form stable complexes on DnaB-bound DNA
DNA bandshifts of (A) Rep and (B) RepΔ2B (1, 5, 10 and 25 nM) with DnaB (100 nM hexamers) on forked DNA having two ssDNA arms (60 bp dsDNA, 38 bp ssDNA; CC139+CC140) in the presence of 10 µM ADP after resolution on a 4% acrylamide gel (n=3). "I" = DNA-DnaB complex; "II" = DNA-DnaB-Rep complex

Only DnaB was able to generate a stable complex on the DNA in the absence of other proteins. Neither wild-type nor RepΔ2B could form stable complexes in the absence of DnaB. Rep was able to form a secondary complex on a DnaB-bound fork ("II"; Figure 4.9A), as reported previously (Guy *et al.*, 2009). In contrast, RepΔ2B failed to form this complex. Since RepΔ2B retains the ability to interact with DnaB (Guy *et al.*, 2009), the inability of RepΔ2B to form a stable interaction with DnaB and DNA was most likely due to an altered interaction with DNA.

The affinity of the helicases to different DNA substrates was going to be tested using SPR. Biotinylated Rep, RepΔ2B and the Rep 2B subdomain were immobilised onto a streptavidin coated SPR chip (GE Healthcare). However, no binding was observed with various ss- (25 to 60-mers) and dsDNA (25 base pairs and 50 base pairs) substrates of concentrations up to 1 μM in the presence or absence of 10 μM ADP or ATP and/or magnesium (data not shown). Since these proteins were functional DNA helicases *in vitro* (Figure 4.3), it was concluded that surface immobilisation onto the streptavidin chips prevented DNA binding by the helicases.

4.2.4 The 2B subdomain of Rep is required for efficient nucleoprotein displacement

4.2.4.1 RepΔ2B cannot promote replisome movement through a nucleoprotein block *in vitro*

Mutations in RNA polymerases that destabilise their interaction with DNA have been shown to suppress the *Δrep ΔuvrD* rich medium lethality, allowing for growth even in the absence of accessory helicases (Baharoglu *et al.*, 2010; Guy *et al.*, 2009). In order to test whether the lack of complementation of Rep function by RepΔ2B (Figure 4.5B.i and ii) was a result of a reduced ability to deal with replication-transcription conflicts, the expression of RepΔ2B was tested in such RNA polymerase mutants (*rpoB*35*, *rpoB* G1260D; Figure 4.10).

Expression of RepΔ2B was toxic in all backgrounds tested, as indicated by reduced colony sizes (Figure 4.10). Therefore in the presence of a chromosomal wild-type

copy of Rep (and UvrD), overexpression of RepΔ2B remained toxic even when transcription complexes were destabilised. In a *Δrep* background, no significant change in the toxicity was observed (Figure 4.10D-E). Hence, the toxicity of RepΔ2B expression was either not related to replication-transcription conflicts or that in the presence of high levels of RepΔ2B, also destabilised replication-transcription complexes pose a significant barrier to cell survival.
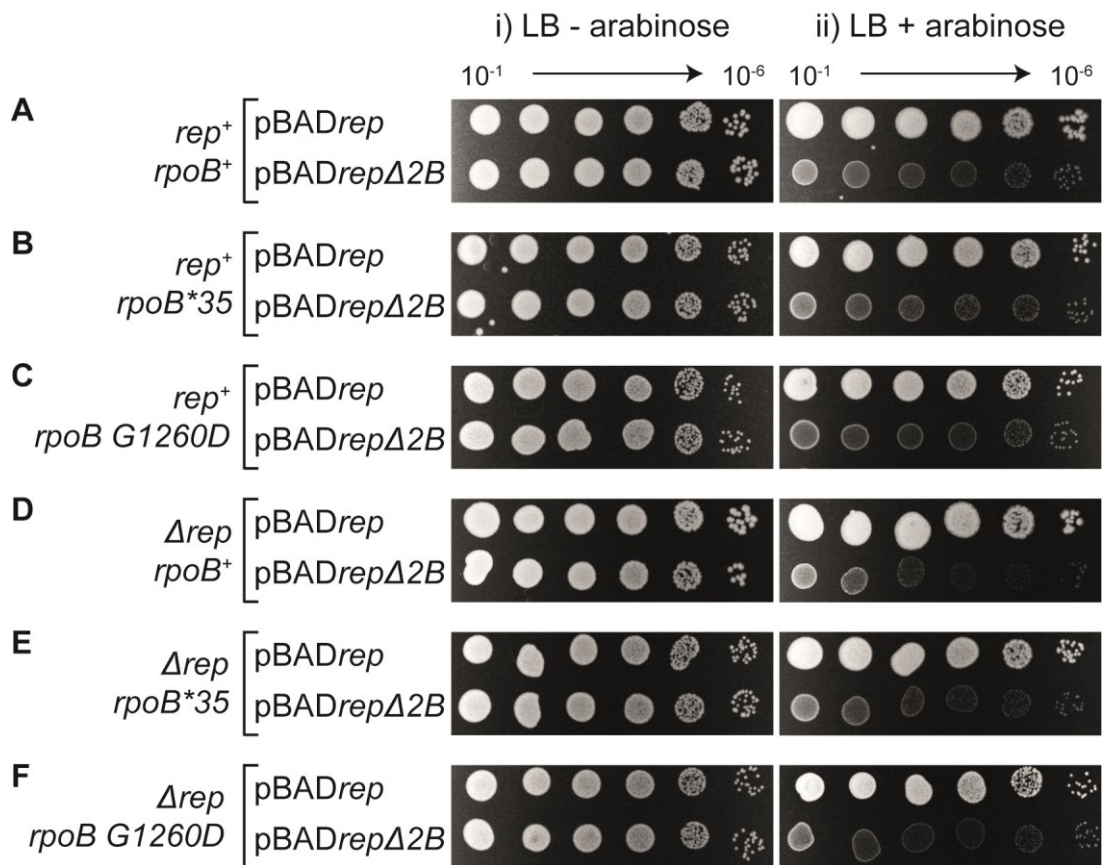
Figure 4.10 The toxicity of RepΔ2B is not suppressed by RNA polymerase mutations
Colony formation of (A) *rep⁺ rpoB⁺* (TB28), (B) *rep⁺ rpoB*35* (N5925), (C) *rep⁺ rpoB G1260D* (AM2158), (D) *Δrep rpoB⁺* (N6577), (E) *Δrep rpoB*35* (N5925) and (F) *Δrep rpoB G1260D* (HB278) strains with different pBAD *rep* derivatives after growth in LB and plating of serial dilutions on LB agar with kanamycin ± arabinose (n=2).

Accessory replicative helicases like Rep, UvrD and PcrA share the ability to underpin replication through protein-bound DNA (Guy *et al.*, 2009). However, RepΔ2B failed to complement Rep function *in vivo* (Figure 4.5) and RNA polymerase mutations did not reduce the toxicity of RepΔ2B (Figure 4.10). It was possible that in the absence of the 2B subdomain, RepΔ2B had a reduced ability to displace nucleoprotein

blocks. Therefore, it was tested whether RepΔ2B retained accessory replicative helicase function *in vitro*.

The ability of helicases to promote replisome movement through nucleoprotein blocks was tested using a plasmid containing an *oriC* and an array of eight EcoRI sites. The EcoRI sites were bound by a EcoRI E111G mutant, which efficiently binds, but that has a very low rate of cleavage of DNA (Figure 4.11A.i) (King *et al.*, 1989). Replication was initiated with a reconstituted *E. coli* replisome (Figure 4.11A.ii). DNA digestion with SmaI (Figure 4.11A.iii) resulted in movement of only a single replication fork towards the nucleoprotein block (Figure 4.11A.iv). The EcoRI-DNA interaction forms an efficient block to replisome movement, when DnaB is the only helicase present within the replisome (Figure 4.11B; +E111G) (Guy *et al.*, 2009). Different candidate accessory replicative helicases were added to the blocked replisomes and assessed for the ability to overcome the EcoRI block, as indicated by the generation of the 4.7 kb replication product (Figure 4.11A.v).
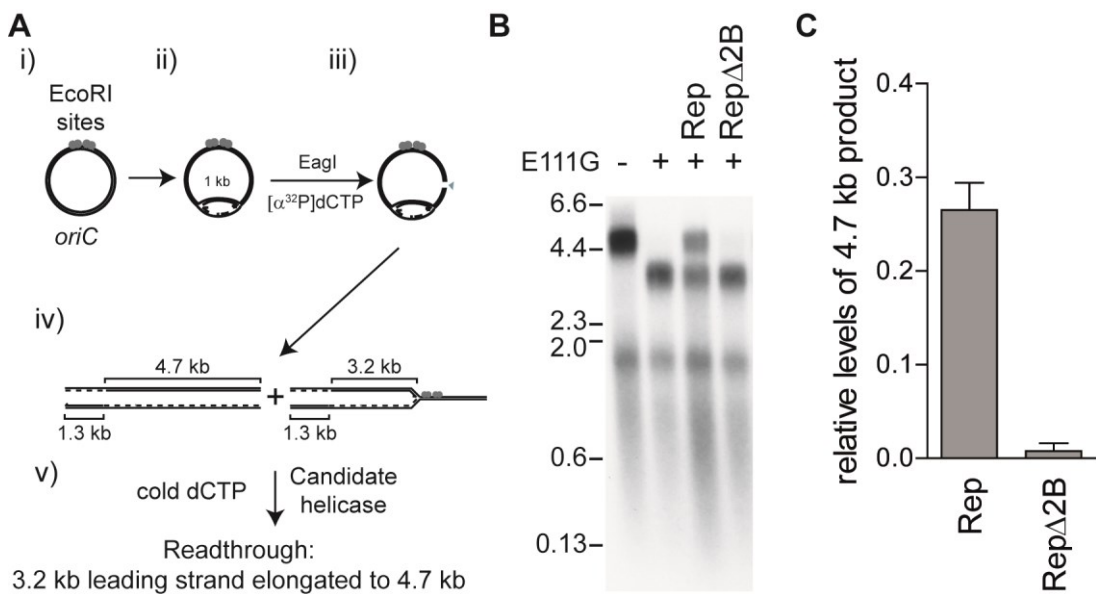
Figure 4.11 RepΔ2B cannot promote replication through a nucleoprotein block
(A) Schematic representation of the assay to monitor promotion of replication fork progression through a nucleoprotein block. (B) Denaturing agarose gel from *in vitro* replication assay of pPM594 containing eight EcoRI sites in absence and presence of EcoRI E111G (200 nM dimers) and different Rep mutants (100 nM). (C) Relative fractions of the full length replication products compared to –EcoRI E111G control. Error bars represent standard error of the mean (n=4).

Rep was able to support replication through the EcoRI block, as demonstrated previously (Guy *et al.*, 2009), whilst addition of RepΔ2B did not result in significant generation of full length leading strand products (Figure 4.11C). These data indicate that RepΔ2B cannot promote replication through this protein-DNA barrier. Thus, accessory replicative helicase function is dependent on the 2B subdomain of Rep.

While the absence of accessory replicative helicase function explains why RepΔ2B failed to complement the rich medium lethality of a *Δrep ΔuvrD* strain (Figure 4.5), it does not explain the RepΔ2B toxicity in cells grown on minimal medium *in vivo* (Figure 4.5B.iv). It has been shown recently that the 5'-3' SF1B helicase RecD2 from *D. radiodurans* inactivates stalled, but not elongating replication forks (Gupta *et al.*, 2013). It is possible that the toxicity of RepΔ2B (Figure 4.10) could be caused by inactivation of paused replisomes by RepΔ2B, given the elevated helicase activity of RepΔ2B (Figure 4.3 and Figure 4.4) (Brendza *et al.*, 2005; Cheng *et al.*, 2002).

To test this hypothesis, replisomes were stalled at a high affinity nucleoprotein block (22 *lac* repressor-operator complexes) that could not be overcome even in the presence of accessory replicative helicases *in vitro* (Gupta *et al.*, 2013). Different helicases were added to the blocked replisome and tested for continuation of replication upon removal of the block by the addition of IPTG (Figure 4.12A).

Replication was fully blocked by the repressor operator array, but upon removal of LacI by the addition of IPTG, the majority of replisomes produced full length products of replication (Figure 4.12B and C, no helicase). The addition of RecD2 inactivated stalled replisomes, as shown previously (Gupta *et al.*, 2013), and no full length replication product was generated. Rep and RepΔ2B both allowed for continuation of replication by a large proportion of replisomes (Figure 4.12C). Previously, wild-type Rep did not show any reduction in levels of full length replication product (Gupta *et al.*, 2013), but due to time constraints the source of this discrepancy could not be investigated. Nonetheless, Rep and RepΔ2B did not inactivate stalled replisomes in a RecD2-like manner. Thus, RepΔ2B is likely not toxic due to a destabilisation of stalled replication forks.
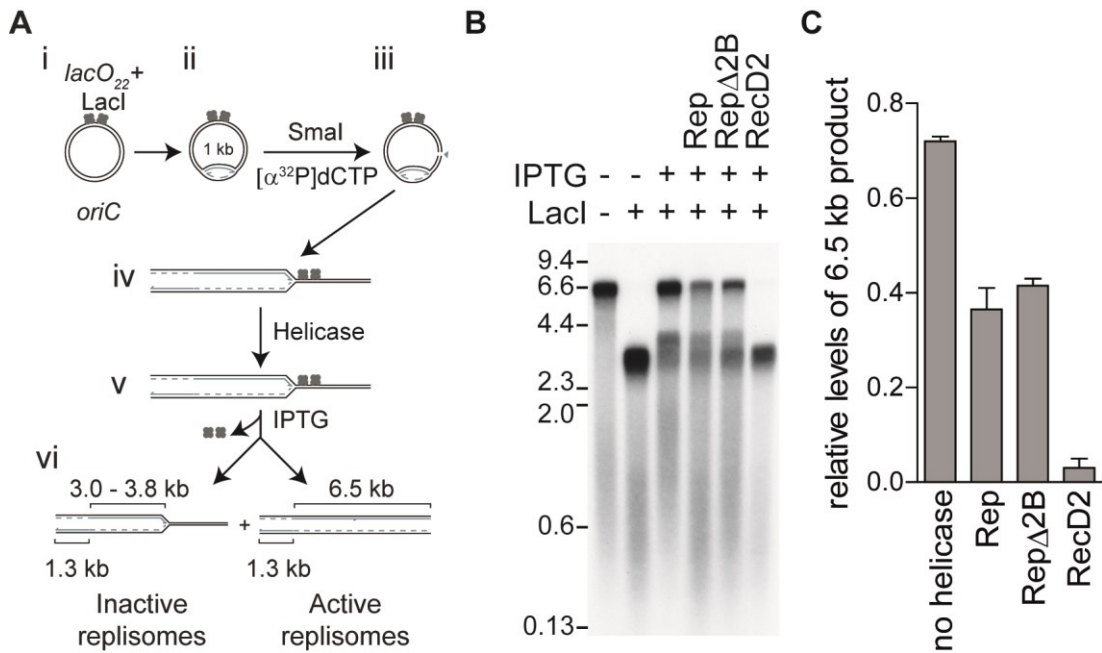
Figure 4.12 RepΔ2B does not inactivate stalled replication forks
(A) Schematic representation of monitoring the inactivation of stalled replication forks by different helicases. (B) Denaturing agarose gel from *in vitro* replication of pPM561 (*lacO₂₂*) in absence and presence of LacI (400 nM tetramers), IPTG (1 mM) and different helicases (100 nM). (C) Histogram of the relative fractions of the full length replication products compared to the –LacI –IPTG control.

4.2.4.2 RepΔ2B cannot efficiently displace a streptavidin block from ssDNA

In the previous section, it was shown that a 2B subdomain is essential for Rep to underpin the replication of protein-bound DNA (Figure 4.11). However, the assay did not test whether the 2B subdomain is involved in the process of simply bypassing the block, actually removing the proteins from DNA or whether it stimulates other replisome components, such as DnaB to clear the obstacle. The displacement of a model nucleoprotein block from ssDNA had been demonstrated before by the SF1B helicase Dda from bacteriophage T4 (Byrd & Raney, 2004). The model block used in these experiments was a streptavidin molecule bound to a biotinylated nucleotide within a short DNA substrate. Streptavidin binds biotin with high affinity thereby mimicking an obstacle to DNA translocases and helicases, whose removal can be assayed by DNA bandshifts. Thus, a ssDNA-streptavidin displacement assay was set up to test different helicases for their ability to displace nucleoprotein blocks from ssDNA.

Different 5'-radiolabelled oligonucleotides with biotin modifications were tested for stable binding by streptavidin (Figure 4.13). In the presence of 1 µM streptavidin all the biotinylated oligonucleotides were completely shifted. In the absence of the biotin modification (substrate 4) no DNA shift occurred, verifying that the bandshifts were specific to the biotin-streptavidin interaction.

In order to prevent rebinding of displaced streptavidin to the oligonucleotides, biotin titrations were performed on substrate 3. The addition of 100 µM free biotin prior to the incubation of the DNA with streptavidin was able to prevent any DNA-streptavidin interaction (biotin first, Figure 4.13B), while the same amount of biotin had no impact on the preformed DNA-streptavidin interaction (SA first, Figure 4.13B). Thus, streptavidin displacement from ssDNA was assayed in the presence of 1 µM streptavidin and 100 µM free biotin.
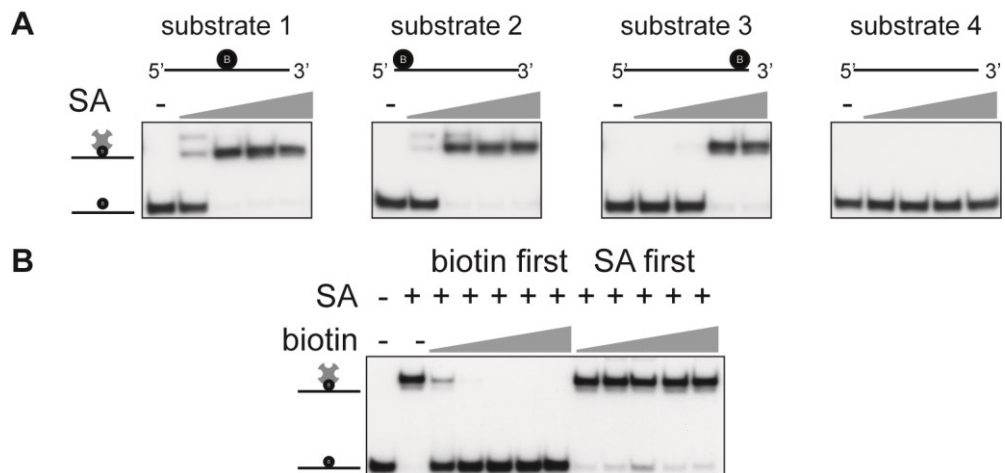
Figure 4.13 Free biotin does not disrupt preformed streptavidin-DNA complexes.
(A) Streptavidin titrations (0.01/0.1/1/10 µM) of dT_{60}-mers (PM326-329) with different biotin modifications (B) Biotin titrations (0.001/0.01/0.1/1/10 mM) added to PM328 before and after the addition of streptavidin (1 µM). The black circle indicates the position of the biotin on the oligonucleotide, the grey cross represents streptavidin (n=2).

The effect of translocation polarity on streptavidin removal by Rep, RepΔ2B and DnaB was tested on all three biotinylated oligonucleotides (Figure 4.14). Substrate 1, which contains 30 base pairs ssDNA each side of the biotin modification, displayed streptavidin displacement by all three helicases. However, Rep was much more efficient at streptavidin removal than RepΔ2B and DnaB (Figure 4.14B.i), indicating that the 2B subdomain of Rep is crucial for efficient

displacement of streptavidin from ssDNA. Substrate 2 was 5'-biotinylated and streptavidin was only displaced by Rep and RepΔ2B, but not DnaB. Conversely, only DnaB was able to remove streptavidin from the 3'-biotinylated substrate 3. This reflects the opposing polarities of the helicases, with Rep and RepΔ2B translocating in the 3'-5' direction and DnaB in the 5'-3' direction (Brendza *et al.*, 2005; LeBowitz & McMacken, 1986; Yarranton & Gefter, 1979). Thus, displacement of ssDNA-protein complexes requires translocation of the helicases towards the block to "push" the obstacle off the DNA, which is in accordance with a previous report (Morris & Raney, 1999). This process is much more efficient for wild-type Rep than for DnaB.
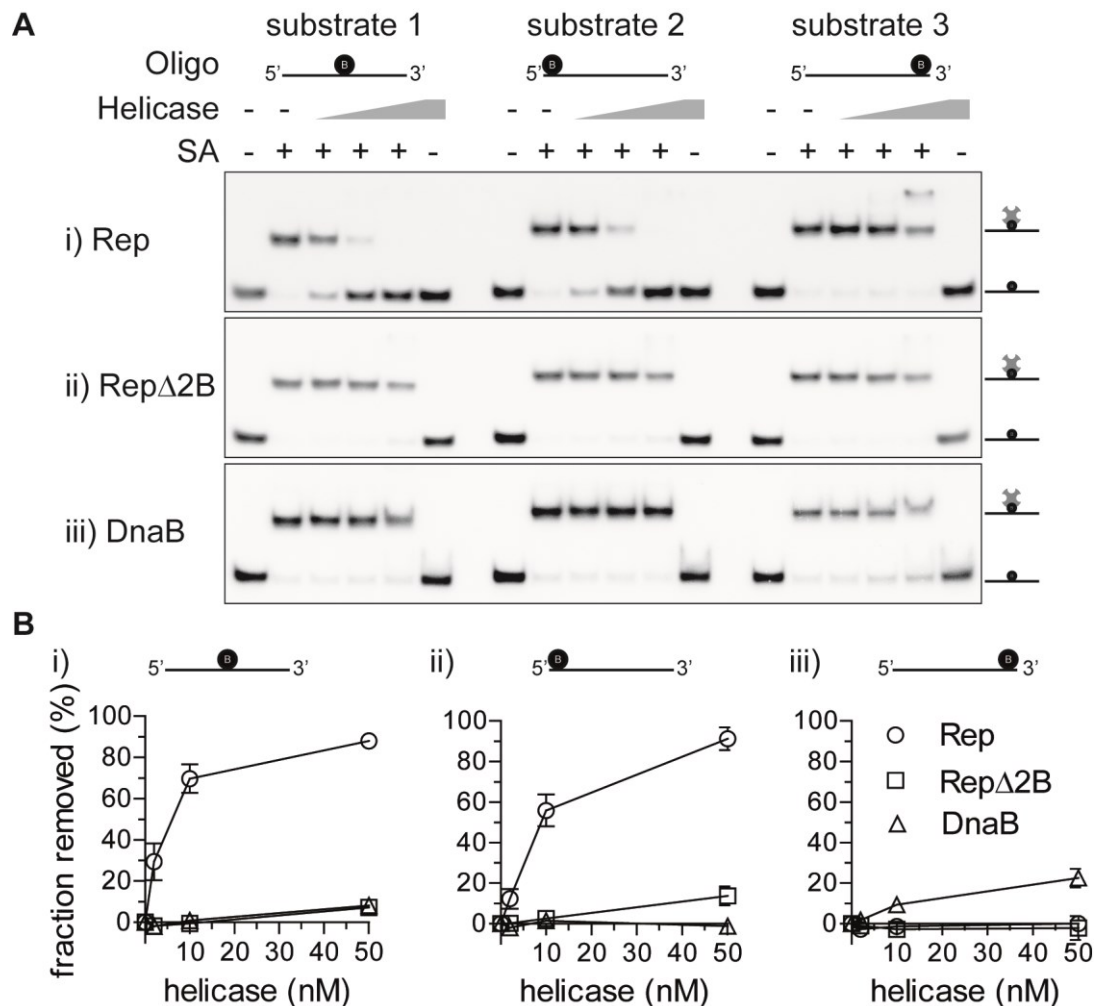
Figure 4.14 RepΔ2B and DnaB cannot efficiently remove a nucleoprotein block from ssDNA
(A) Displacement of streptavidin (1 µM) from biotinylated dT60-mers (PM328, PM326 and PM327) by different helicases (2, 10 and 50 nM) (B) Relative levels of streptavidin displacement from (i) PM328, (ii) PM326 and (iii) PM327 by individual helicases. Error bars represent standard error of the mean (n=2-3). The black circle indicates the position of the biotin on the DNA, the grey cross represents streptavidin.

4.2.4.3 The cooperativity between DnaB and Rep in streptavidin displacement is dependent on translocation of both helicases

Rep and DnaB display cooperativity in DNA unwinding on a forked DNA substrate (Figure 4.4) (Guy *et al.*, 2009). It was therefore tested if the cooperativity was also observed for nucleoprotein displacement from ssDNA.

No cooperativity in streptavidin displacement was observed either on the 5'-biotinylated substrate, where streptavidin removal was specific to the 3'-5' helicases Rep and RepΔ2B, or on the 3'-biotinylated substrate, which was only a substrate for DnaB (Figure 4.15C.ii and iii). With increasing concentrations of both helicases, only DNA bandshifting was observed on these substrates (Figure 4.15A.i, ii, v and vi). Both Rep and RepΔ2B are able to interact with DnaB due to the presence of the Rep C-terminus (Guy *et al.*, 2009). This interaction might therefore stabilise the helicases on the ssDNA and result in DNA bandshifting.

On the other hand, on substrate 3, where the biotin modification is in the centre of the ssDNA, DnaB displayed cooperativity in streptavidin displacement with Rep and also RepΔ2B. Thus, translocation towards the biotin-streptavidin block by both helicases was a prerequisite to result in cooperative streptavidin displacement from ssDNA. It is unlikely that the cooperativity in streptavidin displacement is simply due to the ability of both helicases to displace the block, since both helicases have opposing polarities of ssDNA translocation. Hence, it is more plausible that the interaction between both helicases stabilises and enhances streptavidin displacement by one of the two helicases.

Figure 4.15 Translocation of both helicases towards a streptavidin block is required for cooperative streptavidin removal from ssDNA
(A) Displacement of streptavidin (1 μM) from biotinylated dT_{60}-mers (PM328, PM326 and PM327) by (i-iii) Rep or (iv-vi) RepΔ2B (2 and 10 nM) in the absence or presence of DnaB (2, 10 and 50 nM). (B) Relative levels of streptavidin displacement by (i-iii) Rep or (iv-vi) RepΔ2B. (C) Cooperativity in streptavidin removal from (i) PM328, (ii) PM326 and (iii) PM327 shown as fractions of streptavidin displacement by Rep(Δ2B) with DnaB compared to the sum of the individual levels of streptavidin displacement by each helicase individually. Error bars represent standard error of the mean (n=3).

4.2.4.4 DNA unwinding and nucleoprotein displacement are separable processes

Proteins bound to dsDNA are thought to be the main type of replicative barrier in *E. coli in vivo* (Gupta *et al.*, 2013). However, the experiments above addressed streptavidin displacement from ssDNA. Although replication forks can bypass nucleoprotein blocks *in vitro*, DNA unwinding in the presence of high affinity protein blocks requires accessory replicative helicases (Payne *et al.*, 2006; Pomerantz & O'Donnell, 2008; Pomerantz & O'Donnell, 2010). In line with this, Rep but not DnaB is able to efficiently unwind duplex DNA that is bound by a repressor-operator complex (Yancey-Wrona & Matson, 1992). It was therefore tested whether the deletion of the 2B subdomain of Rep had a direct impact on DNA unwinding in the presence of streptavidin block, using forked DNA substrates that contained biotin modifications close to the ss/dsDNA junction.

Streptavidin binding to 98-mers of identical sequence (CC139 and CC139B53) was specific to the biotinylated oligonucleotide CC139B53 (Figure 4.16A). Annealing of CC139 or CC139B53 to CC140 or CC140B47 resulted in DNA forks, containing a biotin modification on both strands, only the lagging or the leading strand template or lacking biotin completely (Figure 4.16B.i-iv). Again, streptavidin binding to these DNA forks as indicated by bandshifts was specific to the presence of biotin (Figure 4.16B). Finally, the effect of free biotin on the DNA forks was tested (Figure 4.16C). All concentrations of free biotin were sufficient to prevent the formation of the streptavidin-biotin complex on the DNA when addition of the free biotin preceded that of streptavidin (Figure 4.16C). When free biotin was added after streptavidin the dually labelled fork retained streptavidin (Figure 4.16C.i), as seen with individual oligonucleotides (Figure 4.16A.ii). However, with each singly labelled fork, the addition of free biotin after the streptavidin led to the disruption of the DNA-streptavidin interaction (Figure 4.16C.ii and iii). This was more apparent when the biotin modification was on the leading strand template (Figure 4.16C.ii). It is possible that secondary structures in the ssDNA arms might reduce the biotin-streptavidin interaction on the DNA. On the dually labelled fork, the streptavidin tetramer could form a more stable interaction by binding to both biotin

modifications. DNA unwinding in the presence of a strand-specific block could therefore not be tested. Hence, all of the following experiments were performed with the dually labelled fork only (CC139B53+CC140B47; Figure 4.16C.i).
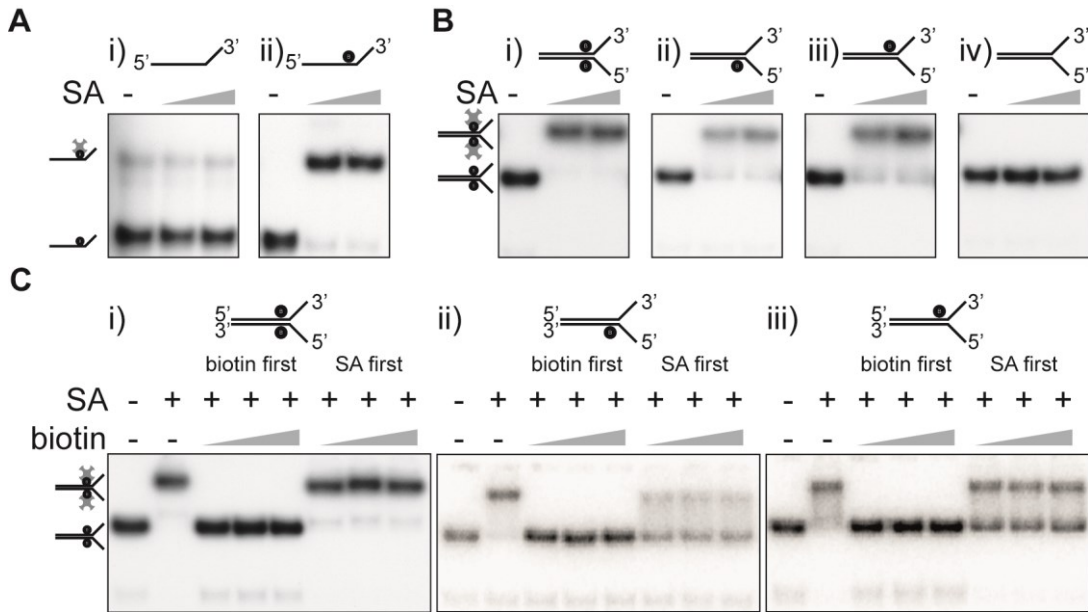
Figure 4.16 Streptavidin binding to biotinylated DNA forks
(A) ssDNA-streptavidin titrations (0.1 µM and 1 µM) of (i) CC139 and (ii) CC139B53. (B) Streptavidin titrations (0.1 µM and 1 µM) of forked DNA (i) dually labelled fork CC139B53+CC140B47; (ii) CC139+CC140B47; (iii) CC139B53+CC140 and (iv) CC139+CC140, no biotinylation. (C) Addition of free biotin (10 µM – 1 mM) to dsDNA forks before and after the addition of streptavidin (1 µM). The black circle indicates the position of the biotin on the DNA, the grey cross represents streptavidin (n=2).

DNA unwinding in the absence or presence of streptavidin was tested on the dually labelled fork. Rep, although displaying only low levels of DNA unwinding, was not inhibited by the presence of streptavidin (Figure 4.17A and B). In contrast, DNA unwinding by RepΔ2B was reduced about four-fold by the presence of streptavidin (Figure 4.17C), but total levels of DNA unwinding in the presence of streptavidin were still higher than wild-type Rep at the same concentration (Figure 4.17B). Nonetheless, this indicated that DNA unwinding and nucleoprotein displacement are two distinct processes and that the 2B subdomain of Rep plays a central role in both. On the one hand, the 2B subdomain is autoinhibitory with respect to helicase activity (Brendza *et al.*, 2005), but on the other hand, the presence of the 2B subdomain was necessary for efficient unwinding of DNA in the presence of protein blocks (Figure 4.17). DNA unwinding by DnaB was inhibited more than 10-fold and

DnaB failed to unwind DNA in the presence of the streptavidin block (~0.1%; Figure 4.17B.i), emphasising the need for accessory replicative helicases to assist replication fork movement through protein blocks *in vivo*.
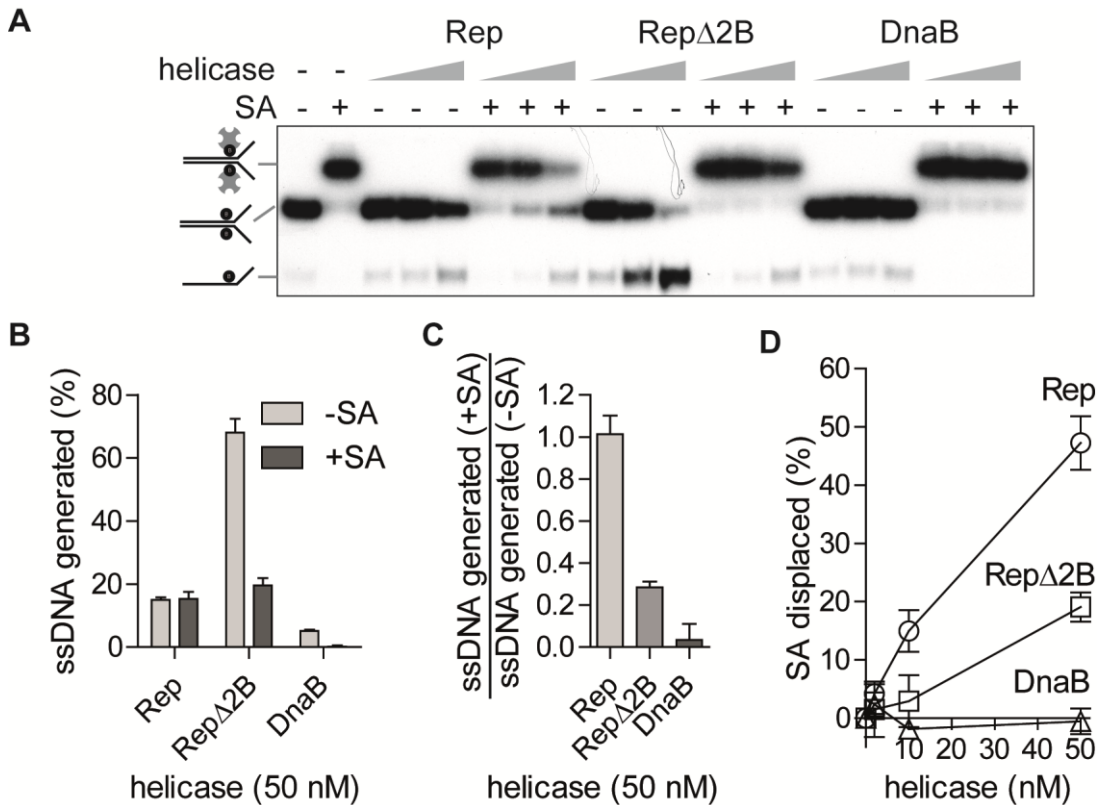
Figure 4.17 The 2B subdomain of Rep is required for efficient unwinding of protein-bound DNA
(A) DNA unwinding of a dually biotinylated DNA fork (CC139B53+CC140B47) in the absence or presence of streptavidin by the denoted helicases (2, 10 and 50 nM). (B) Total levels of DNA unwinding in the absence or presence of streptavidin by 50 nM Rep, RepΔ2B and DnaB. (C) Inhibition of DNA unwinding by streptavidin given as the fraction of DNA unwinding in the presence of streptavidin divided by the levels of DNA unwinding in the absence of streptavidin. Values below 1 indicate inhibition of DNA unwinding by streptavidin (D) Total levels of streptavidin removal from ss- and dsDNA. Error bars represent standard error of the mean (n=4).

In addition to the generation of ssDNA as a measurement of helicase activity, streptavidin displacement from dsDNA without complete unwinding of the DNA could be observed. Rep showed increasing levels of streptavidin-less dsDNA (migrating with the dsDNA control, –helicase –SA; Figure 4.17A). Hence, Rep is efficient at displacing the streptavidin close to the fork junction without fully unwinding the remaining ~50 base pairs of dsDNA. This is in agreement with a low processivity in DNA unwinding by Rep (Brendza *et al.*, 2005). Therefore, total levels of streptavidin removal by Rep accounted to 20% ssDNA unwinding product but

additional 30% removal of streptavidin from DNA without full unwinding of the duplex (Figure 4.17B and D). RepΔ2B gave an all-or-nothing response, as all DNA lacking streptavidin was also fully unwound (compare Figure 4.17B and D). Thus, the removal of a nucleoprotein block is the bottleneck in the DNA unwinding process by RepΔ2B.

Rep and DnaB display cooperativity in DNA unwinding in the absence of a protein block (Figure 4.4) (Guy *et al.*, 2009). In the presence of a protein block, DNA unwinding by DnaB was greatly reduced, while unwinding by Rep was not affected (Figure 4.17). It was therefore tested whether Rep and DnaB also display cooperativity in DNA unwinding in the presence of a protein block.

DNA unwinding by Rep was not affected by the presence or the absence of the streptavidin block but DNA unwinding by RepΔ2B and DnaB was greatly reduced (Figure 4.18B). When DnaB was present at the fork together with Rep or RepΔ2B, DNA unwinding was only stimulated with Rep (Figure 4.18D.i). The cooperativity between Rep and DnaB was enhanced two- to threefold by the presence of the streptavidin block compared to the absence of the block (Figure 4.18D.i). This correlated with the absence of inhibition of DNA unwinding in presence of streptavidin when Rep is additionally present at a DnaB bound fork (Figure 4.18C). In contrast, cooperativity between DnaB and RepΔ2B was observed in the presence of the streptavidin block only at the highest concentration tested and also only to a very moderate level (1.5x increase; Figure 4.18D.ii), suggesting that the interaction between RepΔ2B and DnaB does not stimulate nucleoprotein displacement. These results correlate with the inability of RepΔ2B to promote replication fork movement through a nucleoprotein block (Figure 4.11). Thus, for efficient unwinding of protein-bound DNA, one of the two helicases needs to be able to efficiently displace proteins, which consequently allows Rep but not RepΔ2B to function as an efficient accessory replicative helicase *in vitro* (Figure 4.11).

Due to the instability of biotin-streptavidin complexes on singly labelled DNA forks (Figure 4.16C), it could not be tested how removal of strand-specific blocks was affected.
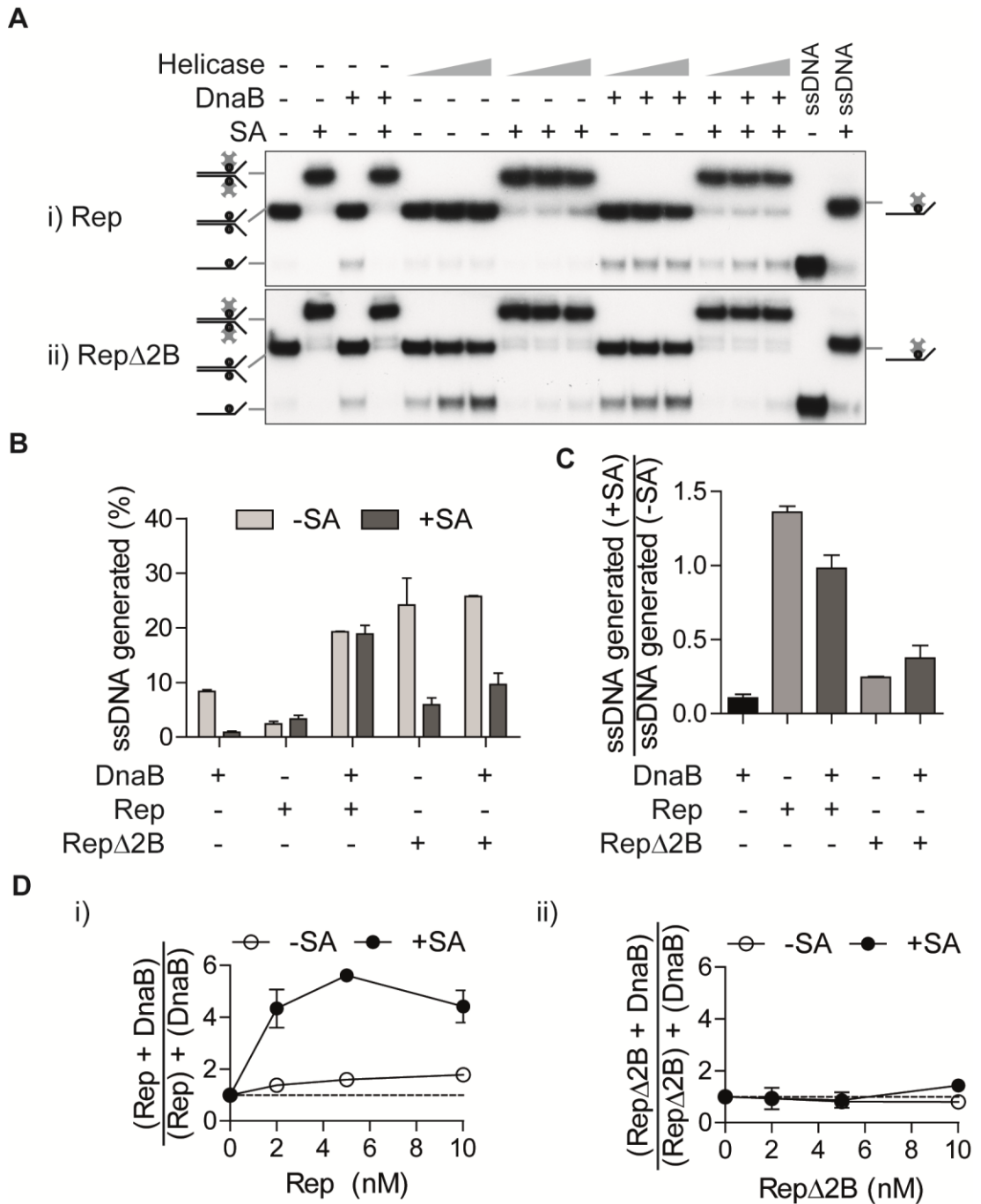
Figure 4.18 The presence of streptavidin enhances the cooperativity between DnaB and Rep
(A) DNA unwinding of a dually biotinylated DNA fork (CC139B53+CC140B47) in the absence or presence of streptavidin and/or 100 nM DnaB by (i) Rep and (ii) RepΔ2B (2, 5 and 10 nM). (B) Total levels of DNA unwinding in the absence or presence of streptavidin by 10 nM helicases. (C) Inhibition of DNA unwinding by streptavidin given as the fraction of DNA unwinding in the presence of streptavidin divided by the levels of DNA unwinding in the absence of streptavidin for 100 nM DnaB or 10 nM Rep or RepΔ2B. Values below 1 indicate inhibition of DNA unwinding by streptavidin (D) Cooperativity in DNA unwinding shown as fractions of unwound DNA by (i) Rep and (ii) RepΔ2B with DnaB compared to the sum of the individual levels of DNA unwinding by both individual helicases in the absence or presence of streptavidin. Error bars represent standard error of the mean (n=2).

4.2.4.5 Inhibition of DNA unwinding by RepΔ2B is block-specific and concentration dependent

In addition to streptavidin blocks, unwinding in presence of a second type of nucleoprotein block was tested to exclude streptavidin-specific results for nucleoprotein displacement and DNA unwinding. A previous study had assessed unwinding of dsDNA containing a single *lacO* sequence in the presence of LacI (Yancey-Wrona & Matson, 1992).

The substrate that was chosen for the assays was similar to all previous DNA forks used, in that it had 60 base pairs dsDNA with two ssDNA arms of 38 bases length (oJA025 annealed to oJA026; Table A.16). The only difference for this assay was that the dsDNA region contained a single *lacO* sequence (5'-AATTGTGAGCGGATAACAA TT-3'). A LacI titration of the $lacO_1$ fork was performed to ensure complete saturation of the operator sites on the DNA by LacI, which was achieved in the presence of 20 nM LacI tetramers (Figure 4.19).
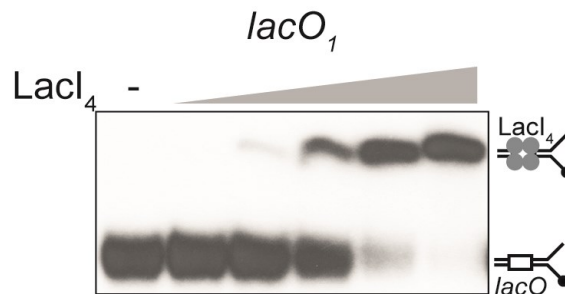
Figure 4.19 LacI titration of the $lacO_1$ fork
DNA bandshift of a LacI titration (0.05, 0.25, 1, 5 and 20 nM tetramers) with a $lacO_1$ fork containing a single *lac* operator sequence within the 60 base pairs duplex DNA (oJA025+oJA026).

Similar to the streptavidin block, DNA unwinding by Rep in the presence of LacI was not inhibited significantly (Figure 4.20B.i). In contrast, DNA unwinding by RepΔ2B was inhibited by LacI, especially at low concentrations of RepΔ2B. At the highest concentrations of RepΔ2B tested, levels of DNA unwinding nearly matched ssDNA fractions generated in the absence of the LacI block (Figure 4.20B.ii). Thus, the amount of inhibition of DNA unwinding by a nucleoprotein block was dependent on

the concentration of the helicase and the type of nucleoprotein block (compare streptavidin and *lacO₁*-LacI; Figure 4.17 and Figure 4.20).
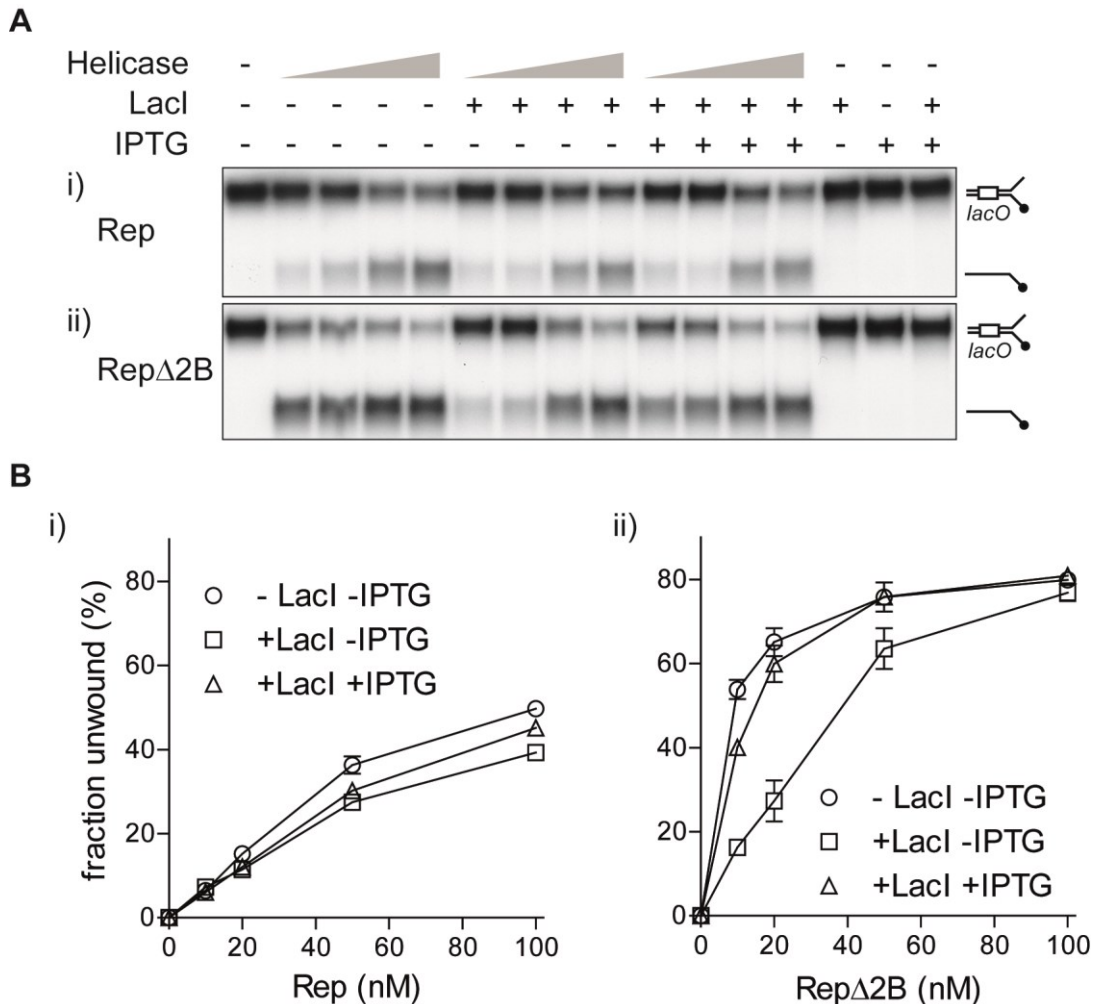
Figure 4.20 DNA unwinding by RepΔ2B is inhibited by a single *lac* repressor-operator complex
(A) Unwinding of a *lacO₁* fork (oJA025+oJA026) in the absence or presence of LacI and/or IPTG by (i) Rep and (ii) RepΔ2B (10, 20, 50 and 100 nM). (B) Relative levels of DNA unwinding by (i) Rep or (ii) RepΔ2B. Error bars represent standard error of the mean (n=3).

Finally, the cooperativity between DnaB and Rep or RepΔ2B in the unwinding of LacI-bound DNA was tested (Figure 4.21). LacI binding to DNA was inhibitory to DNA unwinding by DnaB, although — unlike in the presence of streptavidin previously (Figure 4.17) — residual DNA unwinding was detected (Figure 4.21A and B), which correlated with the reduction of inhibition for DNA unwinding by RepΔ2B (Figure 4.20).
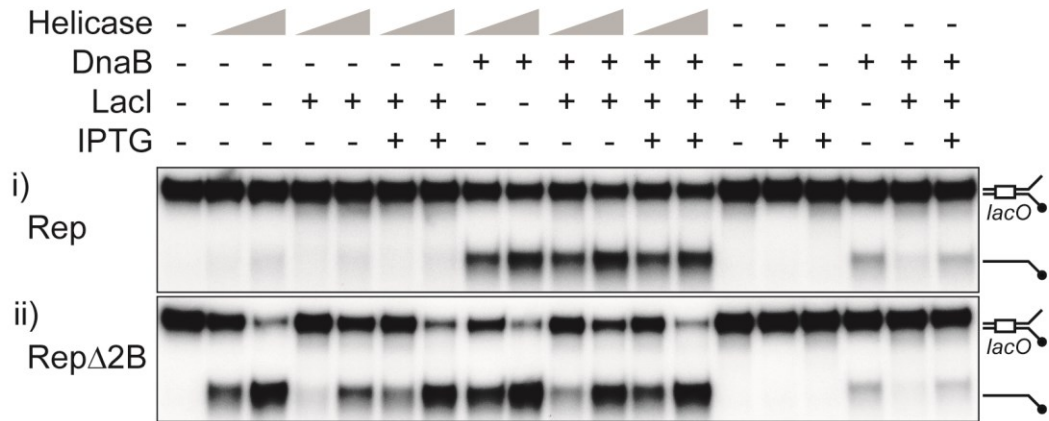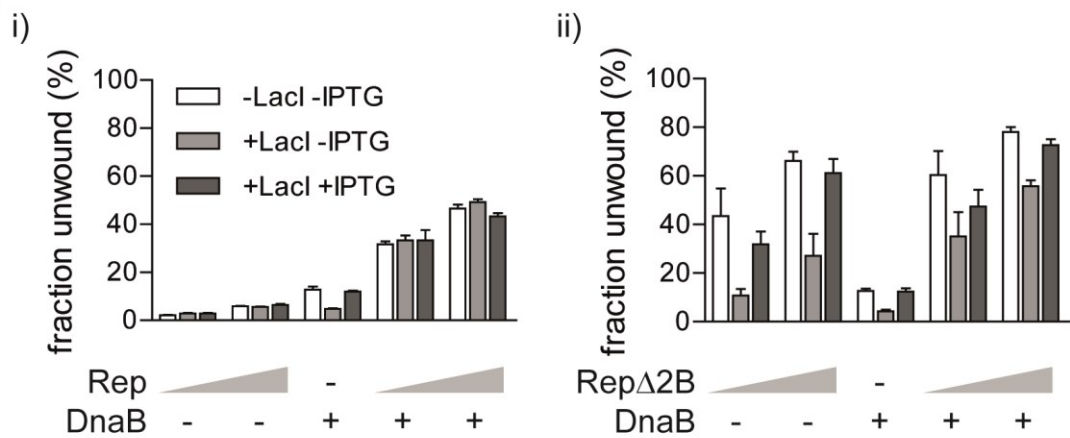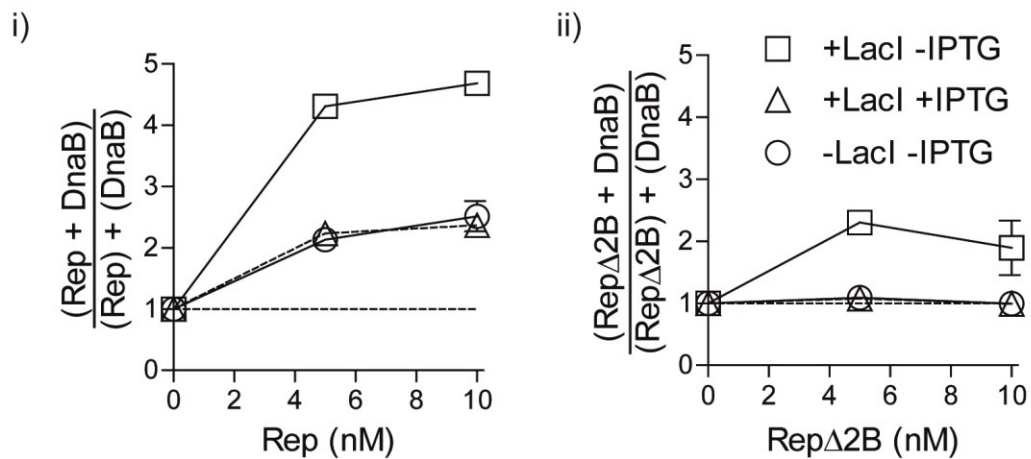
Figure 4.21 A repressor-operator complex stimulates the cooperativity in DNA unwinding
(A) Unwinding of a *lacO₁* fork (oJA025+oJA026) in the absence or presence of LacI and/or IPTG by (i) Rep and (ii) RepΔ2B (5 or 10 nM) without or with DnaB (100 nM). (B) Relative levels of DNA unwinding by (i) Rep or (ii) RepΔ2B in the absence or presence of DnaB (C) Cooperativity in DNA unwinding shown as fractions of unwound DNA by (i) Rep or RepΔ2B with DnaB compared to the sum of the individual levels of DNA unwinding by both individual helicases in the absence or presence of LacI and/or IPTG. Error bars represent standard error of the mean (n=2).

In the absence of LacI, only Rep displayed cooperativity in DNA unwinding with DnaB (-LacI -IPTG and +LacI +IPTG; Figure 4.21C), just as observed previously (Figure 4.4). Cooperativity between Rep and DnaB was further enhanced in the presence of the repressor-operator complex (Figure 4.21C.i). RepΔ2B did also show cooperativity in the presence of the protein block (Figure 4.21C.ii) to even higher levels than previously seen for a streptavidin block (Figure 4.18). Nonetheless, total levels of DNA unwinding by RepΔ2B were slightly reduced compared to levels of unwinding in the absence of LacI (Figure 4.21B.ii). Thus, the interaction between Rep and DnaB is not only crucial for cooperativity in DNA unwinding but also improves protein displacement.

4.2.5 The UvrD 2B subdomain can complement the Rep 2B subdomain *in vivo*

Most SF1A helicases possess a 2B subdomain and it was therefore tested whether the RepΔ2B phenotype could be complemented by the insertion of a 2B subdomain from a related helicase. In this RepΔ2B[uvrD2B] mutant (a kind gift from T. Lohman, Washington University St. Louis), the Rep 2B subdomain is replaced by UvrD residues M380-A542 – the 2B subdomain of UvrD (Figure 4.22).
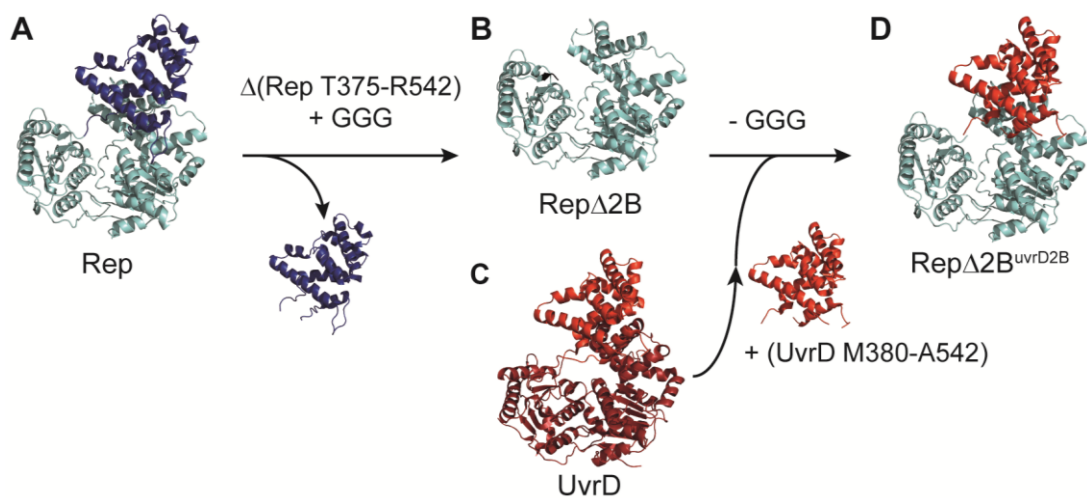
Figure 4.22 The RepΔ2B[uvrD2B] mutant
(A) The 2B subdomain of Rep (PDB: 1UAA, (Korolev *et al.*, 1997)) was deleted and replaced by three glycine residues, creating (B) RepΔ2B. (C) The 2B subdomain of UvrD (PDB 2IS2, (Lee & Yang, 2006)) was inserted in the RepΔ2B mutant, replacing the glycine linker, giving rise to (D) RepΔ2B[uvrD2B].

RepΔ2B^{uvrD2B} was tested for complementation of the *Δrep ΔuvrD* lethality on rich medium. RepΔ2B^{uvrD2B} was able to restore growth to the *Δrep ΔuvrD* strain, but only at high levels of expression (Figure 4.23B.ii). Additionally, the efficiency of complementation was dependent on the interaction with DnaB (Figure 4.23B.ii; compare pBAD*repΔ2B^{uvrD2B}* to pBAD*repΔ2B^{uvrD2B}ΔC33*). These data support a model in which proper function of Rep in the context of the replisome depends on a 2B subdomain. Additionally, the ability of the 2B subdomain of UvrD to substitute for the Rep 2B subdomain indicates a conserved function for 2B subdomains among different SF1A helicases.

RepΔ2B^{uvrD2B} was also tested for complementation of the *rep recB* lethality *in vivo*. Similar to the complementation of *Δrep ΔuvrD* lethality (Figure 4.23), RepΔ2B^{uvrD2B} also allowed for the loss of the complementing pRC7*rep* construct in *rep recB* cells (Figure 4.24C.i). However, colony size and the frequency of pRC7*rep* loss were reduced compared to pBAD-encoded wild-type Rep and even RepΔC33 (Figure 4.24B.i and B.ii). RepΔ2B^{uvrD2B}ΔC33 was able to support growth of a *rep recB* strain, although at a very low frequency (Figure 4.24C.i). Taken together, these data further support the notion that proper Rep function is dependent on a 2B subdomain *in vivo*.
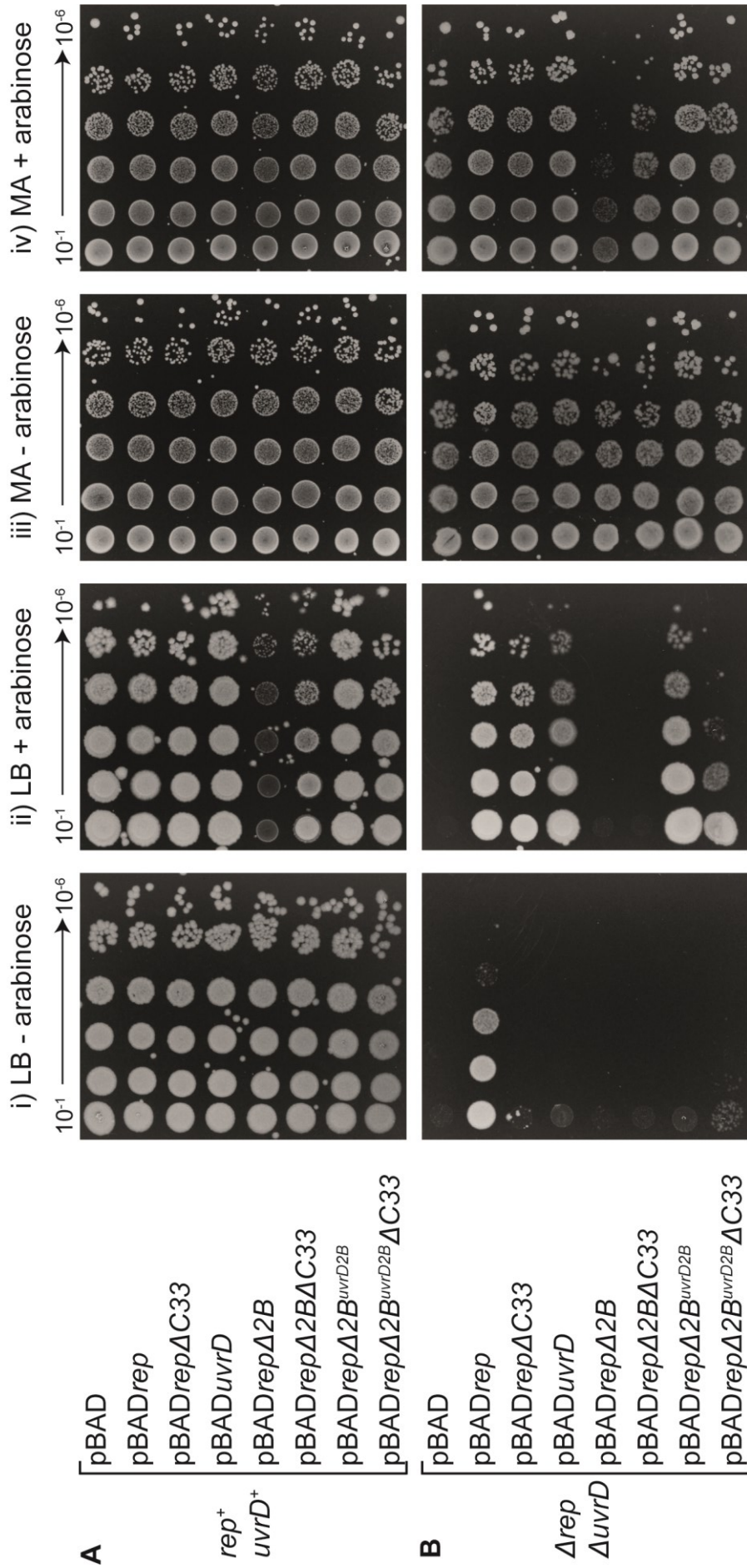
Figure 4.23 Rep function is dependent on a 2B subdomain *in vivo*

rep⁺ uvrD⁺ (N6524) and *Δrep ΔuvrD* (N6556) cells lacking the pRC7*rep* plasmid but carrying the denoted helicases were grown in liquid minimal medium, serially diluted and spotted on LB or MM agar containing kanamycin ± arabinose (n=2). Note that the panels of the first six plasmids have been used in Figure 4.5.
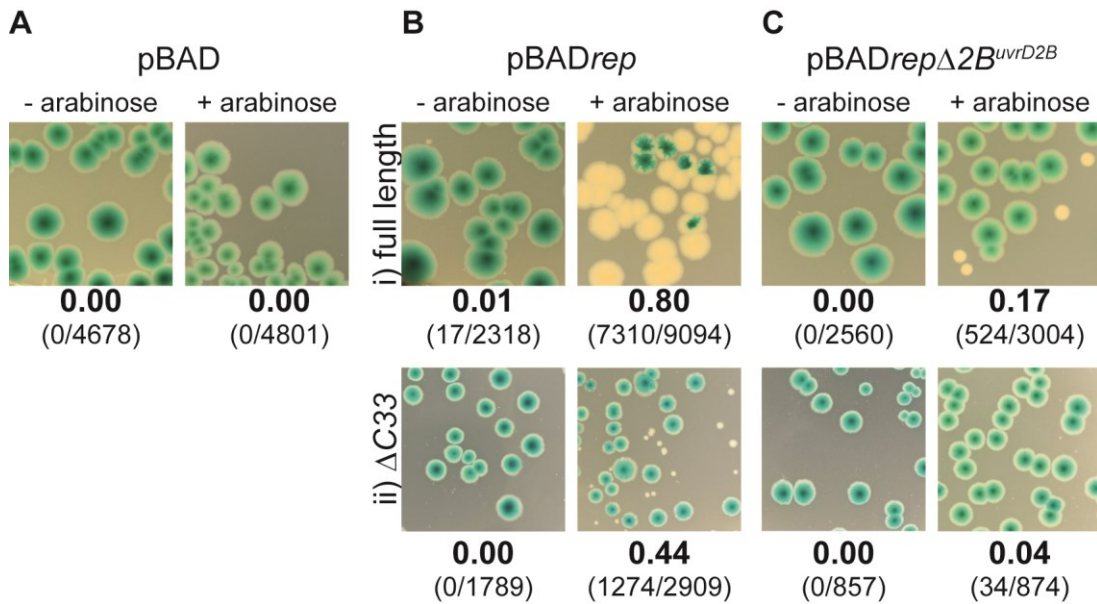
Figure 4.24 RepΔ2B^{uvrD2B} complements the *rep recB* lethality *in vivo*
Blue/white screening for loss or retention of pRC7*rep* in *rep recB* (N7919) strains with different pBAD derivatives encoding (i) full length versions or (ii) C-terminal truncations of *rep* mutants on LB$^{0.5}$ agar with kanamycin ± arabinose in the presence of IPTG and X-Gal. Fractions of white colonies are given, with numbers of white and total numbers of colonies in brackets from at least four independent replicates. Note that A and B have been used in Figure 4.6.

4.2.6 Rep activity is not altered by different N-terminal tags

As the insertion of the UvrD 2B subdomain restored Rep function *in vivo*, I wished to further characterise this mutant protein *in vitro*, in order to assess the general role of a 2B subdomain in Rep. Rep and RepΔ2B had been purified in our laboratory previously using a biotin tag. However, yields were very low. Therefore RepΔ2B^{uvrD2B} and wild-type Rep were purified with a hexahistidine (His-) tag. Purification of His-RepΔ2B failed and alternative purification attempts were abandoned due to time constraints.

DNA unwinding by bio- and His-Rep was compared to untagged Rep. Untagged Rep unwound DNA more efficiently than bio-Rep and His-Rep, similar to previous observations (Cheng *et al.*, 2002). However, the levels of DNA unwinding by the two tagged proteins were indistinguishable (Figure 4.25B). Thus, while a tag on the Rep protein did affect its the behaviour, no differences between different tags could be observed. Comparisons between biotinylated and His-tagged Rep proteins was

therefore possible although it must be borne in mind that the different tags could potentially affect Rep activities differentially within the context of the replisome.
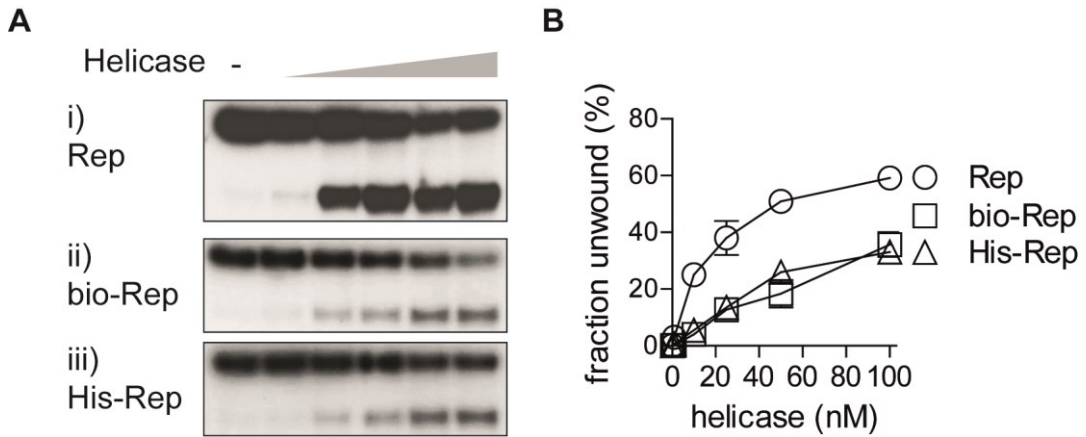
Figure 4.25 Biotin and His-tags reduce DNA unwinding by Rep to the same degree
(A) DNA unwinding by (i) Rep, (ii) bio-Rep or (iii) His-Rep (1, 10, 25, 50 and 100 nM) on DNA fork structures with 60bp dsDNA (CC139+CC140). (B) Fractions of unwound DNA for different helicase concentrations. Error bars represent standard error of the mean (n=3).

4.2.7 Insertion of the UvrD 2B subdomain reduces helicase activity

A DNA helicase assay revealed that the RepΔ2B^{uvrD2B} was a functional helicase, albeit with lower levels of DNA unwinding compared to wild-type Rep (Figure 4.26B). Thus, the presence of an exogenous 2B subdomain is inhibitory for DNA unwinding by Rep.
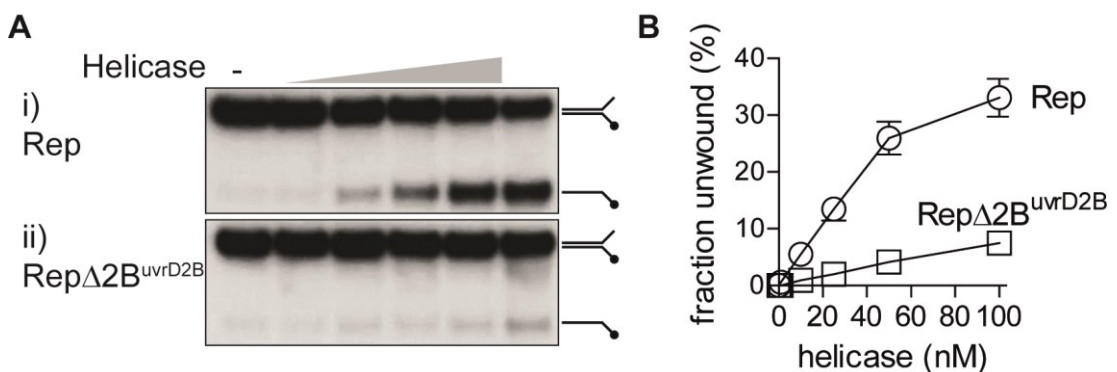
Figure 4.26 A 2B subdomain restricts the DNA helicase activity of Rep
(A) DNA unwinding by (i) Rep and (ii) RepΔ2B^{uvrD2B} (1, 10, 25, 50 and 100 nM) on DNA fork structures with 60bp dsDNA (CC139+CC140). (B) Fractions of unwound DNA for different helicase concentrations. Error bars represent standard error of the mean (n=4).

4.2.8 RepΔ2B^uvrD2B cooperates with DnaB in DNA unwinding

Cooperativity between Rep and DnaB was not observed for RepΔ2B or UvrD (Figure 4.4) (Guy *et al.*, 2009). It was therefore tested whether the cooperativity was specific to wild-type Rep only.

RepΔ2B^uvrD2B showed cooperativity in the presence of DnaB to levels similar to those of wild-type Rep (Figure 4.4C). Thus, the presence of the UvrD 2B subdomain restored cooperativity in DNA unwinding. Since RepΔ2B^uvrD2B was a very inefficient helicase, it cannot be said whether cooperativity depends on a 2B subdomain in general, or whether DNA unwinding by RepΔ2B could not be any further stimulated.
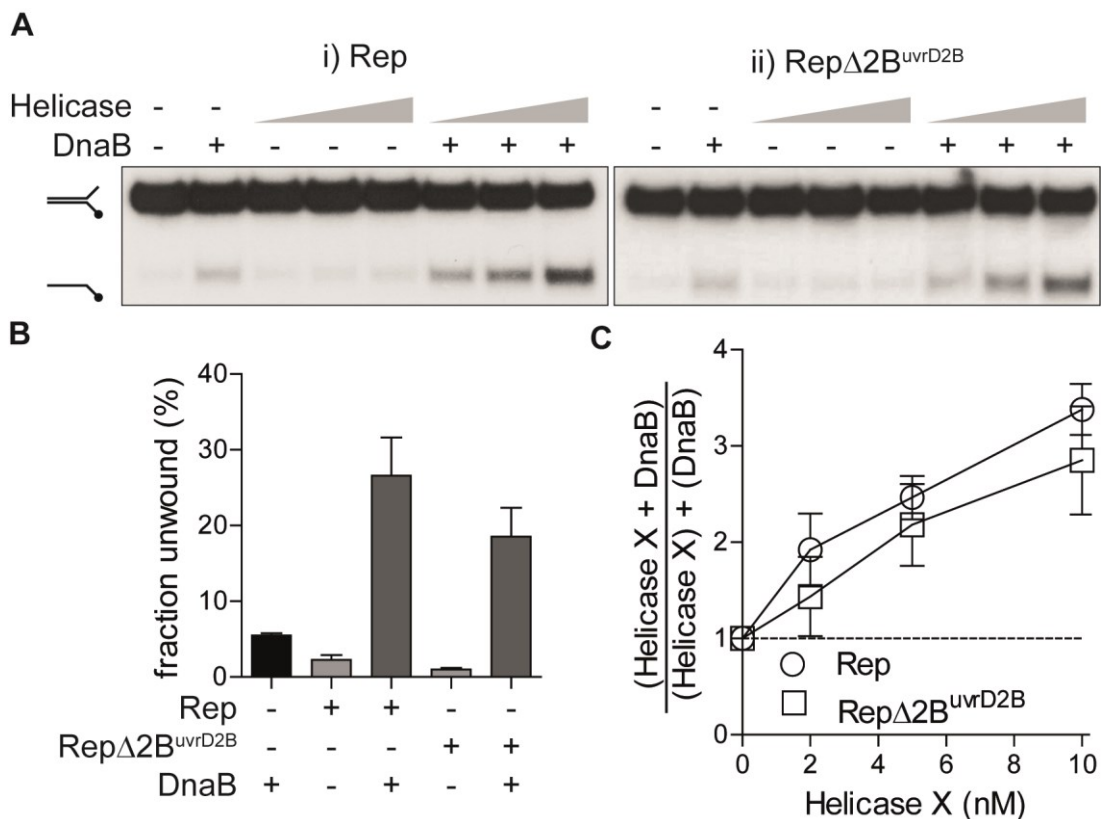
Figure 4.27 RepΔ2B^uvrD2B cooperates with DnaB in DNA unwinding
(A) Cooperativity of DNA unwinding by (i) Rep or (ii) RepΔ2B^uvrD2B (2, 5 and 10 nM) with DnaB (100 nM hexamers) on DNA fork structures with 60 bp dsDNA (CC139+CC140). (B) Fractions of unwound DNA by 10 nM Rep and RepΔ2B^uvrD2B without and with DnaB. Error bars represent standard error of the mean. (C) Cooperativity in DNA unwinding shown as fractions of unwound DNA by Rep and RepΔ2B^uvrD2B with DnaB compared to the sum of the individual levels of DNA unwinding by the two individual helicases. Error bars represent standard error of the mean (n=5).

4.2.9   Nucleoprotein displacement is dependent on a 2B subdomain

In the absence of a 2B subdomain, RepΔ2B was not able to displace streptavidin blocks from ssDNA (Figure 4.14). Substrate 1, which displayed streptavidin removal by helicases of both polarities, was chosen to assay the role of the 2B subdomain in the removal of proteins from ssDNA (Figure 4.14). Wild-type UvrD was used as a control, as it has been demonstrated before that the SF1A helicases Rep and UvrD are able to displace proteins from ssDNA (Myong *et al.*, 2005; Veaute *et al.*, 2005).

All helicases with a 2B subdomain were able to displace streptavidin at least partially (Figure 4.28). UvrD was most efficient with the lowest concentration tested (2 nM) fully displacing the block. Higher concentrations of UvrD resulted in streptavidin-independent bandshifting (Figure 4.28A.iii), indicating a higher affinity of UvrD to ssDNA compared to all other tested helicases. RepΔ2B^{uvrD2B} was less efficient at displacing streptavidin than Rep or UvrD (Figure 4.28), but more efficient than RepΔ2B (Figure 4.14). Thus, the presence of a 2B subdomain is essential for Rep to efficiently displace nucleoprotein blocks from ssDNA.
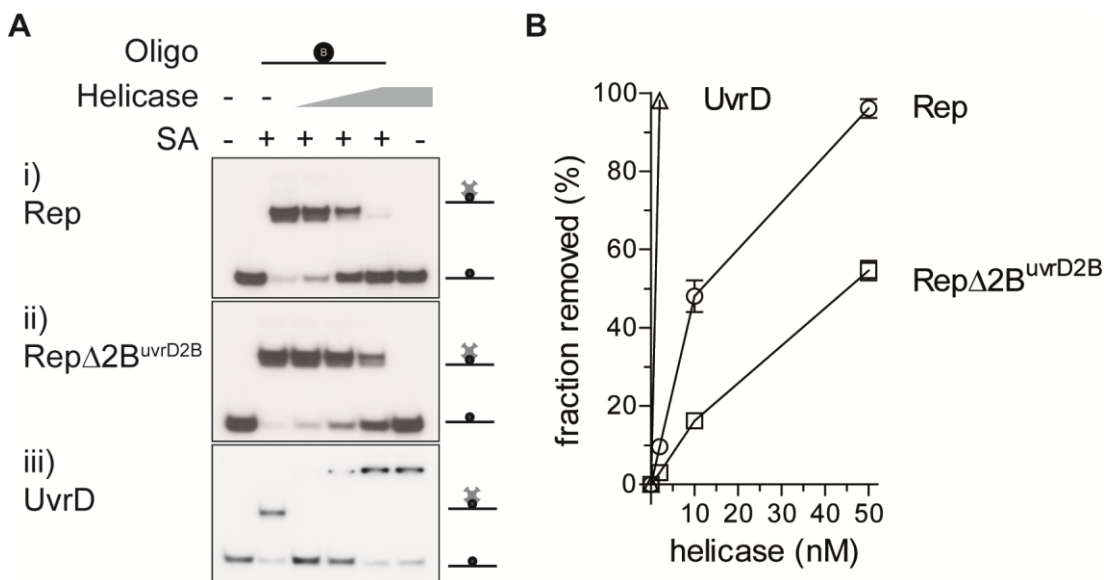
Figure 4.28 Streptavidin displacement depends on the presence of a 2B subdomain
(A) Displacement of streptavidin (1 µM) from biotinylated dT60-mers (PM328) by different helicases (2, 10 and 50 nM). (B) Relative levels of streptavidin displacement from PM328 by individual helicases. Note: UvrD is not shown for concentrations higher than 2 nM due to streptavidin-independent bandshifts. Error bars represent standard error of the mean (n=2).

4.2.10 DNA unwinding by RepΔ2B^{uvrD2B} is not inhibited by biotin-streptavidin complexes

Next, it was assessed whether the presence of the UvrD 2B subdomain also relieved the inhibition of DNA unwinding in the presence of nucleoprotein blocks by RepΔ2B (Figure 4.17).

DNA unwinding by RepΔ2B^{uvrD2B} was not inhibited by streptavidin (Figure 4.17B). Similar to wild-type Rep, RepΔ2B^{uvrD2B} was also able to displace streptavidin from dsDNA without fully unwinding the duplex DNA, although to a lesser extent (2% DNA unwinding + ~5% streptavidin displacement; Figure 4.29D). A 2B subdomain in Rep is therefore crucial to the unwinding of protein-bound DNA.
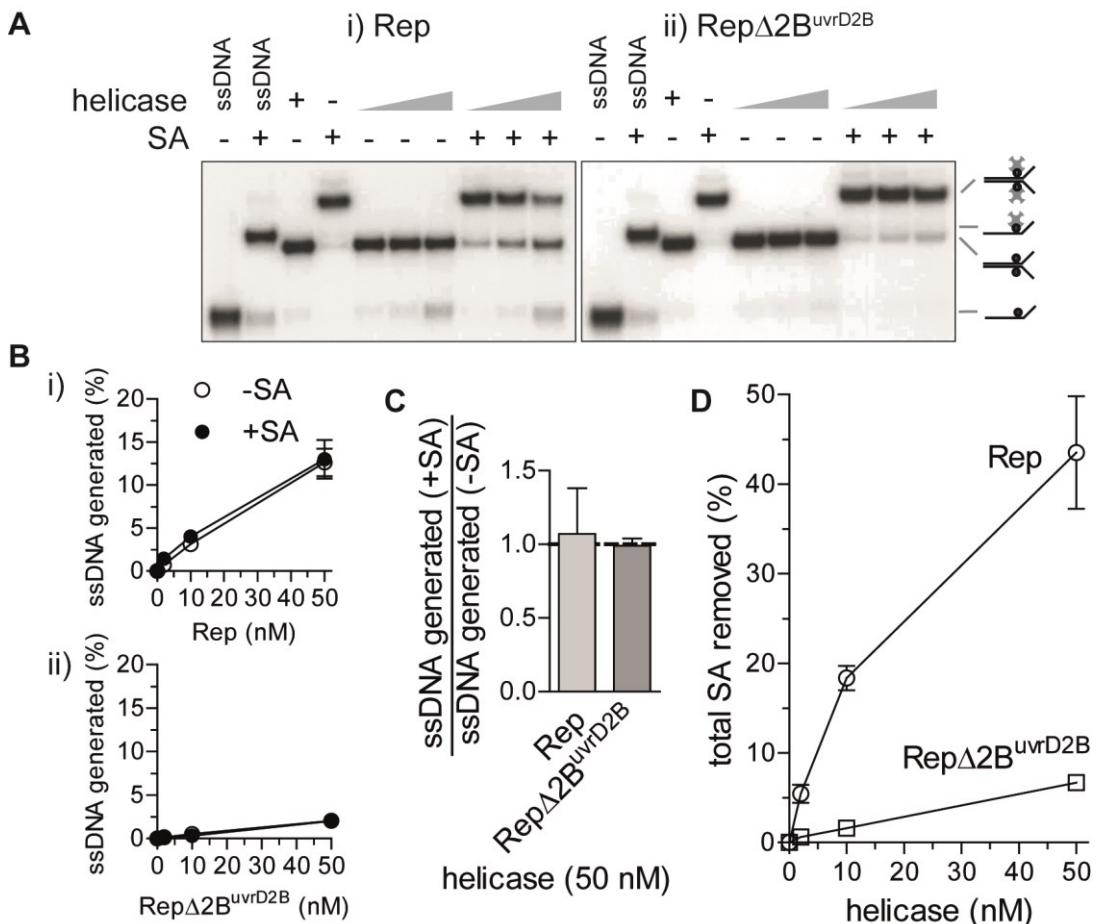
Figure 4.29 DNA unwinding by RepΔ2B^{uvrD2B} is not inhibited by a streptavidin block
(A) DNA unwinding of a dually biotinylated DNA fork (CC139B53+CC140B47) in the absence or presence of streptavidin by the denoted helicases (2, 10 and 50 nM). (B) Total levels of DNA unwinding in the absence or presence of streptavidin by 50 nM Rep and RepΔ2B^{uvrD2B}. (C) Inhibition of DNA unwinding by streptavidin given as the fraction of DNA unwinding in the presence of streptavidin divided by the levels of DNA unwinding in the absence of streptavidin. Values below 1 indicate inhibition of DNA unwinding by streptavidin (D) Total levels of streptavidin removal from ss- and dsDNA. Error bars represent standard error of the mean (n=2).

4.2.11 The presence of a 2B subdomain is necessary for stable interaction with DnaB-bound forked DNA

In the absence of the 2B subdomain, RepΔ2B did not form a stable Rep-DnaB-dsDNA complex (Figure 4.9). In contrast, RepΔ2B^{uvrD2B} was able to form such a complex (lanes 8-10; Figure 4.30B) at similar concentrations to wild-type Rep (lane 10; Figure 4.30B). However, in the absence of DnaB, binding of the forked DNA substrate was reduced by RepΔ2B^{uvrD2B} compared to wild-type Rep, as indicated by reduced levels of DNA smearing in the gel (lanes 5; Figure 4.30A and B). These data demonstrate that a 2B subdomain is essential for Rep to form of a stable complex on DnaB-bound forked DNA.
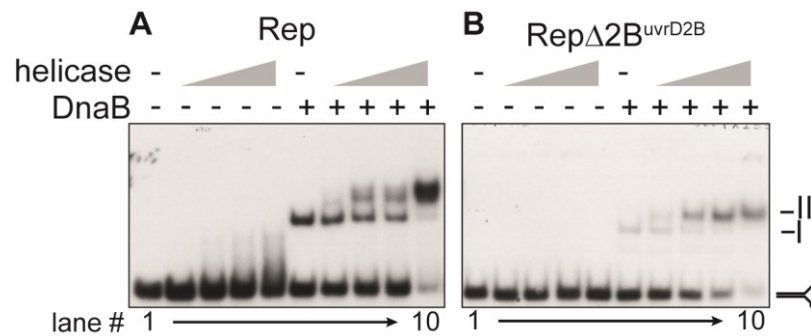
Figure 4.30 RepΔ2B^{uvrD2B} forms a stable complex Rep-DnaB-DNA complex
DNA bandshifts of (A) Rep and (B) RepΔ2B^{uvrD2B} (1, 5, 10 and 25 nM) with DnaB (100 nM hexamers) on forked DNA having two ssDNA arms (60 bp dsDNA, 38 bp ssDNA; CC139+CC140) in the presence of 10 µM ADP after resolution on a 4% acrylamide gel (n=3). "I" = DNA-DnaB complex; "II" = DNA-DnaB-Rep complex.

To differentiate between differences in binding to ssDNA, dsDNA and the branch point, SPR was performed. 5'-biotinylated DNA was immobilised onto streptavidin coated SPR chips and His-Rep and His-RepΔ2B^{uvrD2B} were used as the analyte (His-RepΔ2B could not purified; 4.2.6). The different Rep proteins displayed binding to the DNA, but the proteins also bound non-specifically to the chip surface, as the baseline was not reached again once the channels were washed with salt solutions (data not shown). None of the different buffer conditions tested removed the proteins from the chip surface. Control experiments showed that the non-specific binding was due to the Rep protein itself and not due to the His-tag (data not shown). Thus, these experiments did not give any significant data. Due to time constraints alternative experiments could not be conducted.

4.3   Discussion

In this chapter, the function of the 2B subdomain of Rep was investigated via the characterisation of Rep, RepΔ2B and RepΔ2B^{uvrD2B}. This work shows that the 2B subdomain of Rep is essential for Rep function *in vivo* (Figure 4.23), refuting a previous report (Cheng *et al.*, 2002). Overexpression of RepΔ2B as well as HelD, which naturally lacks a 2B subdomain, was toxic (Figure 4.7). The autoinhibitory function of the 2B subdomain of Rep with respect to helicase function that had been proposed previously (Brendza *et al.*, 2005) is therefore likely required to prevent toxicity from the expression of Rep. Moreover, cellular concentrations of HelD are very low (Mendonca *et al.*, 1993), suggesting that the expression of helicases lacking a 2B subdomain needs to be tightly controlled.

Rep and RepΔ2B^{uvrD2B} showed cooperativity in DNA unwinding with DnaB (Figure 4.27). The Rep-DnaB interaction is dependent on the Rep C-terminus but not the Rep 2B subdomain (Guy *et al.*, 2009). Thus, RepΔ2B^{uvrD2B} is likely able to interact with DnaB. The Rep-DnaB interaction might increase the local concentration of Rep at the replication fork, which could lead to an increased processivity of the leading Rep helicase molecule, in a similar manner to that proposed in the cooperative inchworm model (Byrd & Raney, 2006). In contrast, RepΔ2B is already a very active helicase on its own. The interaction with DnaB (Guy *et al.*, 2009) might therefore not be able to further stimulate DNA unwinding at the replication fork, as shown by the lack of cooperativity between RepΔ2B and DnaB (Figure 4.4). Alternatively, cooperativity between Rep and DnaB could depend on the presence of a 2B subdomain. Crystal structures of a ssDNA-Rep complex show that the 2B subdomain can exist in a "closed" or an "open" conformation, which differ in a 130° rotation of the 2B subdomain along a hinge region that connects the 2B to the 2A subdomain (more details in chapter 5) (Korolev *et al.*, 1997). Interaction with other proteins, such as DnaB, could induce allosteric changes in the Rep 2B subdomain that activate helicase activity of Rep. In such a model, the 2B subdomain would provide a means to restrict Rep helicase activity to sites where it is required (Brendza *et al.*, 2005).

Although RepΔ2B displays higher levels of DNA unwinding compared to wild-type Rep (Cheng *et al.*, 2002) (Figure 4.3), the 2B subdomain of Rep was essential for

efficient nucleoprotein displacement from ssDNA and dsDNA (Figure 4.14, Figure 4.17 and Figure 4.20). The level of inhibition was dependent on the affinity of these protein-ligand interactions. A single *lac* repressor-operator complex has a dissociation constant (K_d) of about 10^{-11} M at 30°C (Gilbert & Muller-Hill, 1967). On the other hand, the biotin-streptavidin interaction with a dissociation constant of about 10^{-14} M at 25°C (Green, 1990; Teulon *et al.*, 2011) is one of the strongest non-covalent interactions known and was consequently more inhibitory to DNA unwinding by RepΔ2B than the repressor-operator complex (Figure 4.17 and Figure 4.20). Due to time constraints it was not tested whether larger numbers of repressor operator complexes would show an additive effect on the inhibition of DNA unwinding by RepΔ2B and also Rep.

A reduction in DNA unwinding in the presence of protein-DNA blocks correlated with a lack of accessory replicative helicase function of RepΔ2B within the context of the replisome *in vitro* (Figure 4.11). Hence, the lack of complementation of Rep function by RepΔ2B in a *Δrep ΔuvrD* strain on rich medium (Figure 4.5D) is likely a result of the inability of RepΔ2B to resolve replication/transcription conflicts, which are thought to be the main source of lethality in the absence of accessory replicative helicases (Guy *et al.*, 2009). Similar to RepΔ2B, DNA unwinding by HelD is also reduced by the presence of a repressor-operator complex (Yancey-Wrona & Matson, 1992). The ability of the UvrD 2B subdomain in RepΔ2B[uvrD2B] to restore nucleoprotein displacement (Figure 4.28 and Figure 4.29), suggests that the 2B subdomain is likely a general requirement for SF1A helicases to displace nucleoprotein blocks efficiently. The low levels of DNA unwinding by DnaB in the presence of protein complexes emphasise the need for accessory replicative helicases *in vivo* (Figure 4.17 and Figure 4.21) (Yancey-Wrona & Matson, 1992).

The SF1B helicase Dda is able to displace streptavidin blocks from ssDNA (Byrd & Raney, 2004). Collisions between a streptavidin block and the Dda cause increased levels of ATP hydrolysis compared to Dda translocation away from the block (Raney & Benkovic, 1995). These reactions did not contain a streptavidin trap and therefore likely represent several cycles of streptavidin displacement by Dda and streptavidin rebinding to the oligonucleotide. The increased ATPase activity suggests that

additional energy input is required, as ssDNA translocation alone does not generate enough force to displace protein blocks. Given that the 2B subdomain of Rep exists in different conformational states (open and closed; see chapter 5) it is possible that these conformational changes play a role in nucleoprotein displacement. One conformation of the 2B subdomain could be activated for protein displacement or alternatively alternations between the open and the closed conformation, as seen during ssDNA translocation (Myong *et al.*, 2005), could act as an ATP-dependent lever that facilitates protein displacement. RepΔ2B lacks this domain and is therefore only able to remove proteins via ssDNA translocation and consequently with a greatly reduced efficiency compared to wild-type Rep. In the light of the results presented above, the 2B subdomain of SF1A helicases is likely required to couple the energy derived from ATP hydrolysis to protein displacement.

Genetic and biochemical studies on UvrDΔ2B could be performed to test whether the absence of the 2B subdomain in UvrD has similar effects on nucleoprotein displacement as in Rep, confirming the role of the 2B subdomain in other SF1A helicases. However, it has been stated that purification of UvrDΔ2B failed due to cytotoxicity and increased levels of plasmid rearrangements, suggesting severe defects for UvrDΔ2B (Cheng *et al.*, 2002).

Wild-type Rep, UvrD and PcrA require additional protein-protein interactions or multiple helicase monomers for self-dimerization or stabilisation to efficiently unwind DNA *in vitro* (cooperative inchworm model) (Byrd & Raney, 2005; Cheng *et al.*, 2001; Maluf *et al.*, 2003; Yang *et al.*, 2008). However, in the absence of a 2B subdomain, monomers of RepΔ2B can unwind DNA (Brendza *et al.*, 2005). The toxicity upon overexpression of RepΔ2B might therefore be caused by unrestricted DNA unwinding in the cell, most likely at the replication fork (compare pBAD*repΔ2B* and pBAD*repΔ2BΔC33*, Figure 4.5). A kinetic model for DNA unwinding by Rep additionally proposed a higher affinity to DNA for RepΔ2B compared to wild-type Rep (Cheng *et al.*, 2002). RepK28AΔ2B was more toxic than RepΔ2B and RepK28A on their own (Figure 4.8). Complementation of this toxicity was more efficient in the presence of chromosomal wild-type Rep compared to UvrD, suggesting that the plasmid-expressed Rep mutants compete with and prevent replication fork access

by the chromosomal helicases. The absence of the 2B subdomain could reduce steric occlusion of the motor core and thereby facilitate ssDNA binding (Figure 4.1), which could explain this phenotype. However, this is in contrast to DNA bandshifts, which indicated a reduced affinity of RepΔ2B with a DnaB-bound DNA fork (Figure 4.9). Further investigation of the affinity of Rep and RepΔ2B to DnaB and different DNA substrates is therefore required to determine whether the RepΔ2B toxicity is linked to an altered DNA affinity.

In summary, these findings demonstrate the function of the 2B subdomain in the SF1A helicase Rep and point to a critical and conserved function of 2B subdomains across SF1A helicases – the removal of nucleoprotein complexes.

Chapter 5

CHARACTERISATION OF POINT MUTATIONS IN REP THAT PHENOCOPY REPΔ2B

Chapter 5 – Characterisation of point mutations in Rep that phenocopy RepΔ2B

5.1 Introduction

In the previous chapter it was shown that Rep function depends on the 2B subdomain. In the absence of the 2B subdomain, RepΔ2B failed to remove nucleoprotein complexes and consequently failed to act as an accessory replicative helicase.

Crystal structures of Rep revealed that the 2B subdomain exists in at least two stable conformations, open and closed (Korolev *et al.*, 1997). Upon binding of a DNA fork, the 2B subdomain of SF1A helicases is usually in the closed conformation and makes contacts with dsDNA (Lee & Yang, 2006; Rasnik *et al.*, 2004; Velankar *et al.*, 1999). Mutations of the 2B subdomain of PcrA and UvrD affecting the interaction with dsDNA impair helicase activity (Lee & Yang, 2006; Soultanas *et al.*, 2000).

In the closed conformation, the 2B subdomain makes contacts with the 1B subdomain, burying the ssDNA in the central cleft between subdomains 1A and 2A. In UvrD, closing of the 2B subdomain was dependent on salt concentration, indicating that the 1B and 2B subdomains form ionic interactions in UvrD (Jia *et al.*, 2011). Mutations in the 2B subdomain of UvrD that are thought to destabilise the closed conformation of the 2B subdomain increase DNA helicase activity (Meiners *et al.*, 2014; Zhang *et al.*, 1998).

The open conformation of Rep is defined by a rotation of 130° along the hinge region of the 2B subdomain (Figure 5.1) (Korolev *et al.*, 1997). Single molecule FRET experiments have shown that the 2B subdomain switches between the open and closed conformations during translocation along ssDNA (Myong *et al.*, 2005). Similar conformational changes were also identified via FRET analysis for the 2B subdomains of UvrD and PcrA (Jia *et al.*, 2011; Park *et al.*, 2010), suggesting that the 2B subdomains of SF1A helicases are highly flexible. A mutation in one of the hinges that was proposed keep the 2B subdomain in a more open conformation decreases DNA binding by UvrD (Lee & Yang, 2006).
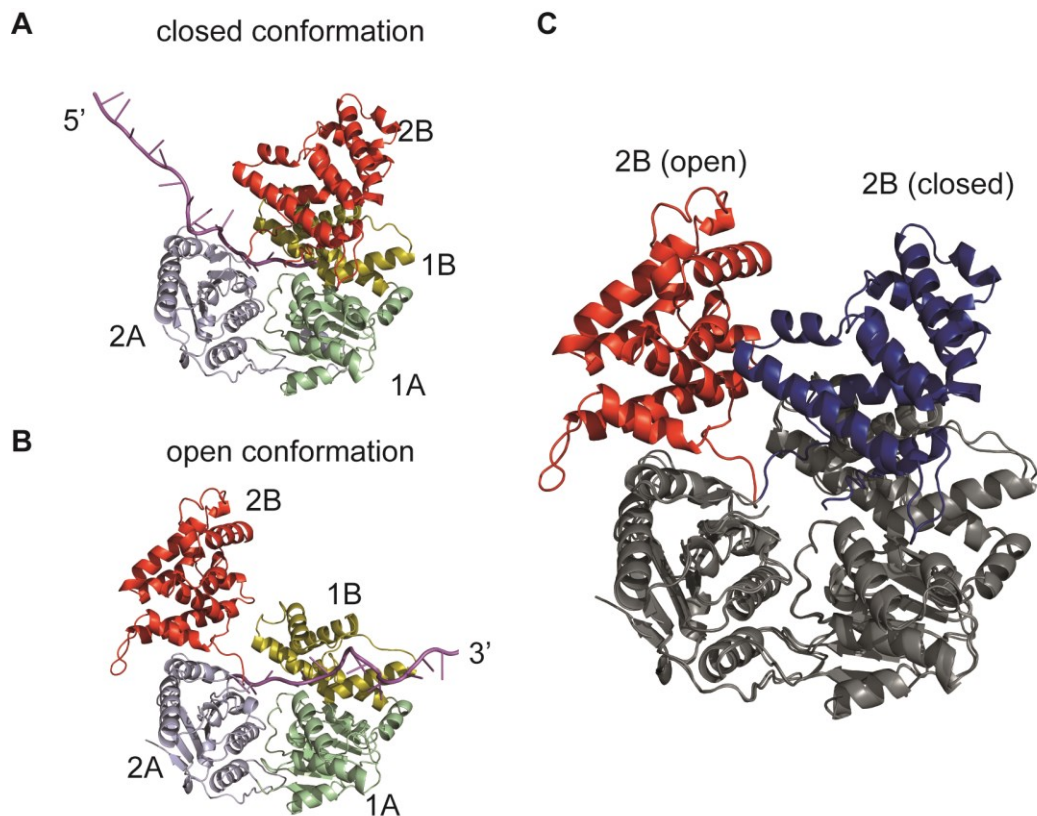
Figure 5.1 Conformational changes of the 2B subdomain of Rep
Crystal structures of *E. coli* Rep with the 2B subdomain in (A) the closed and (B) the open conformation characterised by a rotation of 130° around a hinge region connecting the 2B subdomain to the 2A subdomain. Colour coding as in Figure 1.4 (C) Superimposition of both Rep conformations with the 1A, 1B and 2A subdomains in grey and the 2B subdomain in the open and closed conformation in red and blue, respectively (PDB: 1UAA, (Korolev *et al.*, 1997))

The function of the 2B subdomain in nucleoprotein displacement and the physiological role of the different conformations has however not been addressed previously.

In this chapter selected residues of the 2B subdomain were mutated to identify the function of the 2B subdomain of Rep. Mutations that reconstituted the RepΔ2B phenotype *in vivo* (Figure 4.5) were further characterised. The aim was to find mutations that gave the same properties as RepΔ2B and correlate those properties with structural effects of the point mutation on Rep.

5.2 Results

5.2.1 Mutagenic screens for RepΔ2B like phenotypes

The characterisation of RepΔ2B has shown that the 2B subdomain of Rep was crucial to unwind and displace proteins form DNA. However, RepΔ2B lacked roughly a quarter of the wild-type sequence of Rep and the direct impact of the 2B subdomain on nucleoprotein displacement and DNA unwinding could not be determined. It was therefore attempted to reconstitute the RepΔ2B phenotype via site directed mutagenesis of selected residues in the 2B subdomain of an otherwise full length Rep protein (Figure 5.2).

A

```
UvrD   378 GGMRFFERQEIKDALSYLRLIANRNDDAAFERVVNTPTRGIGDRTLDVVRQTSRDRQLTL
PcrA   382 GGLKFYDRKEIKDILAYLRVIANPDDDLSLLRIIINVPKRGIGASTIDKLVRYAADHELSL
Rep    373 GGTSFFSRPEIKDLLAYLRVLTNPDDDSAFLRIVNTPKREIGPATLKKLGEWAMTRNKSM
           **   *:.* **** *:***:::* :** :: *::*.*.* **  *:. : . :  :: ::

UvrD   438 WQACRELLQEKALAGRAASALQRFMELIDALAQETADMPLHVQTDRVIKDSGLRTMYEQE
PcrA   442 FEALGELEMIG-LGAKAAGALAAFRSQLEQWTQLQEYVSVTELVEEVLDKSGYREMLKAE
Rep    433 FTASFDMGLSQTLSGRGYEALTRFTHWLAEIQRLAEREPIAAVRDLIHGMDYESWLYETS
           : *  ::     *..:.  **   *   :    :      .:    :  :   .   : : .

UvrD   498 KG-EKGQTRIENLEELVTATRQFSYNEEDEDLMPLQAFLSHAALEA----GEG 545
PcrA   501 RT-IEAQSRLENLDEFLSVTKHFENVSDDK---SLIAFLTDLALISDLD---- 548
Rep    493 PSPKAAEMRMKNVNQLFSWMTEMLEGSELDEPMTLTQVVTRFTLRDMMERGES 545
             .: *::*:::::.:   .:    .:  .    .*  .::  :*
```

B

Rep (open conformation)
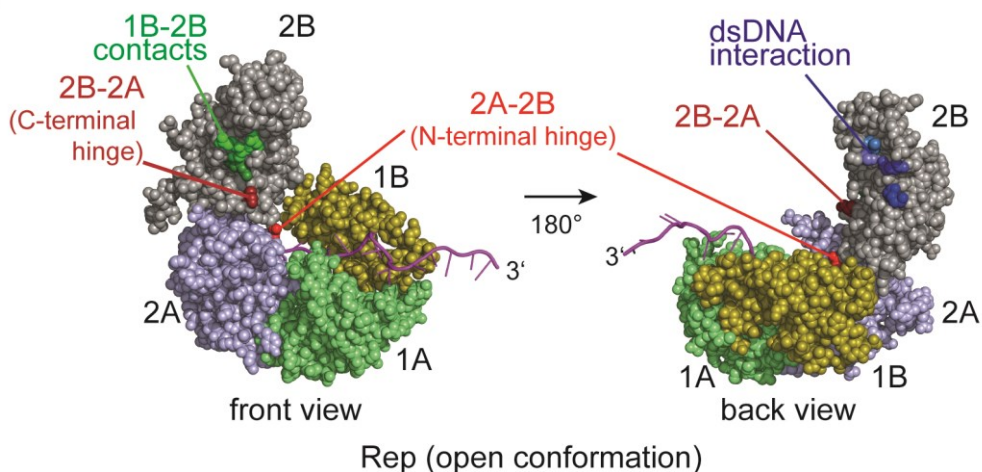
Figure 5.2 Residues for site directed mutagenesis of the Rep 2B subdomain
(A) ClustalW alignment of the 2B subdomains of UvrD (AAs 378-545), PcrA (AAs 382-545) and Rep (AAs 373-545) according to Korolev *et al.* (1997). (B) Crystal structure of Rep in the open conformation (PDB: 1UAA). Residues within the 2B subdomain targeted by SDM: 2B hinges in red, dsDNA interaction in blue and contacts with the 1B subdomain in the closed conformation in green.

Several residues within the 2B subdomain were chosen for mutation, based on previous reports: (1) residues that had been reported to be involved in the interaction with dsDNA in UvrD and PcrA (Lee & Yang, 2006; Park *et al.*, 2010; Soultanas *et al.*, 2000); (2) Residues that make contacts with the 1B subdomain in the closed conformation and were therefore proposed to prevent the formation of the closed conformation of the 2B subdomain in UvrD (Lee & Yang, 2006; Zhang *et al.*, 1998); (3) Residues within the hinge, connecting the 2A and 2B subdomain that were supposed to also destabilise the closed conformation and generally result in the opening of the 2B subdomain of UvrD (Figure 5.2 and Table 5.1) (Lee & Yang, 2006).

Table 5.1 Overview of the Rep 2B subdomain SDM
A list of all residues mutated in the SDM of the 2B subdomain with the amino acid change. Residues were chosen based on previous publications that reported on the function of the 2B subdomain. Note: Only a double mutant of G373 G374 was created, as the original mutation was also a double mutant (UvrD G378T G379T, (Lee & Yang, 2006)).

Rep residue	Change in SDM	Reported / proposed function	Original mutation	Reference
G373	A, T	2A-2B hinge	UvrD G378T	(Lee & Yang, 2006)
G374	A, T	2A-2B hinge	UvrD G379T	(Lee & Yang, 2006)
R391	A	1B-2B contacts	UvrD R396E	(Lee & Yang, 2006)
D397	A	1B-2B contacts	-	(Zhang *et al.*, 1998)
D398	A	1B-2B contacts	UvrD D403A	(Meiners *et al.*, 2014)
D399	A	1B-2B contacts	UvrD D404A	
K410	A	dsDNA interaction	PcrA K419A	(Soultanas *et al.*, 2000)
E412	A, G	dsDNA interaction	PcrA G421E	(Park *et al.*, 2010)
G414	A, T	dsDNA interaction	-	(Lee & Yang, 2006)
			PcrA G423T	(Park *et al.*, 2010)
			UvrD G419T	(Lee & Yang, 2006)
T417	A	dsDNA interaction	PcrA T426A	(Soultanas *et al.*, 2000)
			UvrD T422A	(Lee & Yang, 2006)
R448	A	dsDNA interaction	PcrA K456A	(Soultanas *et al.*, 2000)
G543	A	2B-2A hinge	UvrD G543A	(Lee & Yang, 2006)
S545	A	2B-2A hinge	UvrD G545A	(Lee & Yang, 2006)

Rep genes with the mutated residues in the 2B subdomain were cloned under the control of the arabinose inducible promoter, P_{BAD} (Table 5.1, the full list of plasmids can be found in Table A.18e). These mutants were tested for a lack of complementation of the lethality of *Δrep ΔuvrD* cells on rich medium and possible

toxicity upon growth on minimal agar, in short, a mutation that phenocopied RepΔ2B (Figure 4.5).

Single mutations within the 2B subdomain of Rep corresponding to PcrA and UvrD residues involved in dsDNA binding did not affect Rep function *in vivo* (Figure 5.3), as none of the single mutations resulted in toxicity upon overexpression (Figure 5.3B.iv). Since all of these mutants already complemented the lethality of a *Δrep Δuvrd* strain on rich medium at low levels of expression (Figure 5.3B.i), different mutations potentially affecting the interaction of the 2B subdomain with dsDNA were combined (Figure 5.4). However, none of the combined mutations displayed toxicity or failed to complement Rep function either (Figure 5.4). Thus, a lack of interaction of the 2B subdomain with dsDNA is likely not responsible for the lack of complementation of Rep function by RepΔ2B. However, it cannot be excluded that the residues mutated in Rep have a different effect as their homologous mutations in UvrD and PcrA. Due to time constraints, this could not be tested in detail.

Similar to the dsDNA mutants, none of the Rep mutations located in the 1B-2B interface were toxic upon overexpression and growth on minimal agar (Figure 5.5B.iv). The mutation of residue R391 in Rep, located in the interface between subdomains 1B and 2B, showed a reduction in the complementation of Rep function at low levels of expression (Figure 5.5B.i) but led to full complementation of the *Δrep Δuvrd* lethality on rich medium in the presence of arabinose, albeit with a reduction in colony size compared to the wild-type Rep control (Figure 5.5B.ii). Rep contains three aspartate residues in homologous positions in the 2B subdomain (D397-399) compared to UvrD (D403 D404) and therefore all three residues were tested. None of the single mutations affected the growth of the strains, other than a slight reduction in colony size upon growth in the presence of arabinose (Figure 5.5). A double mutant, which was the equivalent of the original UvrD D403A/D404A mutation based on the 2B subdomain alignment (Figure 5.2A), resulted in a reduction of growth by three orders of magnitude in the absence of arabinose (Figure 5.5B.i). Growth was restored by high levels of expression (Figure 5.5B.ii) but again displaying smaller colonies than the wild-type Rep control. The triple mutant (D397-D399A) and the quadruple mutant (R391A/D397-399A) resulted in complete

lack of complementation of the *Δrep ΔuvrD* lethality on rich medium at low levels of expression, but still retained function at higher levels of expression (Figure 5.5B.i and ii). Both these mutations displayed colony sizes similar to wild-type Rep. However, none of the mutations tested phenocopied RepΔ2B with respect to toxicity on minimal medium. Thus, the suggested destabilisation of the closed conformation led to a slight reduction in Rep function (Figure 5.5B.i), which could be a result of reduced nucleoprotein displacement. However, due time constraints and more severe phenotypes of another point mutation (see below), these mutations were not further investigated.

The hinge connecting the 2B to the 2A subdomain was mutated. The 2B subdomain is an insertion into the 2A motor core domain. Mutations of the conserved residues G373 and G374 in Rep that form the N-terminal linker of the 2B subdomain did not display any toxicity or lack of complementation of growth of the *Δrep ΔuvrD* strain on rich medium. This was independent of the amino acid change to alanine or threonine (homologous to the original UvrD G378T/G379T mutant; Figure 5.6) (Lee & Yang, 2006). On the other hand, the mutation G543A/S545A in the C-terminal linker region of the 2B subdomain phenocopied RepΔ2B, as overexpression of Rep G543A/S545A in a *Δrep ΔuvrD* background did not restore viability upon growth on rich medium (Figure 5.6D.ii). Additionally, Rep G543A/S545A was toxic even at low levels of expression in a *Δrep ΔuvrD* background (Figure 5.6D.iii) and in a *Δrep* strain (Figure 5.6B.ii and iv). Thus, out of all point mutants created, only Rep G543A/S545A phenocopied RepΔ2B *in vivo*.
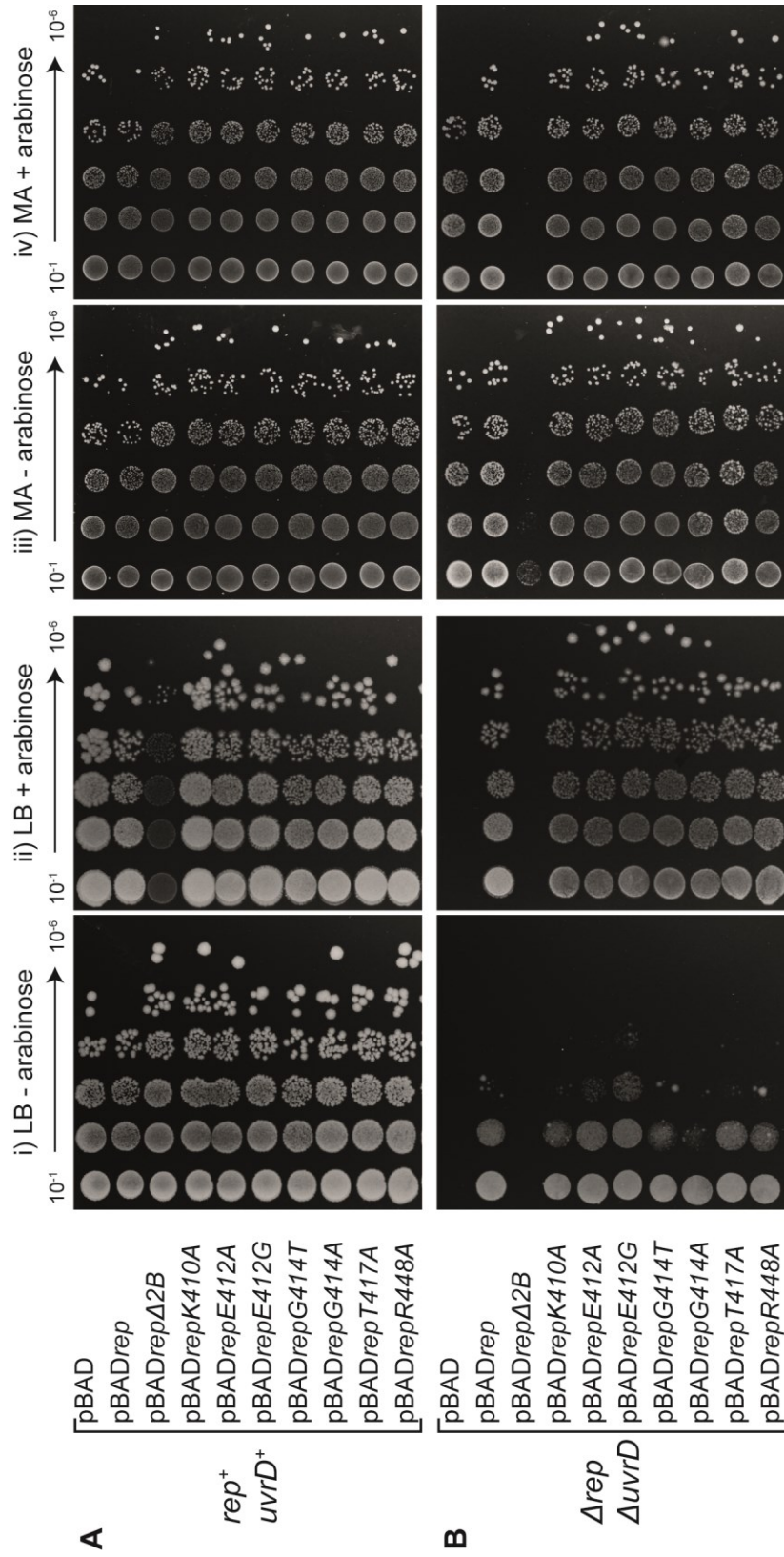
Figure 5.3 Single mutations affecting the dsDNA interaction of the 2B subdomain do not phenocopy RepΔ2B.
Colony formation of (A) *rep+ uvrD+* (N6524) and (B) *Δrep ΔuvrD* (N6556) strains with different pBAD derivatives after loss of pRC7*rep*. Cells were grown in minimal medium, prior to plating of serial dilutions on LB agar (i and ii) or minimal agar (iii and iv) with kanamycin ± arabinose (n=2).
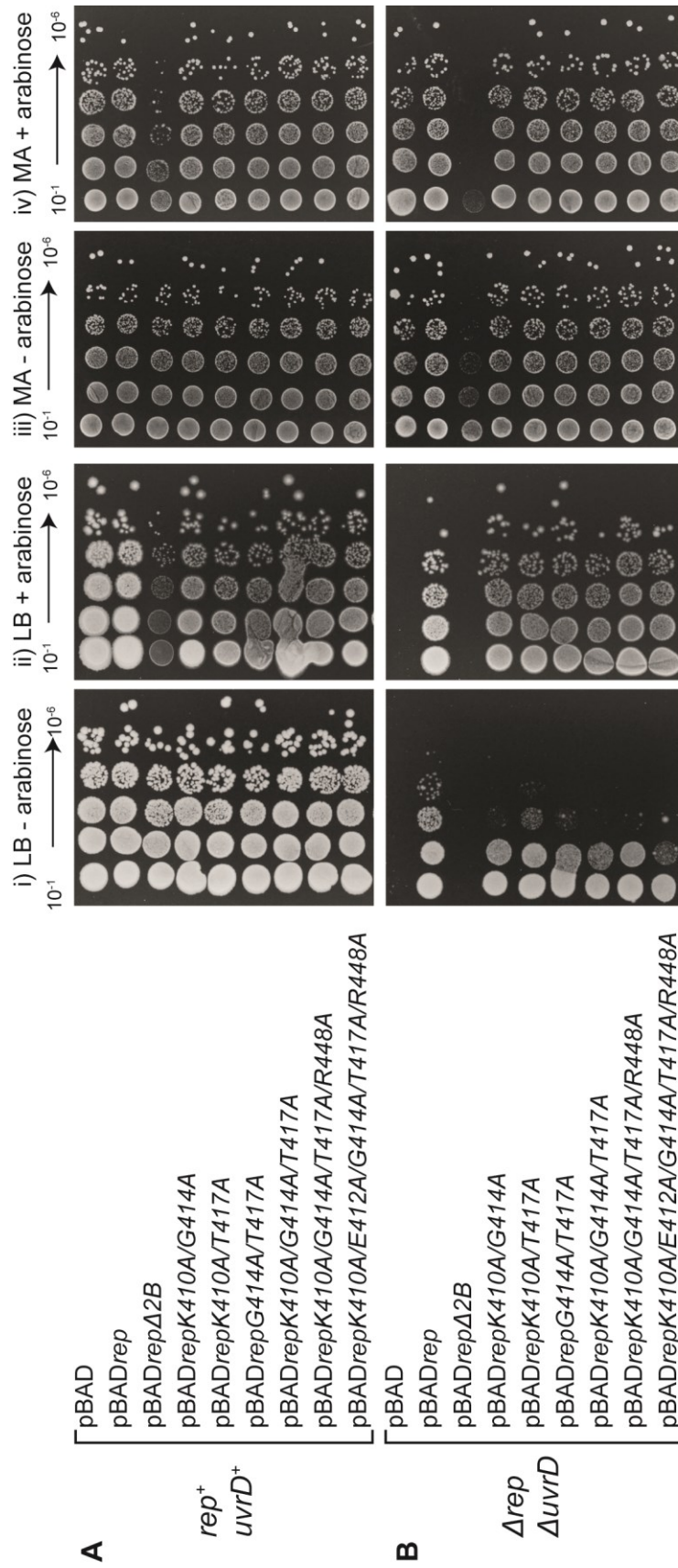
Figure 5.4 Mutations affecting the dsDNA interaction of the 2B subdomain do not phenocopy RepΔ2B
Colony formation of (A) *rep+ uvrD+* (N6524) and (B) *Δrep ΔuvrD* (N6556) strains with different pBAD derivatives after loss of pRC7*rep*. Cells were grown in minimal medium, prior to plating of serial dilutions on LB agar (i and ii) or minimal agar (iii and iv) with kanamycin ± arabinose (n=2).
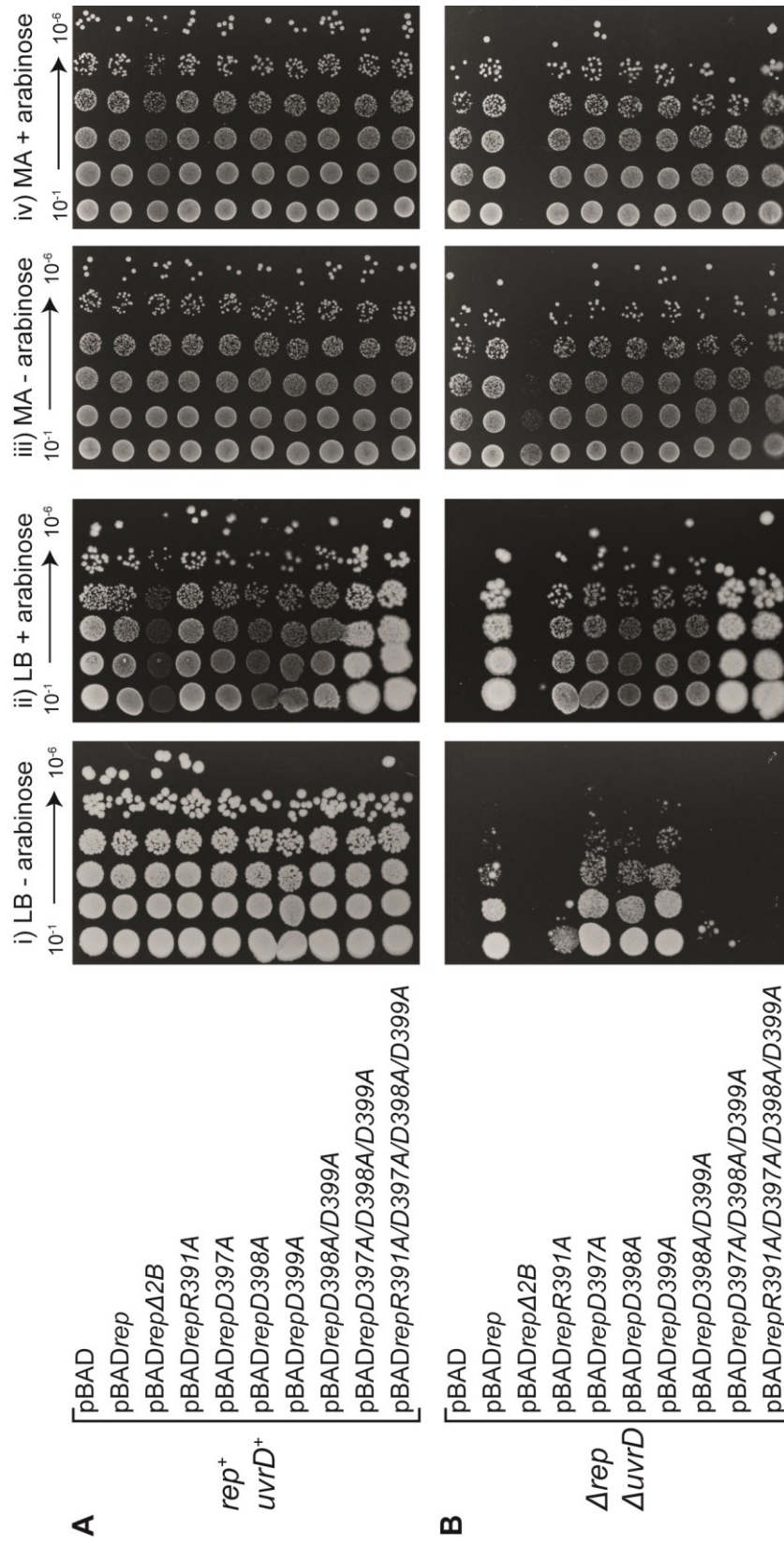
Figure 5.5 Changes in residues of the Rep 2B subdomain interacting with the 1B subdomain in the closed conformation do not phenocopy RepΔ2B
Colony formation of (A) *rep⁺ uvrD⁺* (N6524) and (B) *Δrep ΔuvrD* (N6556) strains with different pBAD derivatives after loss of pRC7*rep*. Cells were grown in minimal medium, prior to plating of serial dilutions on LB agar (i and ii) or minimal agar (iii and iv) with kanamycin ± arabinose (n=2).

137
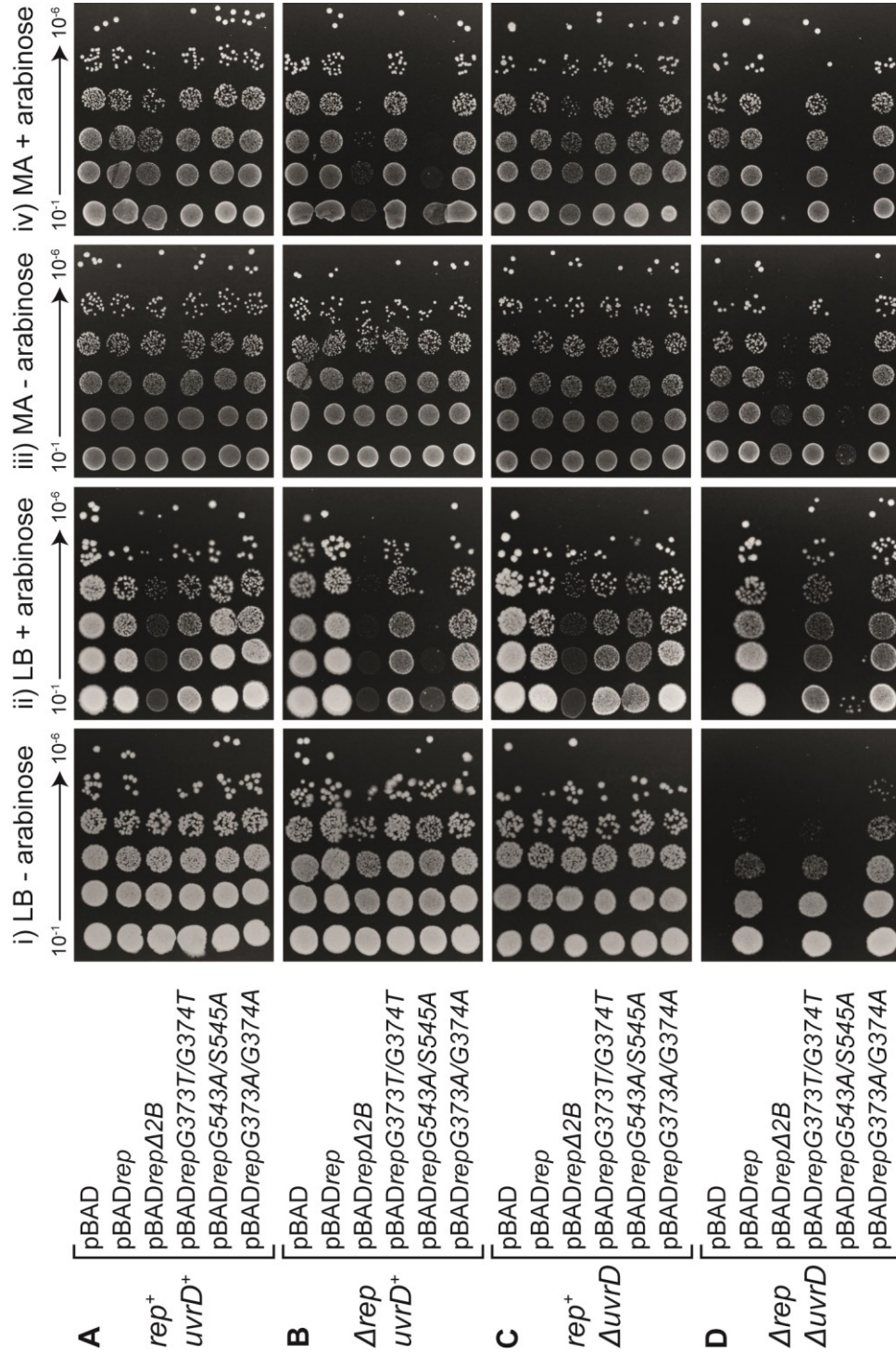
Figure 5.6 Only mutations in the C-terminal hinge of the 2B subdomain phenocopy RepΔ2B.
Colony formation of (A) rep⁺ uvrD⁺ (N6524), (B) Δrep uvrD⁺ (N6540), (C) rep⁺ ΔuvrD (N6568) and (D) Δrep ΔuvrD (N6556) strains with different pBAD derivatives after loss of pRC7rep. Cells were grown in minimal medium, prior to plating of serial dilutions on LB agar (i and ii) or minimal agar (iii and iv) with kanamycin ± arabinose (n=2).

Next, to examine whether the Rep G543A/S545A phenotype was specific to one of the residues, the single mutants Rep G543A and Rep S545A were created. Both single mutants allowed for growth in a *Δrep ΔuvrD* strain on rich medium and were even more efficient than wild-type Rep at low levels of expression (Figure 5.7D.i). Accordingly, neither of the two single mutants was toxic upon overexpression (Figure 5.7D.iv) or displayed any growth defects in the other strains including the *rep* mutant (Figure 5.7A-C). It was concluded that the double mutation in Rep G543A/S545A was essential to phenocopy RepΔ2B *in vivo*.

The interaction between Rep and DnaB is crucial for efficient complementation of the *Δrep ΔuvrD* growth defect on LB (Guy *et al.*, 2009). Conversely in the absence of the interaction between RepΔ2B and DnaB, RepΔ2BΔC33 displayed reduced levels of toxicity (Figure 4.23D and Figure 4.5D.iv). Similarly, when the C-terminus was deleted from Rep G543A/S545A, Rep G543A/S545AΔC33 lost the toxicity in the *rep* single and the *Δrep ΔuvrD* double helicase mutant backgrounds. Surprisingly, in the absence of the interaction with DnaB, Rep G543A/S545AΔC33 was also able to restore growth to the *Δrep ΔuvrD* strain on rich medium (Figure 5.8D.iv). Thus, the toxicity of Rep G543A/S545A seemed to depend on or was caused by the interaction with DnaB.

This hypothesis was additionally tested via the complementation of the synthetic lethality of a *rep recB* strain. Strains containing the empty pBAD vector and the complementing pRC7*rep* construct were unable to lose the latter as indicated by the absence of white colonies (Figure 5.9A). The presence of pBAD*rep* allowed for efficient complementation of the synthetic lethality in presence of arabinose as indicated by the loss of pRC7*rep* (white colonies; Figure 5.9B.i). In accordance with the toxicity and lack of complementation of the *Δrep ΔuvrD* lethality, overexpression of Rep G543A/S545A also resulted in small colonies, which were unable to lose the complementing pRC7*rep* plasmid (0% white colonies; Figure 5.9C.i). In the absence of the interaction with DnaB, Rep G543A/S545AΔC33 allowed the loss of pRC7*rep* to levels similar to those of RepΔC33 (Figure 5.9B.ii and C.ii). These data support the conclusion that the interaction between Rep G543A/S545A and DnaB has a detrimental effect on cell viability.

The mutation of the N-terminal hinge of the Rep 2B subdomain, Rep G373T/G374T, led to a more efficient complementation of growth than wild-type Rep, as white colonies were visible in the absence of arabinose (Figure 5.9D.i). In the presence of arabinose, loss of pRC7*rep* was as high as for strains expressing plasmid-encoded wild-type Rep, but colony size was reduced compared to those with wild-type Rep (79%; Figure 5.9D.i). Overexpression of Rep G373T/G374TΔC33 was less efficient at complementing the *rep recB* lethality than RepΔC33, as indicated by a reduction in number and size of white colonies (compare Figure 5.9B.ii and D.ii). These data emphasise the different effects of mutations in the Rep hinge regions, even though both mutants had been designed to destabilise the UvrD 2B subdomain in the closed conformation (Lee & Yang, 2006).
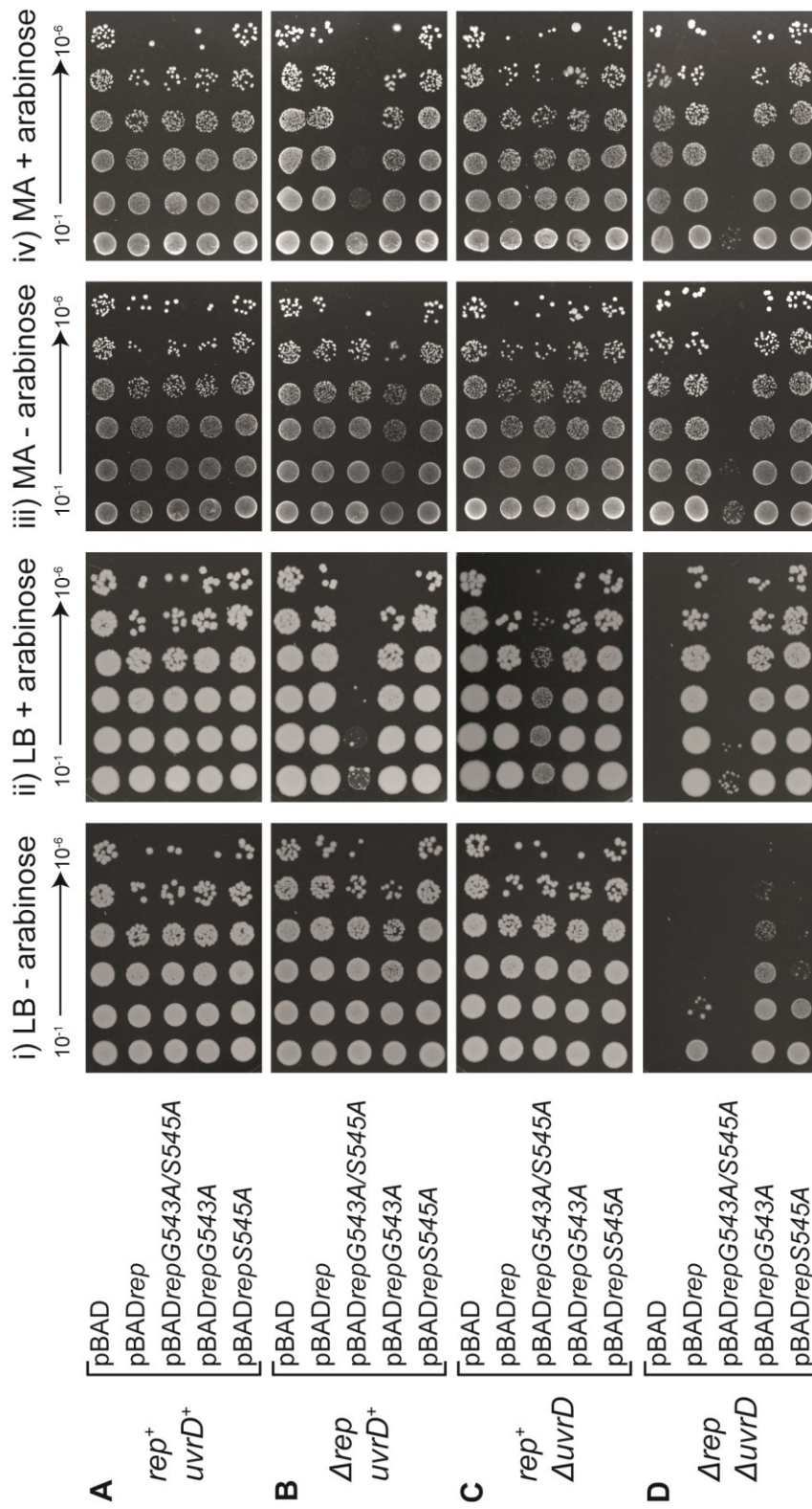
Figure 5.7 Single mutations of the C-terminal hinge do not reconstitute the effect of Rep G543A/S545A
Colony formation of (A) *rep⁺ uvrD⁺* (N6524), (B) *Δrep uvrD⁺* (N6540), (C) *rep⁺ ΔuvrD* (N6556) strains with different pBAD derivatives after loss of pRC7*rep*. Cells were grown in minimal medium, prior to plating of serial dilutions on LB agar (i and ii) or minimal agar (iii and iv) with kanamycin ± arabinose (n=2).
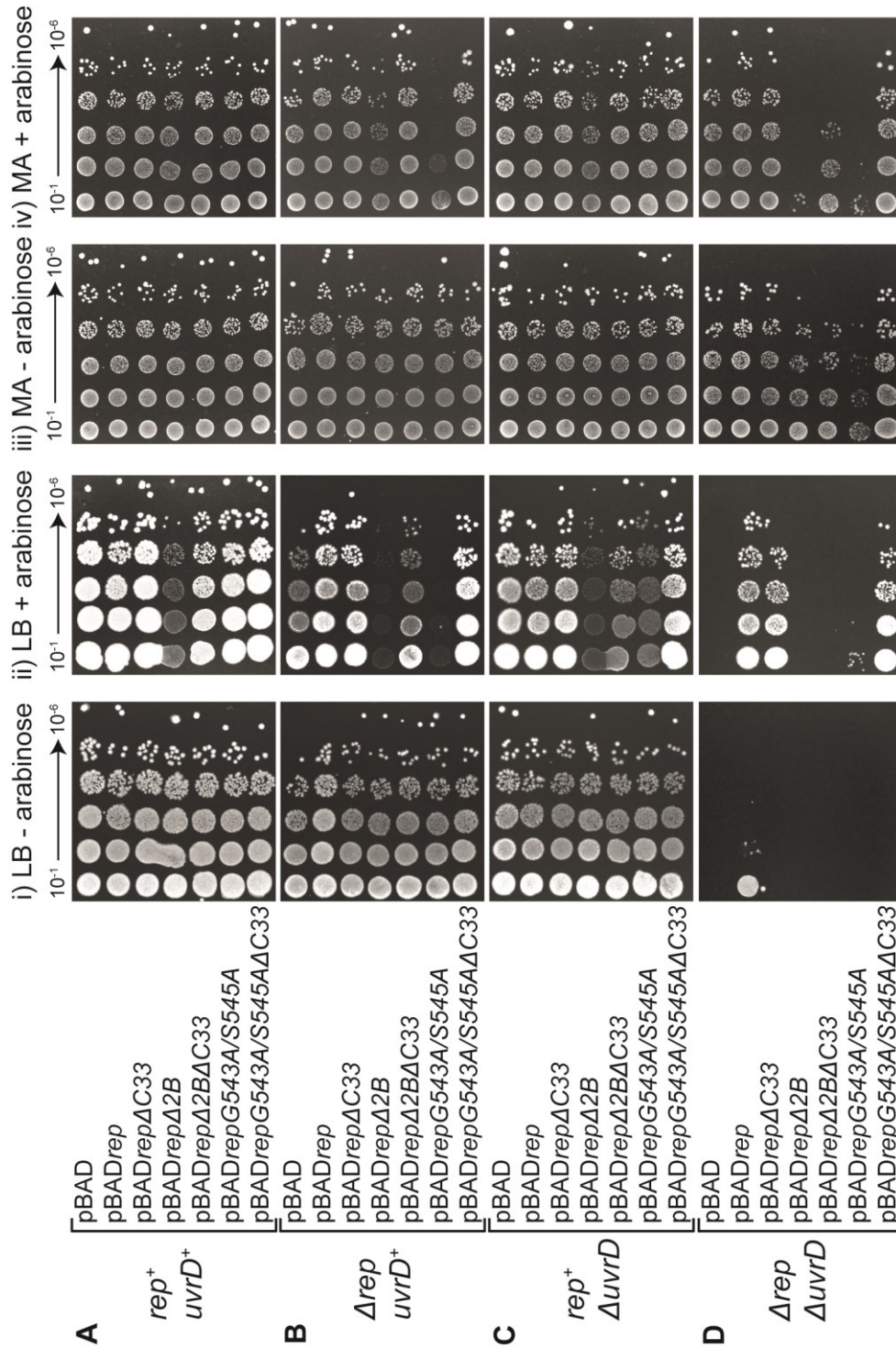
Figure 5.8 The toxicity of RepG543A/S545A depends on the Rep-DnaB interaction
Colony formation of (A) *rep⁺ uvrD⁺* (N6524), (B) *Δrep uvrD⁺* (N6540), (C) *rep⁺ ΔuvrD* (N6568) and (D) *Δrep ΔuvrD* (N6556) strains with different pBAD derivatives after loss of pRC7*rep*. Cells were grown in minimal medium, prior to plating of serial dilutions on LB agar (i and ii) or minimal agar (iii and iv) with kanamycin ± arabinose (n=2).
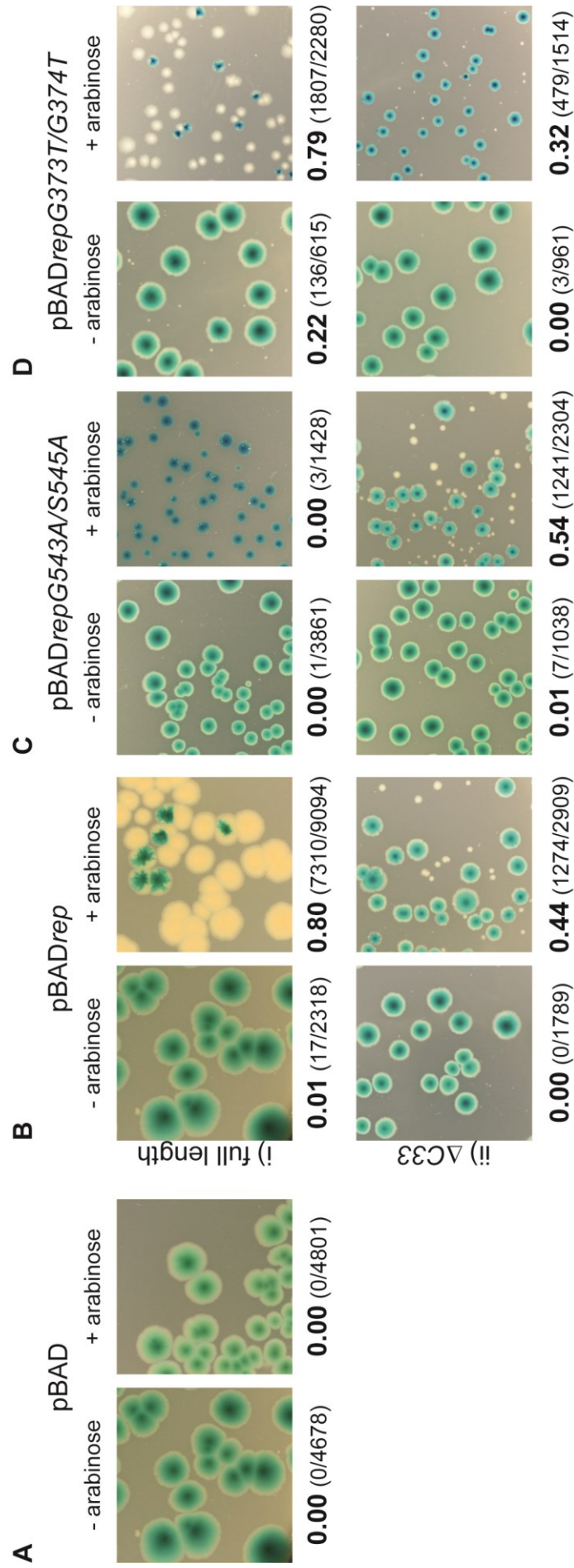
Figure 5.9 Rep G543A/S545A can complement the *rep recB* lethality in the absence of the Rep C-terminus
Blue/white screening for loss or retention of pRC7*rep* in a *rep recB* strain (N7919) with different pBAD derivatives by (i) full length or (ii) truncated Rep genes on LB^0.5 agar with kanamycin ± arabinose in presence of IPTG and X-Gal. Fractions of white colonies are given, with numbers of white and total numbers of colonies in brackets. from at least four independent repeats. A and B have been used in Figure 4.6.

143

5.2.2 Mutations of the Rep 2B hinge activate DNA unwinding

Rep G543A/S545A, Rep G373T/G374T and wild-type Rep were purified as His-tagged proteins to investigate why Rep G543A/S545A, but not Rep G373T/G374T failed to complement Rep function *in vivo*.

One characteristic feature of RepΔ2B was an increased DNA helicase activity *in vitro* (Figure 4.3) (Cheng *et al.*, 2002). Hence, DNA unwinding of a dsDNA fork of 60 base pairs duplex length by the hinge mutants was tested. Both mutant Rep proteins displayed increased helicase activity as compared with wild-type Rep (Figure 5.10B). Rep G373T/G374T was most active (Figure 5.10A.iii). Even at the lowest concentration tested (1:1 stoichiometry of the helicase and DNA), both hinge mutants were able to unwind DNA, indicating that the hinge mutants might also allow for DNA unwinding by monomers, similar to the RepΔ2B mutation (Brendza *et al.*, 2005).
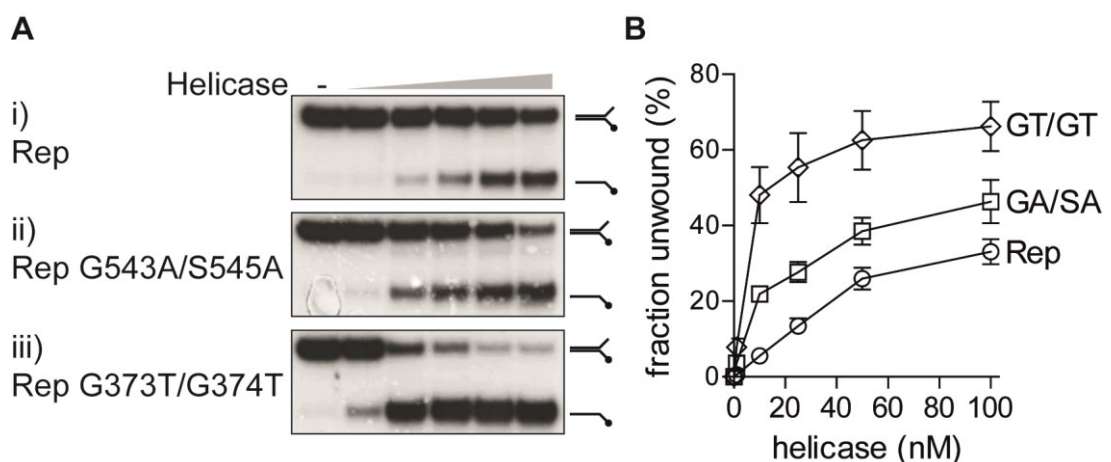
Figure 5.10 Rep hinge mutants are hyperactive helicases
(A) DNA unwinding by (i) Rep, (ii) Rep G543A/S545A or (iii) Rep G373T/G374T (1, 10, 25, 50 and 100 nM) on DNA fork structures with 60bp dsDNA (CC139+CC140). (B) Fractions of unwound DNA for different helicase concentrations. GT/GT = Rep G373T/G374T and GA/SA = Rep G543A/S545A. Error bars represent standard error of the mean (n=4).

5.2.3 Rep G543A/S545A cooperates with DnaB in DNA unwinding

RepΔ2B did not display cooperativity in DNA unwinding with DnaB (Figure 4.4), which suggested that the RepΔ2B helicase activity was near-maximal and could not

be further stimulated by the presence of DnaB or that the cooperativity between Rep and DnaB was dependent on the presence of a 2B subdomain. Therefore, the cooperativity between DnaB and the hinge mutants was tested.
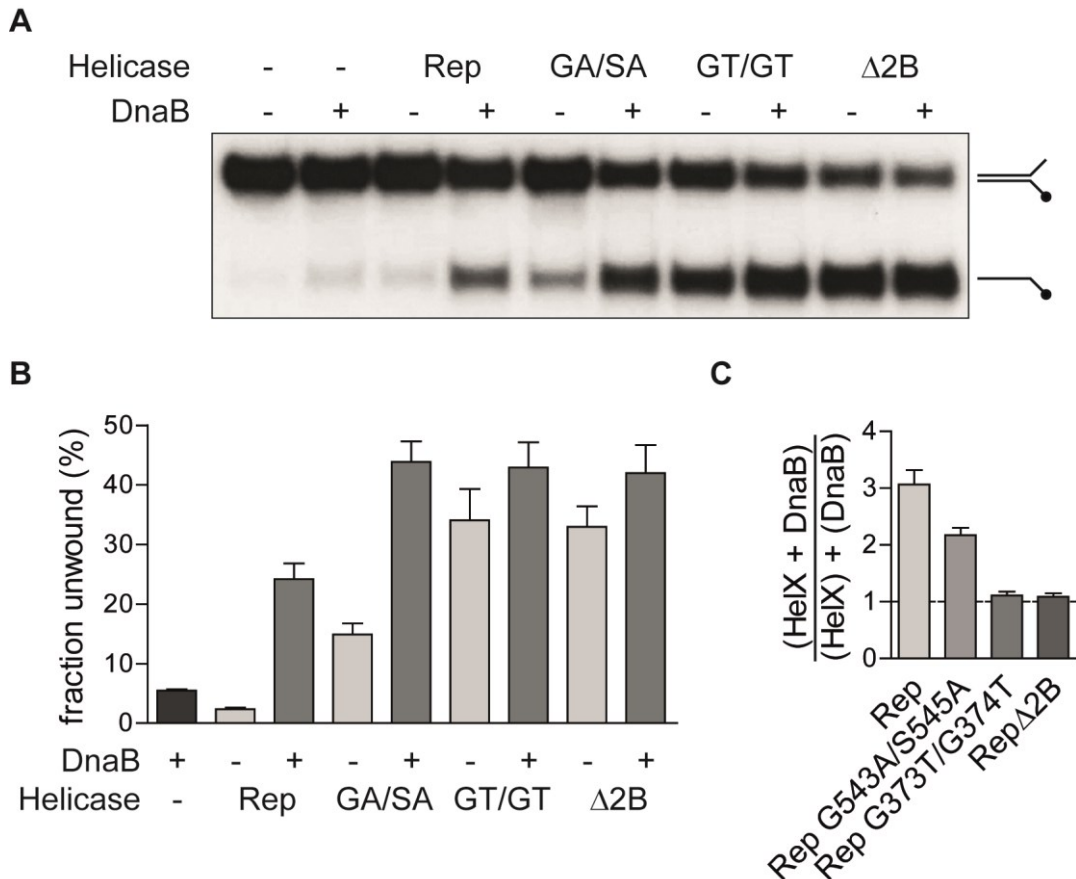
Figure 5.11 Rep G543A/S545A but not Rep G373T/G374T displays cooperativity with DnaB
(A) Cooperativity of DNA unwinding by Rep mutants (10 nM) without and with DnaB (100 nM hexamers) on DNA fork structures with 60bp dsDNA (CC139+CC140). (B) Fractions of unwound DNA by Rep mutants without and with DnaB. (C) Cooperativity in DNA unwinding shown as fractions of unwound DNA by Rep mutants with DnaB compared to the sum of the individual levels of DNA unwinding by both individual helicases. Error bars represent standard error of the mean (n=4).

Levels of DNA unwinding by wild-type Rep alone were low but the cooperativity in DNA unwinding between Rep and DnaB was higher than for the Rep mutants (Figure 5.11B). Out of the hinge mutants, only Rep G543A/S545A displayed cooperativity with DnaB (Figure 5.11C) but total levels of DNA unwinding by Rep G543A/S545A together with DnaB was identical to RepΔ2B and Rep G373T/G374T in the presence of DnaB (Figure 5.11B). Thus, stimulation of DNA unwinding by the presence of DnaB was only achieved when the Rep proteins showed low rates of DNA unwinding. Stimulation of DNA unwinding of Rep and DnaB seemed to be

limited to a maximal rate of DNA unwinding, which was already achieved by RepΔ2B and Rep G373T/G374T in the absence of DnaB (Figure 5.11B).

5.2.4 Mutations of the Rep 2B hinge enhance nucleoprotein displacement from ssDNA

In the absence of the 2B subdomain, RepΔ2B was unable to displace streptavidin from biotin-labelled DNA (Figure 4.14). It was therefore tested whether the hinge mutations of Rep also showed a reduction in the removal of streptavidin from ssDNA.
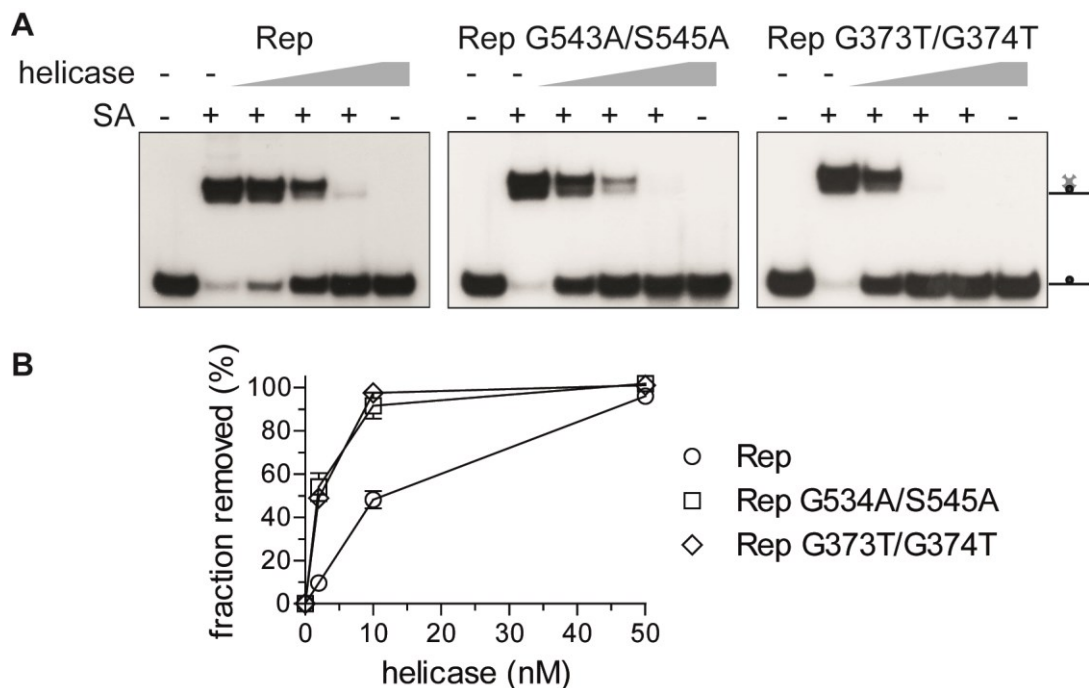
Figure 5.12 Hinge mutants are activated for nucleoprotein removal from ssDNA
(A) Displacement of streptavidin (1 μM) from biotinylated dT60-mer (PM328) by different helicases (2, 10 and 50 nM). (B) Relative levels streptavidin displacement from PM328 by individual helicases. Error bars represent standard error of the mean (n=2).

Both the hinge mutants displayed increased levels of streptavidin displacement from ssDNA compared to wild-type Rep (Figure 5.12A). 10 nM of the hinge mutants completely displaced the streptavidin block, whereas 50 nM of wild-type Rep was required (Figure 5.12B). Although Rep G543A/S545A phenocopied RepΔ2B *in vivo*

(Figure 5.6), neither of the hinge mutants displayed a lack or a reduction in streptavidin displacement from ssDNA.

5.2.5 DNA unwinding of the hinge mutants is not inhibited by streptavidin blocks

DNA unwinding and nucleoprotein displacement were separable processes as shown by the inability of RepΔ2B to efficiently unwind nucleoprotein-bound DNA despite increased levels of helicase activity on "naked" DNA (Figure 4.17 and Figure 4.20). It was therefore tested whether the hinge mutants, despite their ability to remove streptavidin from ssDNA (Figure 5.12), might display defects in the unwinding of protein-bound DNA.

Both hinge mutants displayed increased, rather than decreased levels of DNA unwinding in the presence of streptavidin (Figure 5.13B). DNA unwinding in the presence of a streptavidin-block was stimulated about 1.3x for Rep G373T/G374T and nearly twofold for Rep G543A/S545A, while wild-type Rep did not show any significant stimulation of DNA unwinding in the presence of streptavidin (Figure 5.13C). Additionally, total levels of streptavidin displacement from dsDNA by the hinge mutants were also elevated compared to wild-type Rep (Figure 5.13D). In correlation with the higher efficiency of DNA unwinding, Rep G373T/G374T was also able to displace a greater proportion of streptavidin from dsDNA than Rep G543A/S545A. Rep G373T/G374T nearly fully unwound all dsDNA and removed all of the streptavidin (100 nM; Figure 5.13D). In line with improved streptavidin displacement from ssDNA, the hinge mutations were also hyperactive helicases with respect to DNA unwinding in the presence of a streptavidin block. Thus, Rep G543A/S545A also does not phenocopy RepΔ2B in terms of unwinding of protein bound DNA *in vitro*.
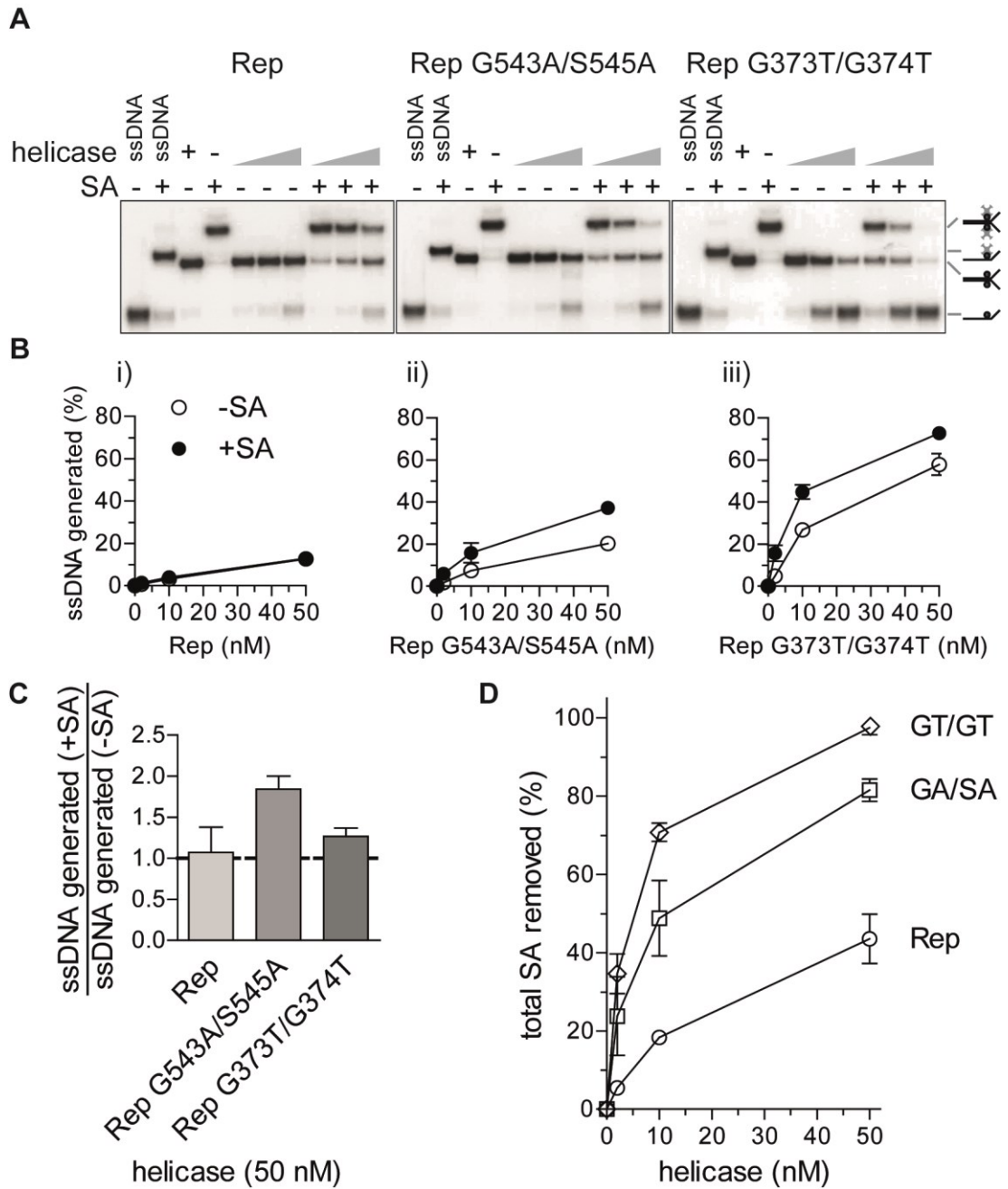
Figure 5.13 DNA unwinding by hinge mutants is not inhibited by a streptavidin block
(A) DNA unwinding of a dually biotinylated DNA fork (CC139B53+CC140B47) in the absence or presence of streptavidin by the denoted helicases. (2, 10 and 50 nM) (B) Total levels of DNA unwinding in the absence or presence of streptavidin by 50 nM (i) Rep, (ii) Rep G5433A/S545A and (iii) Rep G373T/G374T. (C) Inhibition of DNA unwinding by streptavidin given as the fraction of DNA unwinding in the presence of streptavidin divided by the levels of DNA unwinding in the absence of streptavidin. Values below 1 indicate inhibition of DNA unwinding by streptavidin (D) Total levels of streptavidin removal from ss and dsDNA. Error bars represent standard error of the mean (n=2). GA/SA = Rep G543A/S545A; GT/GT = Rep G373T/G374T.

5.2.6 Rep G543A/S545A is able to cooperate with DnaB in the unwinding of streptavidin-bound duplex DNA

The toxicity of Rep G543A/S545A *in vivo* was dependent on the presence of the Rep G543A/S545A C-terminus (Figure 5.9). Thus, the interaction between DnaB and Rep G543A/S545A could be responsible for the toxicity and the complex of DnaB and Rep G543A/S545A might be inactivated for nucleoprotein displacement. Therefore the cooperativity between the hinge mutants and DnaB was tested in the presence of streptavidin.

Wild-type Rep displayed higher levels of cooperativity, but reduced levels of total DNA unwinding and streptavidin displacement compared to both hinge mutants (Figure 5.14B and D). The presence of streptavidin stimulated DNA unwinding by Rep G543A/S545A in the presence of DnaB about two- to threefold (Figure 5.14C). Rep G373T/G374T displayed cooperativity in DNA unwinding with DnaB only in the presence of streptavidin but the level of stimulation was lower than for Rep G543A/S545A and wild-type Rep (Figure 5.14C).

Moreover, streptavidin removal from DNA even in the absence of complete DNA unwinding was enhanced in the presence of DnaB by all three helicases (Figure 5.14D). Thus, the interaction between DnaB and Rep did not affect or reduce the ability of Rep G543A/S545A to displace nucleoproteins.

Figure 5.14 The Rep-DnaB cooperativity is stimulated by the presence of a streptavidin block
(A) DNA unwinding of a dually biotinylated DNA fork (CC139B53+CC140B47) in the absence or presence of streptavidin and/or DnaB (100 nM) by (i) Rep, (ii) Rep G543A/S545A and (iii) Rep G373T/G374T. (2, 5 and 10nM) (B) Total levels of DNA unwinding in the absence or presence of streptavidin by 10 nM helicases. (C) Cooperativity in DNA unwinding shown as fractions of unwound DNA by Rep variants with DnaB compared to the sum of the individual levels of DNA unwinding by both individual helicases in the absence or presence of streptavidin. (D) Total levels of streptavidin removal from ss and dsDNA. Error bars represent standard error of the mean (n=2).

5.2.7 The hinge mutants are more active accessory replicative helicase in the context of the replisome

It was also possible that the toxicity and lack of complementation of Rep function *in vivo* by Rep G543A/S545A was an effect that was depended on the interaction with not just DnaB but rather the whole replisome. It was therefore tested whether the hinge mutants were also able to act as accessory replicative helicases in the context of the replisome *in vitro*.
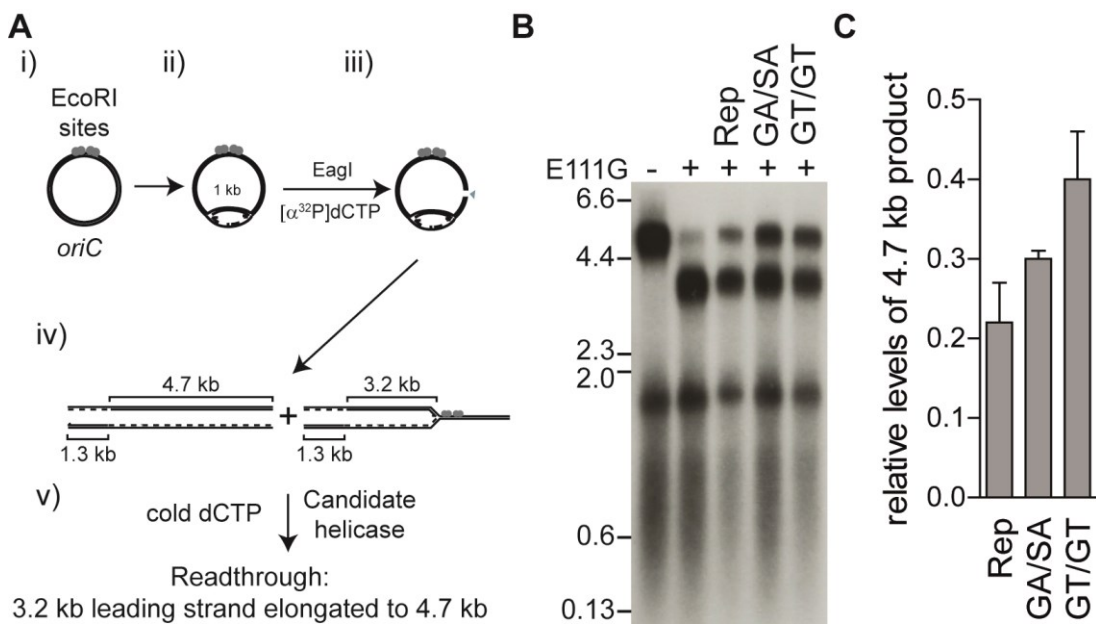
Figure 5.15 The Rep hinge mutants are more efficient accessory replicative helicases
(A) Schematic representation of the assay to monitor promotion of replication fork progression through a nucleoprotein block. (B) Denaturing agarose gel from *in vitro* replication assay of pPM594 containing eight EcoRI sites in absence and presence of EcoRI E111G (200 nM dimers) and different Rep mutants (100 nM). (C) Relative fractions of the full length replication products compared to the control lacking EcoRI E111G. Error bars represent standard error of the mean (n=2). GA/SA = Rep G543A/S545A, GT/GT = Rep G373T/G374T.

Both hinge mutants displayed increased activities at promoting replication fork movement through a nucleoprotein barrier in the context of a reconstituted *E. coli* replisome compared to wild-type Rep (Figure 5.15), which was in agreement with increased levels of nucleoprotein displacement from ss- and dsDNA (Figure 5.12 and Figure 5.13). Thus, the interaction of Rep G543A/S545A with either DnaB or the whole replisome *in vitro* (Figure 5.14 and Figure 5.15) did not reconstitute a phenotype that could explain the toxicity and lack of complementation of Rep

function *in vivo* (Figure 5.6). The hinge mutants therefore were not only hyperactive helicases (Figure 5.10), similar to RepΔ2B (Figure 4.3) (Cheng *et al.*, 2002) but also combined this property with enhanced levels of nucleoprotein displacement and improved accessory replicative helicase function.

5.2.8   Rep G543A/S545A displays an increased affinity for forked DNA

Originally, the hinge mutations in UvrD had been proposed to result in a more open conformation of the 2B subdomain and thereby preventing or reducing the interaction of the 2B subdomain with dsDNA, for which the closed conformation is required (Lee & Yang, 2006). It was therefore tested whether the hinge mutants displayed an altered affinity to DNA, using EMSAs with a forked DNA substrate of 60 base pair duplex with two 38 bases ssDNA arms with or without DnaB.

Wild-type Rep needed the presence of DnaB to form a stable complex on the DNA substrate (II; Figure 5.16A), as shown previously (Figure 4.9) (Guy *et al.*, 2009). The formation of this complex was Rep concentration dependent, reaching complete binding of DnaB-bound forked DNA only in the presence of 50 nM Rep (lane 10; Figure 5.16A). Rep G543A/S545A showed enhanced binding to the DNA fork in the absence of DnaB, as indicated by increased smearing of the fork with Rep G543A/S545A compared with wild-type Rep (lanes 2-5; Figure 5.16B). In the presence of DnaB, the formation of a stable DNA-Rep G543A/S545A-DnaB complex ("II") occurred at the lowest concentrations of Rep G543A/S545A, with only a very small fraction of detectable unbound DNA (lane 7; Figure 5.16B). In contrast, Rep G373T/G374T binding to DNA in the absence of DnaB was similar compared to wild-type Rep. Rep G373T/G374T did however show an increased affinity for DnaB-bound forked DNA, as formation of a stable Rep-DnaB-DNA complex occurred at the lowest concentration of Rep G373T/G374T (lane 7; Figure 5.16C). The formation of this complex was however not significantly enhanced for concentrations higher than 5 nM (lanes 8-10; Figure 5.16C). Thus, both hinge mutants display a higher affinity for the DnaB-bound fork, which could simply reflect an increased affinity for DnaB rather than DNA. However, Rep G543A/S545A displayed a significant increase in DNA binding on its own.
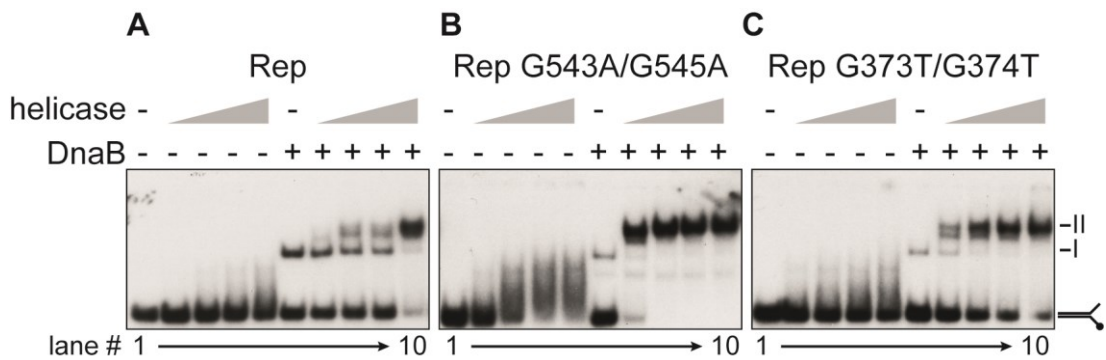
Figure 5.16 Rep hinge mutants have a higher affinity for DNA
Interaction of (A) Rep, (B) Rep G543A/S545A and (C) Rep G373T/G374T (1, 5, 10 and 25 nM) and DnaB (100 nM hexamers) with forked DNA having DNA having two ssDNA arms (60 bp dsDNA, 38 bp ssDNA; CC139+CC140) in the presence of 10 μM ADP after resolution on a 4% acrylamide gel (n=3). "I" = DNA-DnaB complex; "II" = DNA-DnaB-Rep complexes.

Using EMSAs, it is impossible to determine whether the hinge mutations in Rep result in the increased affinity of the protein to ssDNA, dsDNA, and the DNA fork structures as a whole or simply due to an increased affinity to DnaB. To differentiate between these possibilities, the interaction of the mutant proteins with immobilised ssDNA was tested by SPR. However, SPR experiments failed due to non-specific interactions of the Rep proteins with the SPR chip surface (see section 4.2.11) and so other DNA substrates (dsDNA, 3'-overhang) could also not be tested. Alternative experiments like fluorescence anisotropy that test the affinity of these helicase mutants to DNA could not be performed due to time constraints.

To test whether the toxicity of Rep G543A/S545A was caused by an increased affinity to DNA, Rep G543A/S545A was combined with mutations that were suspected to affect dsDNA binding of the 2B subdomain, creating Rep^{dsDNA} G543A/S545A (Rep K410A/E412A/G414A/T417A/R448A/G543A/S545A).

This mutant restored growth of the Rep G543A/S545A mutation in a *Δrep ΔuvrD* strain on rich medium, similar to wild-type Rep and Rep^{dsDNA} (Figure 5.17D.i and ii). Alterations of the interaction with dsDNA of Rep G543A/S545A also abolished the toxicity of Rep G543A/S545A on minimal medium in the *Δrep* and *Δrep ΔuvrD* background (Figure 5.17B and D.iii and iv), as well as on LB in the *Δrep* and *ΔuvrD* single mutant backgrounds (Figure 5.17B.ii and C.ii). These results suggest that the affinity of Rep G543A/S545A to dsDNA could at least partially cause the toxicity of Rep G543A/S545A *in vivo*.
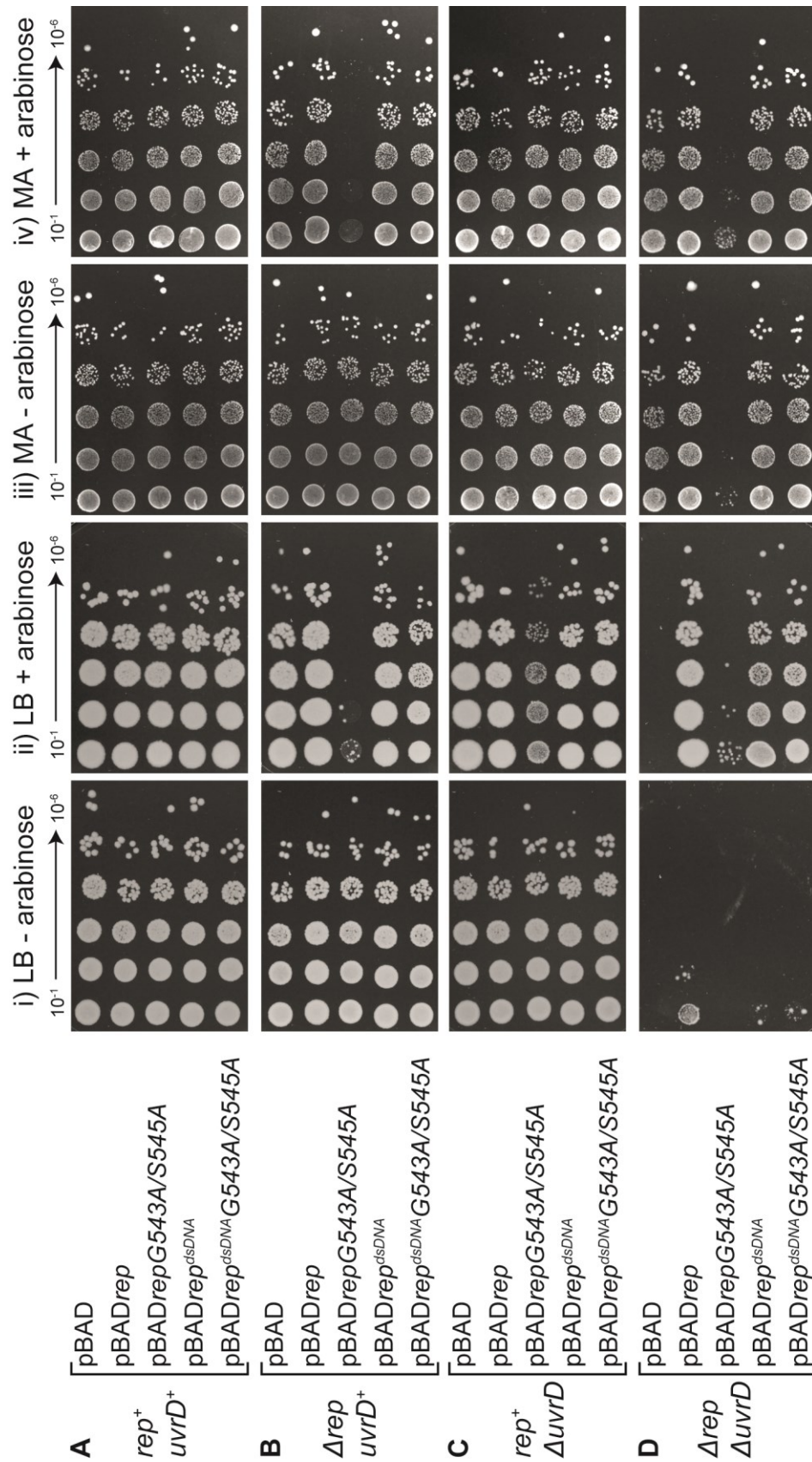
Figure 5.17 The toxicity of Rep G543A/S545 is rescued by mutations affecting the interaction of the Rep 2B subdomain with dsDNA

Colony formation of (A) *rep⁺ uvrD⁺* (N6524), (B) *Δrep uvrD⁺* (N6540), (C) *rep⁺ ΔuvrD* (N6568) and (D) *Δrep ΔuvrD* (N6556) strains with different pBAD derivatives after loss of pRC7*rep*. Cells were grown in minimal medium, prior to plating of serial dilutions on LB agar (i and ii) or minimal agar (iii and iv) with kanamycin ± arabinose. dsDNA stands for Rep mutations K410A/E412A/G414A/T417A/R448A (n=2).

5.2.9   Investigation of conformational changes of the Rep 2B subdomain

It was quite surprising that the two hinge mutants that were both predicted to result in a more open conformation of the 2B subdomain (Lee & Yang, 2006) had such different effects *in vivo* (Figure 5.6). However, direct evidence for such a conformational change was missing and therefore experiments testing the conformation of the 2B subdomain in wild-type Rep and Rep G543A/S545A were set up.

To gain an insight in the possible differences between the N- and C-terminal hinge mutations, different crystal structures of PcrA, UvrD and Rep were compared. The N-terminal hinge is resolved in all available SF1A helicase crystal structures (2A-2B; Table 5.2). This was independent on the conformation of the 2B subdomain. In contrast, stretches of up to twelve amino acids were not resolved around the C-terminal hinge in the majority of available SF1A helicase crystal structures (2B-2A; Table 5.2). In Rep, neither G543 nor S545 are resolved either in the open or closed conformation (Table 5.2). Therefore the 2B subdomain of Rep and also PcrA and UvrD likely possesses more flexibility around the C-terminal as compared with the N-terminal hinge. Thus, the increased toxicity of Rep G543A/S545A might reflect reduced conformational flexibility within this hinge region.

Upon binding of dsDNA, the 2B subdomain of SF1A helicases usually assumes the closed conformation (Lee & Yang, 2006; Rasnik *et al.*, 2004; Velankar *et al.*, 1999). Mutations in the 1B-2B interface of UvrD and possibly also Rep likely form ionic interactions in the closed conformation, as the UvrD subdomain opened at high salt conditions (Jia *et al.*, 2011). If the Rep G543A/S545A mutation locked the 2B subdomain in an open conformation, additional mutations in the 1B-2B subdomain interface should not affect the toxicity. On the other hand, if the toxicity of Rep G543A/S545A was dependent on the formation of the closed conformation of the 2B subdomain, additional mutations in the 1B-2B interface that reduce ionic strength of the closed conformation should alleviate the toxicity of Rep G543A/S545A. To test this idea, Rep[1B-2B] G543A/S545A (Rep R391A/D397-399A/G543A/ S545A) was created.

Table 5.2 Comparison of the 2B hinges in crystal structures of different Superfamily 1 helicases
Crystal structures of Superfamily 1 helicases were checked for possible flexibility of the 2B hinge regions, as indicated by the absence of confinement of amino acids in the crystal structure. The 2A-2B hinge (equivalents to Rep residues G373 G374) was resolved in all crystal structures, while the 2B-2A hinge (equivalents to Rep residues G543 S545) lacked amino acids in nearly all structures.

helicase	PDB ID	in complex with (2B conformation)	2A-2B	2B-2A
Rep	1UAA	ssDNA (open)	yes	M539-E546 missing
		ssDNA (closed)	yes	G543-S545 missing
PcrA	3PJR	dsDNA + ATP (closed)	yes	L547-G549 missing
	1QHH	ADPNP (open)	yes	D543-E555 missing
	2PJR	SO_4^{2-} (closed)	yes	G549-E555 missing
			yes	D548-E555 missing
UvrD	2IS1	dsDNA + SO_4^{2-} (closed)	yes	yes
			yes	Q551-V554 missing
	2IS2	dsDNA + MgF$_3$ (closed)	yes	E544-D548 missing
			yes	A539-A547 missing
	2IS4	dsDNA + ADPNP (closed)	yes	G545-D548 missing
			yes	A538-Q546 missing
	2IS6	dsDNA + ADP + MgF$_3$ (closed)	yes	yes
			yes	yes
	3LFU	SO_4^{2-} (open)	yes	A542 missing

In support of the latter hypothesis, toxicity was abolished from all backgrounds and all growth conditions when the 1B-2B interface mutations were combined with the Rep G543A/S545A (Figure 5.18). Rep function of Rep[1B-2B] G543A/S545A also complemented the *Δrep ΔuvrD* lethality on rich medium to the same extent as the Rep[1B-2B] mutation on its own (Figure 5.18D.ii). These results suggest that the formation of the closed conformation of the 2B subdomain in Rep G543A/S545A plays a central role for the toxicity of Rep G543A/S545A *in vivo*.

To directly investigate the conformation of the 2B subdomain of Rep and Rep G543A/S545A on their own and in the presence of DNA and/or DnaB, single-molecule (sm)FRET techniques, such as multiparameter fluorescence detection (MFD) or total internal reflection (TIRF) microscopy would be performed (Ha *et al.*, 2002; Sisamakis *et al.*, 2010). These experiments require fluorescent labelling of cysteine residues of Rep at discrete sites on the surface of the protein (Joo & Ha, 2012; Rasnik *et al.*, 2004).
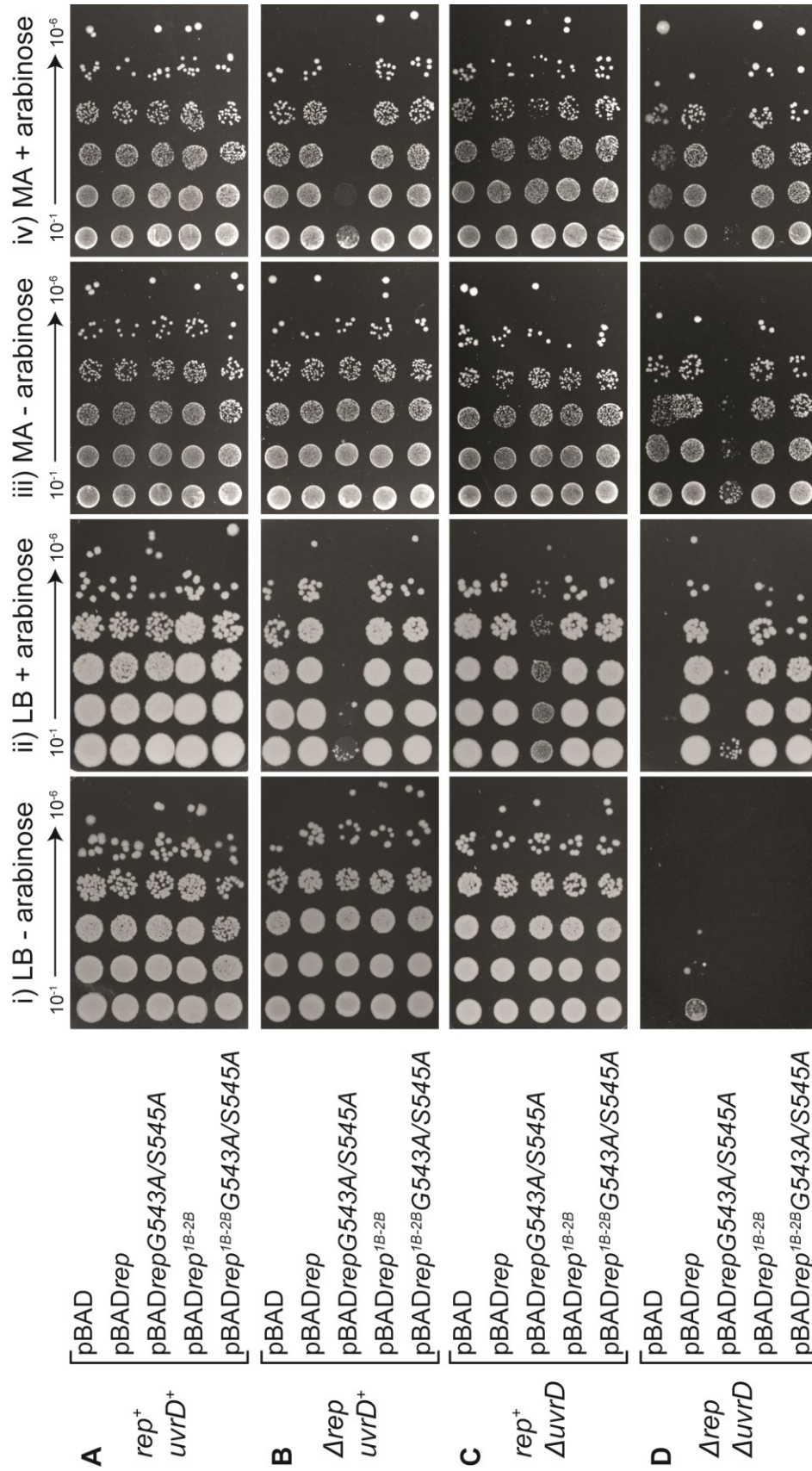
Figure 5.18 The toxicity of Rep G543A/S545 is rescued by mutations affecting the interaction between the 1B and 2B subdomains of Rep

Colony formation of (A) *rep*[+] *uvrD*[+] (N6524), (B) *Δrep uvrD*[+] (N6540), (C) *rep*[+] *ΔuvrD* (N6568) and (D) *Δrep ΔuvrD* (N6556) strains with different pBAD derivatives after loss of pRC7*rep*. Cells were grown in minimal medium, prior to plating of serial dilutions on LB agar (i and ii) or minimal agar (iii and iv) with kanamycin ± arabinose. 1B-2B represents Rep mutations R391A/D397A/D398A/D399A (n=2).

Rep has five native cysteine residues that would interfere with site-specific labelling by fluorophores. Hence, a Rep mutant that had all native cysteine residues replaced (C18L/C43S/C167V/C178A/C612A; RepΔcys) was used as a background (Rasnik *et al.*, 2004). Within this background, wild-type Rep and Rep G543A/S545A were going to be fluorescently labelled via introduced cysteine residues on the 1A subdomain (A97C) and on the 2B subdomain (A473C) (Rep2cys) (Myong *et al.*, 2005). The distances between these two sites were 29 Å in the closed and 68 Å in the open conformation of the 2B subdomain, as determined on Rep crystal structures in PyMol (PDB: 1UAA (Korolev *et al.*, 1997)). These differences resulted in detectable changes in the FRET signal upon opening and closing of the 2B subdomain (Myong *et al.*, 2005). RepΔcys and Rep2cys support replication of φX174 phage and showed only a small reduction in in ATP hydrolysis and DNA helicase activity compared to wild-type Rep (Myong *et al.*, 2005; Rasnik *et al.*, 2004).

However, since Rep2cysG543A/S545A had not been tested for functionality before, the cysteine mutants were tested for the complementation of the *Δrep ΔuvrD* lethality on rich medium. The overexpression of RepΔcys and Rep2cys was not toxic (Figure 5.19A.i or D.iv). However, they were slightly less efficient in complementing Rep function in a *Δrep ΔuvrD* background than wild-type Rep, as complementation in the absence of arabinose was reduced (Figure 5.19D.i). This might be related to the reduced helicase and ATPase activities of RepΔcys and Rep2cys *in vitro* (Rasnik *et al.*, 2004). In a Rep 2cys G543A/S545A, the cysteine mutations abolished the toxicity of the hinge mutation in the *Δrep* and the double mutant background (Figure 5.19B and D). This was also the case for RepΔcysG543A/S545A (Figure 5.19D.ii) and therefore the absence of the native cysteines rather than the introduction of cysteines were the reason for the change in the Rep G543A/S545A phenotype. Due to the lack of toxicity of Rep2cysG543A/S545A, potential conformational changes detected by smFRET experiments would likely not reflect the conformation of the 2B subdomain in Rep G543A/S545A. Due to time constraints smFRET experiments could not be performed to test this hypothesis.
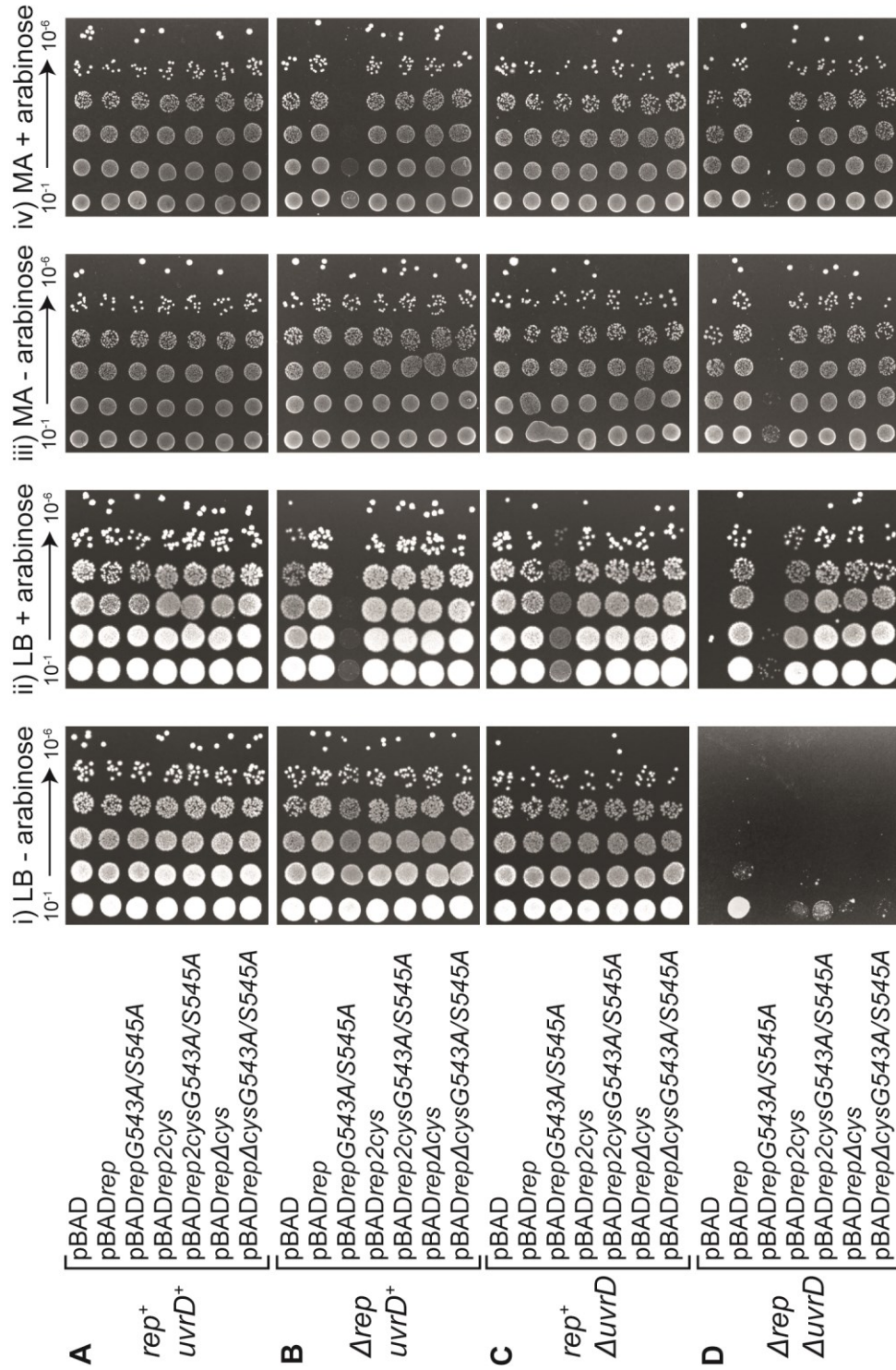
Figure 5.19 Rep cysteine mutants rescue the G543A/S545A phenotype

Colony formation of (A) *rep⁺ uvrD⁺* (N6524), (B) *Δrep uvrD⁺* (N6540), (C) *rep⁺ ΔuvrD* (N6568) and (D) *Δrep ΔuvrD* (N6556) strains with different pBAD derivatives after loss of pRC7*rep*. Cells were grown in minimal medium, prior to plating of serial dilutions on LB agar (i and ii) or minimal agar (iii and iv) with kanamycin ± arabinose. Δcys stands for C18L/C43S/C167V/C178A/C612A; 2cys stands for Rep mutations A97C/A473C in addition to the Δcys mutations (n=2).

5.3   Discussion

In the previous chapter, it was demonstrated that efficient nucleoprotein displacement by Rep was dependent on the presence of a 2B subdomain (Figure 4.14 and Figure 4.17). This was supported by the ability of the UvrD 2B subdomain to complement the RepΔ2B mutation *in vitro* and *in vivo* (Figure 4.28 and Figure 4.29). This chapter aimed to decipher the role of the 2B subdomain of Rep, by creating and characterising a full length mutant Rep protein that displayed similar properties to RepΔ2B both *in vitro* and *in vivo*. Several Rep mutants were constructed by site directed mutagenesis of defined residues in the 2B subdomain. The amino acid substitutions were homologous to residues in the 2B subdomains of UvrD and PcrA and had been proposed to interact with dsDNA, form interactions with the 1B subdomain in the closed conformation or were proposed to be necessary for the flexibility of the 2B subdomain.

Mutations of residues that were predicted to be involved in the interaction of the 2B subdomain with dsDNA neither impacted on complementation of Rep function nor displayed any toxicity upon overexpression *in vivo* (Figure 5.3 and Figure 5.4). Given the importance of nucleoprotein clearance for Rep function *in vivo* (Chapter 4) (Atkinson *et al.*, 2011b; Guy *et al.*, 2009) it is therefore unlikely that these residues play significant roles in facilitating protein displacement.

Although none of the point mutants in the Rep 1B-2B subdomain interface displayed toxicity or failed to restore growth in a *Δrep ΔuvrD* mutant on rich medium (Figure 5.5), it cannot be excluded that some mutations would show a reduction of Rep function *in vitro*. The reduction of complementation of the *Δrep ΔuvrD* lethality by Rep R391A or Rep D398A/D399A (Figure 5.5D.i and ii) could reflect a partial loss of function of these mutants. The homologous mutation of Rep D398A/D399A in UvrD, UvrD D403A/D404A, is a hyperactive helicase, like RepΔ2B but does not cause toxicity *in vivo* (Centore *et al.*, 2009; Meiners *et al.*, 2014; Zhang *et al.*, 1998). Nucleoprotein displacement by UvrD D403A/D404A has however not been tested directly. Purification and biochemical characterisation of these Rep mutants would be required to test whether they are also hyperactive helicases and whether these mutations have an effect on nucleoprotein displacement.

The third group of Rep mutants tested had amino acid substitutions in the N-terminal hinge (Rep G373T/G374T, from the 2A to the 2B subdomain) and the C-terminal hinge (Rep G543A/G545A, from the 2B to the 2A subdomain) of the 2B subdomain. The mutations were homologous to those created in UvrD (UvrD G378T/G379T and UvrD G543A/G545A) that were proposed to destabilise the closed conformation. In the case of UvrD G378T/G379T the 2B subdomain was supposed to be fully opened due to altered φ and ψ angles resulting from the amino acid changes. Overexpression of the UvrD G378T/G379T mutation displayed cytotoxicity (Lee & Yang, 2006), a characteristic that was also seen for RepΔ2B (Figure 4.7). However, a mutation of the N-terminal hinge of the 2B subdomain in Rep (Rep G373T/G374T) did not display any toxicity or lack of complementation of the *Δrep ΔuvrD* lethality on rich medium (Figure 5.6).

In contrast, the UvrD G543A/G545A mutant was only proposed to destabilise the closed conformation of the 2B subdomain (Lee & Yang, 2006). Homologous mutations in the C-terminal hinge of the Rep 2B subdomain (Rep G543A/S545A) displayed phenotypes similar to RepΔ2B (Figure 5.6). This effect was specific to the double mutant, as both single mutants displayed normal Rep function *in vivo* (Figure 5.7). A Rep G543T/S545T mutation could be created to test whether the toxicity of Rep G543A/S545A would be alleviated *in vivo,* similar to Rep G373T/G374T. However, the alanine mutant of the N-terminal hinge (Rep G373A/G374A) did not behave differently to the threonine mutation *in vivo* (Figure 5.6), suggesting that the effects of these mutants were not specific to the amino acid changes.

Both hinge mutants displayed increased levels of DNA unwinding compared to wild-type Rep. These elevated helicase activities reflected the hyperactivity of RepΔ2B. However, the ability of Rep G373T/G374T to complement the *Δrep ΔuvrD* lethality indicates that increased levels of DNA unwinding by SF1A helicases *per se* do not correlate with a lack of Rep functionality or toxicity *in vivo*.

Why are the hinge mutants hyperactive helicases? Unwinding in the presence of a 2B subdomain was proposed to occur via two different mechanisms (Lee & Yang, 2006). At first the 2B subdomain needs to be in the closed conformation to make contacts with the dsDNA. This interaction "feeds" the DNA into the helicase motor

core formed by subdomains 1A and 2A (the so-called "wrench and inchworm mechanism"). During DNA unwinding in this mechanism, the 2B subdomain closes down on the ssDNA and blocks the passage of nucleotides of the ssDNA molecule. During ATP hydrolysis, the 2B subdomain opens and allows translocation along ssDNA for another base pair. Once the duplex DNA is shorter than 14 base pairs, the 2B subdomain cannot make any contacts with the dsDNA anymore and the remaining DNA is unwound in a strand displacement mode that only requires translocation along ssDNA. In the absence of the 2B subdomain the transient inhibition of ssDNA translocation by closing of the 2B subdomain would therefore be absent. Enhanced levels of DNA unwinding by RepΔ2B were therefore attributed to a strand displacement mode during which translocation along ssDNA, without dsDNA binding, stripped the second strand from the first (Lee & Yang, 2006). This wire-stripper mode was used to explain the twofold increase in ssDNA translocation by RepΔ2B (Brendza *et al.*, 2005). If the hinge mutations result in a more open conformation, inhibition of ssDNA translocation by the 2B subdomain might be relieved. Increased levels of DNA unwinding seen for the hinge mutants in Rep (Figure 5.10) might therefore be caused via strand displacement only. To address this idea, the ssDNA translocation velocities of the helicase mutants would need to be tested to establish whether increased ssDNA translocation is also related to increased levels of DNA unwinding.

Cooperativity in DNA unwinding with DnaB was only observed with Rep G543A/S545A (Figure 5.11C). The lack of cooperativity between DnaB and Rep G373T/G374T indicates that the stimulation was not dependent on the presence of a 2B subdomain. Reduced or absent functional cooperativity also correlated with elevated levels of DNA unwinding by Rep enzymes in the absence of DnaB. It might therefore be that RepΔ2B and Rep G373T/G374T are already very efficient helicases in their own rights and that addition of DnaB has no stimulatory effect. There are two possibilities how Rep and DnaB can achieve cooperativity: (1) the interaction between DnaB and Rep stabilises or increases the local concentration of Rep at the replication fork. DNA unwinding by the T4 helicase Dda is enhanced by the association of additional helicase molecules that prevent backslipping of the leading helicase, thereby increasing the processivity of DNA unwinding (cooperative

inchworm model) (Byrd & Raney, 2005). (2) The interaction between DnaB and Rep could induce allosteric changes within the 2B subdomain that enhance DNA unwinding by Rep, e.g. by activating the strand displacement mode (see above). Rep G373T/G374T and RepΔ2B might naturally assume such a conformation, while wild-type Rep and Rep G543A/S545A require the interaction with DnaB to adopt such a conformation. SmFRET experiments are required to address this hypothesis.

How does the 2B subdomain affect nucleoprotein displacement? DNA unwinding and nucleoprotein displacement are separable processes (Figure 4.17). The step size, defined as the number of base pairs unwound per molecule of ATP hydrolysed has been reported as two base pairs for Rep (Kornberg $et\ al.$, 1978; Yarranton & Gefter, 1979), one to 4-5 base pairs (Ali & Lohman, 1997; Lee & Yang, 2006) for UvrD and 4 base pairs for PcrA (Yang $et\ al.$, 2008). Given that the mean energy necessary to separate a single base pair of DNA (6.7 kJ mol^{-1}) is much lower than the free energy of ATP hydrolysis (42 kJ mol^{-1}) (von Hippel & Delagoutte, 2001), the remaining free energy (9 to 35 kJ mol^{-1}) could drive conformational changes of the 2B subdomain. Opening and closing of the 2B subdomain has been observed during ssDNA translocation of Rep. Upon encounter of a streptavidin block on ssDNA it was shown that the 2B subdomain assumes a more closed conformation (Myong $et\ al.$, 2005). It is possible for the 2B subdomain to act as a spring or a lever by coupling conformational changes of the subdomain to nucleoprotein displacement. Subsequent cycles of ATP hydrolysis would in turn cause several cycles of opening and closing of the 2B subdomain, creating enough energy to disrupt the non-covalent bonds between the DNA and the protein block, eventually leading to dissociation of the obstacle. This model would explain why in the absence of the 2B subdomain high affinity protein-DNA interactions were not efficiently removed by RepΔ2B (Figure 4.14). A altered, potentially more open conformation of the 2B subdomain in Rep G543A/S545A and Rep G373T/G374T could generate more force on a nucleoprotein block, related to a greater difference between the open and closed conformations of their 2B subdomains. To address this hypothesis, ssDNA translocation and DNA unwinding could be tested with the fluorescently labelled Rep mutants (Figure 5.19) in the absence and the presence of a nucleoprotein block in stopped-flow experiments (Dillingham $et\ al.$, 2000). Due to time constraints,

experiments investigating the conformation of the 2B subdomain and its relevance to DNA unwinding and nucleoprotein displacement could not be performed. Single molecule analysis of wild-type Rep and the hinge mutants could address the native state of the 2B subdomain.

The question remains, why only Rep G543A/S545A but not Rep G373T/G374T phenocopied RepΔ2B *in vivo*, as both hinge mutants were more active accessory replicative helicases *in vitro* (Figure 5.15). One explanation is that increased DNA binding even in the absence of DnaB (Figure 5.16) results in toxicity due to unrestricted, DnaB-independent DNA unwinding. More detailed analysis of the interaction between DNA and the hinge mutants are however necessary to address this hypothesis. It is also possible that the interaction between Rep G543A/S545A and DnaB causes the toxicity *in vivo*. Deletion of the Rep G543A/S545A C-terminus rescued the cytotoxicity and also restored complementation of Rep function *in vivo* (Figure 5.6 and Figure 5.9). However, the functionality of Rep G543A/S545A as an accessory replicative helicase in the context of the replisome *in vitro* (Figure 5.15) contradicts this idea.

In summary, this work describes two mutations within the 2B hinge of Rep that display very different phenotypes *in vivo*. The characterisation of these hinge mutations suggests a close relationship between nucleoprotein displacement and the conformation of the 2B subdomain in Rep. These results set the basis to investigate the nature and the significance of the 2B subdomain in general and furthermore propose the physiological role of the open conformation of 2B subdomains in Rep and other Superfamily 1A helicases.

Chapter 6

CONCLUDING REMARKS

Chapter 6 – Concluding Remarks

In this thesis, two key features of the Superfamily 1A helicase Rep were addressed that are essential for Rep to properly function as an accessory replicative helicase *in vivo*: (1) its interaction with the main replicative helicase DnaB and (2) the ability of Rep to displace protein blocks from DNA.

My data shows that efficient Rep function *in vivo* was dependent on the last four amino acids of the Rep C-terminus. Based on sequence comparisons of the respective C-terminal regions of Rep and DnaB proteins, the interaction of Rep and DnaB is likely mediated via ionic bond formation between the C-termini of both proteins. Since DnaC interacts with the DnaB C-terminus and prevents the formation of the Rep-DnaB complex, recruitment of Rep to replication forks likely occurs once DnaC dissociates (Galletto *et al.*, 2004c; Guy *et al.*, 2009). Previous work had shown that DnaB translocates along the lagging strand of the replication fork with its C-terminus facing towards the 3' end of ssDNA and the fork junction (Galletto *et al.*, 2004b; Jezewska *et al.*, 1998a). Consequently the interaction of Rep with the DnaB C-terminus could place Rep close to the replication fork junction on the free leading strand template (Figure 1.18A). This would position Rep close to nucleoprotein blocks ahead of the replication fork and promote displacement of obstacles that would otherwise stall replication fork movement driven by DnaB only.

Cells lacking accessory replicative helicases display reduced rates of replication fork movement (Atkinson *et al.*, 2011b; Ivessa *et al.*, 2002; Lane & Denhardt, 1975; Sabouri *et al.*, 2012), since accessory motors are required to underpin replication fork movement through high affinity protein blocks and arrays of protein complexes (Azvolinsky *et al.*, 2009; Guy *et al.*, 2009; Ivessa *et al.*, 2003; Sabouri *et al.*, 2012). The need for an accessory replicative helicase in *E. coli* correlates with the inability of the hexameric helicase DnaB to displace nucleoprotein blocks in isolation and in the context of the replisome *in vitro* (Guy *et al.*, 2009; Yancey-Wrona & Matson, 1992). My work demonstrates that the 2B subdomain of Rep plays a central role in the displacement of nucleoprotein blocks and consequently for Rep to act as the

accessory replicative helicase in *E. coli*. RepΔ2B, a mutant lacking the 2B subdomain did not complement Rep function either *in vivo* or *in vitro*, although RepΔ2B displayed a two-fold increased velocity in ssDNA translocation and was a more active DNA helicase than wild-type Rep (Brendza *et al.*, 2005; Cheng *et al.*, 2002). RepΔ2B failed to efficiently displace nucleoprotein complexes from DNA, demonstrating that ssDNA translocation and DNA unwinding are separable processes from nucleoprotein displacement and that additional energy input is required for efficient displacement of (high-affinity) nucleoprotein complexes. It is therefore possible DNA translocation can be uncoupled from ATP hydrolysis and that additional cycles of ATP hydrolysis can lead to a step-wise disruption of the non-covalent interactions between the DNA and the protein block (Raney & Benkovic, 1995). RepΔ2B^{uvrD2B}, which contains the 2B subdomain of the SF1A helicase UvrD, restored Rep function both *in vitro* and *in vivo*, suggesting that the 2B subdomain in SF1A helicases could be required to channel energy derived from ATP hydrolysis into a mechanistic displacement of nucleoprotein barriers.

The 2B subdomain of Rep was crystallised in an open and a closed conformation (Korolev *et al.*, 1997) and it was shown that the 2B subdomains of Rep, UvrD and PcrA are flexible (Jia *et al.*, 2011; Myong *et al.*, 2005; Park *et al.*, 2010). A site directed mutagenesis approach was performed that aimed to find a full-length Rep protein that displayed a similar phenotype to RepΔ2B *in vivo* and *in vitro*. A Rep mutant that contained mutations in the C-terminal hinge of the 2B subdomain phenocopied RepΔ2B *in vivo*. Conversely, mutations in the N-terminal hinge were fully functional, even though both the hinge mutations had originally been designed in UvrD to result in an opening of the 2B subdomain (Lee & Yang, 2006). Comparison of the available crystal structures of Rep, UvrD and PcrA indicated that the C-terminal hinge likely provides flexibility to the 2B subdomain in SF1A helicases. Biochemical characterisation of the two hinge mutants showed increased levels of DNA unwinding and also enhanced nucleoprotein displacement. Given that the 2B subdomain in these hinge mutants might be in a more open conformation, it is possible that ATP-driven opening of this domain in wild-type Rep could act as a lever to disrupt protein-DNA interactions. Unfortunately, experiments investigating

the conformation of the 2B subdomain could not be performed within the time of this project.

Table 6.1 Overview of biochemical and genetic characterisation of wild-type Rep and Rep mutants

Helicase	wild-type Rep	RepΔ2B	Rep Δ2B^uvrD2B	G543A/ S545A	G373T/ G374T
Complementation of *Δrep ΔuvrD* lethality	++	–	+	–	+++
Helicase activity	+	+++	+	++	+++
DNA supershifts	++	–	++	+++	++
DnaB cooperativity	+++	–	+++	++	–
Streptavidin displacement	++	–	+	+++	+++
In vitro fork progression	++	–	not tested	+++	+++

Rep G543A/S545A only phenocopied RepΔ2B *in vivo*, whereas it was a fully functional helicase *in vitro*. The most likely reason for the toxicity of Rep G543A/S545A *in vivo* is its increased affinity to DNA. In all other assays performed Rep G373T/G374T, which was a functional helicase *in vivo*, either displayed more extreme phenotypes than Rep G543A/S545A or in the case of cooperativity in DNA unwinding with DnaB behaved like RepΔ2B (Table 6.1). RepΔ2B has also been proposed to have a higher affinity to DNA but the experiments performed here did not support this hypothesis. Additional and more direct experiments are therefore required to investigate the interaction of the helicases with DNA. It is however also possible that the reason for the toxicity of RepΔ2B and Rep G543A/S545A is not related.

My work demonstrates that the 2B subdomain is essential for Rep to act as an accessory replicative helicase with different conformations or conformational changes of the 2B subdomain possibly playing a key role in nucleoprotein displacement. In eukaryotes, accessory replicative helicase function is provided by SF1B helicases that translocate with the opposite polarity to SF1A helicases, such as Rep (Figure 1.5). SF1B helicases share the basic structure of four subdomains with

SF1A helicases. The 1B subdomain acts as a separation pin, required for DNA duplex separation (Saikrishnan *et al.*, 2008) but the function of the 2B subdomain is not known. It has been shown that the SF1B helicase Dda is able to displace protein blocks from ssDNA and dsDNA (Byrd & Raney, 2004; Byrd & Raney, 2006). Although the structure of 2B subdomains of SF1B helicases differs from their SF1A equivalents, it is possible that the 2B subdomain also plays a central role in nucleoprotein displacement by SF1B helicases, e.g. the eukaryotic accessory replicative helicases *Sc*Rrm3 or *Sp*Pfh1.

All in all, this work illustrates several key features for accessory replicative helicases. The presence of accessory replicative helicases in eukaryotes shows that these helicases play vital roles in genome maintenance and safeguard the genetic integrity in all domains of life.

APPENDIX

Appendix

A.1　Chemicals and Reagents

Table A.1 Materials and Suppliers

Material	Source/supplier
a)　Media	
Sodium Chloride	VWR
Tryptone	Melford
Technical agar No. 3	Oxoid
Yeast extract	Oxoid
b)　Nucleic acid manipulations	
Taq DNA polymerase	New England Biolabs (NEB)
Phusion DNA polymerase	NEB
Restriction enzymes	NEB
Calf intestinal alkaline phosphatase (CIP)	NEB
T4 DNA ligase	NEB
T4 polynucleotide kinase (PNK)	NEB
Fast Ladder (10kb-50bp)	NEB
dNTPs	Roche
NTPs	Roche
Oligonucleotides	Integrated DNA Technologies (IDT)
QIAprep Spin Miniprep Kit	Qiagen
QIAquick PCR Purification Kit	Qiagen
QIAquick Gel Extraction Kit	Qiagen
Molecular biology grade water, ACS water	Sigma
[γ-32P]-ATP (6000Ci/mmol 10mCi/ml)	Perkin-Elmer
[α-32P]-dCTP (3000Ci/mmol 10mCi/ml)	Perkin-Elmer
c)　Other chemicals and solutions	
acrylamide : bis-acrylamide – 29:1 (40%)	Fisher
agarose	Melford
BSA	Roche

A.2   List of commonly used recipes and buffers in this work

a) General buffers and solutions

Gel loading buffer (GLB)

Gel loading buffer was added to DNA samples prior to agarose gel electrophoresis or polyacrylamide gel electrophoresis.

Table A.2 6× GLB

Chemical	Final concentration
Glycerol	30% (w/v)
Bromophenol blue	0.25% (w/v)

Sequencing gel stock

Denaturing urea polyacrylamide gels were prepared by mixing 60 ml of 12% sequencing gel stock with 60 µl of 25% (w/v) APS and 60 µl TEMED and careful injection into the BIO-RAD SequiGen apparatus with 1 mm spacers using a 50 ml syringe. A 10 well comb was inserted into the top of the gel, covered in cling film and left to set overnight at room temperature.

Table A.3 12% sequencing gel stock

Chemical (stock concentration)	Amount
acrylamide : bis-acrylamide– 29:1 (40%)	90 ml
TBE (5x)	60 ml
urea	138 g
dH$_2$O	filled to 200 ml

Sequencing loading dye

Sequencing loading dye was added to oligonucleotides prior to denaturing urea gel electrophoresis.

Table A.4 2× sequencing loading dye

Chemical	Final concentration
deionised formamide	80%
EDTA pH 8.0	10 mM
Xylene cyanol	1 mg ml^{-1}
Bromophenol blue	1 mg ml^{-1}

SSC

SSC was added to annealing reactions of oligonucleotides.

Table A.5 10× SSC

Chemical	Concentration
sodium citrate pH 7.0	300 mM
NaCl	1 M

TBE

TBE was used as running buffer for agarose gel electrophoresis, polyacrylamide gel electrophoresis and denaturing urea polyacrylamide gel electrophoresis.

Table A.6 5× TBE

Chemical (stock concentration)	Amount l^{-1}
Tris base	54 g
Boric acid	27.5 g
EDTA pH 8.0 (0.5 M)	20 ml

b) DNA helicase assays

Biotin solution

A 100 mM biotin stock solution used in *in vitro* assays containing streptavidin was made up in Tris-HCl pH 8.0 and kept at 4°C.

Dilution buffer (DB)

Protein dilutions for *in vitro* experiments were made in dilution buffer.

Table A.7 Dilution buffer for *in vitro* assays

Chemical	Final concentration
Tris-HCl pH 7.5	50 mM
NaCl	100 mM
EDTA pH 8.0	1 mM
glycerol	20%
BSA	0.5 mg ml^{-1}
β-mercaptoethanol	10 mM

TBE-polyacrylamide gels (TBE/PAA gels)

TBE/PAA gels were cast as 16×16×0.5 cm with a 20 well comb. After setting for a minimum of two hours, the comb was removed and the wells were rinsed in TBE. The gels were then assembled in a BIO-RAD Protean II xi Cell and stored in 1x TBE at 4°C until use.

Table A.8 10% TBE-polyacrylamide gel

Chemical (stock concentration)	Amount
dH$_2$O	32.8 ml
TBE (5×)	12 ml
acrylamide : bis-acrylamide – 29:1 (40%)	15 ml
APS (10%)	600 µl
TEMED (100%)	60 µl

4% TB-gel were used for DNA bandshifts and were prepared as above, just that 89 mM TB, 10 mM MgAc, 10 µM ADP or ATP was used for rinsing the wells and as running buffer.

Table A.9 4% TB-PAA gel

Chemical (stock concentration)	Amount
dH$_2$O	46.7 ml
Tris Borate (890 mM)	6 ml
acrylamide : bis-acrylamide – 29:1 (40%)	6 ml
MgAc (1 M)	600 µl
ADP or ATP (100 mM)	6 µl
APS (10%)	600 µl
TEMED (100%)	60 µl

c) Buffers and recipes used for protein purification

Prior to affinity purification on the His-trap FF column (GE Healthcare), the nickel from previous purifications was removed by 3 CVs of 400 mM EDTA, 2 M NaCl and 8 mM Tris pH 7.9. The column was charged with 3 CVs 0.2 M aqueous NiSO$_4$ before equilibration in 3 CVs of binding buffer (2.6.3).

Heparin columns (GE Healthcare) were washed in 3 CV of 50 mM Tris pH 7.5, 1 mM EDTA and 1 M NaCl to remove residual contaminants. Afterwards, the column was equilibrated in 50 mM Tris pH 7.5 and 1 mM EDTA and 50 mM NaCl, which the conductivity of the protein sample was adjusted to.

Storage buffer (20% ethanol) was removed from the HiLoad 26/60 Superdex 200 prepgrade Gel filtration column (GE Healthcare) by washing with 2 CV sterile filtered dH$_2$0 with a flow rate of 0.5 ml min^{-1}. Prior to the injection of the protein sample, the column was equilibrated with 2 CV of the running buffer (50 mM Tris pH 8.4, 200 mM NaCl, 1 mM EDTA and 5 mM DTT; 0.5 ml min^{-1}).

Sodium dodecyl sulphate polyacrylamide gel electrophoresis (SDS-PAGE)

SDS-PAGE gels were cast in 1 mm Novex gel cassettes (LifeTechnologies). The bottom layer was formed by an 8% resolving gel and after setting topped up with 6% resolving gel containing a 15 well comb.

Table A.10 Recipe for a single SDS gel

Chemical (stock concentration)	8% resolving gel	6% stacking gel
dH$_2$O	5.2 ml	3.525 ml
Tris pH 8.8 (3 M)	1 ml	-
Tris pH 6.8 (1 M)	-	0.625 ml
acrylamide : bis-acrylamide – 29:1 (40%)	1.6 ml	0.75 ml
SDS (10%)	80 µl	50 µl
APS (10%)	80 µl	50 µl
TEMED (100%)	8 µl	5 µl

Protein samples were mixed in SDS loading buffer (1x final concentration) and boiled at 95°C for 5 min before loading onto the SDS gels.

Table A.11 4x SDS loading buffer

Chemical	Concentration
Tris-HCl pH8.0	200 mM
SDS	8% (w/v)
Bromophenol blue	0.4% (w/v)
glycerol	20% (w/v)
DTT	200 mM

SDS-PAGE was performed in 1x SDS running buffer at 220V for 50 min.

Table A.12 1l 10× SDS running buffer

Chemical	Amount
Tris base	30.3 g
glycine	144 g
SDS	10 g

A.3 List of Oligonucleotides

Table A.13 List of PCR primers used for gene amplification and cloning

Name	Gene	Sequence (5' – 3')	5' modification	Pairs with	PCR product (kb)
oJGB216	*dnaB*	GACAAGCTTACATATGGCAGGAAATAAACCCTTCAAC	HindIII, NdeI	various	various
oJGB217	*dnaB*	AGTGGATCCCGGGTTATTATTCGTCGTCGTACTGCG	BamHI, SmaI	oJGB216	*dnaB* (1.41)
oJGB218	*dnaB*	AGTGGATCCCGGGTTATTAGTACTGCGGCCCCGCATAG	BamHI, SmaI	oJGB216	*dnaBΔC3* (1.4)
oJGB219	*dnaB*	AGTGGATCCCGGGTTATTACCCCGCATAGTTGTCGAAGC	BamHI, SmaI	oJGB216	*dnaBΔC6* (1.4)
oJGB220	*dnaB*	AGTGGATCCCGGGTTATTAGTTGTCGAAGCGCGACCATTG	BamHI, SmaI	oJGB216	*dnaBΔC9* (1.4)
oJGB221	*dnaB*	AGTGGATCCCGGGTTATTAGCGCGACCATTGACCGTTAAAG	BamHI, SmaI	oJGB216	*dnaBΔC12* (1.38)
oJGB222	*dnaB*	AGTGGATCCCGGGTTATTACCATTGACCGTTAAAGGTCAGG	BamHI, SmaI	oJGB216	*dnaBΔC14* (1.38)
oJGB253	*dnaB*	AGTGGATCCCGGGTTATTACGTCCCGATTGGGCCGTTAC	BamHI, SmaI	oJGB216	*dnaBΔC23* (1.35)
oJGB254	*dnaB*	AGTGGATCCCGGGTTATTAGATAATAATTTCCGCGATGCC	BamHI, SmaI	oJGB216	*dnaBΔC33* (1.32)
oJGB329	*rep*	AGGTGATTAAGCTTGAGCAGAAC	HindIII	oJGB330	Rep 2B subdomain for cloning into pPM638
oJGB330	*rep*	AGATCGAAGCTTCTCGATTTATTTCCCTCGTTTTGCCGCC	HindIII	oJGB329	

Table A.14 List of sequencing primers

Name	Sequence (5' – 3')	Gene/plasmid	Binding site relative to start codon
PM303	GATGCATGCGTTGCCATTAATTT	*rep* (5' UTR)	(-396) – (-373)
PM304	GCTTATCTGGTGCGTAATCTGGAT	*rep* (3' UTR)	2398-2422 (376-400 after stop codon)
PM319	CTTGTTGGATCAGACCGGAAAATG	*uvrD* (5' UTR)	(-190) – (-166)
PM320	TGGCAACGCTATCCTTTTGTCA	*uvrD* (3' UTR)	2338-2360 (175-197- after stop codon)
PM363	CATACGTTGGGGCTGGAT	*rep*	253-270
PM364	TTATGGGCTGTATGATGC	*rep*	501-518
PM365	TGCACGTCCGCAAAACCT	*rep*	756-773
PM366	TCACTTCGTCAATAAAAC	*rep*	1002-1019
PM367	GCTGAAAAAGCTGGGTGA	*rep*	1251-1268
PM368	CGCATGAAGAACGTCAAC	*rep*	1501-1518
PM375	GTTTTGCGGACGTGCACC	*rep*	771-754
PM376	GTGTGCATCATACAGCCC	*rep*	522-505
PM403	TTCTGTAACAAAGCGGGACCAAAG	pBAD24 and derivatives	(-220) – (-197) (upstream of ATG in NcoI site in pBAD 24)
PM404	AGTTCCCTACTCTCGCATGGG	pBAD24 and derivatives	219-239 (downstream of ATG in NcoI site in pBAD 24)
MKG132	CATCGTGCGTGAACG	*dnaB*	372-386
MKG133	GGTACTTATCTTCTCGC	*dnaB*	765-781
MKG134	AGAAATCTCTCGCTCGC	*dnaB*	1086-1102
oJGB302	AAAGACGCGGGATTCAGCCAG	*dnaB*	498-478

Table A.15 List of primers used for Site Directed Mutagenesis (SDM) of Rep

Base changes in bold. Codons affected shown in red. Bases differing from the wild-type sequence are underlined, if the primers are complementary to a Rep mutant.

Resulting AA change (complementaty to)	Forward Primer	Sequence (5' – 3')	Reverse Primer	Sequence (5' – 3')
G373A/G374A (Rep)	oJGB296	GTACAAAATATCT**GCTGCT**ACGTCGTTTTTC	oJGB297	GAAAAACGACGT**AGCAG**CAGATATTTTGTAC
G373T/G374T (Rep)	oJGB316	GTACAAAATATCT**ACCACC**ACGTCGTTTTTC	oJGB317	GAAAAACGACG**TGGTGG**TAGATATTTTGTAC
R391A (Rep)	oJGB294	CTGGCTTATCTG**GCT**GTGCTGACTAAC	oJGB295	GTTAGTCAGCAC**AGC**CAGATAAGCCAG
D397A (Rep)	oJGB310	CTGACTAACCCG**GCT**GATGACAGCGC	oJGB311	GCGCTGTCATC**AG**CCGGGTTAGTCAG
D398A (Rep)	oJGB308	CTAACCCGGACG**CT**GACAGCGCATTTC	oJGB309	GAAATGCGCTGTCA**GC**GTCCGGGTTAG
D399A (Rep)	oJGB306	CTAACCCGGACGAT**GCT**AGCGCATTTC	oJGB307	GAAATGCGCT**AG**CATCGTCCGGGTTAG
D398A/D399A (Rep)	oJGB312	GACTAACCCGGACG**CTGCT**AGCGCATTTCTG	oJGB313	CAGAAATGCGCT**AGCAG**CGTCCGGGTTAGTC
D397A/D398A/D399A (Rep)	oJGB314	GACTAACCCG**GCTGCTGCT**AGCGCATTTCTG	oJGB315	CAGAAATGCGCT**AGCAGCAG**CCGGGTTAGTC
K410A (Rep) and K410A/T417A (Rep)	oJGB282	CGTTAACACGCCG**GCT**CGAGAGATTGGC	oJGB283	GCCAATCTCTCG**AGC**CGGCGTGTTAACG
E412A (Rep)	oJGB344	GCCGAAGCGAGC**T**ATTGGCCCGG	oJGB345	CCGGGCCAAT**AG**CTCGCTTCGGC
E412G (Rep)	oJGB304	GCCGAAGCGAG**GT**ATTGGCCCGG	oJGB305	CCGGGCCAAT**ACC**TCGCTTCGGC
G414A (Rep)	oJGB284	GAAGCGAGAGATTG**CT**CCGGCTACGC	oJGB285	GCGTAGCCGG**AG**CAATCTCTCGCTTC
G414T (Rep)	oJGB318	GAAGCGAGAGATT**ACC**CCGGCTACGC	oJGB319	GCGTAGCCGG**GGT**AATCTCTCGCTTC
T417A (Rep)	oJGB286	GATTGGCCCGGCTG**CT**CTGAAAAAGC	oJGB287	GCTTTTTCAG**AGC**AGCCGGGCCAATC
K410A (Rep G414A)	oJGB290	CGTTAACACGCCG**GCT**CGAGAGATTG<u>CT</u>	oJGB291	<u>AGC</u>AATCTCT**CGA**GCCGGCGTGTTAACG
T417A (Rep G414A)	oJGB292	GATT<u>GCT</u>CCGGCTG**CT**CTGAAAAAGC	oJGB293	GCTTTTTCAG**AGC**AGCCGG<u>AGC</u>AATC
K410A/G414A/T417A (Rep G414A)	oJGB290	CGTTAACACGCCG**GCT**CGAGAGATTG<u>CT</u>	oJGB293	GCTTTTTCAG**AGC**AGCCGG<u>AGC</u>AATC

Resulting AA change (complementarity to)	Forward Primer	Sequence (5' – 3')	Reverse Primer	Sequence (5' – 3')
E412A (Rep K410A G414A)	oJGB340	GCCGGCTCGAG**CT**ATTGCTCCGG	oJGB341	CCGGAGCAAT**AG**CTCGAGCCGGC
R448A (Rep)	oJGB288	CGCTTAGCGGA**GC**TGGTTATGAAGC	oJGB289	GCTTCATAACCA**GC**TCCGCTAAGCG
G543A (Rep)	oJGB332	GATGGAGCGTG**CT**GAGAGTGAAG	oJGB333	CTTCACTCTCA**G**CACGCTCCATC
S545A (Rep)	oJGB334	GAGCGTGGTGAG**GC**TGAAGAAGAGCTG	oJGB335	CAGCTCTTCTTCA**GC**CTCACCACGCTC
G543A/S545A (Rep)	oJGB298	GATGGAGCGTG**CT**GAG**GC**TGAAGAAGAGCTG	oJGB299	CAGCTCTTCTTCA**GC**CTCA**G**CACGCTCCATC

Table A.16 List of oligonucleotides used in *in vitro* studies

Name	Sequence (5' – 3')	Resulting substrate (<u>dsDNA</u>-ssDNA)
a) Fork substrates		
CC139	<u>GCAAGCCTTCTACAGGTCGACCGTCCATGGCGACTCGAGACCGCAATACGGATAAGGGCTGA</u>GCACGCCGACGAACATTCACCACGCCAGACCACGTA	fork (<u>60</u>-38)
CC140	GACTATCTACGTCCGAGGCTCGCGCCGCAGACTCATTT<u>AGCCCTTATCCGTATTGCGGTCTC</u>GAGTCGCCATGGACGGTCGACCTGTAGAAGGCTTGC	
CC139B53	<u>GCAAGCCTTCTACAGGTCGACCGTCCATGGCGACTCGAGACCGCAATACGGA**B**AAGGGCTGA</u>GCACGCCGACGAACATTCACCACGCCAGACCACGTA	fork (<u>60</u>-38) **biotinylated** 8/9 bp away from the ss/dsDNA junction
CC140B47	GACTATCTACGTCCGAGGCTCGCGCCGCAGACTCATTT<u>AGCCCTTA**B**CCGTATTGCGGTCTC</u>GAGTCGCCATGGACGGTCGACCTGTAGAAGGCTTGC	
oJA025	<u>GCAAGCCTTCTACAGGTCGAATTGTGAGCGGATAACAATTCCGCAATACGGATAAGGGCTGA</u>GCACGCCGACGAACATTCACCACGCCAGACCACGTA	fork (<u>60</u>-38) with *lacO₁*
oJA026	GACTATCTACGTCCGAGGCTCGCGCCGCAGACTCATTT<u>AGCCCTTATCCGTATTGCGGAATTGTTATCCGCTCACAATT</u>CGACCTGTAGAAGGCTTGC	
b) ssDNA substrates		
PM326	T**B**TTTTTTTTTTTTTTTTTTTTTTTTTTTTTTTTTTTTTTTTTTTTTTTTTTTTTTTTTTTTT	5' dT bio-dT dT$_{60}$ (used in SPR)
PM327	TTTTTTTTTTTTTTTTTTTTTTTTTTTTTTTTTTTTTTTTTTTTTTTTTTTTTTTTTTTTT**B**T	3' dT$_{60}$ bio-dT dT
PM328	TTTTTTTTTTTTTTTTTTTTTTTTTTTTTT**B**TTTTTTTTTTTTTTTTTTTTTTTTTTTTTT	5' dT$_{30}$ bio-dT dT$_{30}$ 3'
PM329	TTTTTTTTTTTTTTTTTTTTTTTTTTTTTTTTTTTTTTTTTTTTTTTTTTTTTTTTTTTT	dT$_{60}$
oJGB353	**B**–GTCGGATCCTCTAGACAGCTCCATG	25mer used in SPR
oJGB354	**B**–GTCGGATCCTCTAGACAGCTCCATGATCACTGGCACTGGTAGAATTCGGC	50mer used in SPR

A.4 Full list of plasmids used in this study

Table A.17 List of plasmids used in this study for experiments and subcloning

Name	Relevant Features	Source
a) cloning vectors		
pACT-2	shuttle vector for expression in *E. coli* and *S. cerevisiae*, N-terminal HA-epitope, Ap[r]	Clontech
pBAD24	pBR322 origin, *araC* gene, P_{BAD} promoter, optimised SD sequence, Ap[r]	(Guzman *et al.*, 1995)
pBlueskript SK(-)	phagemid, cloning vector replicating from f1 phage origin; polylinker, T3 and T7 RNA polymerase promoters in *lacZ* gene, blue-white selection, Ap[r]	(Alting-Mees & Short, 1989)
pBR322	pMB1-derived cloning vector, *rop* gene for limiting copy number, Ap[r], Tet[r]	(Bolivar *et al.*, 1977)
pET14b	cloning/expression vector, pBR322-derived origin, N-terminal His-tag followed by thrombine site, T7 promoter, Ap[r]	Novagene
pET21a	cloning/expression vector, pBR322 and f1-derived origins, N-terminal His-tag, *lacI* coding sequence, T7 promoter, *lac* operator, Ap[r]	Novagene
pET21b	cloning/expression vector, as pET21a differing by a 1bp deletion upstream the BamHI site of the MCS	Novagene
pET22b	cloning/expression vector, pBR322 and f1-derived origins, C-terminal His-tag, *pelB* signal sequence for potential periplasmic localisation, *lacI* coding sequence, T7 promoter, *lac* operator, Ap[r]	Novagene
pPM638	as pBAD24 but contains a Kn[r] cassette cloned into the ScaI site of the pBAD24 Ap[r] cassette	(Guy *et al.*, 2009)
pRC7	mini-F plasmid, contains *lacIZYA* genes for blue/white screening, lacks stabilisation system and can be lost at a high frequency, Ap[r]	(Bernhardt & de Boer, 2004)
b) cloning vector derivatives		
pAM403	a pRC7 derivative encoding wild-type *rep*	(Mahdi *et al.*, 2006)

pAM407	as pAM403 but encodes wild-type *uvrD* instead of *rep*	(Guy *et al.*, 2009)
pJLH102	derivative of pET21b, encodes *repΔcys*	J. Howard, unpublished
pJLH103	as pJLH102 but encodes r*ep2cys* instead of *repΔcys*	J. Howard, unpublished
pJLH133	derivative of pET14b, encodes wild-type Rep	J. Howard, unpublished
pJLH120	a pPM638 derivative encoding *repΔcys*	J Howard, unpublished
pJLH121	a pPM638 derivative encoding *rep2cys*	J Howard, unpublished
pJLH134	as pJLH133 but encodes r*epΔcys* instead of *rep*	J. Howard, unpublished
pJLH135	as pJLH133 but encodes r*ep2cys* instead of *rep*	J. Howard, unpublished
pMG32	a pACT-2 derivative, encodes *repΔC2*	M. Gupta, unpublished
pMG33	as pMG32 but encodes r*epΔC4* instead of *repΔC2*	M. Gupta, unpublished
pMG34	as pMG32 but encodes r*epΔC6* instead of *repΔC2*	M. Gupta, unpublished
pMG35	as pMG32 but encodes r*epΔC8* instead of *repΔC2*	M. Gupta, unpublished
pPM561	a pBR322 derivative containing the *E. coli oriC* and an array of 22 *lac* operator complexes	(Gupta *et al.*, 2013)
pPM594	pBlueskript SK(-) derivative containing *E. coli oriC* and 8 EcoRI sites cloned into the XbaI site	(Guy *et al.*, 2009)
pPM657	a pET22b derivative, encodes wild-type *rep* with a N-terminal biotin tag	(Guy *et al.*, 2009)
pPM841	derivative of pET21a, encodes *repΔ2B*[uvrD2B]	P. McGlynn, unpublished
pPM648	a pPM638 derivative encoding wild-type *rep*	(Guy *et al.*, 2009)
pPM682	a pPM638 derivative encoding *repΔ2B*	(Guy *et al.*, 2009)
pPM713	a pPM638 derivative encoding *repK28AΔ2B*	P. McGlynn, unpublished
pPM730	a pPM638 derivative encoding *repK28A*	P. McGlynn, unpublished
pPM759	a pPM638 derivative encoding *repΔC33*	(Guy *et al.*, 2009)
pPM765	a pPM638 derivative encoding *repΔ2BΔC33*	P. McGlynn, unpublished
pPM853	a pPM638 derivative encoding *repΔ2B*[uvrD2B]	P. McGlynn, unpublished

Table A.18 List of plasmids generated in this study

All plasmids were cloned as described in section 2.5.7. Vector and insert DNA were either plasmid DNA (acquired as described in section 2.5.1) or PCR products (section 2.5.5.3). Digests were performed with the indicated restriction enzymes as described in section 2.5.3. The letter "B" after a restriction enzyme indicates the conversion of that restriction site to blunt ends (2.5.3.1).Only vector DNA was dephosphorylated (2.5.3.2) and all DNA sequences were gel purified (2.5.4) prior to DNA ligation.

Plasmid name	Features	Cloning	
		Vector (digest) – relevant features	Insert (digest) – relevant features
a) pPM638 derivatives – *dnaB*			
pJGB143	pBAD*dnaB*	pPM638 (NcoI, B/XmaI, B) – pBAD	PCR of TB28 with oJGB216+217 (HindIII, B/XmaI, B) – *dnaB*
pJGB145	pBAD*dnaBΔC3*	pPM638 (NcoI, B/XmaI, B) – pBAD	PCR of TB28 with oJGB216+218 (HindIII, B/XmaI, B) – *dnaBΔC3*
pJGB147	pBAD*dnaBΔC6*	pPM638 (NcoI, B/XmaI, B) – pBAD	PCR of TB28 with oJGB216+219 (HindIII, B/XmaI, B) – *dnaBΔC6*
pJGB148	pBAD*dnaBΔC9*	pPM638 (NcoI, B/XmaI, B) – pBAD	PCR of TB28 with oJGB216+220 (HindIII, B/XmaI, B) – *dnaBΔC9*
pJGB149	pBAD*dnaBΔC14*	pPM638 (NcoI, B/XmaI, B) – pBAD	PCR of TB28 with oJGB216+222 (HindIII, B/XmaI, B) – *dnaBΔC14*
pJGB177	pBAD*dnaBΔC12*	pPM638 (NcoI, B/XmaI, B) – pBAD	PCR of TB28 with oJGB216+221 (HindIII, B/XmaI, B) – *dnaBΔC12*
pJGB181	pBAD*dnaΔC23*	pPM638 (NcoI, B/XmaI, B) – pBAD	PCR of TB28 with oJGB216+253 (HindIII, B/XmaI, B) – *dnaBΔC23*
pJGB183	pBAD*dnaBΔC33*	pPM638 (NcoI, B/XmaI, B) – pBAD	PCR of TB28 with oJGB216+254 (HindIII, B/XmaI, B) – *dnaB ΔC33*
b) pBAD24 derivatives (Ap^r) — *dnaB*			
pJGB234	pBAD*dnaB*	pBAD24 (XmaI, B/PstI) – pBAD	pJGB143 (NdeI, B/PstI) – *dnaB*
pJGB235	pBAD*dnaBΔC3*	pBAD24 (XmaI, B/PstI) – pBAD	pJGB145 (NdeI, B/PstI) – *dnaBΔC3*

Plasmid name	Features	Cloning	
		Vector (digest) – relevant features	Insert (digest) – relevant features
pJGB236	pBAD*dnaBΔC6*	pBAD24 (XmaI, B/PstI) – pBAD	pJGB147 (NdeI, B/PstI) – *dnaBΔC6*
pJGB237	pBAD*dnaBΔC9*	pBAD24 (XmaI, B/PstI) – pBAD	pJGB148 (NdeI, B/PstI) – *dnaBΔC9*
pJGB238	pBAD*dnaBΔC12*	pBAD24 (XmaI, B/PstI) – pBAD	pJGB177 (NdeI, B/PstI) – *dnaBΔC12*
pJGB239	pBAD*dnaBΔC14*	pBAD24 (XmaI, B/PstI) – pBAD	pJGB149 (NdeI, B/PstI) – *dnaBΔC14*
pJGB240	pBAD*dnaBΔC23*	pBAD24 (XmaI, B/PstI) – pBAD	pJGB181 (NdeI, B/PstI) – *dnaBΔC23*
pJGB241	pBAD*dnaBΔC33*	pBAD24 (XmaI, B/PstI) – pBAD	pJGB183 (NdeI, B/PstI) – *dnaBΔC33*

c) **pPM638 derivatives (Kn^r) — *rep***

Plasmid name	Features	Cloning	
pJGB1	pBAD*repΔC2*	pPM638 (XmaI, B) – pBAD	pMG32 (NdeI, B/XhoI, B) – *repΔC2*
pJGB2	pBAD*repΔC4*	pPM638 (XmaI, B) – pBAD	pMG33 (NdeI, B/XhoI, B) – *repΔC4*
pJGB3	pBAD*repΔC6*	pPM638 (XmaI, B) – pBAD	pMG34 (NdeI, B/XhoI, B) – *repΔC6*
pJGB4	pBAD*repΔC8*	pPM638 (XmaI, B) – pBAD	pMG35 (NdeI, B/XhoI, B) – *repΔC8*
pJGB9	pBAD*repK28AΔC33*	pPM730 (HindIII) – pBAD*repK28A*	pPM759 (HindIII) – *repΔC33*
pJGB10	pBAD*repK28AΔC2*	pPM730 (HindIII) – pBAD*repK28A*	pJGB1 (HindIII) – *repΔC2*
pJGB11	pBAD*repK28AΔC4*	pPM730 (HindIII) – pBAD*repK28A*	pJGB2 (HindIII) – *repΔC4*
pJGB12	pBAD*repK28AΔC6*	pPM730 (HindIII) – pBAD*repK28A*	pJGB3 (HindIII) – *repΔC6*
pJGB13	pBAD*repK28AΔC8*	pPM730 (HindIII) – pBAD*repK28A*	pJGB4 (HindIII) – *repΔC8*
pJGB185	pBAD*repΔ2B^{uvrD2B}ΔC33*	pPM765 (BseRI/PstI) – pBAD*rep Δ2BΔC33*	pPM853 (BseRI/PstI) – *repΔ2B^{uvrD}*
pJGB328	pBAD*repG543A/S545Aδcys*	pJLH120 (BseRI-BstXI) – pBAD*repΔcys*	pJGB304 (BseRI-BstXI) – *repΔcysG543A/S545A*
pJGB329	pBAD*repG543A/S545A2cys*	pJLH121 (BseRI-BstXI) – pBAD*rep2cys*	pJGB305 (BseRI-BstXI) – *rep2cysG543A/S545A*

Plasmid name	Features	Cloning	
		Vector (digest) – relevant features	Insert (digest) – relevant features
d) pET22b bio-rep derivatives (Site Directed Mutagenesis)			
pJGB195	pET22b*bio-repG414T*	pPM657 (pET22b*bio-rep*)	SDM with oJGB318+319 (G414T)
pJGB196	pET22b*bio-repD397A*	pPM657 (pET22b*bio-rep*)	SDM with oJGB310+311 (D397A)
pJGB197	pET22b*bio-repG543A/S545A*	pPM657 (pET22b*bio-rep*)	SDM with oJGB298+299 (G543A/S545A)
pJGB198	pET22b*bio-repD398A/D399A*	pPM657 (pET22b*bio-rep*)	SDM with oJGB312+313 (D398A/D399A)
pJGB215	pET22b*bio-repR448A*	pPM657 (pET22b*bio-rep*)	SDM with oJGB288+289 (R448A)
pJGB217	pET22b*bio-repT417A*	pPM657 (pET22b*bio-rep*)	SDM with oJGB286+287 (T417A)
pJGB220	pET22b*bio-repG414A*	pPM657 (pET22b*bio-rep*)	SDM with oJGB284+285 (G414A)
pJGB221	pET22b*bio-repD397A/D398A/ D399A*	pPM657 (pET22b*bio-rep*)	SDM with oJGB314+315 (D397A/D398A/D399A)
pJGB226	pET22b*bio-repK410A/G414A*	pJGB220 (pET22b*bio-repG414A*)	SDM with oJGB290+291 (K410A)
pJGB227	pET22b*bio-repK410A/T417A*	pJGB217 (pET22b*bio-repT417A*)	SDM with oJGB282+283 (K410A)
pJGB228	pET22b*bio-rep K410A/G414A/ T417A*	pJGB220 (pET22b*bio-repG414A*)	SDM with oJGB290+293 (K410A /T417A)
pJGB229	pET22b*bio-repR391A*	pPM657 (pET22b*bio-rep*)	SDM with oJGB294+295 (R391A)
pJGB230	pET22b*bio-repE412G*	pPM657 (pET22b*bio-rep*)	SDM with oJGB304+305 (E412G)
pJGB231	pET22b*bio-repD398A*	pPM657 (pET22b*bio-rep*)	SDM with oJGB308+309 (D398A)
pJGB243	pET22b*bio-repG414A/T417A*	pPM657 (pET22b*bio-rep*)	SDM with oJGB292+293 (G414A/T417A)
pJGB244	pET22b*bio-repG373A/G374A*	pPM657 (pET22b*bio-rep*)	SDM with oJGB296+297 (G373A/G374A)
pJGB255	pET22b*bio-repD399A*	pPM657 (pET22b*bio-rep*)	SDM with oJGB306+307 (D399A)
pJGB274	pET22b*bio-repG543A*	pPM657 (pET22b*bio-rep*)	SDM with oJGB294+295 (G543A)

Plasmid name	Features	Cloning	
		Vector (digest) – relevant features	Insert (digest) – relevant features
pJGB275	pET22b*bio-repS545A*	pPM657 (pET22b*bio-rep*)	SDM with oJGB294+295 (S545A)
pJGB286	pET22b*bio-repK410A/G414A/ T417A/R448A*	pJGB228 (pET22b*bio-repK410A/G414A/T417A*)	SDM with oJGB288+289 (R448A)
pJGB289	pET22b*bio-repK410A/E412A/ G414A/T417A/ R448A*	pJGB286 (pET22b*bio-repK410A/G414A/ T417A/R448A*)	SDM with oJGB340+341 (E412A)
pJGB291	pET22b*bio-repR391A/D397A/ D398A/D399A*	pJGB221 (pET22b*bio-rep*D397A/D398A/D399A)	SDM with oJGB294+295 (R391A)
pJGB303	pET22b*bio-repE412A*	pPM657 (pET22b*bio-rep*)	SDM with oJGB340+341 (E412A)
pJGB307	pET22b*bio-repG373T/G374T*	pPM657 (pET22b*bio-rep*)	SDM with oJGB316+317 (G373T/G374T)
pJGB320	pET22bbio-rep*K410A*	pPM657 (pET22b*bio-rep*)	SDM with oJGB282+283 (K410A)
pJGB321	pET22b*bio-repK410A/E412A/ G414A/T417A/R448A/G543A/ S545A*	pJGB289 (NcoI/BseRI) – pET22b*bio-repK410A/ E412A/G414A/T417A/R448A*)	pJGB197 (NcoI/BseRI) – *repG543A/S545A*
pJGB330	pET22b*bio-repR391A/D397A/ D398A/D399A/ G543A/S545A*	pJGB291 (NcoI/BseRI) – pET22b *bio-rep R391A/D397A/D398A/D399A*	pJGB197 (NcoI/BseRI) – *repG543A/S545A*

e) Subcloning of the Rep 2B subdomain mutants (from SDM) in pPM638

Plasmid name	Features	Cloning	
pJGB210	pBAD*repG543A/S545A*	pPM682 (HindIII) – pBAD*repΔ2B*	PCR of pJGB197 with oJGB329+330 (HindIII) – *rep*G543A/S545A
pJGB211	pBAD*repD398A/D399A*	pPM682 (HindIII) – pBAD*repΔ2B*	PCR of pJGB198 with oJGB329+330 (HindIII) – *rep*D398A/D399A
pJGB213	pBAD*repT417A*	pPM682 (HindIII) – pBAD*rep Δ2B*	PCR of pJGB217 with oJGB329+330 (HindIII) – *repT417A*

Table A.18 continued

Plasmid name	Features	Cloning	
		Vector (digest) – relevant features	Insert (digest) – relevant features
pJGB214	pBAD*repR448A*	pPM682 (HindIII) – pBAD*rep Δ2B*	PCR of pJGB215 with oJGB329+330 (HindIII) – *repR448A*
pJGB218	pBAD*repD397A*	pPM682 (HindIII) – pBAD*rep Δ2B*	PCR of pJGB196 with oJGB329+330 (HindIII) – *repD397A*
pJGB246	pBAD*repG414A*	pPM682 (BstXI/BseRI) – pBAD*repΔ2B*	pJGB220 (BstXI/BseRI) – rep*G414A*
pJGB247	pBAD*repD397A/D398A/D399A*	pPM682 (BstXI/BseRI) – pBAD*repΔ2B*	pJGB221 (BstXI/BseRI) – *repD397A/D398A/D399A*
pJGB248	pBAD*repK410A/G414A*	pPM682 (BstXI/BseRI) – pBAD*repΔ2B*	pJGB226 (BstXI/BseRI) – *repK410A/G414A*
pJGB249	pBAD*repK410A/G414A/T417A*	pPM682 (BstXI/BseRI) – pBAD*repΔ2B*	pJGB228 (BstXI/BseRI) – *repK410A/G414A/T417A*
pJGB250	pBAD*repR391A*	pPM682 (BstXI/BseRI) – pBAD*repΔ2B*	pJGB229 (BstXI/BseRI) – *repR391A*
pJGB251	pBAD*repE412G*	pPM682 (BstXI/BseRI) – pBAD*repΔ2B*	pJGB230 (BstXI/BseRI) – *repE412G*
pJGB252	pBAD*repD398A*	pPM682 (BstXI/BseRI) – pBAD*repΔ2B*	pJGB231 (BstXI/BseRI) – *repD398A*
pJGB253	pBAD*repK410A/T417A*	pPM682 (BstXI/BseRI) – pBAD*repΔ2B*	pJGB227 (BstXI/BseRI) – *repK410A/T417A*
pJGB256	pBAD*repG414A/T417A*	pPM682 (BstXI/BseRI) – pBAD*repΔ2B*	pJGB243 (BstXI/BseRI) – *repG414A/T417A*
pJGB258	pBAD*repD399A*	pPM682 (BstXI/BseRI) – pBAD*repΔ2B*	pJGB255 (BstXI/BseRI) – *repD399A*
pJGB260	pBAD*repG373A/G374A*	pPM682 (BstXI/BseRI) – pBAD*repΔ2B*	pJGB244 (BstXI/BseRI) – *repG373A/G374A*
pJGB262	pBAD*repG373A/G374AΔC33*	pPM765 (BstXI/BseRI) – pBAD*repΔ2BΔC33*	pJGB244 (BstXI/BseRI) – *repG373A/G374A*
pJGB264	pBAD*repG543A/S545AΔC33*	pPM765 (BstXI/BseRI) – pBAD*repΔ2BΔC33*	pJGB210 (BstXI/BseRI) – *repG543A/S545A*
pJGB276	pBAD*repG543A*	pPM682 (BstXI/BseRI) – pBAD*repΔ2B*	pJGB274 (BstXI/BseRI) – *repG543A*
pJGB280	pBAD*repS545A*	pPM682 (BstXI/BseRI) – pBAD*repΔ2B*	pJGB275 (BstXI/BseRI) – *repS545A*
pJGB296	pBAD*repK410A/E412A/G414A/ T417A/R448A*	pPM682 (BstXI/BseRI) – pBAD*repΔ2B*	pJGB289 (BstXI/BseRI) – *repK410A/E412A/G414A/ T417A/R448A*
pJGB298	pBAD*repR391A/D397A/D398A/ D399A*	pPM682 (BstXI/BseRI) – pBAD*repΔ2B*	pJGB291 (BstXI/BseRI) – *repR391A/D397A/D398A/D399A*

Table A.18 continued

Plasmid name	Features	Cloning	
		Vector (digest) – relevant features	Insert (digest) – relevant features
pJGB315	pBAD*repK410A/G414A/T417A/ R448A*	pPM682 (BstXI/BseRI) – pBAD*repΔ2B*	pJGB286 (BstXI/BseRI) – *rep*K410A/G414A/T417A/R448A
pJGB318	pBAD*repE412A*	pPM682 (BstXI/BseRI) – pBAD*repΔ2B*	pJGB303 (BstXI/BseRI) – *repE412A*
pJGB326	pBAD*repK410A*	pPM682 (BstXI/BseRI) – pBAD*repΔ2B*	pJGB320 (BstXI/BseRI) – *repK410A*
pJGB327	pBAD*repG373T/G374T*	pPM682 (BstXI/BseRI) – pBAD*repΔ2B*	pJGB307 (BstXI/BseRI) – *repG373T/G374T*
pJGB331	pBAD*repG373T/G374T ΔC33*	pPM765 (BstXI/BseRI) – pBAD*repΔ2BΔC33*	pJGB307 (BstXI/BseRI) – *repG373T/G374T*
pJGB332	pBAD*repK410A/E412A/G414A/ T417A/R448A/G543A/S545A*	pPM682 (BstXI/BseRI) – pBAD*repΔ2B*	pJGB321 (BstXI/BseRI) – *repK410A/E412A/G414A/ T417A/R448A/G543A/S545A*
pJGB333	pBAD*repR391A/D397A/D398A/ D399A/G543A/S545A*	pPM682 (BstXI/BseRI) – pBAD*repΔ2B*	pJGB330 (BstXI/BseRI) – *rep*R391A/*D397A/D398A/ D399A/G543A/S545A*
pJGB362	pBAD*rep G373T/G374T ΔC33*	pPM765 (BstXI/BseRI) – pBAD*repΔ2BΔC33*	pJGB327 (BstXI/BseRI) – *repG373T/G374T*
f) pET vector derivatives, Ap^r			
pJGB312	pET14b*repG543A/S545A*	pJLH133 (BseRI/BstXI) – pET14b*rep*	pJGB197 (BseRI/BstXI) – pET22b*bio-repG543A/S545A*
pJGB340	pET14b*repΔ2B*	pJGB312 (BseRI/BstXI) – pET14b*repG543A/S545A*	pPM682 (BseRI/BstXI) – *repΔ2B*
pJGB342	pET14b*repΔ2B^{uvrD2B}*	pJGB312 (BseRI/BstXI) – pET14b*repG543A/S545A*	pPM841 (BseRI/BstXI) – *repΔ2B^{uvrD2B}*
pJGB344	pET14b*repG373T/G374T*	pJGB312 (BseRI/BstXI) – pET14b*repG543A/S545A*	pJGB327 (BseRI/BstXI) – *repG373T/G374T*

Appendix

A.5 Sequence alignments

```
BstDnaB  -----------------MSELFSERIPPQSIEAEQAVLGAVFLDPAALVPASEILIPEDF    43
EcDnaB   MAGNKPFNKQQAEPRERDPQVAGLKVPPHSIEAEQSVLGGLMLDNERWDDVAERVVADDF    60
                          :: . ::**:*****:***.::**      .:* :: :**

BstDnaB  YRAAHQKIFHAMLRVADRGEPVDLVTVTAELAASEQLEEIGGVSYLSELADAVPTAANVE   103
EcDnaB   YTRPHRHIFTEMARLQESGSPIDLITLAESLERQGQLDSVGGFAYLAELSKNTPSAANIS   120
            *    *::** * *: : *.*:**:*:: .*  . **:.:**.:**:**: .*:***:.

BstDnaB  YYARIVEEKSVLRRLIRTATSIAQDGYTREDEID-VLLDEADRKIMEVSQ--RKHSGAFK   160
EcDnaB   AYADIVRERAVVREMISVANEIAEAGFDPQGRTSEDLLDLAESRVFKIAESRANKDEGPK   180
          ** **.*::*:*.:* .*..**: *:  : .   *** *: :::::::   ::. . *

BstDnaB  NIKDILVQTYDNIEM-LHNRDGEITGIPTGFTELDRMTSGFQRSDLIIVAARPSVGKTAF   219
EcDnaB   NIADVLDATVARIEQLFQQPHDGVTGVNTGYDDLNKKTAGLQPSDLIIVAARPSMGKTTF   240
          ** *:*   * .** :::  .  :**: **: *:: *:*:* **********:***.*

BstDnaB  ALNIAQNVATKTNENVAIFSLEMSAQQLVMRMLCAEGNINAQNLRTGKLTPEDWGKLTMA   279
EcDnaB   AMNLVENAAMLQDKPVLIFSLEMPSEQIMMRSLASLSRVDQTKIRTGQLDDEDWARISGT   300
          *:*::*.*   :: * ****** ::*::** *.: ..:: ::***:*  ***.::: :

BstDnaB  MGSLS-NAGIYIDDTPSIRVSDIRAKCRRLKQ-ESGLGMIVIDYLQLIQGSGRSKENRQQ   337
EcDnaB   MGILLEKRNIYIDDSSGLTPTEVRSRARRIAREHGGIGLIMIDYLQLMRVPAL-SDNRTL   359
          ** *   :  *****: .: :::*::.**: :  ..*:*:*:******:: .   .:**

BstDnaB  EVSEISRSLKALARELEVPVIALSQLSRSVEQRQDKRPMMSDIRESGSIEQDADIVAFLY   397
EcDnaB   EIAEISRSLKALAKELNVPVVALSQLNRSLEQRADKRPVNSDLRESGSIEQDADLIMFIY   419
          *::*********:**:**.***:*****.**:*** ****: **:***********:: *:*

BstDnaB  RDDYYNKDSENKNIIEIIIAKQRNGPVGTVQLAFIKEYNKFVNLERRFDEAQIPPGA   454
EcDnaB   RDEVYHENSDLKGIAEIIIGKQRNGPIGTVRLTFNGQWSRFDNYAGPQYDDE-----   471
          **: *.::*: * * **** .******:***:*:*  ::.:* *      : :
```

Figure A.1 The mutation of the *dnaB107*^{ts} allele is located close to the linker domain
BLAST alignment of *B. stearothermophilus* DnaB (Uniprot: P0ACB0) and *E. coli* DnaB (Uniprot: Q9X4C9). The linker domain of *Bst*DnaB is highlighted in yellow. The position of the G206A mutation in the *E. coli dnaB107*^{ts} allele is highlighted in red.

A

```
Rep   ------------------------------------------------------------
UvrD  ------------------------------------------------------------
HelD  MELKATTLGKRLAQHPYDRAVILNAGIKVSGDRHEYLIPFNQLLAIHCKRGLVWGELEFV   60


Rep   ------------------------------------------------------------
UvrD  ------------------------------------------------------------
HelD  LPDEKVVRLHGTEWGETQRFYHHLDAHWRRWSGEMSEIASGVLRQQLDLIATRTGENKWL  120


Rep   ------------------------------------------------------------
UvrD  ------------------------------------------------------------
HelD  TREQTSGVQQQIRQALSALPLPVNRLEEFDNCREAWRKCQAWLKDIESARLQHNQAYTEA  180


Rep   --------------MRLNPGQQQAVEFVTGPCLVLAGAGSGKTRVITNKIAHLIRGCYQ    46
UvrD  -------MDVSYLLDSLNDKQREAVAAPRSNLLVLAGAGSGKTRVLVHRIAWLMSVENCS    53
HelD  MLTEYADFFRQVESSPLNPAQARAVVNGEHSLLVLAGAGSGKTSVLVARAGWLLARGEAS   240
                  **   *  .**       **********  *:. : . *:      .

Rep   ARHIAAVTFTNKAAREMKERVGQTLGRKEARGLMISTFHTLGLDIIKREYAALGMKANFS   106
UvrD  PYSIMAVTFTNKAAAEMRHRIGQLMGTSQ-GGMWVGTFHGLAHRLLRAHHMDANLPQDFQ   112
HelD  PEQILLLAFGRKAAEEMDERIRERLHTED---ITARTFHALALHIIQQGSKKVPIVSKLE   297
          *  ::* .*** ** .*: : : .:   :    *** *. :::       :  .:.

Rep   --------LFD—DTDQLA-----------------LLKELTEGLIEDDKVLLQQLISTIS   140
UvrD  --------ILD—SEDQLR-----------------LLKRLIKAMNLDEKQWPPR----QA   142
HelD  NDTAARHELFIAEWRKQCSEKKAQAKGWRQWLTEEMQWSVPEGNFWDDEKLQRRLASRLD   357
                ::      .*              :     : :. *:: :

Rep   NWKNDLKTP----SQAAASAIGERDRI-------FAHCYGLYDAHLKACNVLDFDDLILL   189
UvrD  MWYINSQKDEGLRPHHIQSYGNPVEQT-------WQKVYQAYQEACDRAGLVDFAELLLR   195
HelD  RWVSLMRMHGGAQAEMIASAPEEIRDLFSKRIKLMAPLLKAWKGALKAENAVDFSGLIHQ   417
       *      :     .   *           :.  .     :** *:

Rep   PTLLLQRNEEVRKRWQNKIRYLLVDEYQDTNTSQYELVKLLVG—-SRARFTVVGDDDQSI   247
UvrD  AHELWLNKPHILQHYRERFTNILVDEFQDTNNIQYAWIRLLAG—-DTGKVMIVGDDDQSI   253
HelD  AIVILEKG-----RFISPWKHILVDEFQDISPQRAALLAALRKQNSQTTLFAVGDDWQAI   472
       :  .          :: .   :****:** . :   : *    .   .   **** *:*

Rep   YSWRGARPQNLVLLSQDFPALKVIKLEQNYRSSGRILKAANILIANNPHVFEKRLFSELG   307
UvrD  YGWRGAQVENIQRFLNDFPGAETIRLEQNYRSTSNILSAANALIENNNGRLGKKLWTDGA   313
HelD  YRFSGAQMSLTTAFHENFGEGERCDLDTTYRFNSRIGEVANRFIQQNPGQLKKPLNSLTN   532
       * : **: .   : ::*   :   *: .** ...* ..** :* :*   : * * :

Rep   YGAE-LKVLSANNEEHEAERVTGELIAHHFVNKTQYKDYAILYRGNHQSRVFEKFLMQNR   366
UvrD  DGEP-ISLYCAFNELDEARFVVNR-IKTWQDNGGALAECAILYRSNAQSRVLEEALLQAS   371
HelD  GDKKAVTLLDE-SQLD---ALLDKLSG----YAKPEERILILARYHHM------------   572
       :.:    .:.  :     . * ** *  .

Rep   IPYKISGGTSFFSRPEIKDLLAYLRVLTNPDDDSAFLRIVNTPKREIGPATLKKLGEWAM   426
UvrD  MPYRIYGGMRFFERQEIKDALSYLRLIANRNDDAAFERVVNTPTRGIGDRTLDVVRQTSR   431
HelD  RPA---------------------------------------------------------   575
       *

Rep   TRNKSMFTASFDMGLSQTLSGRGYEALTRFTHWLAEIQRLAEREPIAAVRDLIHGMDYES   486
UvrD  DRQLTLWQACRELLQEKALAGRAASALQRFMELIDALAQETADMPLHVQTDRVIKDSGLR   491
HelD  ------------------------------------------------------------


Rep   WLYETSPSPKAAEMRMKNVNQLFSWMTEMLEGSELDEPMTLTQVVTRFTLRDMMERGES-   544
UvrD  TMYEQEKGE-KGQTRIENLEELVTATRQFSYNEEDEDLMPLQA----FLSHAALEAGEGQ   546
HelD  ------------------------------------SL--------------EKA   580
                                           *                 *
```

```
Rep   -EEE-LDQVQLMTLHASKGLEFPYVYMVGMEEGFLPHQSS------------IDED-NID 590
UvrD  ADTW-QDAVQLMTLHSAKGLEFPQVFIVGMEEGMFPSQMS------------LDEGGRLE 593
HelD  ATRWPKLQIDFMTIHASKGQQADYVIIVGLQEGSDGFPAAARESIMEEALLPPVEDFPDA 640
      :       :::**:*::**  :    * :**::**       :              *

Rep   EERRLAYVGITRAQKELTFTLCKERRQYGELVRPEPSRFLLELPQDDLIWEQERKVVSAE 650
UvrD  EERRLAYVGVTRAMQKLTLTYAETRRLYGKEVYHRPSRFIGELPEECVEEVRLRATVSRP 653
HelD  EERRLMYVALTRARHRVWALFN---------KENPSPFVEILKNLDVPVARKP------ 684
      ***** **.:*** :.:                  .** *:   * :   :    :

Rep   ERMQK-GQSHLANLKAM------MAAKRGK------------------------------ 673
UvrD  VSHQRMGTPMVENDSGYKLGQRVRHAKFGEGTIVNMEGSGEHSRLQVAFQGQGIKWLVAA 713
HelD  ------------------------------------------------------------

Rep   -------
UvrD  YARLESV 720
HelD  -------
```

B
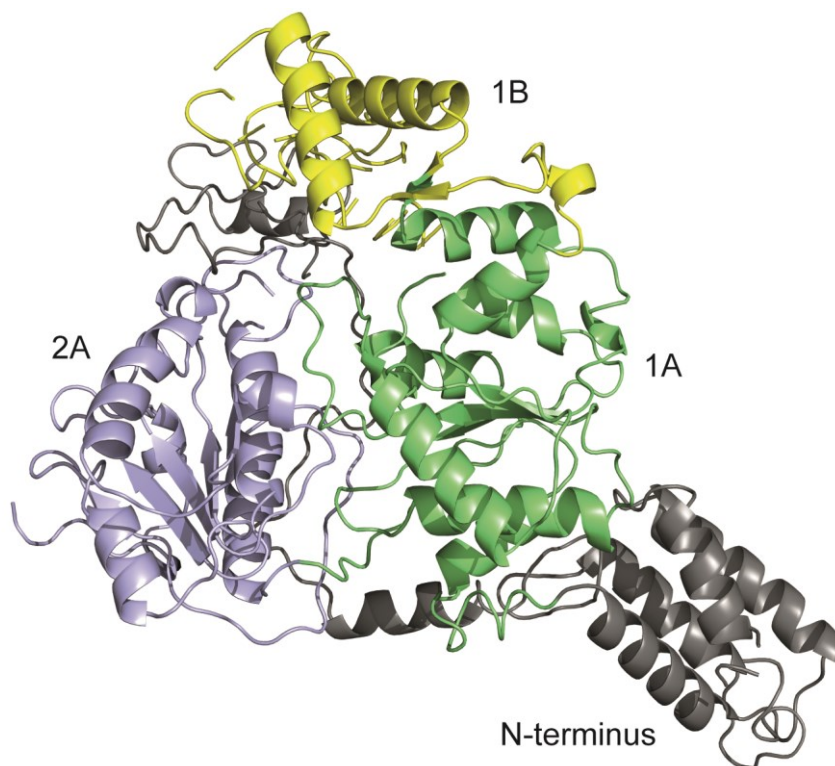
Figure A.2 *E. coli* HelD does not contain a 2B subdomain
(A) BLAST alignment of *E. coli* Rep (Uniprot P099080), *E. coli* UvrD (P03018) and *E. coli* HelD (P15038).
Rep and UvrD 2B subdomains in red. Identical residues are marked with an asterisk while conserved
substitutions are marked with a colon and semi-conserved substitutions are marked with one dot.
(B) Structure prediction of HelD generated using Phyre2 (Kelley & Sternberg, 2009). 87% of residues
modelled at >90% confidence. Highest confidence for the 1A (green), 1B (yellow) and 2A (blue)
subdomains. The N-terminal extension is labelled in grey.

A.6 List of Abbreviations

::	insertion
Δ	deletion
A	absorbance
AA	amino acid
Ap	ampicillin
ARS	autonomous replication sequence
APS	ammonium persulphate
ATP	adenosine triphosphate
bp	base pair(s)
Bq	Becquerel
BSA	bovine serum albumin
cfu	colony forming unit
CIP	calf intestine alkaline phosphatase
Cm	chloramphenicol
CTP	cytosine triphosphate
CV	column volume
DMSO	dimethyl sulfoxide
DNA	deoxynucleotide acid
DTT	dithiothreitol
FRET	Förster resonance energy transfer
FRT	FLP recognition target
dH_2O	deionised water
dNTP	deoxyribonucleotide
ds	double-stranded
DTT	dithiothreitol
EDTA	ethylenediaminetetraacetic acid
EMSA	electrophoretic mobility shift assay
et al.	et alia (and others)
g	gram(s)
GLB	gel loading buffer
GTP	guanosine-5'-triphosphate
h	hour(s)
HEPES	2-[4-(2-hydroxyethyl)piperazin-1-yl]ethanesulfonic acid
IHF	integration host factor
IPTG	isopropyl β-D-1-thiogalactopyranoside
kb	kilobase(s)
K_d	dissociation constant
Kn	kanamycin
LB	lysogeny broth
MA	minimal agar (56/2 salts with vitamin B_1, glucose and 1.5% agar)

MM	minimal medium (56/2 salts with vitamin B$_1$, glucose)
min	minute(s)
MMR	methyl-directed mismatch repair
NA	nucleic acid (DNA or RNA)
NER	nucleotide excision repair
nt	nucleotide(s)
NTP	nucleoside triphosphate
ORC	origin recognition complex
PAA	polyacrylamide
PAGE	polyacrylamide gel electrophoresis
PCR	polymerase chain reaction
pfu	plaque forming unit
^{r}	conferring resistance to an antibiotic
RNA	ribonucleic acid
rpm	rounds per minute
s	second(s)
SA	streptavidin
ss	single-stranded
SDM	site directed mutagenesis
SDS	sodium dodecyl sulphate
SF	Superfamily (classification of helicases)
sm	single molecule
SSC	saline sodium citrate
TBE	Tris-borate-EDTA
TCR	transcription-coupled repair
TEMED	tetramethylethylenediamine
Tris	tris(hydroxymethyl)methylamine
U	unit
UTP	uridine-5'-triphosphate
UV	ultra violet
v/v	volume per volume
w/v	weight per volume
X-gal	5-bromo-4-chloro-3-indolyl-β-D-galactopyranoside

References

Abarzua P, Soeller W, Marians KJ (1984) Mutational analysis of primosome assembly sites. I. Distinct classes of mutants in the pBR322 Escherichia coli factor Y DNA effector sequences. *J Biol Chem* **259:** 14286-14292

Ahn JS, Osman F, Whitby MC (2005) Replication fork blockage by RTS1 at an ectopic site promotes recombination in fission yeast. *EMBO J* **24:** 2011-2023

Ali Azam T, Iwata A, Nishimura A, Ueda S, Ishihama A (1999) Growth phase-dependent variation in protein composition of the Escherichia coli nucleoid. *J Bacteriol* **181:** 6361-6370

Ali JA, Lohman TM (1997) Kinetic measurement of the step size of DNA unwinding by Escherichia coli UvrD helicase. *Science* **275:** 377-380

Alting-Mees MA, Short JM (1989) pBluescript II: gene mapping vectors. *Nucleic Acids Res* **17:** 9494

Alzu A, Bermejo R, Begnis M, Lucca C, Piccini D, Carotenuto W, Saponaro M, Brambati A, Cocito A, Foiani M, Liberi G (2012) Senataxin associates with replication forks to protect fork integrity across RNA-polymerase-II-transcribed genes. *Cell* **151:** 835-846

Amundsen SK, Taylor AF, Reddy M, Smith GR (2007) Intersubunit signaling in RecBCD enzyme, a complex protein machine regulated by Chi hot spots. *Genes Dev* **21:** 3296-3307

Amundsen SK, Taylor AF, Smith GR (2000) The RecD subunit of the Escherichia coli RecBCD enzyme inhibits RecA loading, homologous recombination, and DNA repair. *Proc Natl Acad Sci U S A* **97:** 7399-7404

Anand SP, Zheng H, Bianco PR, Leuba SH, Khan SA (2007) DNA helicase activity of PcrA is not required for the displacement of RecA protein from DNA or inhibition of RecA-mediated strand exchange. *J Bacteriol* **189:** 4502-4509

Arias-Palomo E, O'Shea VL, Hood IV, Berger JM (2013) The Bacterial DnaC Helicase Loader Is a DnaB Ring Breaker. *Cell* **153:** 438-448

Atkinson J (2007) Regulation of the E. coli replicative helicase DnaB by the helicase loader DnaC. PhD Thesis, Institute of Medical Sciences, University of Aberdeen, Aberdeen

Atkinson J, Gupta MK, McGlynn P (2011a) Interaction of Rep and DnaB on DNA. *Nucleic Acids Res* **39:** 1351-1359

Atkinson J, Gupta MK, Rudolph CJ, Bell H, Lloyd RG, McGlynn P (2011b) Localization of an accessory helicase at the replisome is critical in sustaining efficient genome duplication. *Nucleic Acids Res* **39:** 949-957

Atkinson J, Guy CP, Cadman CJ, Moolenaar GF, Goosen N, McGlynn P (2009) Stimulation of UvrD helicase by UvrAB. *J Biol Chem* **284:** 9612-9623

Atkinson J, McGlynn P (2009) Replication fork reversal and the maintenance of genome stability. *Nucleic Acids Res* **37:** 3475-3492

Azvolinsky A, Dunaway S, Torres JZ, Bessler JB, Zakian VA (2006) The S. cerevisiae Rrm3p DNA helicase moves with the replication fork and affects replication of all yeast chromosomes. *Genes Dev* **20:** 3104-3116

Azvolinsky A, Giresi PG, Lieb JD, Zakian VA (2009) Highly transcribed RNA polymerase II genes are impediments to replication fork progression in Saccharomyces cerevisiae. *Mol Cell* **34:** 722-734

Bachmann BJ (1996) Derivations and Genotypes of Some Mutant Derivatives of *Escherichia coli* K-12. In *Escherichia coli and Salmonella cellular and molecular biology*, F.C. Neidhardt RCI, J.L. Ingraham,

References

E.C.C. Lin, K.B. Low, B. Magasanik, W.S., Reznikoff MR, M. Schaechter, and H.E. Umbarger (eds), pp 2460-2488. Washington, DC: ASM Press

Baharoglu Z, Bradley AS, Le Masson M, Tsaneva I, Michel B (2008) ruvA Mutants that resolve Holliday junctions but do not reverse replication forks. *PLoS Genet* **4:** e1000012

Baharoglu Z, Lestini R, Duigou S, Michel B (2010) RNA polymerase mutations that facilitate replication progression in the rep uvrD recF mutant lacking two accessory replicative helicases. *Mol Microbiol* **77:** 324-336

Bailey S, Eliason WK, Steitz TA (2007) Structure of hexameric DnaB helicase and its complex with a domain of DnaG primase. *Science* **318:** 459-463

Barcena M, Ruiz T, Donate LE, Brown SE, Dixon NE, Radermacher M, Carazo JM (2001) The DnaB.DnaC complex: a structure based on dimers assembled around an occluded channel. *EMBO J* **20:** 1462-1468

Bedinger P, Hochstrasser M, Jongeneel CV, Alberts BM (1983) Properties of the T4 bacteriophage DNA replication apparatus: the T4 dda DNA helicase is required to pass a bound RNA polymerase molecule. *Cell* **34:** 115-123

Bell SP, Stillman B (1992) ATP-dependent recognition of eukaryotic origins of DNA replication by a multiprotein complex. *Nature* **357:** 128-134

Bernhardt TG, de Boer PA (2004) Screening for synthetic lethal mutants in Escherichia coli and identification of EnvC (YibP) as a periplasmic septal ring factor with murein hydrolase activity. *Mol Microbiol* **52:** 1255-1269

Bertani G (1951) Studies on lysogenesis. I. The mode of phage liberation by lysogenic Escherichia coli. *J Bacteriol* **62:** 293-300

Bessler JB, Torredagger JZ, Zakian VA (2001) The Pif1p subfamily of helicases: region-specific DNA helicases? *Trends Cell Biol* **11:** 60-65

Bianco PR, Kowalczykowski SC (1997) The recombination hotspot Chi is recognized by the translocating RecBCD enzyme as the single strand of DNA containing the sequence 5'-GCTGGTGG-3'. *Proc Natl Acad Sci U S A* **94:** 6706-6711

Bird LE, Subramanya HS, Wigley DB (1998) Helicases: a unifying structural theme? *Curr Opin Struct Biol* **8:** 14-18

Biswas EE, Biswas SB (1999) Mechanism of DnaB helicase of Escherichia coli: structural domains involved in ATP hydrolysis, DNA binding, and oligomerization. *Biochemistry* **38:** 10919-10928

Biswas SB, Flowers S, Biswas-Fiss EE (2004) Quantitative analysis of nucleotide modulation of DNA binding by DnaC protein of Escherichia coli. *Biochem J* **379:** 553-562

Boehmer PE, Emmerson PT (1992) The RecB subunit of the Escherichia coli RecBCD enzyme couples ATP hydrolysis to DNA unwinding. *J Biol Chem* **267:** 4981-4987

Bolivar F, Rodriguez RL, Greene PJ, Betlach MC, Heyneker HL, Boyer HW, Crosa JH, Falkow S (1977) Construction and characterization of new cloning vehicles. II. A multipurpose cloning system. *Gene* **2:** 95-113

Boubakri H, de Septenville AL, Viguera E, Michel B (2010) The helicases DinG, Rep and UvrD cooperate to promote replication across transcription units in vivo. *EMBO J* **29:** 145-157

Bramhill D, Kornberg A (1988) Duplex opening by dnaA protein at novel sequences in initiation of replication at the origin of the E. coli chromosome. *Cell* **52:** 743-755

References

Brendza KM, Cheng W, Fischer CJ, Chesnik MA, Niedziela-Majka A, Lohman TM (2005) Autoinhibition of Escherichia coli Rep monomer helicase activity by its 2B subdomain. *Proc Natl Acad Sci U S A* **102:** 10076-10081

Brennan CA, Steinmetz EJ, Spear P, Platt T (1990) Specificity and efficiency of rho-factor helicase activity depends on magnesium concentration and energy coupling to NTP hydrolysis. *J Biol Chem* **265:** 5440-5447

Brewer BJ (1988) When polymerases collide: replication and the transcriptional organization of the E. coli chromosome. *Cell* **53:** 679-686

Brewer BJ, Fangman WL (1988) A replication fork barrier at the 3' end of yeast ribosomal RNA genes. *Cell* **55:** 637-643

Brown PO, Cozzarelli NR (1979) A sign inversion mechanism for enzymatic supercoiling of DNA. *Science* **206:** 1081-1083

Bruand C, Ehrlich SD (2000) UvrD-dependent replication of rolling-circle plasmids in Escherichia coli. *Mol Microbiol* **35:** 204-210

Budd ME, Reis CC, Smith S, Myung K, Campbell JL (2006) Evidence suggesting that Pif1 helicase functions in DNA replication with the Dna2 helicase/nuclease and DNA polymerase delta. *Mol Cell Biol* **26:** 2490-2500

Bujalowski W, Klonowska MM, Jezewska MJ (1994) Oligomeric structure of Escherichia coli primary replicative helicase DnaB protein. *J Biol Chem* **269:** 31350-31358

Byrd AK, Matlock DL, Bagchi D, Aarattuthodiyil S, Harrison D, Croquette V, Raney KD (2012) Dda helicase tightly couples translocation on single-stranded DNA to unwinding of duplex DNA: Dda is an optimally active helicase. *J Mol Biol* **420:** 141-154

Byrd AK, Raney KD (2004) Protein displacement by an assembly of helicase molecules aligned along single-stranded DNA. *Nat Struct Mol Biol* **11:** 531-538

Byrd AK, Raney KD (2005) Increasing the length of the single-stranded overhang enhances unwinding of duplex DNA by bacteriophage T4 Dda helicase. *Biochemistry* **44:** 12990-12997

Byrd AK, Raney KD (2006) Displacement of a DNA binding protein by Dda helicase. *Nucleic Acids Res* **34:** 3020-3029

Calendar R, Lindqvist B, Sironi G, Clark AJ (1970) Characterization of REP- mutants and their interaction with P2 phage. *Virology* **40:** 72-83

Carl PL (1970) Escherichia coli mutants with temperature-sensitive synthesis of DNA. *Mol Gen Genet* **109:** 107-122

Caruthers JM, McKay DB (2002) Helicase structure and mechanism. *Curr Opin Struct Biol* **12:** 123-133

Centore RC, Leeson MC, Sandler SJ (2009) UvrD303, a hyperhelicase mutant that antagonizes RecA-dependent SOS expression by a mechanism that depends on its C terminus. *J Bacteriol* **191:** 1429-1438

Chandler M, Bird RE, Caro L (1975) The replication time of the Escherichia coli K12 chromosome as a function of cell doubling time. *J Mol Biol* **94:** 127-132

Chang P, Marians KJ (2000) Identification of a region of Escherichia coli DnaB required for functional interaction with DnaG at the replication fork. *J Biol Chem* **275:** 26187-26195

Chaudhury AM, Smith GR (1984) A new class of Escherichia coli recBC mutants: implications for the role of RecBC enzyme in homologous recombination. *Proc Natl Acad Sci U S A* **81:** 7850-7854

References

Chen C, Natale DA, Finn RD, Huang H, Zhang J, Wu CH, Mazumder R (2011) Representative proteomes: a stable, scalable and unbiased proteome set for sequence analysis and functional annotation. *PLoS One* **6:** e18910

Cheng W, Brendza KM, Gauss GH, Korolev S, Waksman G, Lohman TM (2002) The 2B domain of the Escherichia coli Rep protein is not required for DNA helicase activity. *Proc Natl Acad Sci U S A* **99:** 16006-16011

Cheng W, Hsieh J, Brendza KM, Lohman TM (2001) E. coli Rep oligomers are required to initiate DNA unwinding in vitro. *J Mol Biol* **310:** 327-350

Chuang RY, Weaver PL, Liu Z, Chang TH (1997) Requirement of the DEAD-Box protein ded1p for messenger RNA translation. *Science* **275:** 1468-1471

Churchill JJ, Anderson DG, Kowalczykowski SC (1999) The RecBC enzyme loads RecA protein onto ssDNA asymmetrically and independently of chi, resulting in constitutive recombination activation. *Genes Dev* **13:** 901-911

Clerici M, Mourao A, Gutsche I, Gehring NH, Hentze MW, Kulozik A, Kadlec J, Sattler M, Cusack S (2009) Unusual bipartite mode of interaction between the nonsense-mediated decay factors, UPF1 and UPF2. *EMBO J* **28:** 2293-2306

Colavito S, Prakash R, Sung P (2010) Promotion and regulation of homologous recombination by DNA helicases. *Methods* **51:** 329-335

Company M, Arenas J, Abelson J (1991) Requirement of the RNA helicase-like protein PRP22 for release of messenger RNA from spliceosomes. *Nature* **349:** 487-493

Cordin O, Banroques J, Tanner NK, Linder P (2006) The DEAD-box protein family of RNA helicases. *Gene* **367:** 17-37

Cox MM, Lehman IR (1981) Directionality and polarity in recA protein-promoted branch migration. *Proc Natl Acad Sci U S A* **78:** 6018-6022

Cox MM, Lehman IR (1982) recA protein-promoted DNA strand exchange. Stable complexes of recA protein and single-stranded DNA formed in the presence of ATP and single-stranded DNA binding protein. *J Biol Chem* **257:** 8523-8532

Cox MM, Soltis DA, Lehman IR, DeBrosse C, Benkovic SJ (1983) ADP-mediated dissociation of stable complexes of recA protein and single-stranded DNA. *J Biol Chem* **258:** 2586-2592

Crampton DJ, Guo S, Johnson DE, Richardson CC (2004) The arginine finger of bacteriophage T7 gene 4 helicase: role in energy coupling. *Proc Natl Acad Sci U S A* **101:** 4373-4378

Crooks GE, Hon G, Chandonia JM, Brenner SE (2004) WebLogo: a sequence logo generator. *Genome Res* **14:** 1188-1190

Dallmann HG, Kim S, Pritchard AE, Marians KJ, McHenry CS (2000) Characterization of the unique C terminus of the Escherichia coli tau DnaX protein. Monomeric C-tau binds alpha AND DnaB and can partially replace tau in reconstituted replication forks. *J Biol Chem* **275:** 15512-15519

Denhardt DT, Dressler DH, Hathaway A (1967) THE ABORTIVE REPLICATION OF PhiX174 DNA IN A RECOMBINATION-DEFICIENT MUTANT OF Escherichia coli. *Proc Natl Acad Sci U S A* **57:** 813-820

Dereeper A, Guignon V, Blanc G, Audic S, Buffet S, Chevenet F, Dufayard JF, Guindon S, Lefort V, Lescot M, Claverie JM, Gascuel O (2008) Phylogeny.fr: robust phylogenetic analysis for the non-specialist. *Nucleic Acids Res* **36:** W465-469

Dillingham MS (2011) Superfamily I helicases as modular components of DNA-processing machines. *Biochem Soc Trans* **39:** 413-423

References

Dillingham MS, Kowalczykowski SC (2008) RecBCD enzyme and the repair of double-stranded DNA breaks. *Microbiol Mol Biol Rev* **72:** 642-671, Table of Contents

Dillingham MS, Spies M, Kowalczykowski SC (2003) RecBCD enzyme is a bipolar DNA helicase. *Nature* **423:** 893-897

Dillingham MS, Wigley DB, Webb MR (2000) Demonstration of unidirectional single-stranded DNA translocation by PcrA helicase: measurement of step size and translocation speed. *Biochemistry* **39:** 205-212

Doetsch PW, Cunningham RP (1990) The enzymology of apurinic/apyrimidinic endonucleases. *Mutat Res* **236:** 173-201

Dutta D, Shatalin K, Epshtein V, Gottesman ME, Nudler E (2011) Linking RNA polymerase backtracking to genome instability in E. coli. *Cell* **146:** 533-543

Eki T, Ishihara T, Katsura I, Hanaoka F (2007) A genome-wide survey and systematic RNAi-based characterization of helicase-like genes in Caenorhabditis elegans. *DNA Res* **14:** 183-199

Elias-Arnanz M, Salas M (1999) Resolution of head-on collisions between the transcription machinery and bacteriophage phi29 DNA polymerase is dependent on RNA polymerase translocation. *EMBO J* **18:** 5675-5682

Enemark EJ, Joshua-Tor L (2006) Mechanism of DNA translocation in a replicative hexameric helicase. *Nature* **442:** 270-275

Epshtein V, Kamarthapu V, McGary K, Svetlov V, Ueberheide B, Proshkin S, Mironov A, Nudler E (2014) UvrD facilitates DNA repair by pulling RNA polymerase backwards. *Nature*

Fairman-Williams ME, Guenther UP, Jankowsky E (2010) SF1 and SF2 helicases: family matters. *Curr Opin Struct Biol* **20:** 313-324

Fay PJ, Johanson KO, McHenry CS, Bambara RA (1981) Size classes of products synthesized processively by DNA polymerase III and DNA polymerase III holoenzyme of Escherichia coli. *J Biol Chem* **256:** 976-983

Flores MJ, Bierne H, Ehrlich SD, Michel B (2001) Impairment of lagging strand synthesis triggers the formation of a RuvABC substrate at replication forks. *EMBO J* **20:** 619-629

French S (1992) Consequences of replication fork movement through transcription units in vivo. *Science* **258:** 1362-1365

Fu YV, Yardimci H, Long DT, Ho TV, Guainazzi A, Bermudez VP, Hurwitz J, van Oijen A, Scharer OD, Walter JC (2011) Selective bypass of a lagging strand roadblock by the eukaryotic replicative DNA helicase. *Cell* **146:** 931-941

Fugger K, Mistrik M, Danielsen JR, Dinant C, Falck J, Bartek J, Lukas J, Mailand N (2009) Human Fbh1 helicase contributes to genome maintenance via pro- and anti-recombinase activities. *J Cell Biol* **186:** 655-663

Fujiwara Y, Tatsumi M (1976) Replicative bypass repair of ultraviolet damage to DNA of mammalian cells: caffeine sensitive and caffeine resistant mechanisms. *Mutat Res* **37:** 91-110

Futami K, Shimamoto A, Furuichi Y (2007) Mitochondrial and nuclear localization of human Pif1 helicase. *Biol Pharm Bull* **30:** 1685-1692

Galletto R, Jezewska MJ, Bujalowski W (2003) Interactions of the Escherichia coli DnaB helicase hexamer with the replication factor the DnaC protein. Effect of nucleotide cofactors and the ssDNA on protein-protein interactions and the topology of the complex. *J Mol Biol* **329:** 441-465

References

Galletto R, Jezewska MJ, Bujalowski W (2004a) Unzipping mechanism of the double-stranded DNA unwinding by a hexameric helicase: quantitative analysis of the rate of the dsDNA unwinding, processivity and kinetic step-size of the Escherichia coli DnaB helicase using rapid quench-flow method. *J Mol Biol* **343:** 83-99

Galletto R, Jezewska MJ, Bujalowski W (2004b) Unzipping mechanism of the double-stranded DNA unwinding by a hexameric helicase: the effect of the 3' arm and the stability of the dsDNA on the unwinding activity of the Escherichia coli DnaB helicase. *J Mol Biol* **343:** 101-114

Galletto R, Maillard R, Jezewska MJ, Bujalowski W (2004c) Global conformation of the Escherichia coli replication factor DnaC protein in absence and presence of nucleotide cofactors. *Biochemistry* **43:** 10988-11001

Gautam A, Mulugu S, Alexander K, Bastia D (2001) A single domain of the replication termination protein of Bacillus subtilis is involved in arresting both DnaB helicase and RNA polymerase. *J Biol Chem* **276:** 23471-23479

Gefter ML, Hirota Y, Kornberg T, Wechsler JA, Barnoux C (1971) Analysis of DNA polymerases II and 3 in mutants of Escherichia coli thermosensitive for DNA synthesis. *Proc Natl Acad Sci U S A* **68:** 3150-3153

Gellert M, Mizuuchi K, O'Dea MH, Nash HA (1976) DNA gyrase: an enzyme that introduces superhelical turns into DNA. *Proc Natl Acad Sci U S A* **73:** 3872-3876

George JW, Brosh RM, Jr., Matson SW (1994) A dominant negative allele of the Escherichia coli uvrD gene encoding DNA helicase II. A biochemical and genetic characterization. *J Mol Biol* **235:** 424-435

George T, Wen Q, Griffiths R, Ganesh A, Meuth M, Sanders CM (2009) Human Pif1 helicase unwinds synthetic DNA structures resembling stalled DNA replication forks. *Nucleic Acids Res* **37:** 6491-6502

Gilbert W, Muller-Hill B (1967) The lac operator is DNA. *Proc Natl Acad Sci U S A* **58:** 2415-2421

Gilchrist CA, Denhardt DT (1987) Escherichia coli rep gene: sequence of the gene, the encoded helicase, and its homology with uvrD. *Nucleic Acids Res* **15:** 465-475

Gilhooly NS, Gwynn EJ, Dillingham MS (2013) Superfamily 1 helicases. *Front Biosci (Schol Ed)* **5:** 206-216

Glover BP, McHenry CS (1998) The chi psi subunits of DNA polymerase III holoenzyme bind to single-stranded DNA-binding protein (SSB) and facilitate replication of an SSB-coated template. *J Biol Chem* **273:** 23476-23484

Gorbalenya AE, Koonin EV (1993) Helicases: Amino acid sequence comparisons and structure-function relationships. *Current Opinion in Structural Biology* **3:** 419-429

Gore J, Bryant Z, Stone MD, Nollmann M, Cozzarelli NR, Bustamante C (2006) Mechanochemical analysis of DNA gyrase using rotor bead tracking. *Nature* **439:** 100-104

Green NM (1990) Avidin and streptavidin. *Methods Enzymol* **184:** 51-67

Guenther UP, Handoko L, Laggerbauer B, Jablonka S, Chari A, Alzheimer M, Ohmer J, Plottner O, Gehring N, Sickmann A, von Au K, Schuelke M, Fischer U (2009) IGHMBP2 is a ribosome-associated helicase inactive in the neuromuscular disorder distal SMA type 1 (DSMA1). *Hum Mol Genet* **18:** 1288-1300

Gupta MK, Atkinson J, McGlynn P (2010) DNA structure specificity conferred on a replicative helicase by its loader. *J Biol Chem* **285:** 979-987

Gupta MK, Guy CP, Yeeles JT, Atkinson J, Bell H, Lloyd RG, Marians KJ, McGlynn P (2013) Protein-DNA complexes are the primary sources of replication fork pausing in Escherichia coli. *Proc Natl Acad Sci U S A* **110:** 7252-7257

References

Guy CP, Atkinson J, Gupta MK, Mahdi AA, Gwynn EJ, Rudolph CJ, Moon PB, van Knippenberg IC, Cadman CJ, Dillingham MS, Lloyd RG, McGlynn P (2009) Rep provides a second motor at the replisome to promote duplication of protein-bound DNA. *Mol Cell* **36:** 654-666

Guyer MS, Reed RR, Steitz JA, Low KB (1981) Identification of a sex-factor-affinity site in E. coli as gamma delta. *Cold Spring Harb Symp Quant Biol* **45 Pt 1:** 135-140

Guzman LM, Belin D, Carson MJ, Beckwith J (1995) Tight regulation, modulation, and high-level expression by vectors containing the arabinose PBAD promoter. *J Bacteriol* **177:** 4121-4130

Gwynn EJ, Smith AJ, Guy CP, Savery NJ, McGlynn P, Dillingham MS (2013) The Conserved C-Terminus of the PcrA/UvrD Helicase Interacts Directly with RNA Polymerase. *PLoS One* **8:** e78141

Ha T, Rasnik I, Cheng W, Babcock HP, Gauss GH, Lohman TM, Chu S (2002) Initiation and re-initiation of DNA unwinding by the Escherichia coli Rep helicase. *Nature* **419:** 638-641

Hall MC, Matson SW (1997) Mutation of a highly conserved arginine in motif IV of Escherichia coli DNA helicase II results in an ATP-binding defect. *J Biol Chem* **272:** 18614-18620

Hanahan D (1983) Studies on transformation of Escherichia coli with plasmids. *J Mol Biol* **166:** 557-580

He X, Byrd AK, Yun MK, Pemble CWt, Harrison D, Yeruva L, Dahl C, Kreuzer KN, Raney KD, White SW (2012) The T4 phage SF1B helicase Dda is structurally optimized to perform DNA strand separation. *Structure* **20:** 1189-1200

Heller RC, Marians KJ (2005a) The disposition of nascent strands at stalled replication forks dictates the pathway of replisome loading during restart. *Mol Cell* **17:** 733-743

Heller RC, Marians KJ (2005b) Unwinding of the nascent lagging strand by Rep and PriA enables the direct restart of stalled replication forks. *J Biol Chem* **280:** 34143-34151

Heller RC, Marians KJ (2006) Replication fork reactivation downstream of a blocked nascent leading strand. *Nature* **439:** 557-562

Heller RC, Marians KJ (2007) Non-replicative helicases at the replication fork. *DNA Repair (Amst)* **6:** 945-952

Helmrich A, Ballarino M, Nudler E, Tora L (2013) Transcription-replication encounters, consequences and genomic instability. *Nat Struct Mol Biol* **20:** 412-418

Hiasa H, Marians KJ (1994) Primase couples leading- and lagging-strand DNA synthesis from oriC. *J Biol Chem* **269:** 6058-6063

Higgins NP, Kato K, Strauss B (1976) A model for replication repair in mammalian cells. *J Mol Biol* **101:** 417-425

Hodgman TC (1988) A new superfamily of replicative proteins. *Nature* **333:** 22-23

Holliday R (1964) A mechanism for gene conversion in fungi. *Genet. Res.* **5:** 282-304

Hotchkiss RD (1974) Models of genetic recombination. *Annu Rev Microbiol* **28:** 445-468

Hwang DS, Kornberg A (1992) Opening of the replication origin of Escherichia coli by DnaA protein with protein HU or IHF. *J Biol Chem* **267:** 23083-23086

Ideue T, Sasaki YT, Hagiwara M, Hirose T (2007) Introns play an essential role in splicing-dependent formation of the exon junction complex. *Genes Dev* **21:** 1993-1998

Ilyina TV, Gorbalenya AE, Koonin EV (1992) Organization and evolution of bacterial and bacteriophage primase-helicase systems. *J Mol Evol* **34:** 351-357

References

Iordanescu S (1993) Characterization of the Staphylococcus aureus chromosomal gene pcrA, identified by mutations affecting plasmid pT181 replication. *Mol Gen Genet* **241:** 185-192

Itsathitphaisarn O, Wing RA, Eliason WK, Wang J, Steitz TA (2012) The Hexameric Helicase DnaB Adopts a Nonplanar Conformation during Translocation. *Cell* **151:** 267-277

Ivessa AS, Lenzmeier BA, Bessler JB, Goudsouzian LK, Schnakenberg SL, Zakian VA (2003) The Saccharomyces cerevisiae helicase Rrm3p facilitates replication past nonhistone protein-DNA complexes. *Mol Cell* **12:** 1525-1536

Ivessa AS, Zhou JQ, Schulz VP, Monson EK, Zakian VA (2002) Saccharomyces Rrm3p, a 5' to 3' DNA helicase that promotes replication fork progression through telomeric and subtelomeric DNA. *Genes Dev* **16:** 1383-1396

Iwasaki H, Takahagi M, Nakata A, Shinagawa H (1992) Escherichia coli RuvA and RuvB proteins specifically interact with Holliday junctions and promote branch migration. *Genes Dev* **6:** 2214-2220

Iwasaki H, Takahagi M, Shiba T, Nakata A, Shinagawa H (1991) Escherichia coli RuvC protein is an endonuclease that resolves the Holliday structure. *EMBO J* **10:** 4381-4389

Jankowsky E, Gross CH, Shuman S, Pyle AM (2001) Active disruption of an RNA-protein interaction by a DExH/D RNA helicase. *Science* **291:** 121-125

Jezewska MJ, Rajendran S, Bujalowska D, Bujalowski W (1998a) Does single-stranded DNA pass through the inner channel of the protein hexamer in the complex with the Escherichia coli DnaB Helicase? Fluorescence energy transfer studies. *J Biol Chem* **273:** 10515-10529

Jezewska MJ, Rajendran S, Bujalowski W (1998b) Complex of Escherichia coli primary replicative helicase DnaB protein with a replication fork: recognition and structure. *Biochemistry* **37:** 3116-3136

Jia H, Korolev S, Niedziela-Majka A, Maluf NK, Gauss GH, Myong S, Ha T, Waksman G, Lohman TM (2011) Rotations of the 2B sub-domain of E. coli UvrD helicase/translocase coupled to nucleotide and DNA binding. *J Mol Biol* **411:** 633-648

Joo C, Ha T (2012) Labeling Proteins for Single-Molecule FRET. *Cold Spring Harb Protoc* **2012**

Kaplan DL (2000) The 3'-tail of a forked-duplex sterically determines whether one or two DNA strands pass through the central channel of a replication-fork helicase. *J Mol Biol* **301:** 285-299

Kaplan DL, O'Donnell M (2002) DnaB drives DNA branch migration and dislodges proteins while encircling two DNA strands. *Mol Cell* **10:** 647-657

Kelley LA, Sternberg MJ (2009) Protein structure prediction on the Web: a case study using the Phyre server. *Nat Protoc* **4:** 363-371

Khatri GS, MacAllister T, Sista PR, Bastia D (1989) The replication terminator protein of E. coli is a DNA sequence-specific contra-helicase. *Cell* **59:** 667-674

Kim DR, McHenry CS (1996) In vivo assembly of overproduced DNA polymerase III. Overproduction, purification, and characterization of the alpha, alpha-epsilon, and alpha-epsilon-theta subunits. *J Biol Chem* **271:** 20681-20689

Kim JL, Morgenstern KA, Griffith JP, Dwyer MD, Thomson JA, Murcko MA, Lin C, Caron PR (1998) Hepatitis C virus NS3 RNA helicase domain with a bound oligonucleotide: the crystal structure provides insights into the mode of unwinding. *Structure* **6:** 89-100

Kim S, Dallmann HG, McHenry CS, Marians KJ (1996) Coupling of a replicative polymerase and helicase: a tau-DnaB interaction mediates rapid replication fork movement. *Cell* **84:** 643-650

King K, Benkovic SJ, Modrich P (1989) Glu-111 is required for activation of the DNA cleavage center of EcoRI endonuclease. *J Biol Chem* **264:** 11807-11815

References

Kobori JA, Kornberg A (1982) The Escherichia coli dnaC gene product. III. Properties of the dnaB-dnaC protein complex. *J Biol Chem* **257:** 13770-13775

Kogoma T, Cadwell GW, Barnard KG, Asai T (1996) The DNA replication priming protein, PriA, is required for homologous recombination and double-strand break repair. *J Bacteriol* **178:** 1258-1264

Komissarova N, Kashlev M (1997) Transcriptional arrest: Escherichia coli RNA polymerase translocates backward, leaving the 3' end of the RNA intact and extruded. *Proc Natl Acad Sci U S A* **94:** 1755-1760

Kong XP, Onrust R, O'Donnell M, Kuriyan J (1992) Three-dimensional structure of the beta subunit of E. coli DNA polymerase III holoenzyme: a sliding DNA clamp. *Cell* **69:** 425-437

Kornberg A, Scott JF, Bertsch LL (1978) ATP utilization by rep protein in the catalytic separation of DNA strands at a replicating fork. *J Biol Chem* **253:** 3298-3304

Korolev S, Hsieh J, Gauss GH, Lohman TM, Waksman G (1997) Major domain swiveling revealed by the crystal structures of complexes of E. coli Rep helicase bound to single-stranded DNA and ADP. *Cell* **90:** 635-647

Korolev S, Yao N, Lohman TM, Weber PC, Waksman G (1998) Comparisons between the structures of HCV and Rep helicases reveal structural similarities between SF1 and SF2 super-families of helicases. *Protein Sci* **7:** 605-610

Kowalski D, Eddy MJ (1989) The DNA unwinding element: a novel, cis-acting component that facilitates opening of the Escherichia coli replication origin. *EMBO J* **8:** 4335-4344

Krejci L, Van Komen S, Li Y, Villemain J, Reddy MS, Klein H, Ellenberger T, Sung P (2003) DNA helicase Srs2 disrupts the Rad51 presynaptic filament. *Nature* **423:** 305-309

Lahaye A, Stahl H, Thines-Sempoux D, Foury F (1991) PIF1: a DNA helicase in yeast mitochondria. *EMBO J* **10:** 997-1007

Lahue RS, Au KG, Modrich P (1989) DNA mismatch correction in a defined system. *Science* **245:** 160-164

Lambert S, Mizuno K, Blaisonneau J, Martineau S, Chanet R, Freon K, Murray JM, Carr AM, Baldacci G (2010) Homologous recombination restarts blocked replication forks at the expense of genome rearrangements by template exchange. *Mol Cell* **39:** 346-359

Lambert S, Watson A, Sheedy DM, Martin B, Carr AM (2005) Gross chromosomal rearrangements and elevated recombination at an inducible site-specific replication fork barrier. *Cell* **121:** 689-702

Lane HE, Denhardt DT (1975) The rep mutation. IV. Slower movement of replication forks in Escherichia coli rep strains. *J Mol Biol* **97:** 99-112

Lark KG, Wechsler JA (1975) DNA replication in dnaB mutants of Escherichia coli: gene product interaction and synthesis of 4 S pieces. *J Mol Biol* **92:** 145-163

LeBowitz JH, McMacken R (1986) The Escherichia coli dnaB replication protein is a DNA helicase. *J Biol Chem* **261:** 4738-4748

Lee EH, Kornberg A (1991) Replication deficiencies in priA mutants of Escherichia coli lacking the primosomal replication n' protein. *Proc Natl Acad Sci U S A* **88:** 3029-3032

Lee JK, Hurwitz J (2000) Isolation and characterization of various complexes of the minichromosome maintenance proteins of Schizosaccharomyces pombe. *J Biol Chem* **275:** 18871-18878

Lee JY, Yang W (2006) UvrD helicase unwinds DNA one base pair at a time by a two-part power stroke. *Cell* **127:** 1349-1360

References

Lee MS, Marians KJ (1987) Escherichia coli replication factor Y, a component of the primosome, can act as a DNA helicase. *Proc Natl Acad Sci U S A* **84:** 8345-8349

Lindahl T (1993) Instability and decay of the primary structure of DNA. *Nature* **362:** 709-715

Lindahl T (1996) The Croonian Lecture, 1996: endogenous damage to DNA. *Philos Trans R Soc Lond B Biol Sci* **351:** 1529-1538

Liu B, Alberts BM (1995) Head-on collision between a DNA replication apparatus and RNA polymerase transcription complex. *Science* **267:** 1131-1137

Liu J, Marians KJ (1999) PriA-directed assembly of a primosome on D loop DNA. *J Biol Chem* **274:** 25033-25041

Liu J, Nurse P, Marians KJ (1996) The ordered assembly of the phiX174-type primosome. III. PriB facilitates complex formation between PriA and DnaT. *J Biol Chem* **271:** 15656-15661

Lohman TM, Tomko EJ, Wu CG (2008) Non-hexameric DNA helicases and translocases: mechanisms and regulation. *Nat Rev Mol Cell Biol* **9:** 391-401

Lopper M, Boonsombat R, Sandler SJ, Keck JL (2007) A hand-off mechanism for primosome assembly in replication restart. *Mol Cell* **26:** 781-793

Lorenz A, Osman F, Folkyte V, Sofueva S, Whitby MC (2009) Fbh1 limits Rad51-dependent recombination at blocked replication forks. *Mol Cell Biol* **29:** 4742-4756

Louarn J, Patte J, Louarn JM (1977) Evidence for a fixed termination site of chromosome replication in Escherichia coli K12. *J Mol Biol* **115:** 295-314

Lovett ST (2006) Replication arrest-stimulated recombination: Dependence on the RecA paralog, RadA/Sms and translesion polymerase, DinB. *DNA Repair (Amst)* **5:** 1421-1427

Lyubimov AY, Strycharska M, Berger JM (2011) The nuts and bolts of ring-translocase structure and mechanism. *Curr Opin Struct Biol* **21:** 240-248

Mahdi AA, Buckman C, Harris L, Lloyd RG (2006) Rep and PriA helicase activities prevent RecA from provoking unnecessary recombination during replication fork repair. *Genes Dev* **20:** 2135-2147

Maki H, Horiuchi T, Kornberg A (1985) The polymerase subunit of DNA polymerase III of Escherichia coli. I. Amplification of the dnaE gene product and polymerase activity of the alpha subunit. *J Biol Chem* **260:** 12982-12986

Maluf NK, Fischer CJ, Lohman TM (2003) A Dimer of Escherichia coli UvrD is the active form of the helicase in vitro. *J Mol Biol* **325:** 913-935

Manelyte L, Guy CP, Smith RM, Dillingham MS, McGlynn P, Savery NJ (2009) The unstructured C-terminal extension of UvrD interacts with UvrB, but is dispensable for nucleotide excision repair. *DNA Repair (Amst)* **8:** 1300-1310

Manosas M, Perumal SK, Bianco P, Ritort F, Benkovic SJ, Croquette V (2013) RecG and UvsW catalyse robust DNA rewinding critical for stalled DNA replication fork rescue. *Nat Commun* **4:** 2368

Manosas M, Xi XG, Bensimon D, Croquette V (2010) Active and passive mechanisms of helicases. *Nucleic Acids Res* **38:** 5518-5526

Marians KJ (1987) DNA gyrase-catalyzed decatenation of multiply linked DNA dimers. *J Biol Chem* **262:** 10362-10368

Marians KJ (1995) Phi X174-type primosomal proteins: purification and assay. *Methods Enzymol* **262:** 507-521

References

Marians KJ, Hiasa H, Kim DR, McHenry CS (1998) Role of the core DNA polymerase III subunits at the replication fork. Alpha is the only subunit required for processive replication. *J Biol Chem* **273:** 2452-2457

Matson SW (1986) Escherichia coli helicase II (urvD gene product) translocates unidirectionally in a 3' to 5' direction. *J Biol Chem* **261:** 10169-10175

McGlynn P, Al-Deib AA, Liu J, Marians KJ, Lloyd RG (1997) The DNA replication protein PriA and the recombination protein RecG bind D-loops. *J Mol Biol* **270:** 212-221

McGlynn P, Guy CP (2008) Replication forks blocked by protein-DNA complexes have limited stability in vitro. *J Mol Biol* **381:** 249-255

McGlynn P, Lloyd RG (1999) RecG helicase activity at three- and four-strand DNA structures. *Nucleic Acids Res* **27:** 3049-3056

McGlynn P, Lloyd RG (2001) Action of RuvAB at replication fork structures. *J Biol Chem* **276:** 41938-41944

McGlynn P, Savery NJ, Dillingham MS (2012) The conflict between DNA replication and transcription. *Mol Microbiol* **85:** 12-20

McHenry CS (1988) The asymmetric dimeric polymerase hypothesis: a progress report. *Biochim Biophys Acta* **951:** 240-248

McInerney P, O'Donnell M (2004) Functional uncoupling of twin polymerases: mechanism of polymerase dissociation from a lagging-strand block. *J Biol Chem* **279:** 21543-21551

Meiners MJ, Tahmaseb K, Matson SW (2014) The UvrD303 Hyper-helicase Exhibits Increased Processivity. *J Biol Chem*

Mendonca VM, Kaiser-Rogers K, Matson SW (1993) Double helicase II (uvrD)-helicase IV (helD) deletion mutants are defective in the recombination pathways of Escherichia coli. *J Bacteriol* **175:** 4641-4651

Merrikh H, Machon C, Grainger WH, Grossman AD, Soultanas P (2011) Co-directional replication-transcription conflicts lead to replication restart. *Nature* **470:** 554-557

Meselson M, Stahl FW (1958) The replication of DNA. *Cold Spring Harb Symp Quant Biol* **23:** 9-12

Michel B, Ehrlich SD, Uzest M (1997) DNA double-strand breaks caused by replication arrest. *EMBO J* **16:** 430-438

Michel B, Grompone G, Flores MJ, Bidnenko V (2004) Multiple pathways process stalled replication forks. *Proc Natl Acad Sci U S A* **101:** 12783-12788

Mischo HE, Gomez-Gonzalez B, Grzechnik P, Rondon AG, Wei W, Steinmetz L, Aguilera A, Proudfoot NJ (2011) Yeast Sen1 helicase protects the genome from transcription-associated instability. *Mol Cell* **41:** 21-32

Mizukoshi T, Tanaka T, Arai K, Kohda D, Masai H (2003) A critical role of the 3' terminus of nascent DNA chains in recognition of stalled replication forks. *J Biol Chem* **278:** 42234-42239

Mizuno K, Miyabe I, Schalbetter SA, Carr AM, Murray JM (2012) Recombination-restarted replication makes inverted chromosome fusions at inverted repeats. *Nature*

Morimatsu K, Kowalczykowski SC (2003) RecFOR proteins load RecA protein onto gapped DNA to accelerate DNA strand exchange: a universal step of recombinational repair. *Mol Cell* **11:** 1337-1347

Morris PD, Byrd AK, Tackett AJ, Cameron CE, Tanega P, Ott R, Fanning E, Raney KD (2002) Hepatitis C virus NS3 and simian virus 40 T antigen helicases displace streptavidin from 5'-biotinylated

References

oligonucleotides but not from 3'-biotinylated oligonucleotides: evidence for directional bias in translocation on single-stranded DNA. *Biochemistry* **41:** 2372-2378

Morris PD, Raney KD (1999) DNA helicases displace streptavidin from biotin-labeled oligonucleotides. *Biochemistry* **38:** 5164-5171

Mott ML, Erzberger JP, Coons MM, Berger JM (2008) Structural synergy and molecular crosstalk between bacterial helicase loaders and replication initiators. *Cell* **135:** 623-634

Moyer SE, Lewis PW, Botchan MR (2006) Isolation of the Cdc45/Mcm2-7/GINS (CMG) complex, a candidate for the eukaryotic DNA replication fork helicase. *Proc Natl Acad Sci U S A* **103:** 10236-10241

Mulcair MD, Schaeffer PM, Oakley AJ, Cross HF, Neylon C, Hill TM, Dixon NE (2006) A molecular mousetrap determines polarity of termination of DNA replication in E. coli. *Cell* **125:** 1309-1319

Myong S, Rasnik I, Joo C, Lohman TM, Ha T (2005) Repetitive shuttling of a motor protein on DNA. *Nature* **437:** 1321-1325

Naktinis V, Onrust R, Fang L, O'Donnell M (1995) Assembly of a chromosomal replication machine: two DNA polymerases, a clamp loader, and sliding clamps in one holoenzyme particle. II. Intermediate complex between the clamp loader and its clamp. *J Biol Chem* **270:** 13358-13365

Nelson SW, Benkovic SJ (2010) Response of the bacteriophage T4 replisome to noncoding lesions and regression of a stalled replication fork. *J Mol Biol* **401:** 743-756

Ng JY, Marians KJ (1996) The ordered assembly of the phiX174-type primosome. I. Isolation and identification of intermediate protein-DNA complexes. *J Biol Chem* **271:** 15642-15648

Noirot-Gros MF, Dervyn E, Wu LJ, Mervelet P, Errington J, Ehrlich SD, Noirot P (2002) An expanded view of bacterial DNA replication. *Proc Natl Acad Sci U S A* **99:** 8342-8347

Nurse P, Liu J, Marians KJ (1999) Two modes of PriA binding to DNA. *J Biol Chem* **274:** 25026-25032

Nurse P, Zavitz KH, Marians KJ (1991) Inactivation of the Escherichia coli priA DNA replication protein induces the SOS response. *J Bacteriol* **173:** 6686-6693

O'Donnell M, Kuriyan J, Kong XP, Stukenberg PT, Onrust R (1992) The sliding clamp of DNA polymerase III holoenzyme encircles DNA. *Mol Biol Cell* **3:** 953-957

Okazaki R, Okazaki T, Sakabe K, Sugimoto K, Sugino A (1968) Mechanism of DNA chain growth. I. Possible discontinuity and unusual secondary structure of newly synthesized chains. *Proc Natl Acad Sci U S A* **59:** 598-605

Olson MW, Dallmann HG, McHenry CS (1995) DnaX complex of Escherichia coli DNA polymerase III holoenzyme. The chi psi complex functions by increasing the affinity of tau and gamma for delta.delta' to a physiologically relevant range. *J Biol Chem* **270:** 29570-29577

Onrust R, Finkelstein J, Naktinis V, Turner J, Fang L, O'Donnell M (1995) Assembly of a chromosomal replication machine: two DNA polymerases, a clamp loader, and sliding clamps in one holoenzyme particle. I. Organization of the clamp loader. *J Biol Chem* **270:** 13348-13357

Orlova M, Newlands J, Das A, Goldfarb A, Borukhov S (1995) Intrinsic transcript cleavage activity of RNA polymerase. *Proc Natl Acad Sci U S A* **92:** 4596-4600

Orren DK, Selby CP, Hearst JE, Sancar A (1992) Post-incision steps of nucleotide excision repair in Escherichia coli. Disassembly of the UvrBC-DNA complex by helicase II and DNA polymerase I. *J Biol Chem* **267:** 780-788

Pages V, Fuchs RP (2003) Uncoupling of leading- and lagging-strand DNA replication during lesion bypass in vivo. *Science* **300:** 1300-1303

References

Papadopoulos JS, Agarwala R (2007) COBALT: constraint-based alignment tool for multiple protein sequences. *Bioinformatics* **23:** 1073-1079

Parada CA, Marians KJ (1991) Mechanism of DNA A protein-dependent pBR322 DNA replication. DNA A protein-mediated trans-strand loading of the DNA B protein at the origin of pBR322 DNA. *J Biol Chem* **266:** 18895-18906

Park J, Myong S, Niedziela-Majka A, Lee KS, Yu J, Lohman TM, Ha T (2010) PcrA helicase dismantles RecA filaments by reeling in DNA in uniform steps. *Cell* **142:** 544-555

Park JS, Marr MT, Roberts JW (2002) E. coli Transcription repair coupling factor (Mfd protein) rescues arrested complexes by promoting forward translocation. *Cell* **109:** 757-767

Parsons CA, Tsaneva I, Lloyd RG, West SC (1992) Interaction of Escherichia coli RuvA and RuvB proteins with synthetic Holliday junctions. *Proc Natl Acad Sci U S A* **89:** 5452-5456

Paul S, Million-Weaver S, Chattopadhyay S, Sokurenko E, Merrikh H (2013) Accelerated gene evolution through replication-transcription conflicts. *Nature* **495:** 512-515

Payne BT, van Knippenberg IC, Bell H, Filipe SR, Sherratt DJ, McGlynn P (2006) Replication fork blockage by transcription factor-DNA complexes in Escherichia coli. *Nucleic Acids Res* **34:** 5194-5202

Perkins G, Diffley JF (1998) Nucleotide-dependent prereplicative complex assembly by Cdc6p, a homolog of eukaryotic and prokaryotic clamp-loaders. *Mol Cell* **2:** 23-32

Petit MA, Dervyn E, Rose M, Entian KD, McGovern S, Ehrlich SD, Bruand C (1998) PcrA is an essential DNA helicase of Bacillus subtilis fulfilling functions both in repair and rolling-circle replication. *Mol Microbiol* **29:** 261-273

Pinter SF, Aubert SD, Zakian VA (2008) The Schizosaccharomyces pombe Pfh1p DNA helicase is essential for the maintenance of nuclear and mitochondrial DNA. *Mol Cell Biol* **28:** 6594-6608

Pomerantz RT, O'Donnell M (2008) The replisome uses mRNA as a primer after colliding with RNA polymerase. *Nature* **456:** 762-766

Pomerantz RT, O'Donnell M (2010) Direct restart of a replication fork stalled by a head-on RNA polymerase. *Science* **327:** 590-592

Postow L, Crisona NJ, Peter BJ, Hardy CD, Cozzarelli NR (2001) Topological challenges to DNA replication: conformations at the fork. *Proc Natl Acad Sci U S A* **98:** 8219-8226

Prado F, Aguilera A (2005) Impairment of replication fork progression mediates RNA polII transcription-associated recombination. *EMBO J* **24:** 1267-1276

Prescott DM, Kuempel PL (1972) Bidirectional replication of the chromosome in Escherichia coli. *Proc Natl Acad Sci U S A* **69:** 2842-2845

Ramakrishnan C, Dani VS, Ramasarma T (2002) A conformational analysis of Walker motif A [GXXXXGKT (S)] in nucleotide-binding and other proteins. *Protein Eng* **15:** 783-798

Randell JC, Bowers JL, Rodriguez HK, Bell SP (2006) Sequential ATP hydrolysis by Cdc6 and ORC directs loading of the Mcm2-7 helicase. *Mol Cell* **21:** 29-39

Raney KD, Benkovic SJ (1995) Bacteriophage T4 Dda helicase translocates in a unidirectional fashion on single-stranded DNA. *J Biol Chem* **270:** 22236-22242

Rasnik I, Myong S, Cheng W, Lohman TM, Ha T (2004) DNA-binding orientation and domain conformation of the E. coli rep helicase monomer bound to a partial duplex junction: single-molecule studies of fluorescently labeled enzymes. *J Mol Biol* **336:** 395-408

References

Rehrauer WM, Kowalczykowski SC (1993) Alteration of the nucleoside triphosphate (NTP) catalytic domain within Escherichia coli recA protein attenuates NTP hydrolysis but not joint molecule formation. *J Biol Chem* **268:** 1292-1297

Reyes-Lamothe R, Sherratt DJ, Leake MC (2010) Stoichiometry and architecture of active DNA replication machinery in Escherichia coli. *Science* **328:** 498-501

Rocha EP (2004) The replication-related organization of bacterial genomes. *Microbiology* **150:** 1609-1627

Rocha EP, Cornet E, Michel B (2005) Comparative and evolutionary analysis of the bacterial homologous recombination systems. *PLoS Genet* **1:** e15

Sabouri N, McDonald KR, Webb CJ, Cristea IM, Zakian VA (2012) DNA replication through hard-to-replicate sites, including both highly transcribed RNA Pol II and Pol III genes, requires the S. pombe Pfh1 helicase. *Genes Dev* **26:** 581-593

Saikrishnan K, Griffiths SP, Cook N, Court R, Wigley DB (2008) DNA binding to RecD: role of the 1B domain in SF1B helicase activity. *EMBO J* **27:** 2222-2229

Saikrishnan K, Powell B, Cook NJ, Webb MR, Wigley DB (2009) Mechanistic basis of 5'-3' translocation in SF1B helicases. *Cell* **137:** 849-859

Sancar A, Sancar GB (1988) DNA repair enzymes. *Annu Rev Biochem* **57:** 29-67

Sandler SJ (2000) Multiple genetic pathways for restarting DNA replication forks in Escherichia coli K-12. *Genetics* **155:** 487-497

Sandler SJ, Marians KJ (2000) Role of PriA in replication fork reactivation in Escherichia coli. *J Bacteriol* **182:** 9-13

Sandler SJ, Marians KJ, Zavitz KH, Coutu J, Parent MA, Clark AJ (1999) dnaC mutations suppress defects in DNA replication- and recombination-associated functions in priB and priC double mutants in Escherichia coli K-12. *Mol Microbiol* **34:** 91-101

Sandler SJ, McCool JD, Do TT, Johansen RU (2001) PriA mutations that affect PriA-PriC function during replication restart. *Mol Microbiol* **41:** 697-704

Saveson CJ, Lovett ST (1997) Enhanced deletion formation by aberrant DNA replication in Escherichia coli. *Genetics* **146:** 457-470

Saveson CJ, Lovett ST (1999) Tandem repeat recombination induced by replication fork defects in Escherichia coli requires a novel factor, RadC. *Genetics* **152:** 5-13

Scheffzek K, Ahmadian MR, Kabsch W, Wiesmuller L, Lautwein A, Schmitz F, Wittinghofer A (1997) The Ras-RasGAP complex: structural basis for GTPase activation and its loss in oncogenic Ras mutants. *Science* **277:** 333-338

Scheuermann RH, Echols H (1984) A separate editing exonuclease for DNA replication: the epsilon subunit of Escherichia coli DNA polymerase III holoenzyme. *Proc Natl Acad Sci U S A* **81:** 7747-7751

Schmidt KH, Derry KL, Kolodner RD (2002) Saccharomyces cerevisiae RRM3, a 5' to 3' DNA helicase, physically interacts with proliferating cell nuclear antigen. *J Biol Chem* **277:** 45331-45337

Schulz VP, Zakian VA (1994) The saccharomyces PIF1 DNA helicase inhibits telomere elongation and de novo telomere formation. *Cell* **76:** 145-155

Sclafani RA, Wechsler JA (1981) Deletion map of the Escherichia coli K-12 dnaB gene. *Mol Gen Genet* **183:** 314-317

References

Seigneur M, Bidnenko V, Ehrlich SD, Michel B (1998) RuvAB acts at arrested replication forks. *Cell* **95:** 419-430

Seitz H, Weigel C, Messer W (2000) The interaction domains of the DnaA and DnaB replication proteins of Escherichia coli. *Mol Microbiol* **37:** 1270-1279

Selby CP, Drapkin R, Reinberg D, Sancar A (1997) RNA polymerase II stalled at a thymine dimer: footprint and effect on excision repair. *Nucleic Acids Res* **25:** 787-793

Selby CP, Sancar A (1993) Molecular mechanism of transcription-repair coupling. *Science* **260:** 53-58

Shiratori A, Shibata T, Arisawa M, Hanaoka F, Murakami Y, Eki T (1999) Systematic identification, classification, and characterization of the open reading frames which encode novel helicase-related proteins in Saccharomyces cerevisiae by gene disruption and Northern analysis. *Yeast* **15:** 219-253

Simandlova J, Zagelbaum J, Payne MJ, Chu WK, Shevelev I, Hanada K, Chatterjee S, Reid DA, Liu Y, Janscak P, Rothenberg E, Hickson ID (2013) FBH1 disrupts RAD51 filaments in vitro and modulates homologous recombination in mammalian cells. *J Biol Chem*

Singleton MR, Dillingham MS, Wigley DB (2007) Structure and mechanism of helicases and nucleic acid translocases. *Annu Rev Biochem* **76:** 23-50

Singleton MR, Scaife S, Wigley DB (2001) Structural analysis of DNA replication fork reversal by RecG. *Cell* **107:** 79-89

Sisamakis E, Valeri A, Kalinin S, Rothwell PJ, Seidel CA (2010) Accurate single-molecule FRET studies using multiparameter fluorescence detection. *Methods Enzymol* **475:** 455-514

Soultanas P, Dillingham MS, Papadopoulos F, Phillips SE, Thomas CD, Wigley DB (1999) Plasmid replication initiator protein RepD increases the processivity of PcrA DNA helicase. *Nucleic Acids Res* **27:** 1421-1428

Soultanas P, Dillingham MS, Wigley DB (1998) Escherichia coli ribosomal protein L3 stimulates the helicase activity of the Bacillus stearothermophilus PcrA helicase. *Nucleic Acids Res* **26:** 2374-2379

Soultanas P, Dillingham MS, Wiley P, Webb MR, Wigley DB (2000) Uncoupling DNA translocation and helicase activity in PcrA: direct evidence for an active mechanism. *EMBO J* **19:** 3799-3810

Srivatsan A, Tehranchi A, MacAlpine DM, Wang JD (2010) Co-orientation of replication and transcription preserves genome integrity. *PLoS Genet* **6:** e1000810

Stano NM, Jeong YJ, Donmez I, Tummalapalli P, Levin MK, Patel SS (2005) DNA synthesis provides the driving force to accelerate DNA unwinding by a helicase. *Nature* **435:** 370-373

Steinacher R, Osman F, Dalgaard JZ, Lorenz A, Whitby MC (2012) The DNA helicase Pfh1 promotes fork merging at replication termination sites to ensure genome stability. *Genes Dev* **26:** 594-602

Stewart J, Hingorani MM, Kelman Z, O'Donnell M (2001) Mechanism of beta clamp opening by the delta subunit of Escherichia coli DNA polymerase III holoenzyme. *J Biol Chem* **276:** 19182-19189

Story RM, Weber IT, Steitz TA (1992) The structure of the E. coli recA protein monomer and polymer. *Nature* **355:** 318-325

Studwell-Vaughan PS, O'Donnell M (1993) DNA polymerase III accessory proteins. V. Theta encoded by holE. *J Biol Chem* **268:** 11785-11791

Stukenberg PT, Studwell-Vaughan PS, O'Donnell M (1991) Mechanism of the sliding beta-clamp of DNA polymerase III holoenzyme. *J Biol Chem* **266:** 11328-11334

Subramanya HS, Bird LE, Brannigan JA, Wigley DB (1996) Crystal structure of a DExx box DNA helicase. *Nature* **384:** 379-383

References

Sun B, Wei KJ, Zhang B, Zhang XH, Dou SX, Li M, Xi XG (2008) Impediment of E. coli UvrD by DNA-destabilizing force reveals a strained-inchworm mechanism of DNA unwinding. *EMBO J* **27:** 3279-3287

Tackett AJ, Wei L, Cameron CE, Raney KD (2001) Unwinding of nucleic acids by HCV NS3 helicase is sensitive to the structure of the duplex. *Nucleic Acids Res* **29:** 565-572

Tanaka H, Ryu GH, Seo YS, Tanaka K, Okayama H, MacNeill SA, Yuasa Y (2002) The fission yeast pfh1(+) gene encodes an essential 5' to 3' DNA helicase required for the completion of S-phase. *Nucleic Acids Res* **30:** 4728-4739

Tanner NA, Hamdan SM, Jergic S, Loscha KV, Schaeffer PM, Dixon NE, van Oijen AM (2008) Single-molecule studies of fork dynamics in Escherichia coli DNA replication. *Nat Struct Mol Biol* **15:** 170-176

Tanner NK, Cordin O, Banroques J, Doere M, Linder P (2003) The Q motif: a newly identified motif in DEAD box helicases may regulate ATP binding and hydrolysis. *Mol Cell* **11:** 127-138

Taucher-Scholz G, Abdel-Monem M, Hoffmann-Berling H (1983) Functions of helicases in E. coli. In *Mechanisms of DNA replication and recombination*, Cozzarelli NR (ed), Functions of helicases in E. coli, pp 65-76. New York: Alan R. Liss Inc.

Taylor AF, Amundsen SK, Guttman M, Lee KK, Luo J, Ranish J, Smith GR (2014) Control of RecBCD Enzyme Activity by DNA Binding- and Chi Hotspot-dependent Conformational Changes. *J Mol Biol*

Taylor AF, Smith GR (1985) Substrate specificity of the DNA unwinding activity of the RecBC enzyme of Escherichia coli. *J Mol Biol* **185:** 431-443

Taylor SD, Solem A, Kawaoka J, Pyle AM (2010) The NPH-II helicase displays efficient DNA x RNA helicase activity and a pronounced purine sequence bias. *J Biol Chem* **285:** 11692-11703

Teulon JM, Delcuze Y, Odorico M, Chen SW, Parot P, Pellequer JL (2011) Single and multiple bonds in (strept)avidin-biotin interactions. *J Mol Recognit* **24:** 490-502

Tornaletti S (2005) Transcription arrest at DNA damage sites. *Mutat Res* **577:** 131-145

Tornaletti S, Maeda LS, Hanawalt PC (2006) Transcription arrest at an abasic site in the transcribed strand of template DNA. *Chem Res Toxicol* **19:** 1215-1220

Tougu K, Peng H, Marians KJ (1994) Identification of a domain of Escherichia coli primase required for functional interaction with the DnaB helicase at the replication fork. *J Biol Chem* **269:** 4675-4682

Trautinger BW, Jaktaji RP, Rusakova E, Lloyd RG (2005) RNA polymerase modulators and DNA repair activities resolve conflicts between DNA replication and transcription. *Mol Cell* **19:** 247-258

Trautinger BW, Lloyd RG (2002) Modulation of DNA repair by mutations flanking the DNA channel through RNA polymerase. *EMBO J* **21:** 6944-6953

Truglio JJ, Croteau DL, Skorvaga M, DellaVecchia MJ, Theis K, Mandavilli BS, Van Houten B, Kisker C (2004) Interactions between UvrA and UvrB: the role of UvrB's domain 2 in nucleotide excision repair. *EMBO J* **23:** 2498-2509

Uzest M, Ehrlich SD, Michel B (1995) Lethality of rep recB and rep recC double mutants of Escherichia coli. *Mol Microbiol* **17:** 1177-1188

Veaute X, Delmas S, Selva M, Jeusset J, Le Cam E, Matic I, Fabre F, Petit MA (2005) UvrD helicase, unlike Rep helicase, dismantles RecA nucleoprotein filaments in Escherichia coli. *EMBO J* **24:** 180-189

Veaute X, Jeusset J, Soustelle C, Kowalczykowski SC, Le Cam E, Fabre F (2003) The Srs2 helicase prevents recombination by disrupting Rad51 nucleoprotein filaments. *Nature* **423:** 309-312

References

Velankar SS, Soultanas P, Dillingham MS, Subramanya HS, Wigley DB (1999) Crystal structures of complexes of PcrA DNA helicase with a DNA substrate indicate an inchworm mechanism. *Cell* **97:** 75-84

Verhoeven EE, van Kesteren M, Moolenaar GF, Visse R, Goosen N (2000) Catalytic sites for 3' and 5' incision of Escherichia coli nucleotide excision repair are both located in UvrC. *J Biol Chem* **275:** 5120-5123

von Hippel PH, Delagoutte E (2001) A general model for nucleic acid helicases and their "coupling" within macromolecular machines. *Cell* **104:** 177-190

Wahba L, Amon JD, Koshland D, Vuica-Ross M (2011) RNase H and multiple RNA biogenesis factors cooperate to prevent RNA:DNA hybrids from generating genome instability. *Mol Cell* **44:** 978-988

Wahle E, Lasken RS, Kornberg A (1989) The dnaB-dnaC replication protein complex of Escherichia coli. II. Role of the complex in mobilizing dnaB functions. *J Biol Chem* **264:** 2469-2475

Walker JE, Saraste M, Runswick MJ, Gay NJ (1982) Distantly related sequences in the alpha- and beta-subunits of ATP synthase, myosin, kinases and other ATP-requiring enzymes and a common nucleotide binding fold. *EMBO J* **1:** 945-951

Walsh BW, Bolz SA, Wessel SR, Schroeder JW, Keck JL, Simmons LA (2014) RecD2 helicase limits replication fork stress in Bacillus subtilis. *J Bacteriol* **196:** 1359-1368

Wang W, Li GW, Chen C, Xie XS, Zhuang X (2011) Chromosome organization by a nucleoid-associated protein in live bacteria. *Science* **333:** 1445-1449

Washburn RS, Gottesman ME (2011) Transcription termination maintains chromosome integrity. *Proc Natl Acad Sci U S A* **108:** 792-797

Watson JD, Crick FH (1953) Molecular structure of nucleic acids; a structure for deoxyribose nucleic acid. *Nature* **171:** 737-738

Wechsler JA, Gross JD (1971) Escherichia coli mutants temperature-sensitive for DNA synthesis. *Mol Gen Genet* **113:** 273-284

Weiss B, Grossman L (1987) Phosphodiesterases involved in DNA repair. *Adv Enzymol Relat Areas Mol Biol* **60:** 1-34

Welch MM, McHenry CS (1982) Cloning and identification of the product of the dnaE gene of Escherichia coli. *J Bacteriol* **152:** 351-356

Wessel SR, Marceau AH, Massoni SC, Zhou R, Ha T, Sandler SJ, Keck JL (2013) PriC-mediated DNA replication restart requires PriC complex formation with the single-stranded DNA-binding protein. *J Biol Chem*

West SC, Cassuto E, Mursalim J, Howard-Flanders P (1980) Recognition of duplex DNA containing single-stranded regions by recA protein. *Proc Natl Acad Sci U S A* **77:** 2569-2573

Wickner S, Hurwitz J (1975) Interaction of Escherichia coli dnaB and dnaC(D) gene products in vitro. *Proc Natl Acad Sci U S A* **72:** 921-925

Wu CA, Zechner EL, Reems JA, McHenry CS, Marians KJ (1992) Coordinated leading- and lagging-strand synthesis at the Escherichia coli DNA replication fork. V. Primase action regulates the cycle of Okazaki fragment synthesis. *J Biol Chem* **267:** 4074-4083

Xu L, Marians KJ (2000) Purification and characterization of DnaC810, a primosomal protein capable of bypassing PriA function. *J Biol Chem* **275:** 8196-8205

Yamashita T, Hanada K, Iwasaki M, Yamaguchi H, Ikeda H (1999) Illegitimate recombination induced by overproduction of DnaB helicase in Escherichia coli. *J Bacteriol* **181:** 4549-4553

References

Yancey-Wrona JE, Matson SW (1992) Bound Lac repressor protein differentially inhibits the unwinding reactions catalyzed by DNA helicases. *Nucleic Acids Res* **20:** 6713-6721

Yancey-Wrona JE, Wood ER, George JW, Smith KR, Matson SW (1992) Escherichia coli Rep protein and helicase IV. Distributive single-stranded DNA-dependent ATPases that catalyze a limited unwinding reaction in vitro. *Eur J Biochem* **207:** 479-485

Yancey JE, Matson SW (1991) The DNA unwinding reaction catalyzed by Rep protein is facilitated by an RHSP-DNA interaction. *Nucleic Acids Res* **19:** 3943-3951

Yang Y, Dou SX, Ren H, Wang PY, Zhang XD, Qian M, Pan BY, Xi XG (2008) Evidence for a functional dimeric form of the PcrA helicase in DNA unwinding. *Nucleic Acids Res* **36:** 1976-1989

Yao NY, Georgescu RE, Finkelstein J, O'Donnell ME (2009) Single-molecule analysis reveals that the lagging strand increases replisome processivity but slows replication fork progression. *Proc Natl Acad Sci U S A* **106:** 13236-13241

Yao NY, O'Donnell M (2010) SnapShot: The replisome. *Cell* **141:** 1088, 1088 e1081

Yarranton GT, Gefter ML (1979) Enzyme-catalyzed DNA unwinding: studies on Escherichia coli rep protein. *Proc Natl Acad Sci U S A* **76:** 1658-1662

Ye J, Osborne AR, Groll M, Rapoport TA (2004) RecA-like motor ATPases--lessons from structures. *Biochim Biophys Acta* **1659:** 1-18

Yeeles JT, Marians KJ (2011) The Escherichia coli replisome is inherently DNA damage tolerant. *Science* **334:** 235-238

Yeeles JT, Poli J, Marians KJ, Pasero P (2013) Rescuing stalled or damaged replication forks. *Cold Spring Harb Perspect Biol* **5**

Yoda K, Okazaki T (1991) Specificity of recognition sequence for Escherichia coli primase. *Mol Gen Genet* **227:** 1-8

Zavitz KH, Marians KJ (1992) ATPase-deficient mutants of the Escherichia coli DNA replication protein PriA are capable of catalyzing the assembly of active primosomes. *J Biol Chem* **267:** 6933-6940

Zechner EL, Wu CA, Marians KJ (1992) Coordinated leading- and lagging-strand synthesis at the Escherichia coli DNA replication fork. III. A polymerase-primase interaction governs primer size. *J Biol Chem* **267:** 4054-4063

Zhang DH, Zhou B, Huang Y, Xu LX, Zhou JQ (2006) The human Pif1 helicase, a potential Escherichia coli RecD homologue, inhibits telomerase activity. *Nucleic Acids Res* **34:** 1393-1404

Zhang G, Deng E, Baugh L, Kushner SR (1998) Identification and characterization of Escherichia coli DNA helicase II mutants that exhibit increased unwinding efficiency. *J Bacteriol* **180:** 377-387

Zhou JQ, Qi H, Schulz VP, Mateyak MK, Monson EK, Zakian VA (2002) Schizosaccharomyces pombe pfh1+ encodes an essential 5' to 3' DNA helicase that is a member of the PIF1 subfamily of DNA helicases. *Mol Biol Cell* **13:** 2180-2191